SYNTHESIS AND APPLICATIONS OF DEPOLYMERIZABLE POLYALDEHYDES

BY

JOSHUA ANDREW KAITZ

DISSERTATION

Submitted in partial fulfillment of the requirements
for the degree of Doctor of Philosophy in Chemistry
in the Graduate College of the
University of Illinois at Urbana-Champaign, 2015

Urbana, Illinois

Doctoral Committee:

Professor Jeffrey S. Moore, Chair
Professor Paul V. Braun
Professor Steven C. Zimmerman
Professor M. Christina White

Abstract

Depolymerizable polymers are stimuli-responsive materials that can be triggered to rapidly and completely depolymerize into their constituting monomers on command. Their applications include use in triggered release, recyclable and restructurable materials, disappearing or transient materials, and many others functions. Polyaldehyde materials were selected as a candidate system for study due to their known ability to depolymerize rapidly; however, they are also known to generally suffer from limited synthetic accessibility and sensitivity toward post-polymerization modification, thus restricting widespread adoption. My research has broadly focused in two areas: Chapters 2-5 focus on the development of a general and scalable cationic polymerization and copolymerization of aldehydes; Chapters 6-7 describe the installation of functional handles for post-polymerization elaboration of polyaldehydes into various nanostructures. Chapter 8 includes more recent work aimed at the preparation of a novel class of sustainable, recyclable, and eco-friendly depolymerizable polyesters. In short, the cationic polymerization of aldehydes was found to be a robust and scalable reaction, and mechanistic analysis of the polymerization has revealed a reversible cyclization process that produces macrocyclic architectures in high yield and with high purity. It was also found that copolymerization of *o*-phthalaldehyde with substituted benzaldehydes, generally considered unreactive to polymerization, yielded stimuli-responsive polyaldehyde materials that could be further elaborated to generate depolymerizable single-chain polymeric nanoparticles and polymer networks. These and other studies on the preparation and development of depolymerizable materials have advanced the state-in-the-art in polyaldehyde synthesis and paved the way for new applications in triggered depolymerization.

Acknowledgments

I want to take a few paragraphs here to express my gratitude for the many people in my life who have helped me get to this point. Nobody can get a PhD on their own, and I'm fortunate to have been surrounded by amazing people throughout my short time in both academia and industry. My career in chemistry really would not exist without great teachers like Mrs. Krashes and Dr. Corcoran at FHS, and without Professor Mike Gagné at UNC who took a chance on me and let a young, naïve, and inexperienced undergrad join his research group. He partnered me up with an amazing mentor, Dr. Mee-Kyung Chung, who trained me in synthetic organic chemistry and gave me so many of the technical skills I needed to succeed.

I also want to thank people like Dr. Chris Loose and David Lucchino who took a chance on a green, unproven chemist and gave me the opportunity to join the team at Semprus BioSciences. There, I got to team up with a huge influence in my life, Professor Chad Huval, my P.I.C. and mentor. "Chadbo" taught me the skills I need to succeed in my career and in life, and encouraged me to take the plunge and head off to grad school. I also want to give a shout-out to Dr.'s Jonathan "JZ" Zhang and Jun Li who taught me an enormous amount about polymer chemistry and introduced me to such a fascinating field. None of this would have been possible without you.

Of course, I will be forever indebted to my advisor, Professor Jeff Moore. My #1 favorite "Jeffism," which he shared with me early in my first year in a rare and fleeting stroll through the lab, is to "never trust your advisor." He gives us the independence and leeway to pursue our interests and helps us grow into independent scientists in the safe confines of his "incubator" at UIUC. Likewise, I cannot adequately express my gratitude toward Professor Charles Diesendruck, my unscripted mentor during my early years in graduate school. Our many helpful discussions and his insightful suggestions have enabled me to get to this point.

Ashley Trimmell, the architect behind the group, and the kind and caring staff in the organic office have been invaluable resources throughout my time in the department. Thank you to Ashley, Stacy Olson, Becky Duffield, Susan Lighty, Lori Johnson, Gayle Adkisson, Erica Malloch, and any others I may have missed.

The Moore group and the interdisciplinary AMS group have provided an incredible atmosphere to pursue research for the past four years. Getting a chance to work with great engineers from the AMS collaboration like Dr. Marta Baginska, Dr. Sen Kang, Hector Lopez Hernandez, Dr. Chan Woo Park, and others has been a great and enjoyable learning experience. Likewise, the Moore group is a tremendous team

of researchers and I have appreciated getting a chance to work with each and every member of both the RAL and Beckman halves. The RAL crew has grown a lot since my early days, and I want to especially thank the people who helped me find proper footing when I first started like Dr. Dustin Gross, Dr. Bora Inci, Dr. James Herbison, Dr. Scott Sisco, Nina Sekerak, and Dr. Mike Evans. Also, thank you to my more recent colleagues in depolymerizable materials, Dr. Olivia Lee and Dr. Etienne Chenard, who are a pleasure to work with. I won't list the entire Beckman crew, but I will say that even though we are separated by fifteen minutes of campus, I always enjoyed my times hanging around Beckman and bothering you guys. And an extra special thanks to my original boss, and friend through it all, Dr. Windy Santa Cruz. Also, thank you to Windy, Nina, Olivia, and Dr. Maxwell Robb for their assistance in editing this dissertation.

It goes without saying that grad school has its ups and downs, and especially in Champaign, its periods of boredom. But like so many journeys, the thing that matters most is the people who have surrounded me. My friends have helped me to really treasure the past four years and share with me some great memories. The last (almost) year has been a joy to share with Dr. Lea Nienhaus. I'll forever remember our fun times at the Ohio Street house, Jeremy "Smitty" Smith, Stephen "Esteban" Ammann, Ariane "Boomer" Vartanian, Elissa "The Grizz" Grzincic, Sarah "Slow" White, and Tracey "T-Bone" Codding. Weekly lunches and nights out with friends like Tony Grillo and Andrea Ambrosi helped me get through the (occasional) tiring weeks. And playing with and briefly coaching the Esquire Speed Marvels with a roster full of friends kept my weeks interesting throughout the summer and fall months.

Finally, I want to thank my family and friends back home for all of their support. My folks, who might not understand a single paragraph beyond this section, have given me the love and support, and genes, to get to where I am today. I cannot thank them enough. I am happy to say that I have come full circle in the past four years and will be shipping back to Boston soon to start the next phase of my life!

Table of Contents

Chapter 1: Depolymerizable Polymers: An Overview of Discovery, Preparation and Applications

1.1 Abstract

Depolymerizable polymers are stimuli-responsive materials that can be triggered to depolymerize rapidly and completely into their constituting monomers on command. Their applications include use as triggerable vehicles for controlled release, recyclable and restructurable materials, disappearing or sacrificial composites, lithographic resists, and many others functions. Due to their widespread utility across many disciplines, significant efforts have been put forth in recent years to explore, prepare and study a variety of depolymerizable polymers along with their corresponding triggering modes. This introductory chapter aims to highlight the discovery of these polymers over a half-century ago, discuss methods to prepare the polymers, and present recent advances in triggered depolymerization. It also surveys applications that take advantage of these polymers' unique properties, while offering insights into new research directions that may directly contribute to the future development of this dynamic field.

1.2 The Ceiling Temperature Phenomenon

The concept of a ceiling temperature was first described and reported by Snow and Frey in 1943, followed by further elucidation by Dainton and Ivin in several seminal studies on poly(olefin sulfone) polymerizations.[1] The researchers independently discovered that copolymerizations between sulfur dioxide and olefins were paused as temperatures increased; further increasing the temperature to drive the polymerization to completion led to reduced monomer conversions and polymer molecular weights. On the contrary, decreasing polymerization temperature correlated with increasing tendency for the monomers to polymerize and higher polymer molecular weights.[2]

The authors correctly interpreted this counterintuitive result to be a consequence of unfavorable thermodynamics in poly(olefin sulfone) polymerizations.[3] With few exceptions, polymerizations are inherently exothermic and exoentropic ($\Delta H < 0$ and $\Delta S < 0$; there are few known examples of endothermic and endoentropic polymerizations, which exhibit a floor temperature[3c]). It was surmised that all polymerizations are reversible processes, and that there exists a temperature at which the free energy for a polymerization crosses from negative to positive (Scheme 1.1). If the temperature of polymerization is raised to this point, the propagation reaction is halted, and increasing temperature further favors the reverse reaction, resulting in depropagation or "unzipping."

Scheme 1.1 | *Schematic of monomer-polymer equilibrium.*

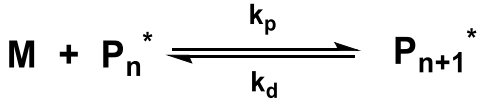

The cross-over temperature was termed a ceiling temperature (T_c), as it represents a critical threshold above which depropagation is the spontaneous process.[3-4] The T_c is an inherent thermodynamic constraint in any polymerization, and depends solely on free energy parameters for any given monomer:

$$\Delta G_p = \Delta H_p - T\Delta S_p \quad (1)$$

$$\Delta G = 0 \; at \; T_C \quad (2)$$

$$T_c = \frac{\Delta H_p}{\Delta S_p} \quad (3)$$

Since the entropy of polymerization depends on concentration, pressure, and effects of solvation, the T_c is generally reported for any given monomer at standard pressure and for an initial monomer concentration of 1.0 mol/L.[3] A more general form of the monomer-polymer equilibrium is expressed below, where $[M]_e$ is the equilibrium monomer concentration at a given temperature:

$$T = \frac{\Delta H_p}{\Delta S_p^\circ + Rln[M]_e} \quad (4)$$

These relationships enable facile determination of polymer ceiling temperatures. Rearranged, a linear relationship is evident between $\frac{1}{T}$ and $\ln[M]_e$, with a slope of $\frac{\Delta H_p}{R}$ and a y-intercept of $-\frac{\Delta S_p^\circ}{R}$:

$$ln[M]_e = \frac{\Delta H_p}{R}\left(\frac{1}{T}\right) - \frac{\Delta S_p^\circ}{R} \quad (5)$$

Thus, measuring monomer equilibrium concentrations at various temperatures enables accurate determination of thermodynamic parameters and gives a reliable estimate of a polymer's T_c. It can be seen that with increasing temperature, the monomer concentration at equilibrium likewise increases. Alternatively, it is possible to measure the rates of polymerization or the polymer molecular weights at various temperatures, and to extrapolate to zero in either case.[3-4] While these last two techniques are less accurate than the first, they were the methods of choice in many early studies on the thermodynamics of polymerization in low T_c polymers.

That the existence of a T_c was not discovered until the 1940s is a direct result of the fact that typical olefin polymerizations are extremely exothermic and have impractically high T_c's.[4] Compared to typical olefin polymerizations known at the time, the exotherm in poly(olefin sulfone) preparation is significantly

reduced (i.e. more positive). The less exothermic polymerization results in a concomitant decrease in T_c, which was impressively recognized and interpreted by the early researchers, paving the way for the discovery of other polymers with low T_c's.

It is worth noting here that reverse propagation above T_c, which will be henceforth termed "depolymerization," is a concept distinct from degradation. Many polymers have been prepared with cleavable bonds within their backbone or side-chains; however, cleaving these bonds, by hydrolysis for example, constitutes degradation and not depolymerization. All polymers are theoretically capable of depolymerization if the temperature is raised above their T_c. However, the majority of common polymers have such high T_c's that thermal degradation is observed before depolymerization. Depolymerizable polymers are thus a special class of polymers with a low T_c, such that depropagation is possible at or near ambient temperatures. Other commonly known depolymerizable polymers besides poly(olefin sulfone)s include many different polyaldehydes, polymers from certain cyclic ethers or acetals, α-methyl styrene, and an emergent class of "self-immolative" polymers, which will be discussed in later sections.[4-7]

1.3 Preparation of Depolymerizable Polymers by Kinetic Stabilization of Chain-Ends

Low T_c, depolymerizable polymers are inherently thermodynamically unstable at, or just above, room temperature. This property raises an important question: how then can low T_c polymers be prepared and exploited as useful materials in ambient conditions? To prepare stable, isolable polymers based on these types of monomers, it is critical to prepare the materials below their T_c and then block or impede the depolymerization process at elevated temperatures. This feat has been achieved in several different manners for various methods of polymerization, but all necessitate "capping" chain-ends to block the depolymerization pathway. End-capping kinetically stabilizes depolymerizable polymers above their T_c because there is not sufficient energy at room temperature to cleave capping groups and permit depropagation to the lowest energy state—monomer.

For radical polymerizations such as poly(olefin sulfone) preparation, blocking the chain-ends from unzipping is relatively trivial.[2] Polymerization at low temperature is accompanied by termination via radical combination or disproportionation, which effectively quenches the reactive chain-ends and end-caps the polymer to inactivate it from depropagation (Scheme 1.2).[8] Only by re-initiating the capped chain-ends or cleaving the polymer backbone to expose new chain-ends can unzipping proceed to effect depolymerization. In this manner, low T_c polymers synthesized by free radical polymerizations essentially stabilize themselves spontaneously by termination.

Scheme 1.2 **|** *Termination "end-capping" processes in free radical polymerizations.*

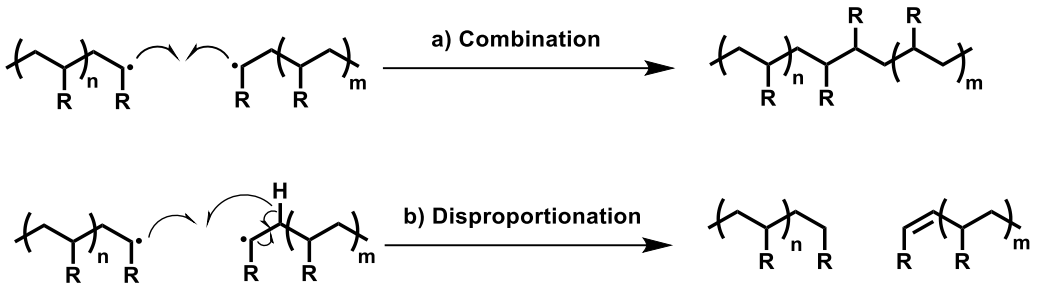

However, in living chain-growth and step-growth polymerizations, termination steps that quench or otherwise inactivate chain-ends do not occur spontaneously (barring termination by cyclization or chain-transfer). It was not until the late 1950s that researchers at DuPont began to identify strategies that effectively stabilize low T_c polymers from depropagation. Polyoxymethylene (POM, or polyformaldehyde) was known at the time to be thermally unstable, thereby limiting interest in its study and industrial application.[9] Several pioneering efforts demonstrated that anionic polymerization of formaldehyde below its T_c followed by a post-polymerization esterification greatly enhanced the thermal stability of the polymer, culminating in a series of publications that for the first time characterized the polymer's physical, thermal, and mechanical properties (Scheme 1.3).[10] The enhanced thermal stability is a consequence of esterification of the chain-end hemiacetal, blocking the polymer from depolymerization at elevated temperatures.

Scheme 1.3 **|** *End-capping polyoxymethylene by esterification. R depends on polymerization initiator.*

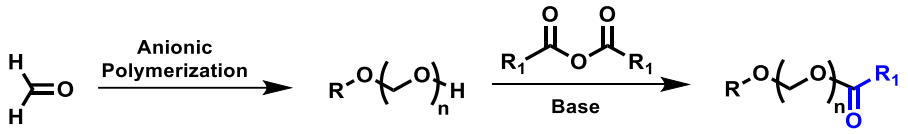

A later discovery introduced an alternative method to effectively stabilize depolymerizable polymers: copolymerization with small quantities of comonomers that do not depolymerize, thereby acting as "chain-stoppers" within the polymer chain.[9] Polymers formed in this way unzip until they reach a unit incapable of depropagation, subsequently stopping depolymerization and leaving the polymers end-capped. One example of such chain-stoppering approach is the cationic copolymerization of 1,3,5-trioxane—the cyclic trimer of formaldehyde—with epoxides (Scheme 1.4). The aldehyde units can unzip via their acetal linkages. However, the additional carbon spacer introduced by the epoxide halts depropagation so that the ehtyelene unit persists as a stable chain-end. A variety of other cyclic ethers and acetals have also been used as comonomers to stabilize polyaldehydes.[9] Although polymers prepared with this method cannot fully depolymerize from head-to-tail due to the blocking comonomers, they can be activated to depolymerize into smaller subunits by cleaving sites within the backbone to create new chain-ends.

Scheme 1.4 | *Copolymerization of trioxane with chain-stoppering ethylene oxide. R depends on initiator.*

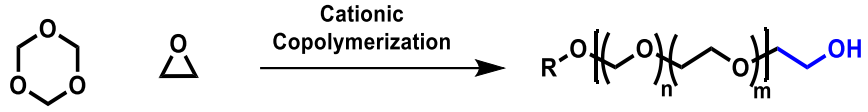

The discovery of these methods for end-capping ionic chain-growth polymerizations immediately stimulated a large outgrowth in the synthesis and study of a range of polyaldehydes.[11-12] Vogl and coworkers notably embarked on the preparation of a wide range of higher aliphatic polyaldehydes, demonstrating that these polymers could be stabilized by post-polymerization esterification as well (Table 1.1).[11] Later, the first aromatic polyaldehydes were discovered by the Aso group in the low-temperature cyclopolymerization of *o*-phthalaldehyde and related monomers (Scheme 1.5, Table 1.1).[12] Advantages of aromatic polyaldehydes include enhanced monomer stability relative to aliphatic counterparts, and improved polymer solubility due to their atactic nature, unlike the highly crystalline aliphatic polyaldehydes.[6, 11-12]

Table 1.1 | *Aldehyde monomers and associated ceiling temperatures.*[6]

Aldehyde	T_c *(°C)*
CH_2O	119
CH_3CHO	-39
$CH_3(CH_2)_2CHO$	-18
$CH_3OCOCHO$	26
$CH_3CH_2OCOCHO$	35
CF_3CHO	85
CCl_3CHO	17
CBr_3CHO	-75
CFClBrCHO	41
o-phthalaldehyde	-43

Scheme 1.5 | *Cyclopolymerization and stabilization of* o*-phthalaldehyde.*[12b]

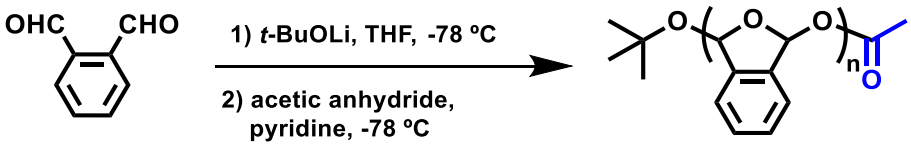

More recently, depolymerizable polymers prepared by step-growth polymerizations have emerged in the literature.[5,7] The first such linear polymer, termed a "self-immolative polymer," was reported in 2008, and many other classes of similar polymers based on quinone-methide backbones have since been reported.[7,13] Synthesis of these materials is accomplished with AB-type monomers containing a blocked

reactive unit. Polymerization ensues on activation of blocked functional groups, for example by catalytic activation of blocked isocyanates or deprotection of amines, to form linear polyurethanes and polycarbonates.[13] These polymers depolymerize via a mechanism unique from low T_c polymers, expelling gaseous byproducts to drive the depolymerization process forward (discussed in section 1.4). However, preventing these polymers from unwanted head-to-tail depolymerization again relies on adding a reagent to end-cap the reactive polymer chains. In this case, a monofunctional reactive species, which is added near the end of the polymerization, is employed to serve as a chain-end and stabilizing group (Scheme 1.6).

Scheme 1.6 | *Polymerization and stabilization of self-immolative polymers.*[13a]

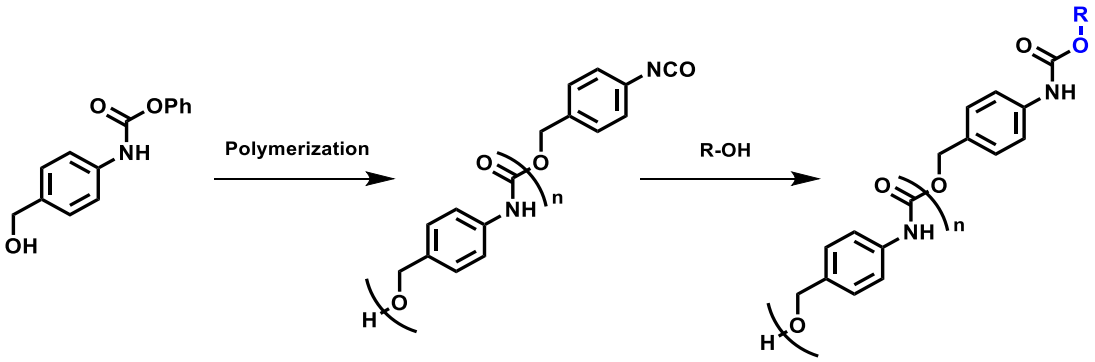

1.4 Recent Advances in Triggered Depolymerization

Depolymerizable polymers have witnessed a resurgence in the literature over the past decade due to their capacity to undergo triggered depolymerization.[5] There are numerous applications of triggered depolymerization, which will be discussed in the ensuing section. Regardless of polymer type, triggered depolymerization relies on a physical or chemical stimulus that reacts with either the polymer end-caps to expose chain-ends, or the polymer backbone to create new chain-ends capable of unzipping.

The first example of triggered head-to-tail depolymerization in linear polymers was reported by Shabat and coworkers in 2008. They employed self-immolative polymers for this purpose, which were derived from self-immolative dendrimers previously prepared by the same group.[7, 13a] They demonstrated that, in order to enact triggered depolymerization, it was necessary to end-cap the polymers with a stimulus-responsive functionality rather than the conventional, inert blocking group. When the responsive cap is removed, head-to-tail depolymerization is initiated and driven to completion by expulsion of CO_2 (Scheme 1.7). Specifically, they employed 4-hydroxy-2-butanone as a trigger, which is removed by enzymatic cleavage, subsequently activating the depolymerization cascade. Later examples expanded the triggering modes to groups that respond to acid, base, UV light, near-IR light, heat, and redox reagents.[13c-g]

Scheme 1.7 | *Triggered depolymerization of self-immolative polymers.*[13a]

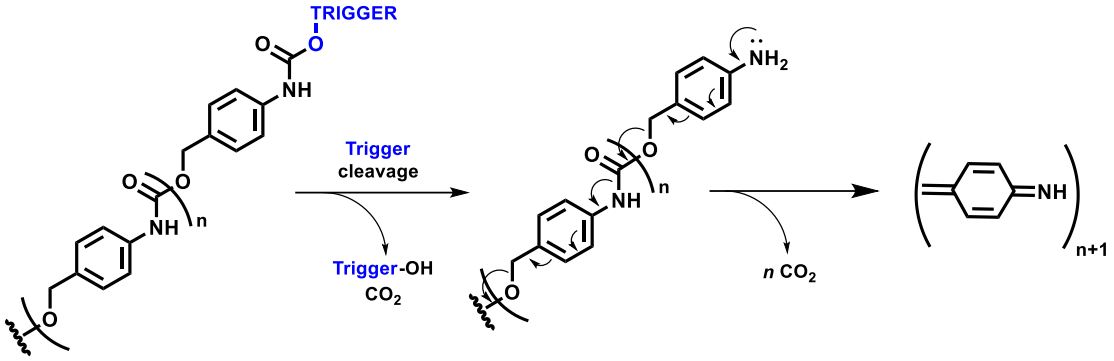

The Gillies group successfully expanded the scope of linear self-immolative polymers and modulated the rates of their depolymerization by designing analogs with cyclizing spacers and alternative main-chain atoms.[13f-i] They demonstrated that by using a cyclizable thiol spacer with a polycarbonate backbone, depolymerization rates could be amplified by several orders of magnitude (Scheme 1.8).[13h] They further prepared small, monodisperse self-immolative polymers by stepwise synthesis to conclusively demonstrate that, as expected, the rate of depolymerization is directly related to the chain-length for this class of polymer.[13i]

Scheme 1.8 | *Triggered depolymerization with enhanced rates by alternating cyclization-elimination.*[13h]

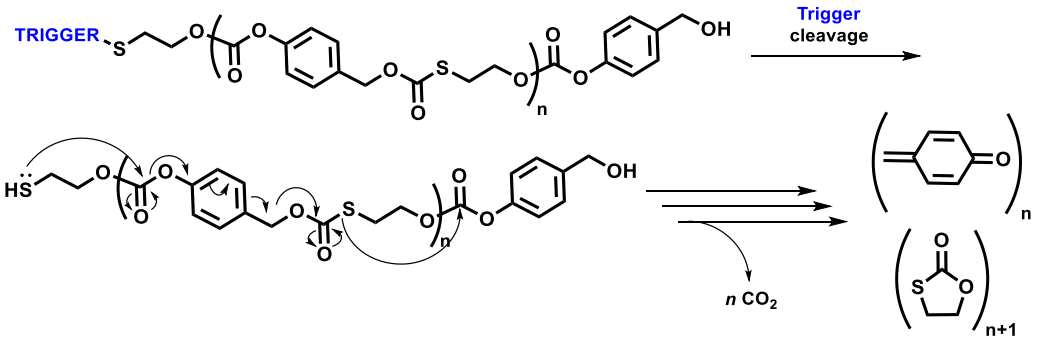

An analogous class of polymers, the "chain-shattering" polymers, also undergoes triggered depolymerization by a similar quinone-methide elimination mechanism. However, rather than head-to-tail depolymerization proceeding from chain-ends, these polymers cleave and depolymerize from alternating sites within their backbone (Scheme 1.9).[14] Compared to self-immolative polymers capable of head-to-tail depolymerization, functionalizing the polymer backbone with multiple triggering sites enhances rates of depolymerization.[14a] Further, preparation of chain-shattering polymers by step-growth copolymerization between activated, bifunctional quinone-methide moieties and bifunctional comonomers enables integration of a wide variety of functional motifs into polymer chains.[14f] In fact, the Cheng group

demonstrated that copolymerization with a reactive therapeutic allows for direct insertion of target drugs into polymer backbones for on-demand release.[14g] One could further envision the incorporation of multiple unique, stimuli-responsive triggers to afford chain-shattering polymers responsive to multiple stimuli.

***Scheme 1.9** | Triggered depolymerization of chain-shattering polymers.[14f]*

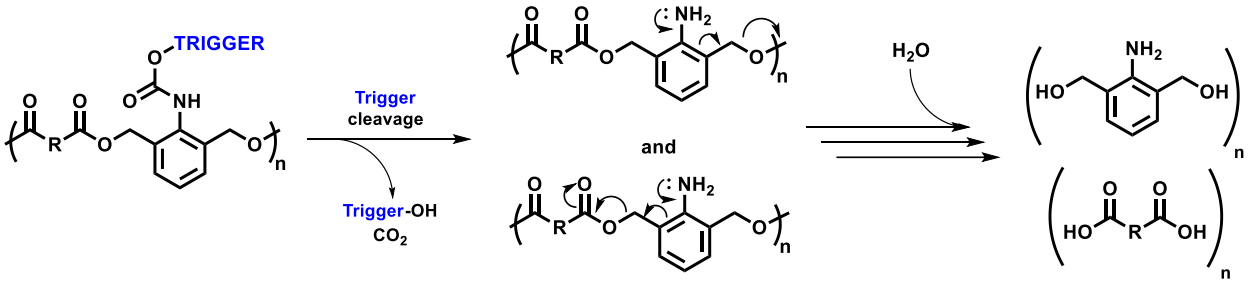

Triggered depolymerization from head-to-tail was first demonstrated for low T_c polyaldehydes in 2010.[15a] It was already known that acid exposure was a viable route to achieve polyaldehyde depolymerization by random chain-scission along the acetal backbone.[16] However, triggering stimuli were limited to acidic reagents capable of backbone cleavage. Taking inspiration from the self-immolative polymer literature, researchers demonstrated that end-capping poly(phthalaldehyde) with a responsive functionality enabled triggered depolymerization (Scheme 1.10). They employed protective groups sensitive to palladium sources or fluoride ions, and showed that complete depolymerization to monomer is nearly instantaneous upon exposure to the chemical stimulants. In this case, unzipping at room temperature is not driven by expulsion of gaseous byproducts, but rather results from the extremely low T_c of the polyaldehyde (-43 °C). Using available thermodynamic data,[12a] it can be estimated that the equilibrium monomer concentration for this polymer at room temperature is 14 mol/L (at 25 °C), so depolymerization continues until reaching this condition, which is unachievable in practice.

***Scheme 1.10** | Triggered depolymerization of poly(phthalaldehyde).[15a]*

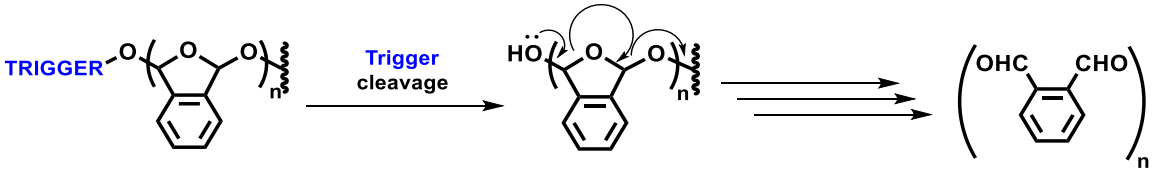

Triggered depolymerization of low T_c polyaldehydes, specifically poly(phthalaldehyde), has many advantages compared to self-immolative polymers, which has made this class of polymers a system of choice for continued research over several decades. High molecular weight poly(phthalaldehyde) can be readily prepared and end-capped with a variety of stimuli-responsive triggers from commercially available reagents.[13b-c] Further, it is possible to functionalize related polymers by post-polymerization modification in order to achieve cross-linking or tailor the polymer with specific moieties.[13d-e] Most importantly, the

depolymerization process is nearly instantaneous on exposure to acid, heat, or triggering reagents. As a result, polyaldehydes have found widespread use in a variety of applications.[5]

1.5 Applications of Depolymerizable, Low T_c Polyaldehydes

1.5.1 Lithographic Materials

One of the earliest applications of depolymerizable polymers was for lithographic purposes. In the 1980s, researchers at IBM began to explore the use of low T_c polyaldehydes as photoresist materials for lithography.[16] Poly(phthalaldehyde) was chosen for research due to its ease of preparation and solubility in common organic solvents. When combined with photoacid generators, exposure of poly(phthalaldehyde) films to light triggers acid-catalyzed depolymerization, permitting fabrication of patterned films. Depolymerization was found to be a particularly effective mechanism in lithography because of the drastic and rapid physical changes between polymer and monomer that occur on exposure.[16a-d] More recently, IBM has shown probe-based nanolithography to be a useful tool for patterning poly(phthalaldehyde) by thermal depolymerization. A heated scanning probe is used to stimulate depolymerization and evaporation of the resultant monomer, permitting rapid patterning with high resolution. Remarkable 2-D and 3-D architectures were fabricated with unprecedented resolution (Figure 1.1).[16e-f]

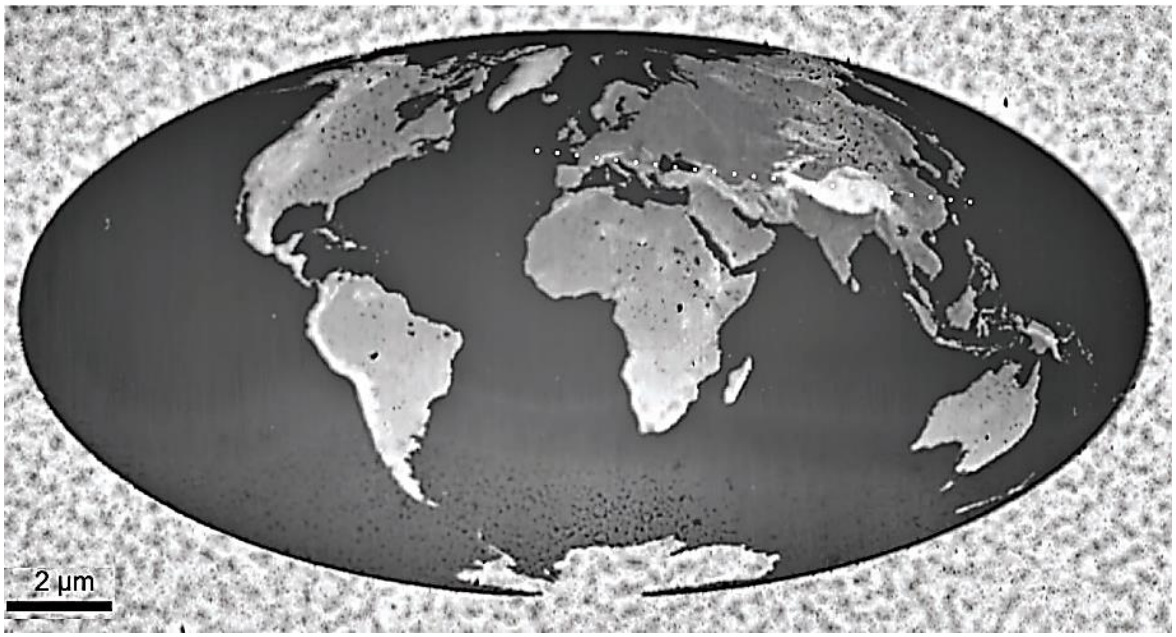

***Figure 1.1** | AFM topographic image of a 3D world map written into a poly(phthalaldehyde) layer by thermally induced depolymerization via probe-based nanolithography (Reproduced with permission from Reference 16f. Copyright 2010 John Wiley and Sons).*

1.5.2 Triggered Release

Perhaps the most ubiquitous application of depolymerizable polymers is their use in triggered release.[5-7, 17] Several methods to achieve triggered release are possible and have been reported with depolymerizable polymers. The monomer itself may serve as the compound of interest or disassemble further to release a compound of interest; alternatively, the depolymerizable material may serve as a structural container that releases sequestered active agents on triggered destruction. Triggered release itself can be categorized further, as liberated compounds may serve as reporter molecules for signal-amplified sensing, fluorescent probes, active drug components for drug delivery, healing agents in autonomic self-healing, or they may serve many other functions.[5-7, 17] The focus herein will be given to reports of depolymerizable polyaldehydes used in triggered release.

Two different low T_c polyaldehydes have been reported thus far for application in triggered release: poly(phthalaldehyde) and poly(glyoxylate)s.[17c-d] In either case, the polyaldehyde serves as a structural container for sequestered active compounds (Figure 1.2). Phillips and coworkers demonstrated that core-shell microcapsules could be fabricated with poly(phthalaldehyde) shell walls. Encapsulated actives are successfully released upon triggering shell wall depolymerization by subjecting capsules to chemical reagents that cleave polymer end-groups.[17c] Gillies and coworkers later reported the preparation of micellar nanoparticles with amphiphilic poly(ethyl glyoxylate)-poly(ethylene glycol) block copolymers. Triggered release was achieved via photolysis of poly(glyoxylate) end-groups to induce depolymerization and initiate nanoparticle decomposition, thereby liberating core contents.[17d]

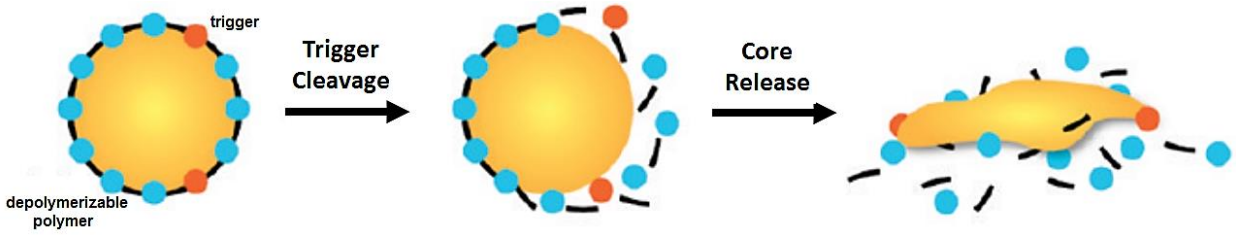

***Figure 1.2** | Schematic of triggered release: core-shell containers are disassembled by triggering shell wall depolymerization to release sequestered actives (Reproduced with permission from Reference 17b. Copyright 2011 American Chemical Society).*

Unlike self-immolative polymers, generating active or reporter molecules directly from depolymerized polyaldehydes has not yet been reported.[7] One could envision that future systems will take advantage of the inherently amplified response in depolymerizable polyaldehydes by incorporating a monomer designed for a targeted purpose like drug delivery or sensing. Alternatively, monomers could undergo further disassembly to autonomically produce an active agent, as has been reported for "self-immolative comb polymers."[13b]

1.5.3 Adaptive Structural Materials

One remarkable feature of depolymerizable polymers is their capacity to serve as dynamic structural materials. By selectively triggering their depolymerization, structural materials can be designed to erode at specified times to permit recycling, patterning, regeneration, or other relevant shape-shifting transformations. Phillips and coworkers capitalized on this application by fabricating a patterned plastic block composed of poly(phthalaldehyde) with two distinct and responsive end-groups. Exposure to one triggering condition selectively etched the corresponding polymers, thereby disintegrating portions of the plastic to reveal predesigned patterns while leaving the remainder polymer intact.[13a]

Researchers later extended the concept of adaptive polyaldehyde materials by demonstrating a reversible cycle of depolymerization followed by repolymerization, mimicking regenerative biomaterials such as bone (Figure 1.3).[18] It was found that depolymerization of poly(phthalaldehyde) could be mechanically activated by ultrasonication, which cleaves polymer chains that subsequently unzip to monomer. Incredibly, the monomer thus generated was directly repolymerized to poly(phthalaldehyde), albeit by first cooling below its T_c and adding initiator. This finding highlights the potential for poly(phthalaldehyde) to serve as a recyclable or regenerative synthetic material. While these studies served merely as preliminary proof-of-concept demonstrations, they emphasize the potential importance of adaptive, dynamic structural materials in future material designs.

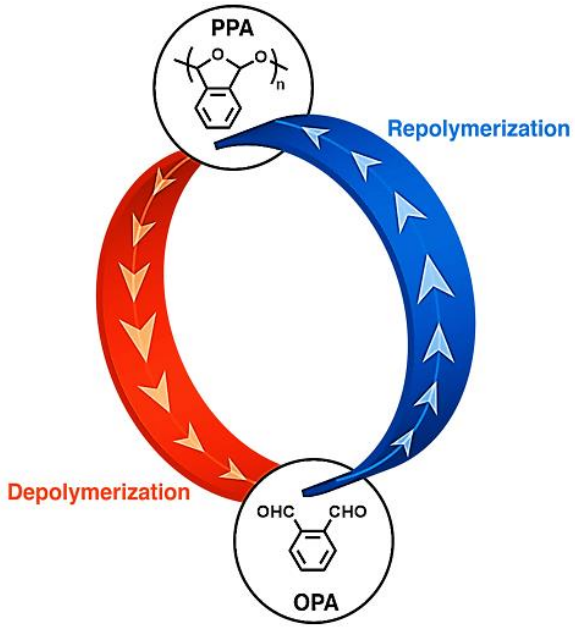

Figure 1.3 *| Adaptive polyaldehyde material exhibiting reversible cycle of depolymerization and orthogonal repolymerization. Poly(phthalaldehyde) was mechanically depolymerized by exposure to high-intensity ultrasonication, and resulting monomer (*o*-phthalaldehyde) repolymerized by anionic polymerization.*[18a]

1.5.4 Transient Substrate and Template Materials

A final key application of depolymerizable polyaldehyde materials has been their use as temporary substrate or template materials. While most prior polymer research has focused on preparing permanent, mechanically and thermally robust structures, there is a growing interest in depolymerizable substrates that could serve as temporary barrier materials, transient substrate materials, or other adaptive structures. In one example, triggered depolymerization of poly(phthalaldehyde) films was employed to activate a microfluidic pumping system on command.[19a] It was shown that modification of end-group polarity in polyaldehyde films, such that chain-end triggers are exposed to interfaces rather than buried within polymer layers, was a productive means to enhance solid-state depolymerization capabilities in the microscale pumps. Toward depolymerizable packaging, it was shown that in conjunction with photoacid generators, light-sensitive poly(phthalaldehyde) films could be fabricated and employed as substrate materials for transient electronics.[19b] When suitably irradiated, film depolymerization induces loss of mechanical integrity and concomitant electronic device destruction (Figure 1.4). One could envision expanding this concept to a range of other applications where triggered destruction is desirable.

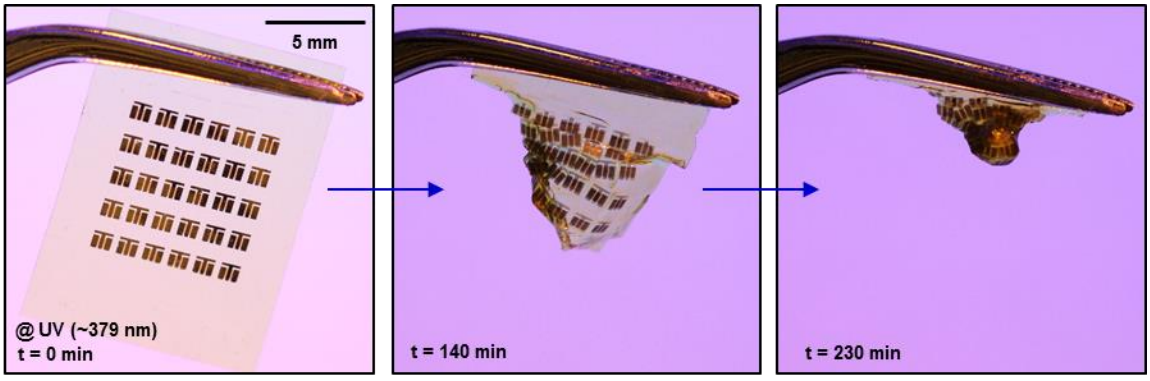

***Figure 1.4** | Triggered depolymerization of poly(phthalaldehyde) films for transient electronics. Films are embedded with photoacid generators such that UV irradiation initiates acid-catalyzed depolymerization of substrate and electronic destruction (Reproduced with permission from Reference 19b. Copyright 2014 John Wiley and Sons).*

In analogous efforts, depolymerizable polyaldehydes have been utilized as removable templating materials to drive nanostructure formation. Patterned poly(phthalaldehyde) films were shown to be effective, removable scaffolds for directed gold nanoparticle assembly.[20a] Likewise, poly(phthalaldehyde)-polystyrene block copolymers were shown to self-assemble under suitable conditions, and subsequent acid treatment depolymerized and etched away the poly(phthalaldehyde) blocks, leaving behind porous nanochannels.[20b] With the growing importance of nanostructured and nanoporous materials, there is a clear opportunity for additional utilization of depolymerizable polymers as sacrificial templating scaffolds.

1.6 Current Status and Future Directions

A great deal of research effort has been invested into the field of depolymerizable polymers. While many different depolymerizable polymer scaffolds have been prepared and studied, there is still demand for novel and versatile materials. For one, new materials are needed that are more robust toward environmental conditions; polyaldehydes are exceedingly sensitive to acidic conditions, while self-immolative polymers are known to undergo unwanted side reactions with nucleophiles.[5] There is undoubtedly a great challenge in the preparation of materials that can be triggered to fall apart on command, yet are stable to any orthogonal conditions. The Phillips group has begun exploring new materials to address this need and has pioneered a class of poly(benzyl ether)s that depolymerize on triggering but are stable to both acid and base.[21] The window for achieving these contrasting properties in synthetic polymers is exceedingly small, leaving a high demand for similar types of robust yet depolymerizable structures.

Opportunities also exist in the rational design of aldehyde monomers with programmed function. As detailed in the preceding section, the development of polyaldehyde materials where the generated monomer performs a function could be exploited, as in the case for self-immolative polymers. Likewise, small molecules released by further disassembly of aldehyde monomers would be an effective means to add functionality to depolymerizable polyaldehydes.

In the context of biomaterials and drug delivery, there is an increasing demand for biocompatible materials and triggers sensitive to biologically relevant small molecules, receptors, and enzymes. New triggers will need to be developed and evaluated in terms of their capability to initiate stimulus-responsive depolymerization in complex biological environments. Furthermore, it is crucial to expand the availability and scope of biocompatible polyaldehyde materials. While poly(phthalaldehyde) depolymerizes to the toxic *o*-phthalaldehyde monomer, the poly(glyoxylate) family represents a biocompatible class of depolymerizable polyaldehydes that merits further exploration for biological applications.[17d, 22]

Finally, with further refinement in the preparation of depolymerizable polymers, the materials will undoubtedly find expanded use in diverse, and perhaps unexpected, applications. The use of sacrificial templates for the fabrication of nanoporous materials or other relevant degradable composites, and the use of these polymers for transient or other adaptive structures will almost surely continue. One might additionally expect new depolymerizable materials to be developed specifically to address the rising challenge of finding green, recyclable materials that minimally impact the environment. Depolymerizable polymers, notably those prepared from renewable resources, would represent an ideal way to achieve materials capable of recycling on command. Beyond that, could these reversible materials be used for energy storage and delivery? It remains to be seen how this field will grow and into which areas it will

expand, but the prospects certainly look bright that the coming years will witness major progress in this dynamic field.

1.7 References

(1) (a) Snow, R. D.; Frey, F. E. *J. Am. Chem. Soc.* **1943**, 65, 2417-2418. (b) Dainton, F. S.; Ivin, K. J. *Nature* **1948**, 162, 705-707.

(2) (a) Dainton, F. S.; Ivin, K. J. *Proc. R. Soc. Lond. A* **1952**, 212, 207-220. (b) Cook, R. E.; Dainton, F. S.; Ivin, K. J. *J. Polym. Sci.* **1957**, 26, 351-364. (c) Cook, R. E.; Dainton, F. S.; Ivin, K. J. *J. Polym. Sci.* **1958**, 29, 549-556.

(3) (a) Dainton, F. S.; Ivin, K. J. *Q. Rev. Chem. Soc.* **1958**, 12, 61-92. (b) Ivin, K. J. *Angew. Chem. Int. Ed.* **1973**, 12, 487-494. (c) Ivin, K. J. *J. Polym. Sci., Part A: Polym. Chem.* **2000**, 38, 2137-2146.

(4) (a) Sawada, H. *J. Macromol. Sci., Part C: Polym. Rev.* **1969**, 3, 313-338. (b) Sawada, H. *J. Macromol. Sci., Part C: Polym. Rev.* **1972**, 8, 235-288.

(5) (a) Peterson, G. I.; Larsen, M. B.; Boydston, A. J. *Macromolecules* **2012**, 45, 7317-7328. (b) Phillips, S. T.; DiLauro, A. M. *ACS Macro Lett.* **2014**, 3, 298-304. (c) Phillips, S. T.; Robbins, J. S.; DiLauro, A. M.; Olah, M. G. *J. Appl. Polym. Sci.* **2014**, 131, 40992-41003.

(6) (a) Vogl, O. *J. Polym. Sci., Part A: Polym. Chem.* **2000**, 38, 2293-2299. (b) Kostler, S. *Polym. Int.* **2012**, 61, 1221-1227. (c) Kubisa, P.; Neeld, K.; Starr, J.; Vogl, O. *Polymer* **1980**, 21, 1433-1447. (d) Vogl, O. *J. Macromol. Sci., Part C: Polym. Rev.* **1975**, 12, 109-164.

(7) (a) Gnaim, S.; Shabat, D. *Acc. Chem. Res.* **2014**, 47, 2970-2984. (b) Avital-Scmilovici, M.; Shabat, D. *Soft Matter* **2010**, 6, 1073-1080. (c) Wong, A. D.; DeWit, M. A.; Gillies, E. R. *Adv. Drug Delivery Rev.* **2012**, 64, 1031-1045.

(8) Odian, G. *Principles of Polymerization*, 4th ed.; Wiley-Interscience: New York, 2004; pp 204-206.

(9) (a) Brown, N. *J. Macromol. Sci., Part A: Pure Appl. Chem.* **1967**, 1, 209-230. (b) Masamoto, J. *Prog. Polym. Sci.* **1993**, 18, 1-84.

(10) (a) Schweitzer, C. E.; MacDonald, R. N.; Punderson, J. O. *J. Appl. Polym. Sci.* **1959**, 1, 158-163. (b) Koch, T. A.; Lindvig, P. E. *J. Appl. Polym. Sci.* **1959**, 1, 164-168. (c) Hammer, C. F.; Koch, T. A.; Whitney, J. F. *J. Appl. Polym. Sci.* **1959**, 1, 169-178. (d) Linton, W. H.; Goodman, H. H. *J. Appl. Polym. Sci.* **1959**, 1, 179-184. (e) Alsup, R. G.; Punderson, J. O.; Leverett, G. F. *J. Appl. Polym. Sci.* **1959**, 1, 185-191.

(11) (a) Vogl, O. *J. Polym. Sci.* **1960**, 46, 261-264. (b) Furukawa, Saegusa, T.; Fujii, H. *Die Makromol. Chem.* **1960**, 44, 398-407. (c) Vogl, O. *J. Polym. Sci., Part A: Polym. Chem.* **1964**, 2, 4591-4606. (d) Vogl, O. *J. Polym. Sci., Part A: Polym. Chem.* **1964**, 2, 4607-4620. (e) Vogl, O. *J. Polym. Sci.,*

Part A: Polym. Chem. **1964**, 2, 4621-4631. (f) Vogl, O.; Bryant, W. M. D. *J. Polym. Sci., Part A: Polym. Chem.* **1964**, 2, 4633-4645. (g) Brame, Jr., E. G.; Sudol, R. S.; Vogl, O. *J. Polym. Sci., Part A: Polym. Chem.* **1964**, 2, 5337-5346. (h) Mark, H. F.; Ogata, N. *J. Polym. Sci., Part A: Polym. Chem.* **1963**, 1, 3439-3447.

(12) (a) Chuji, A.; Tagami, S.; Kunitake, T. *J. Polym. Sci. Part A: Polym. Chem.* **1969**, 7, 497-511. (b) Chuji, A.; Tagami, S. *Macromolecules* **1969**, 2, 414-419. (c) Aso, C. *Pure Appl. Chem.* **1970**, 23, 287-304. (d) Tagami, S.; Kagiyama, T.; Aso, C. *Polym. J.* **1971**, 2, 101-108.

(13) (a) Sagi, A.; Weinstain, R.; Karton, N.; Shabat, D. *J. Am. Chem. Soc.* **2008**, 130, 5434-5435. (b) Weinstain, R.; Sagi, A.; Karton, N.; Shabat, D. *Chem. Eur. J.* **2008**, 14, 6857-6861. (c) Esser-Kahn, A. P.; Sottos, N. R.; White, S. R.; Moore, J. S. *J. Am. Chem. Soc.* **2010**, 132, 10266-10268. (d) Lux, C. D. G.; McFearin, C. L.; Joshi-Barr, S.; Sankaranarayanan, J.; Fomina, N.; Almutairi, A. *ACS Macro Lett.* **2012**, 1, 922-926. (e) Peterson, G. I.; Church, D. C.; Yakelis, N. A.; Boydston, A. J. *Polymer* **2014**, 55, 5980-5985. (f) DeWit, M. A.; Gillies, E. R. *J. Am. Chem. Soc.* **2009**, 131, 18327-18334. (g) DeWit, M. A.; Beaton, A.; Gillies, E. R. *J. Polym. Sci., Part A: Polym. Chem.* **2010**, 48, 3977-3985. (h) Chen, E. K. Y.; McBride, R. A.; Gillies, E. R. *Macromolecules* **2012**, 45, 7364-7374. (i) McBride, R. A.; Gillies, E. R. *Macromolecules* **2013**, 46, 5157-5166. (j) Wong, A. D.; Gungor, T. M.; Gillies, E. R. *ACS Macro Lett.* **2014**, 3, 1191-1195. (k) DeWit, M. A.; Nazemi, A.; Karamdoust, S.; Beaton, A.; Gillies, E. R. *ACS Symposium Series* **2011**, 1066, 9-21. (l) Robbins, J. S.; Schmid, K. M.; Phillips, S. T. *J. Org. Chem.* **2013**, 78, 3159-3169. (m) Lewis, G. G.; Robbins, J. S.; Phillips, S. T. *Macromolecules* **2013**, 46, 5177-5183. (n) Baker, M. S.; Yadav, V.; Sen, A.; Phillips, S. T. *Angew. Chem. Int. Ed.* **2013**, 52, 10295-10299. (o) Liu, G.; Wang, X.; Hu, J.; Zhang, G.; Liu, S. *J. Am. Chem. Soc.* **2014**, 136, 7492-7497.

(14) (a) Fomina, N.; McFearin, C. L.; Sermsakdi, M.; Edigin, O.; Almutairi, A. *J. Am. Chem. Soc.* **2010**, 132, 9540-9542. (b) Fomina, N.; McFearin, C. L.; Sermsakdi, M.; Morachis, J. M.; Almutairi, A. *Macromolecules* **2011**, 44, 8590-8597. (c) Lux, C. D. G.; Joshi-Barr, S.; Nguyen, T.; Mahmoud, E.; Schopf, E.; Fomina, N.; Almutairi, A. *J. Am. Chem. Soc.* **2012**, 134, 15758-15764. (d) Lux, C. D. G.; Almutairi, A. *ACS Macro Lett.* **2013**, 2, 432-435. (e) Olejniczak, J.; Sankaranarayanan, J.; Viger, M. L.; Almutairi, A. *ACS Macro Lett.* **2013**, 2, 683-687. (f) Zhang, Y.; Ma, L.; Deng, X.; Cheng, J. *Polym. Chem.* **2013**, 4, 224-228. (g) Zhang, Y.; Yin, Q.; Yin, L.; Ma, L.; Tang, L.; Cheng, J. *Angew. Chem. Int. Ed.* **2013**, 52, 6435-6439.

(15) (a) Seo, W.; Phillips, S. T. *J. Am. Chem. Soc.* **2010**, 132, 9234-9235. (b) Dilauro, A. M.; Robbins, J. S.; Phillips, S. T. *Macromolecules* **2013**, 46, 2963-2968. (c) Winter, J. D.; Dove, A. P.; Knoll, A.; Gerbaux, P.; Dubois, P.; Coulembier, O. *Polym. Chem.* **2014**, 5, 706-711. (d) Kaitz, J. A.; Moore, J. S. *Macromolecules* **2013**, 46, 608-612. (e) Kaitz, J. A.; Possanza, C. M.; Song, Y.;

Diesendruck, C. E.; Spiering, A. J. H.; Meijer, E. W.; Moore, J. S. *Polym. Chem.* **2014**, 5, 3788-3794.

(16) (a) Ito, H.; Willson, C. G. *Polym. Eng. Sci.* **1983**, 23, 1012-1018. (b) Willson, C. G.; Ito, H.; Frechet, J. M. J.; Tessier, T. G.; Houlihan, F. M. *J. Electrochem. Soc.* **1986**, 133, 181-187. (c) Ito, H.; Schwalm, R. *J. Electrochem. Soc.* **1989**, 136, 241-245. (d) Ito, H.; Ueda, M.; Renaldo, A. F. *J. Electrochem. Soc.* **1989**, 136, 245-249. (e) Coulembier, O.; Knoll, A.; Pires, D.; Gotsmann, B.; Duerig, U.; Frommer, J.; Miller, R. D.; Dubois, P.; Hedrick, J. L. *Macromolecules* **2010**, 43, 572-574. (f) Knoll, A. W.; Pires, D.; Coulembier, O.; Dubois, P.; Hedrick, J. L.; Frommer, J.; Duerig, U. *Adv. Mater.* **2010**, 22, 3361-3365.

(17) (a) Blencowe, C. A.; Russell, A. T.; Gerco, F.; Hayes, W.; Thornthwaite, D. W. *Polym. Chem.* **2011**, 2, 773-790. (b) Esser-Kahn, A. P.; Odom, S. A.; Sottos, N. R.; White, S. R.; Moore, J. S. *Macromolecules* **2011**, 44, 5539-5553. (c) Dilauro, A. M.; Abbaspourrad, A.; Weitz, D. A.; Phillips, S. T. *Macromolecules* **2013,** 46, 3309-3313. (d) Fan, B.; Trant, J. F.; Wong, A. D.; Gillies, E. R. *J. Am. Chem. Soc.* **2014**, 136, 10116-10123.

(18) (a) Diesendruck, C. E.; Peterson, G. I.; Kulik, H. J. Kaitz, J. A.; Mar, B. D.; May, P. A.; White, S. R.; Martinez, T. J.; Boydston, A. J.; Moore, J. S. *Nat. Chem.* **2014**, 6, 623-628. (b) Peterson, G. I.; Boydston, A. J. *Macromol. Rapid. Commun.* **2014**, 35, 1611-1614.

(19) (a) DiLauro, A. M.; Zhang, H.; Baker, M. S.; Wong, F.; Sen, A.; Phillips, S. T. *Macromolecules*, **2013**, 46, 7257-7265. (b) Hernandez, H. L.; Kang, S. -K.; Lee, O. P.; Hwang, S. -W.; Kaitz, J. A.; Inci, B.; Park, C. W.; Chung, S.; Sottos, N. R.; Moore, J. S.; Rogers, J. A.; White, S. R. *Adv. Mater.* **2014**, 26, 7637-7642. (c) Kaitz, J. A.; Moore, J. S. *Macromolecules* **2014**, 47, 5509-5513.

(20) (a) Holzner, F.; Kuemin, C.; Paul, P.; Hedrick, J. L.; Wolf, H.; Spencer, N. D.; Duerig, U.; Knoll, A. W. *Nano Lett.* **2011**, 11, 3957-3962. (b) Vogt, A. P.; Winter, J. D.; Krolla-Sidenstein, P.; Geckle, U.; Coulembier, O.; Barner-Kowollik, C. *J. Mater. Chem. B* **2014**, 2, 3578-3581.

(21) Olah, M. G.; Robbins, J. S.; Baker, M. S.; Phillips, S. T. *Macromolecules* **2013**, 46, 5924-5928.

(22) (a) Vairon, J. P.; Muller, E.; Bunel, C. *Macromol. Symp.* **1994**, 85, 307-312. (b) Brachais, C. H.; Huguet, J.; Bunel C. *Polymer* **1997**, 38, 4959-4964. (c) Brachais, C. H.; Duclos, R.; Vaugelade, C.; Huguet, J.; Capelle-Hue, M. -L.; Bunel, C. *Int. J. Pharm.* **1998**, 169, 23-31. (d) Burel, F.; Rossignol, L.; Pontvianne, P.; Hartman, J.; Couesnon, N.; Bunel, C. *e-Polymers* **2003**, 3, 407-411. (e) Belloncle, B.; Burel, F.; Oulyadi, H.; Bunel, C. *Polym. Degr. Stab.* **2008**, 93, 1151-1157. (f) Kaitz, J. A.; Diesendruck, C. E.; Moore, J. S. *Macromolecules* **2014**, 47, 3603-3607.

Chapter 2: End Group Characterization of Poly(phthalaldehyde): Discovery of a Reversible, Cationic Macrocyclization Mechanism*

2.1 Abstract

End-capped poly(phthalaldehyde) (PPA) synthesized by anionic polymerization has garnered significant interest due to its ease of synthesis and rapid depolymerization. Yet, alternative ionic polymerizations to produce PPA have been largely unexplored. It was found that a cationic polymerization of *o*-phthalaldehyde initiated by boron trifluoride results in cyclic PPA in high yield, high molecular weight, and with extremely high cyclic purity. The cyclic structure is confirmed by NMR spectroscopy, MALDI-TOF mass spectrometry, and triple detection GPC. The cyclic polymers are reversibly opened and closed under the polymerization conditions. Owing to PPA's low ceiling temperature, cyclic PPA is capable of chain-extension to larger molecular weights, controlled depolymerization to smaller molecular weights, or dynamic intermixing with other polymer chains, both cyclics and end-capped linears. These unusual properties endow the system with great flexibility in the synthesis and isolation of pure cyclic polymers of high molecular weight. Further, it is speculated that the absence of end-groups enhances the stability of cyclic PPA and makes it an attractive candidate for lithographic applications.

2.2 Introduction

Poly(phthalaldehyde) (PPA) is a stimuli-responsive polymer that has garnered significant interest in recent years.[1-3] PPA has been shown to have a ceiling temperature around -40 °C,[4] i.e., at room temperature without a kinetically stabilizing end-cap, it spontaneously depolymerizes to monomer. Since its first syntheses in the 1960s, PPA has been widely used as an acid-sensitive, radiation-sensitive, or thermally sensitive degradable film for lithography.[5] Recently, Philips and coworkers demonstrated that end-capped PPA prepared via anionic polymerization is activated to depolymerize with specific triggering moieties that remove the end-cap.[2] Relative to other depolymerizable polymer classes, PPA benefits from its ease of synthesis[3] and rapid and complete depolymerization.

* Portions of this chapter have been published: Kaitz, J. A.; Diesendruck, C. E.; Moore, J. S. *J. Am. Chem. Soc.* **2013**, 135, 12755-12761.

Interestingly, the cationic polymerization of *o*-phthalaldehyde (*o*-PA) has been studied to a far lesser extent than its anionic counterpart.[4,6] PPA prepared with a boron trifluoride initiator is reportedly isolated without end-capping,[6] prompting the authors to speculate that chain entanglement at high molecular weights affords polymer stability above its ceiling temperature. A rigorous assessment of the end group structure of PPA prepared by cationic polymerization is lacking in the literature, and as a result, the polymer prepared by the cationic route has not found wide use in stimuli-responsive applications. We therefore initiated a rigorous study of PPA prepared under cationic conditions, with the intent to attain control over the final molecular weight of the chains, as well as to understand the end-capping of the polymers, with the aim to eventually use these polymers for stimuli-responsive applications.

2.3 Results and Discussion

2.3.1 Anionic and Cationic Polymerization of o-*Phthalaldehyde*

The polymerization of *o*-phthalaldehyde was conducted with both anionic and cationic initiators following reported procedures (See Tables 2.1 and 2.2).[1,3-4] The cationic polymerization is very fast, yielding PPA within minutes, while the anionic polymerization requires several hours to reach full conversion (see section 2.5 for full details). PPAs generated under cationic conditions have molecular weights ranging from M_n ca. 3 kDa to greater than ca. 100 kDa, with polydispersities ranging from ca. 1.5 to 4.5 (Table 2.1). The molecular weights of the cationic polymers do not conform to predictions based on monomer conversion and initial monomer-to-initiator ratios, a known issue with the cationic polymerization of *o*-phthalaldehyde which will be discussed in subsequent sections.[4,6] Consistent with prior observation, PPA was collected without quenching by addition of a neutralizing base (Entry 10).[6] Stable PPA was also isolated without a methanol washing step (Entry 11), suggesting that neither pyridine nor methanol are involved in end-capping the polymer chains. Instead, pyridine's role is to neutralize the Lewis acidic initiator, but this step is not essential to successfully isolate polymer. Polymerizations were also performed with alternative cationic initiators triethyloxonium tetrafluoroborate (Entry 14), tin (IV) chloride (Entry 15), and triphenylcarbenium tetrafluoroborate (Entry 16). Regardless of cationic initiator, PPA was produced with similar yields and molecular weights as with boron trifluoride initiation.

***Table 2.1 | Cationic polymerization reaction**: Polymer collected after precipitation into methanol and washing with methanol and diethyl ether.*

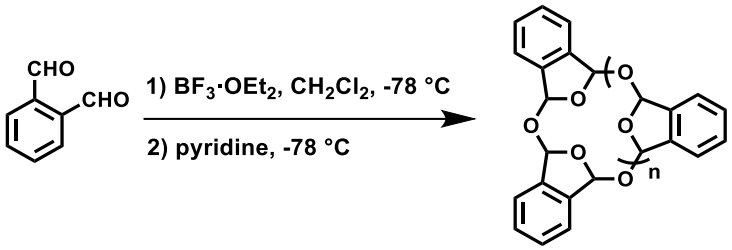

Entry	*[o-PA]*[a]	*$[M]_0/[I]_0$*	*Yield*	*M_n (kDa)*[b]	*M_p (kDa)*[b]	*PDI*[b]
1	1.0 M	10 / 1	86%	36.1	158	4.5
2	0.7 M	7 / 1	99%	109	199	2.5
3	0.7 M	11 / 1	73%	13.2	31.5	2.5
4	0.5 M	10 / 1	77%	6.7	10.1	2.4
5	0.1 M	10 / 1	48%	14.9	54.1	3.5
6	0.1 M	5 / 1	52%	7.9	9.1	1.7
7	0.4 M	5 / 1	60%	5.9	17.2	3.0
8[c]	0.1 M	1 / 2	17%	2.7	2.5	1.6
9[d]	0.2 M	10 / 1	63%	10.5	22.0	2.2
10[e]	0.7 M	6 / 1	76%	15.4	73.7	4.4
11[f]	0.7 M	8 / 1	99%	51.5	107	2.0
12[g]	0.2 M	6 / 1	68%	25.0	71.4	2.8
13	0.9 M	20 / 1	94%	104	218	2.3
14[h]	0.9 M	20 / 1	92%	88.6	158	2.2
15[i]	0.9 M	20 / 1	86%	89.4	181	2.3
16[j]	0.8 M	20 / 1	92%	26.2	57.2	2.3

[a]Monomer purified before use according to literature procedure.[1a] [b]Average molecular weights and polydispersity determined by gel permeation chromatography (GPC), calibrated with monodisperse polystyrene standards. [c]Polymer made by inverse addition of monomer to two equivalents initiator. Low yield attributed to low monomer concentration and use of excess initiator. [d]3-fluoropyridine substituted in place of pyridine. [e]No pyridine added. Polymer precipitated directly at -78 °C in diethyl ether and washed in diethyl ether and methanol. [f]Precipitation and washing conducted in hexanes and diethyl ether only. [g]Addition of 1-pyrene methanol following reaction and precipitation into diethyl ether. [h]Triethyloxonium tetrafluoroborate initiator. [i]Tin (IV) chloride initiator. [j]Triphenylcarbenium tetrafluoroborate initiator.

As a comparison, we also prepared PPA by an anionic polymerization of *o*-phthalaldehyde. In conjunction with an alcohol initiator, the phosphazene base P_2-t-Bu [1-tert-butyl-2,2,4,4,4-pentakis-(dimethylamino)-2Λ^5,4Λ^5-catenadi(phosphazene)] is a known potent catalyst for anionic *o*-phthalaldehyde polymerization.[1a, 3] The polymerization reaction is terminated by addition of an electrophile; both trichloroacetyl isocyanate and acetic anhydride effectively end-cap the polymer chains. The PPA chains generated under anionic conditions have molecular weights ranging from M_n ca. 4 kDa to ca. 20 kDa, with polydispersities ranging from ca. 2-3 (Table 2.2). The molecular weights obtained under anionic conditions

are lower than the theoretically calculated values from conversion and monomer-to-initiator ratios, but this was attributed to impurities in the monomer causing side reactions or providing additional initiation sites.[1a]

Table 2.2 | Anionic polymerization reaction*: Polymer collected by precipitation into methanol and washed in methanol and diethyl ether.*

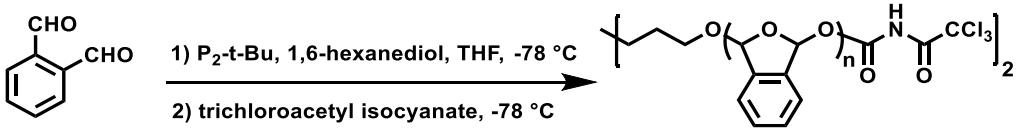

Entry	*[o-PA]*[a]	*$[M]_0/[I]_0/[P_2]_0$*[b]	*Yield*	*M_n (kDa)*[c]	*M_p (kDa)*[c]	*PDI*[c]
1	0.7	125/1/2	83%	4.4	5.4	1.8
2	0.7	250/ 1/2	92%	6.3	8.1	3.0
3	0.7	625/1/2	92%	9.0	11.5	2.1
4	0.7	2500/1/3	36%	16.1	26.5	2.7
5	0.7	5000/1/3	34%	20.4	40.9	2.0

[a]Monomer purified before use according to literature procedure.[1a] [b]Initial monomer-to-initiator-to catalyst ratio.[3] [c]Average molecular weights and polydispersity determined by gel permeation chromatography (GPC), calibrated with monodisperse polystyrene standards.

2.3.2 Spectroscopic Characterization of PPAs

PPAs prepared by cationic and anionic polymerization were examined by a combination of spectroscopic techniques, including nuclear magnetic resonance (NMR) spectroscopy and matrix-assisted laser desorption ionization time-of-flight (MALDI-TOF) mass spectrometry in an attempt to definitively identify the end groups produced by the different polymerization mechanisms.

End-groups are clearly observed by ^{1}H NMR in PPA prepared by anionic polymerization of *o*-phthalaldehyde. When trichloroacetyl isocyanate was used for end-capping, only the 1,6-hexanediol initiator is observed (Figure 2.1a); moreover, we have previously demonstrated the presence of various anhydride end-capping reagents in the *n*-BuLi initiated anionic polymerization of *o*-phthalaldehyde.[1b] On the other hand, end groups are not observed in the ^{1}H NMR of a PPA of similar molecular weight prepared by cationic polymerization when comparable signal to noise is attained (Figure 2.1b). Fluorinated end groups are also not detected by ^{19}F NMR on quenching a cationically initiated polymerization with 3-fluoropyridine (Table 2.1, Entry 9), and only trace solvent peaks are observed on addition of various nucleophilic end-capping reagents. Alternative cationic initiators also fail to show the presence of an end group. In an attempt to incorporate a chromophore end cap, 1-pyrene methanol was added to the polymerization reaction prior to precipitation (Table 2.1, Entry 12), but the UV detector on the GPC confirmed that pyrene was not incorporated into the polymer.[7]

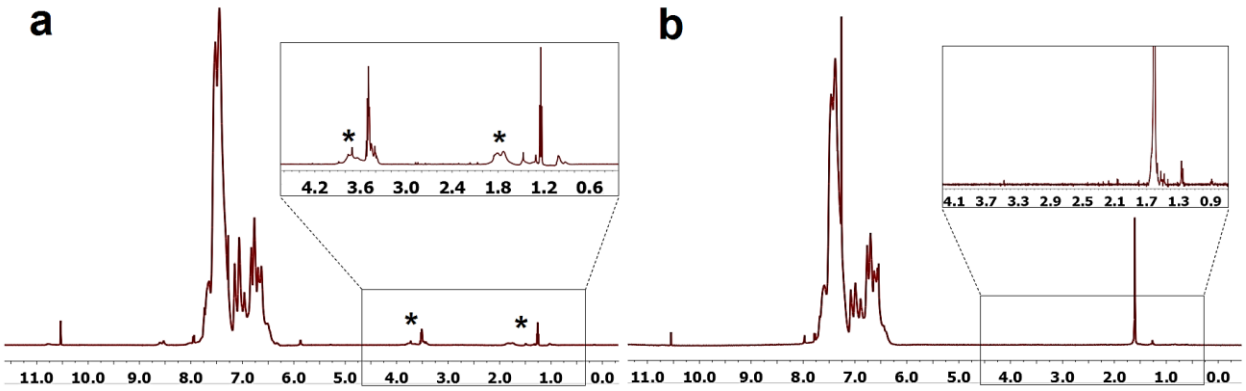

Figure 2.1 | ^{1}H NMR spectra of PPA prepared by anionic and cationic polymerization*: a) NMR spectra of M_n = 6.3 kDa PPA prepared by anionic polymerization (Table 2.2, Entry 2) in $CDCl_3$. Stars indicate peaks corresponding to 1,6-hexandiol initiator. Residual* o*-phthalaldehyde monomer is also observed. Inset region magnification of δ 0-5 ppm. b) NMR spectra of M_n = 5.9 kDa PPA prepared by cationic polymerization (Table 2.1, Entry 7) in $CDCl_3$. No end-groups are observed. Additional peaks correspond to water and residual* o*-phthalaldehyde monomer. Inset region magnification of δ 0-5 ppm.*

All analytical techniques failed to identify end groups in PPA samples polymerized by cationic initiation. Without end-caps, PPA is expected to rapidly depolymerize to monomer due to its known ceiling temperature of -40 °C.[4] This depolymerization reaction has been shown to occur rapidly and completely on end-cap removal by specific deprotecting reagents for PPA samples produced by anionic polymerization.[2] We therefore hypothesized that a cyclic polymer is the sole product of the boron trifluoride-initiated polymerization. We envisioned the possibility of a back-biting mechanism leading to cyclic poly(phthalaldehyde) (cPPA) in a process analogous to the zwitterionic ring-opening polymerization of lactides established by Waymouth.[8a-c] The Aso group has previously demonstrated the formation of small cyclic oligomers in the cationic polymerization *o*-formylphenylacetaldehyde by boron trifluoride.[9]

Cyclic polymers have interested chemists in recent decades due to the unique structural and physical properties imbued into the large macrocycles through the topological constraint of connected chain-ends.[10] Several synthetic strategies exist for the preparation of cyclic polymers including the use of solid supports,[11] the coupling of reactive chain-ends of linear precursors at high dilution,[12] and ring-expansion strategies utilizing cyclic initiators.[8,13-14] Ring-expansion strategies are advantageous in that they produce cyclic polymer in high purity and circumvent additional synthetic steps in high dilutions to generate cyclic macromolecules in high yields. However, the synthetic methods currently available are still limited by the inability to effectively separate residual linear contaminants.[10] The Waymouth and Zhang groups have recently demonstrated a zwitterionic ring-opening polymerization strategy toward the synthesis of

cyclic polyesters and polyamides.[8] Cyclic polymers were obtained in high yields with good control over molecular weight and polydispersity, and the cyclic structure was confirmed by several analytical methods.[8]

The proposed cyclic structure of PPA prepared by cationic polymerization was further elucidated by MALDI-TOF mass spectrometry and comparisons of the solution properties to analogs of similar molecular weight PPAs prepared by anionic polymerization. The MALDI-TOF mass spectrum clearly shows molecular ions for the sodium-complexed cPPA (Figure 2.2). The signals are spaced by 134 mass units and correspond perfectly to *o*-phthalaldehyde monomer units plus a sodium ion. A series of minor peaks separated by +18 mass units from the major peak series is also occasionally observed. This presumably corresponds to PPA with hemiacetal groups produced by hydrolysis on reacting with the acidic MALDI matrix (2,5-dihydroxybenzoic acid, DHB). Importantly, since uncapped linear PPA rapidly degrades to monomer, cPPA is solely obtained in high yield without residual linear contaminants, as confirmed by the presence of a single distribution of cyclic polymer species in the MALDI-TOF mass spectra (Figure 2.2).

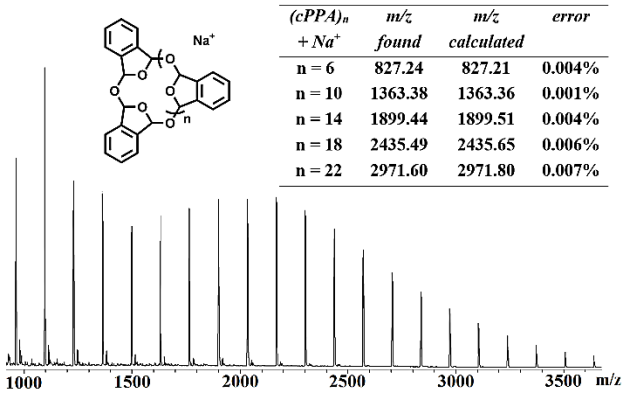

$(cPPA)_n + Na^+$	m/z found	m/z calculated	error
n = 6	827.24	827.21	0.004%
n = 10	1363.38	1363.36	0.001%
n = 14	1899.44	1899.51	0.004%
n = 18	2435.49	2435.65	0.006%
n = 22	2971.60	2971.80	0.007%

Figure 2.2 | MALDI-TOF mass spectrum of cPPA*: Peaks match sodium adduct of cyclic PPA. DHB (2,5-dihydroxybenzoic acid) was used as the matrix and sodium iodide as the cationization agent.*

2.3.3 Size-Molecular Weight Correlations by Triple Detection GPC

Additional evidence for the cyclic structure of the cationic PPA was provided by GPC coupled with refractometer, light-scattering detector and viscometer. PPAs of comparable molecular weight distributions were synthesized by cationic and anionic polymerizations and analyzed. Cationic PPA elutes later than anionic counterparts of the same molecular weight (Figure 2.3a – molecular weights were calculated by Zimm plot), indicative of the compact cyclic structure. Furthermore, Mark-Houwink-Sakurada plots demonstrate that PPA prepared by cationic polymerization has a lower intrinsic viscosity than its anionic analog (Figure 2.3b). Both polymers presented a Mark-Houwink coefficient of ca. 0.6, and the calculated $[\eta]_{cationic}/[\eta]_{anionic}$ was found to be 0.7, consistent with the cyclic/linear ratio based on theoretical predictions

and experimental findings on other cyclic polymers.[8,12-15] These results, in conjunction with MALDI-TOF measurements and ^{1}H NMR spectroscopy, were taken as ample evidence for the cyclic structure of PPA synthesized by cationic polymerization.

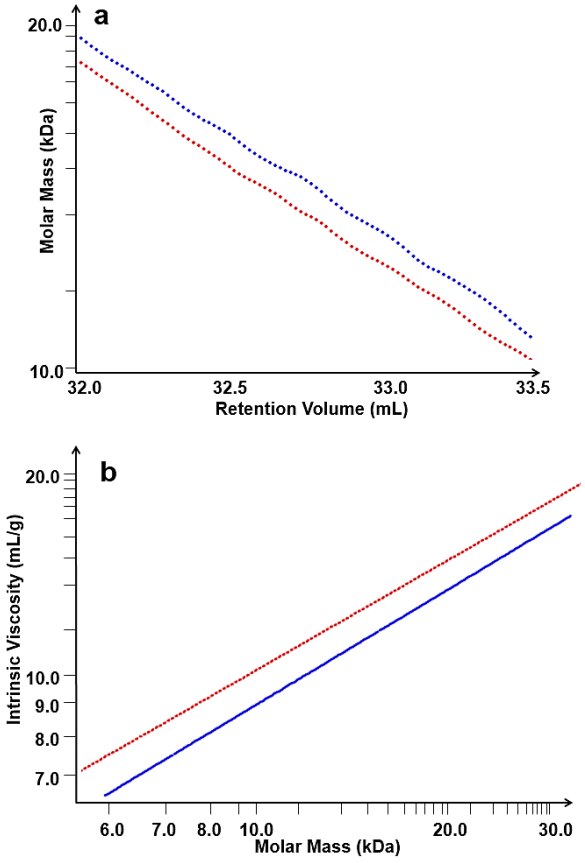

Figure 2.3 | Comparison of the physical properties of PPA prepared by cationic and anionic polymerization*: a) Plot of molecular weight (logarithmic axis) versus retention volume. PPA prepared by cationic polymerization (blue trace) exhibits greater retention volume than PPA prepared by anionic polymerization (red trace); b) Mark-Houwink-Sakurada double log plot of intrinsic viscosity versus molecular weight. PPA prepared by cationic polymerization (blue trace) exhibits lower intrinsic viscosity than PPA prepared by anionic polymerization (red trace).*

2.3.4 Reversible Macrocyclization Polymerization

Upon confirming the cyclic structure of PPA prepared by cationic polymerization, we questioned the reversibility of ring-closure under the polymerization conditions. In the case of anionic PPA, end-capping terminates the reaction (and this stabilizes the resulting chains from depolymerization); the obtained chains are unreactive. In the cationic polymerization, stabilization is achieved by an intramolecular ring closure rather than end-capping. Similarly, ring-closure could represent an irreversible termination step

that inactivates the polymer from further growth or contraction. We hypothesized, however, that the cPPA acetal backbone is re-opened under the Lewis acidic polymerization conditions. To test this hypothesis, the isolated macrocycles were subjected to boron trifluoride at temperatures below the ceiling temperature in an attempt to carry out further propagation on the stable, linear chains produced.

Ring-opening and ring-expansion of cPPA to larger molecular weights was achieved under the polymerization conditions in the presence of boron trifluoride and additional monomer (Figure 2.4a). Interestingly, the polymer was also made to controllably depolymerize to smaller cyclic polymers or even remain at an identical molecular weight after monomer addition, depending on monomer concentration (Figure 2.4b). This unique property is a result of polymerization occurring close to the polymer ceiling temperature, rendering propagation and depropagation dependent on monomer concentration.[4a] The cyclic polymer molecular weight is therefore under thermodynamic control and is tuned by both the polymerization temperature[4a] and the monomer concentration (defined as the amount of *o*-phthalaldehyde added plus the amount of phthalaldehyde repeat units in the cPPA).[16] Attempts to make low molecular weight polymer by inverse addition of monomer to excess initiator confirmed that molecular weight does not strongly correlate with percent initiator. Significantly, this property enables the reversible ring-expansion and ring-contraction of cPPA to form cyclic polymer of various sizes with reasonable control.

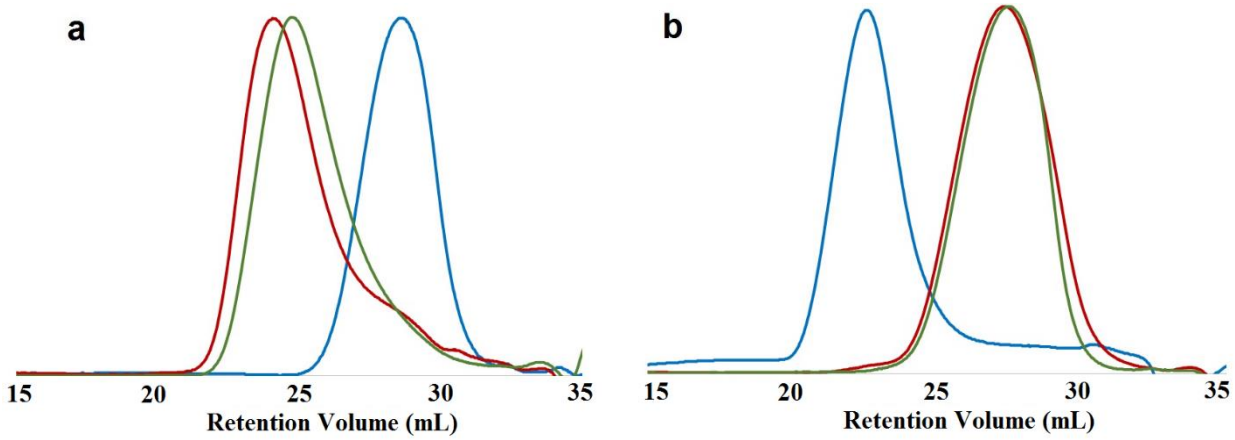

Figure 2.4 | cPPA ring-opening testing*: a) Normalized GPC chromatogram of cPPA (blue, M_p = 5.1 kDa) repolymerized to higher molecular weight at a total monomer concentration of 0.6 M (red, M_p = 67 kDa), and the resulting product repolymerized again at 0.6 M (green, M_p = 46 kDa). All polymerizations were conducted at -78 °C. b) Normalized GPC chromatogram of cPPA (blue, M_p = 199 kDa) repolymerized to lower molecular weight at a total monomer concentration of 0.5 M (red, M_p = 10 kDa) and the resulting product repolymerized again at 0.5 M (green, M_p = 9.1 kDa). All polymerizations were conducted at -78 °C.*

To conclusively illustrate the dynamic reversibility of cPPA polymerization and demonstrate the unique features of the system, we designed two control experiments. In the first, polymerization reactions were carried out at monomer concentrations of 1.0 M and 0.1 M. A third reaction was run in parallel in

which the monomer concentration began at 1.0 M, and then a second batch of monomer was added such that the overall concentration dropped to 0.1 M. In analogous experiments investigating the zwitterionic macrocyclic polymerization of lactones, researchers identified two outcomes: either chain extension to larger cyclic polymer was observed, or re-initiation occurred to generate a second distribution of cyclic polymer.[8a] In this case, though, the molecular weight distribution mirrors that of the polymerization at 0.1 M after the addition of the second batch of monomer (Figure 2.5a), demonstrating the dynamic equilibrium nature of the polymerization.

As a second control experiment, two cPPA polymers of different molecular weights were mixed together and subjected to the cationic polymerization conditions. In one reaction, boron trifluoride etherate was added, while no initiator was added to the second. GPC analysis of the molecular weight distributions clearly reveal the dynamic intermixing of polymers in the presence of boron trifluoride, whereas the polymer blend remained unchanged in the absence of initiator (Figure 2.5b). Interestingly, linear PPA prepared by anionic polymerization can be converted to cPPA using cationic polymerization conditions. By subjecting linear PPA as well as mixtures of linear PPA and cPPA to cationic polymerization conditions, the dynamic polymer intermixing to a single distribution of macrocyclic product is observed. Polymer recoveries of 90% and higher corroborate the incorporation of linear polymer into cyclic polymer products, with remaining uncapped PPA presumably depolymerized and removed in the work-up.

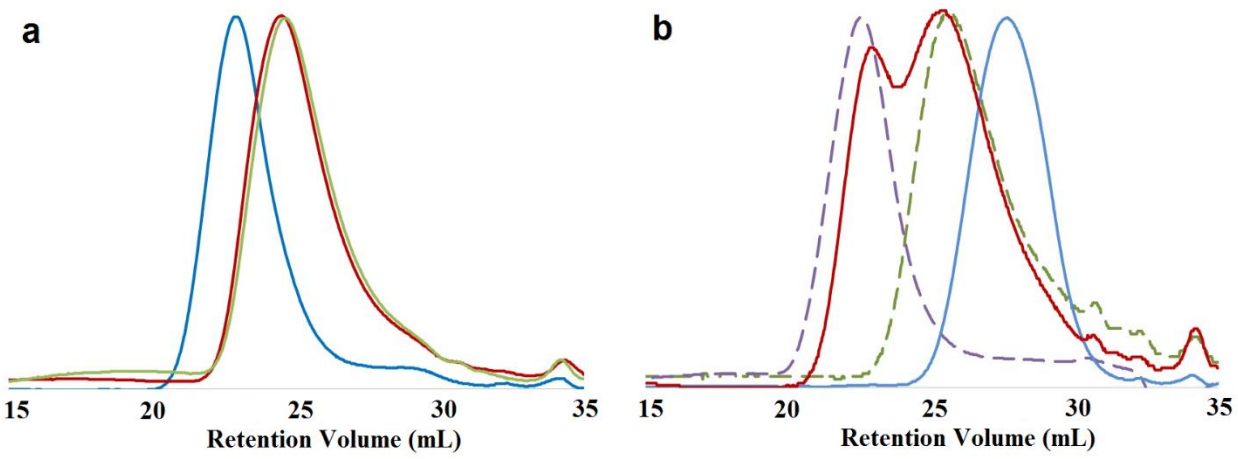

Figure 2.5 | Cycloreversible polymerization studies*: a) Normalized GPC chromatogram of cPPA polymerized at monomer concentrations of 1.0 M (blue), 0.1 M (red), and an initial [o-PA] of 1.0 M followed by addition of a second batch of o-PA to final concentration of 0.1 M (green). The monomodal peak at lower molecular weight is indicative of reversible polymerization. b) Normalized GPC chromatogram of two cPPA polymers (green and purple, dashed lines) and blends of the two polymers in the presence (blue, 0.5 M monomer) and absence (red, 0.5 M monomer) of initiator. Mixing of polymers to monomodal peak at lower molecular weight again indicative of dynamic, reversible polymerization.*

This unique property of cPPA is intriguing because the polymer can be grown, depolymerized, and repolymerized by adjusting reaction temperature and concentration. The thermodynamic control over the final product allows for precise production of polymers with predefined molecular weights and sizes. Whereas some cyclic polymers cannot be re-opened and polymerized to different molecular weights after initiator removal (since cyclization is an irreversible termination process), cPPA is capable of participating in reversible activation-deactivation processes. Furthermore, cPPA can be made to intermingle with and redistribute repeat units of other polymer chains, even linear chains. One could imagine mixing cPPA, or linear PPA, with a second similar polymer such as poly(4-bromophthalaldehyde)[17] to arrive at a completely intermixed, cyclic copolymer where the product composition is completely defined by thermodynamics. Such structural reorganization of distinct polymer blends could facilitate the preparation of complex and novel cyclic copolymers.

2.3.5 Cyclic PPA Mechanism

On the basis of these observations, we propose a cationic propagation mechanism for the cyclopolymerization of *o*-phthalaldehyde, generating cPPA by a back-biting reaction (Scheme 2.1). While a zwitterionic propagation mechanism with negatively charged boron trifluoride bound at one polymer terminus is possible, polymerizations performed with alternative cationic initiators suggest that the chains grow via cationic propagation. In the proposed mechanism, initiation by an acidic or cationic species (**RX**) generates the charged monomer **1**. Propagation proceeds by monomer addition to the cationic center, and cyclization to produce cPPA extrudes the acidic species, which is neutralized by addition of a base (**4**). Back-biting can theoretically occur at any position along the chain to produce cPPA and a shortened cationic chain, but ring closure from only the terminal position is shown for simplicity. As discussed previously, the macrocyclization is entirely reversible. The polymers presumably grow by a reversible activation-deactivation (RAD) process, much like controlled radical polymerization[18] mechanisms, except in this case rings equilibrate between closed (cyclic; **2C**) and open (cationic; **2, 3**) forms. This enables cyclic polymers to re-engage in the polymerization, even after their isolation. Cyclic PPA could potentially react with growing cationic chain ends, cationic monomeric intermediate, or initiator itself; only cPPA ring-opening by reaction with the acidic "**RX**" (reverse termination) is shown, again for simplicity. Notably, the equilibrium dramatically shifts to favor monomer (**M**) under dilute conditions and at temperatures above -40 °C. Therefore, non-cyclized PPA rapidly degrades to monomer such that cPPA is obtained in high yield with high purity.

***Scheme 2.1** | Proposed mechanism of reversible, cationic macrocyclization PPA polymerization.*

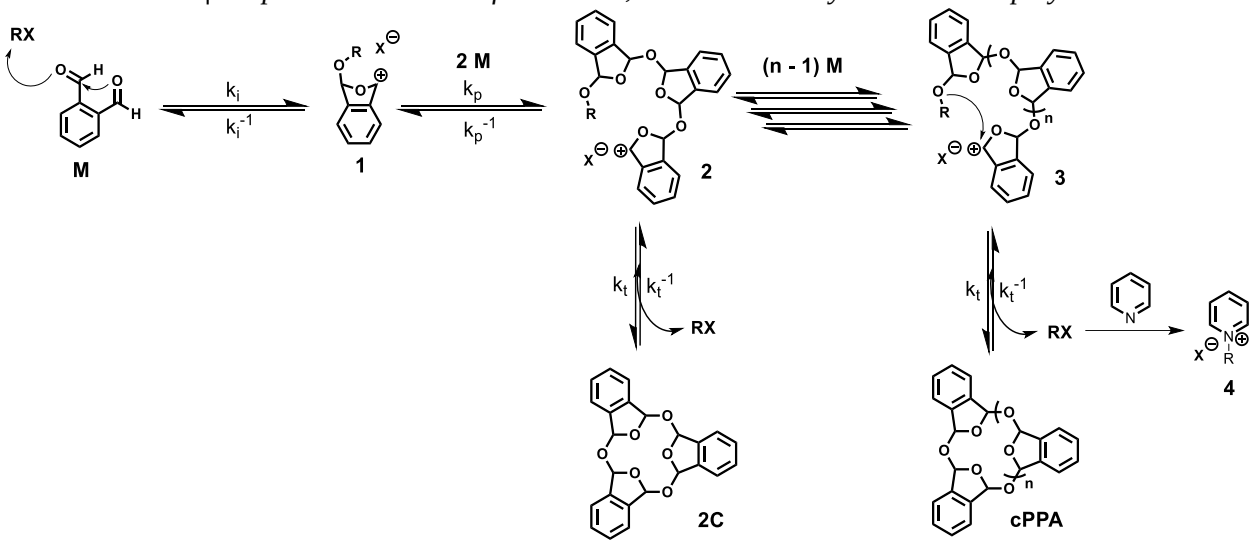

2.4 Conclusions

To conclude, while trying to incorporate specific end-caps to cationically polymerized *o*-phthalaldehyde, we unexpectedly discovered an expedient cationic polymerization to generate high molecular weight cyclic polymer with high purity via a thermodynamically controlled process. The cyclic structure of the polymer product was confirmed by a variety of techniques, namely NMR spectroscopy, MALDI-TOF mass spectrometry, and triple-detection GPC. Significantly, the cyclic polymers were shown to be reversible; the macrocycles are ring-opened to produce either larger cPPA by propagation or smaller cPPA by depropagation, depending on the reaction conditions. These cyclic polymers scramble with other PPA (cyclic or linear) or similar polymer chains and dynamically intermix to a monomodal distribution of macrocyclic product.

The flexibility in sequence and molecular weight distributions make cPPA an exceptional polymer system that merits further exploration. The dynamic polymer is completely recyclable given that it is composed entirely of phthalaldehyde repeat units and therefore will undergo re- or depolymerization depending on conditions. The lack of end-groups in cPPA is additionally advantageous in that it could overcome issues from residual non-volatile end-groups in applications that require total material removal. For example, this could improve capabilities in highly sensitive applications such as lithography or packaging of transient electronics.[3,5,19] We also note that cPPA is remarkably stable in comparison to linear PPA. Samples left on the bench-top have been observed to remain a pristine white polymer for several

months in air, while linear PPA analogs require meticulous storage or risk depolymerizing within days, likely as a result of end-cap removal.[1a]

Finally, we highlight that polymerization near the ceiling temperature may provide a general route to cyclic polymer synthesis with near perfect purity. We anticipate that when an avenue is available for cyclization, and when transfer reactions or other side reactions are avoided, cyclic polymer can be obtained as the sole product without resorting to high dilution conditions.[20] Cyclization would be enforced by the thermodynamic preference to self-correct, i.e., to stabilize by ring-closure, and cyclic polymer would be obtained in high purity by concurrent depolymerization of linear, uncapped products. This potentially general route to cyclic polymer synthesis is currently under investigation in further experimental and computational studies.

2.5 Synthetic Procedures

Scheme 2.2 **|** *General cationic polymerization.*

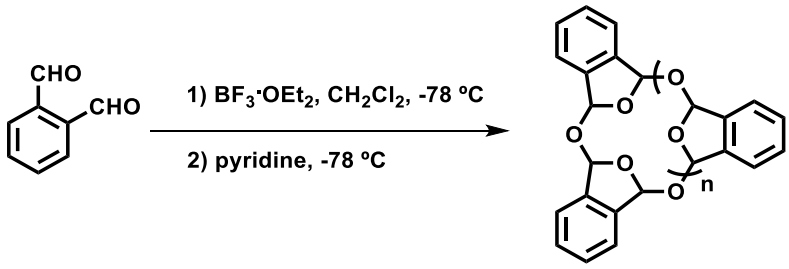

O-Phthalaldehyde (*o*-PA) is purified according to a literature procedure[1a] and dried under high vacuum for 24 hours. *o*-PA (1.00 g, 7.5 mmol) is weighed into a Schlenk flask and dissolved in dichloromethane (10 mL). The solution is cooled to -78 °C and boron trifluoride etherate is added (0.02 mL, 0.16 mmol). The reaction mixture is left stirring at -78 °C for 2 h, then pyridine (0.12 mL, 1.5 mmol) is added. The mixture is left stirring 2 h at -78 °C, then brought to room temperature and the polymer precipitated by pouring into methanol (100 mL). The product is collected by filtration, then further purified by dissolving in dichloromethane and re-precipitating from methanol/diethyl ether (0.84 g, 84%). ^{1}H NMR (500 MHz, $CDCl_3$) δ 7.80-7.15 ppm (br, 4H, aromatic), 7.15-6.25 ppm (br, 2H, acetal). $^{13}C\{^{1}H\}$ NMR (125 MHz, $CDCl_3$) δ 138.8 ppm, 130.2 ppm, 123.5 ppm, 105.0-101.8 ppm.

Table 2.3 | Cationic polymerization samples.

Entry	*[o-PA]*	*$[M]_0/[I]_0$*	*Yield*	*M_n (kDa)[a]*	*M_p (kDa)[a]*	*PDI[a]*
1	1.0 M	10 / 1	86%	36.1	158	4.5
2	0.7 M	7 / 1	99%	109	199	2.5
3	0.5 M	10 / 1	77%	6.7	10.1	2.4
4	0.1 M	10 / 1	48%	14.9	54.1	3.5
5[b]	0.2 M	10 / 1	63%	10.5	22.0	2.2
6[c]	0.7 M	6 / 1	76%	15.4	73.7	4.4
7[d]	0.7 M	8 / 1	99%	51.5	107	2.0
8[e]	0.2 M	6 / 1	68%	25.0	71.4	2.8
9	0.9 M	20 / 1	94%	104	218	2.3
10[f]	0.9 M	20 / 1	92%	88.6	158	2.2
11[g]	0.9 M	20 / 1	86%	89.4	181	2.3
12[h]	0.8 M	20 / 1	92%	26.2	57.2	2.3

[a]Average molecular weights and polydispersity determined by gel permeation chromatography (GPC), calibrated with monodisperse polystyrene standards. [b]3-fluoropyridine used in place of pyridine. [c]No pyridine added. Polymer precipitated directly at -78 °C in diethyl ether and washed in diethyl ether and methanol. [d]Precipitation and washing conducted in hexanes and diethyl ether only. [e]Addition of 1-pyrene methanol following reaction and precipitation into diethyl ether. [f]Triethyloxonium tetrafluoroborate initiator. [g]Tin(IV) chloride initiator. [h]Triphenylcarbenium tetrafluoroborate initiator.

Scheme 2.3 | *General anionic polymerization.*

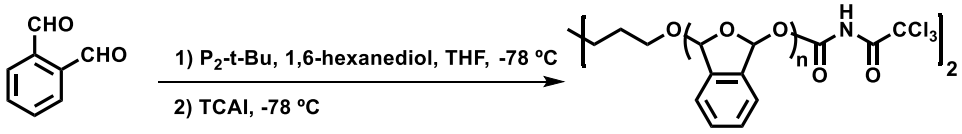

In a glovebox, purified *o*-PA (0.20 g, 1.5 mmol) is weighed into a Schlenk flask and dissolved in THF (2 mL). The solution is removed from the glovebox and degassed by three freeze-pump-thaw cycles. Then, 1,6-hexanediol in THF (0.10 mL of a 0.03 M solution, 3 μmol) is added, and the solution stirred 2 minutes then cooled to -78 °C. Finally, P_2-t-Bu phosphazene base in THF (0.03 mL of a 0.20 M solution, 6 μmol) is added to initiate polymerization. The reaction mixture is left stirring at -78 °C for 2.5 h, then the polymer is end-capped by adding trichloroacetyl isocyanate (0.05 mL, 0.4 mmol) and allowing the mixture to stir an additional 2 h at -78 °C. The reaction mixture is then brought to room temperature and polymer precipitated by pouring into methanol (100 mL) and collected by filtration. If necessary, the polymer is further purified by dissolving in dichloromethane and re-precipitating from methanol/diethyl ether (0.18 g, 90%). ^{1}H NMR (500 MHz, $CDCl_3$) δ 7.80-7.15 (b, 4H, aromatic), 7.15-6.25 (b, 2H, acetal), 3.80-3.30 (b, initiator), 1.85-0.75 (b, initiator).

Table 2.4 | Anionic polymerization samples.

Entry	*[o-PA]*	*$[M]_0/[I]_0/[P_2]_0$*[a]	*Yield*	*M_n (kDa)*[b]	*M_p (kDa)*[b]	*PDI*[b]
1	0.7	125 / 1 / 2	83%	4.4	5.4	1.8
2	0.7	250 / 1 / 2	92%	6.3	8.1	3.0
3	0.7	625 / 1 / 2	92%	9.0	11.5	2.1
4	0.7	2500 / 1 / 3	36%	16.1	26.5	2.7
5	0.7	5000 / 1 / 3	34%	20.4	40.9	2.0

[a]Initial monomer-to-initiator-to catalyst ratio.[2] [b]Average molecular weights and polydispersity determined by gel permeation chromatography (GPC), calibrated with monodisperse polystyrene standards.

Scheme 2.4 | *Inverse addition cationic polymerization.*

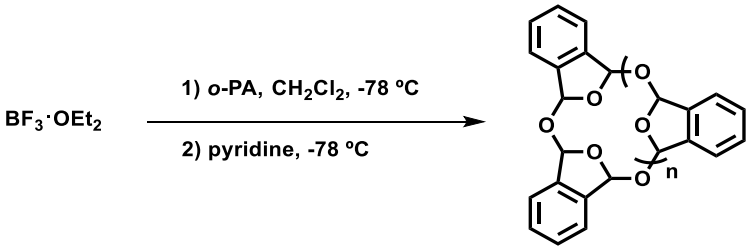

In a clean, dry Schlenk flask, boron trifluoride etherate (0.15 mL, 1.2 mmol) is dissolved in dichloromethane (3 mL). The solution is cooled to -78 °C and *o*-PA (0.30 g, 2.2 mmol) in dichloromethane (2 mL) is added dropwise to the stirring mixture. The reaction mixture is left stirring at -78 °C for 10 minutes, then pyridine (0.15 mL, 1.9 mmol) is added. The mixture is left stirring 10 minutes at -78 °C, then brought to room temperature and the polymer precipitated by pouring into methanol (100 mL). The product is collected by filtration, then further purified by dissolving in dichloromethane and re-precipitating from methanol/diethyl ether (0.25 g, 83%). ^{1}H NMR (500 MHz, $CDCl_3$) δ 7.80-7.15 ppm (br, 4H, aromatic), 7.15-6.25 ppm (br, 2H, acetal).

Table 2.5 | Inverse addition cationic polymerization samples.

Entry	*[o-PA]*	*$[M]_0/[I]_0$*	*Yield*	*M_n (kDa)*[a]	*M_p (kDa)*[a]	*PDI*[a]
1	0.6 M	5 / 1	99%	61.3	124.6	2.5
2	0.4 M	2 / 1	83%	25.8	165.3	4.5
3[b]	0.1 M	1 / 2	17%	2.7	2.5	1.6

[a]Average molecular weights and polydispersity determined by gel permeation chromatography (GPC), calibrated with monodisperse polystyrene standards. [b]Low yield attributed to low monomer concentration and use of excess initiator.

Scheme 2.5 | *Cationic repolymerization reactions (Figure 2.4).*

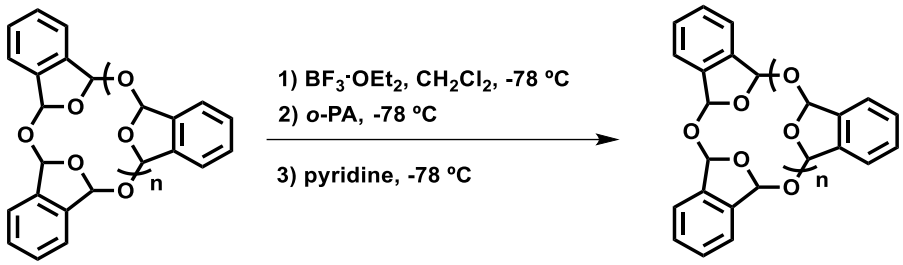

Poly(phthalaldehyde) [PPA] (0.20 g) is weighed into a Schlenk flask and dissolved in dichloromethane (2 mL). The solution is cooled to -78 °C and boron trifluoride etherate is added (0.02 mL, 0.16 mmol). Then, *o*-PA (0.20 g, 1.5 mmol) in dichloromethane (2 mL) is added dropwise to the stirring mixture. The reaction mixture is left stirring at -78 °C for 2 h, then pyridine (0.12 mL, 1.5 mmol) is added. The mixture is left stirring 2 h at -78°C, then brought to room temperature and then the polymer precipitated by pouring into methanol (100 mL). The product is collected by filtration, then further purified by dissolving in dichloromethane and re-precipitating from methanol/diethyl ether (0.29 g, 73%). ^{1}H NMR (500 MHz, $CDCl_3$) δ 7.80-7.15 ppm (br, 4H, aromatic), 7.15-6.25 ppm (br, 2H, acetal).

Table 2.6 | Repolymerization samples.

Entry	*[o-PA]*	$[M]_0/[I]_0$	*Yield*	*Initial Polymer* M_p *(kDa)*	*Final Polymer* M_n *(kDa)*[a]	*Final Polymer* M_p *(kDa)*[a]	*PDI*[a]
1	0.1 M	6 / 1	21%	- - -	4.0	5.1	1.6
2[b]	0.6 M	18 / 1	86%	5.1	12.5	67.4	5.1
3[c]	0.6 M	18 / 1	86%	67.4	16.8	45.6	2.7
4	0.7 M	7 / 1	99%	- - -	109	199	2.5
5[d]	0.5 M	4 / 1	77%	199	6.7	10.1	2.4
6[e]	0.4 M	5 / 1	52%	10.1	7.9	9.1	1.7

[a]Average molecular weights and polydispersity determined by gel permeation chromatography (GPC), calibrated with monodisperse polystyrene standards. [b]Repolymerization of Entry 1. [c]Repolymerization of Entry 2. [d]Repolymerization of Entry 4. [e]Repolymerization of Entry 5.

Scheme 2.6 | *Second batch monomer addition reactions (Figure 2.5a).*

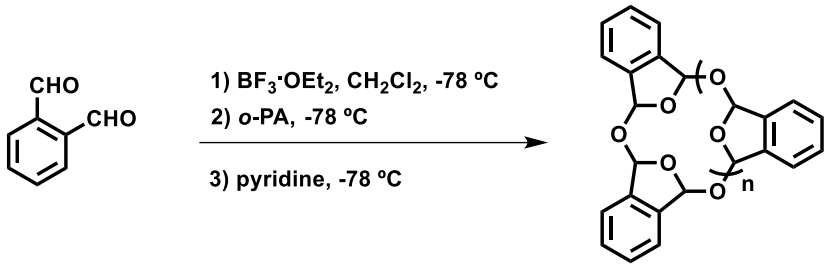

o-PA (0.10 g, 0.7 mmol) is weighed into a Schlenk flask and dissolved in dichloromethane (0.7 mL). The solution is cooled to -78 °C and boron trifluoride etherate is added (0.02 mL, 0.16 mmol). The reaction mixture is left stirring at -78 °C for 1 h, then *o*-PA (0.10 g, 0.7 mmol) in dichloromethane (14 mL) is added dropwise. After stirring for another 1 h at -78 °C, pyridine (0.12 mL, 1.5 mmol) is added. Finally, the mixture is stirred 2 h at -78 °C, then brought to room temperature and the polymer precipitated by pouring into methanol (100 mL). The product is collected by filtration, then further purified by dissolving in dichloromethane and re-precipitating from methanol/diethyl ether (96 mg, 48%). ^{1}H NMR (500 MHz, $CDCl_3$) δ 7.80-7.15 ppm (br, 4H, aromatic), 7.15-6.25 ppm (br, 2H, acetal).

Table 2.7 | Second batch monomer addition samples.

Entry	*[o-PA]*	*$[M]_0/[I]_0$*	*Yield*	*M_n (kDa)[a]*	*M_p (kDa)[a]*	*PDI[a]*
1	1.0 M	10 / 1	86%	36.1	158	4.5
2	0.1 M	10 / 1	48%	14.9	54.1	3.5
3[b]	1.0 → 0.1 M	10 / 1	48%	11.8	48.6	4.1

[a]Average molecular weights and polydispersity determined by gel permeation chromatography (GPC), calibrated with monodisperse polystyrene standards. [b]Initial monomer concentration of 1.0 M, total concentration after addition of second batch of monomer 0.1 M.

Scheme 2.7 | *Polymer mixing reactions (Figure 2.5b).*

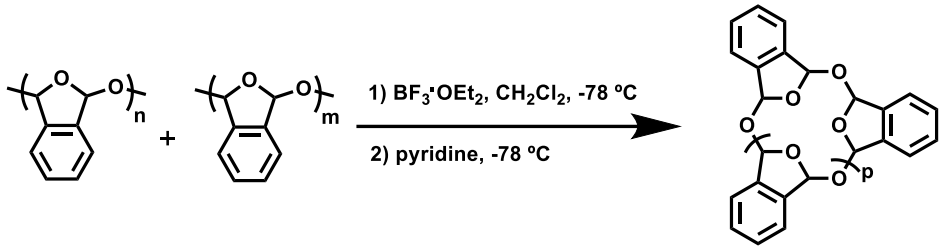

High molecular weight PPA (75 mg, M_p = 199 kDa) and low molecular weight PPA (75 mg, M_p = 30 kDa) are weighed into a Schlenk flask and dissolved in dichloromethane (2.2 mL). The solution is cooled to -78°C and boron trifluoride etherate is added (0.03 mL, 0.24 mmol). The reaction mixture is left stirring at -78 °C for 2 h, then pyridine (0.10 mL, 1.2 mmol) is added. The mixture is left stirring 2 h at -78 °C, then brought to room temperature and then the polymer precipitated by pouring into methanol (100 mL). The product is collected by filtration, then further purified by dissolving in dichloromethane and re-precipitating from methanol/diethyl ether (0.13 g, 87%). ^{1}H NMR (500 MHz, $CDCl_3$) δ 7.80-7.15 ppm (br, 4H, aromatic), 7.15-6.25 ppm (br, 2H, acetal).

Table 2.8 | Polymer mixing samples.

Entry	*[o-PA]*	*$[M]_0/[I]_0$*	*Yield*	*M_n (kDa)[a]*	*M_p (kDa)[a]*	*PDI[a]*
1	0.7 M	7 / 1	99%	109	199	2.5
2	0.5 M	14 / 1	83%	11.7	29.5	2.1
3[b]	0.5 M	5 / 1	87%	8.3	6.0	1.6
4[c,d]	0.5 M	- - -	99%	10.5	30.7, 155	7.8
5[e]	0.7 M	125 / 1	83%	4.4	5.4	1.8
6	1.0 M	10 / 1	86%	36.1	158	4.5
7[f]	0.6 M	3 / 1	90%	7.5	32.9	2.2

[a]Average molecular weights and polydispersity determined by gel permeation chromatography (GPC), calibrated with monodisperse polystyrene standards. [b]Polymers 1 and 2 mixed and initiator added. [c]Control reaction; polymers 1 and 2 mixed, no initiator added. [d]Bimodal molecular weight distribution. [e]Polymer prepared by anionic polymerization. [f]Polymers 5 and 6 mixed and initiator added.

2.6 NMR Spectra, MALDI Spectra, and Thermal Characterization

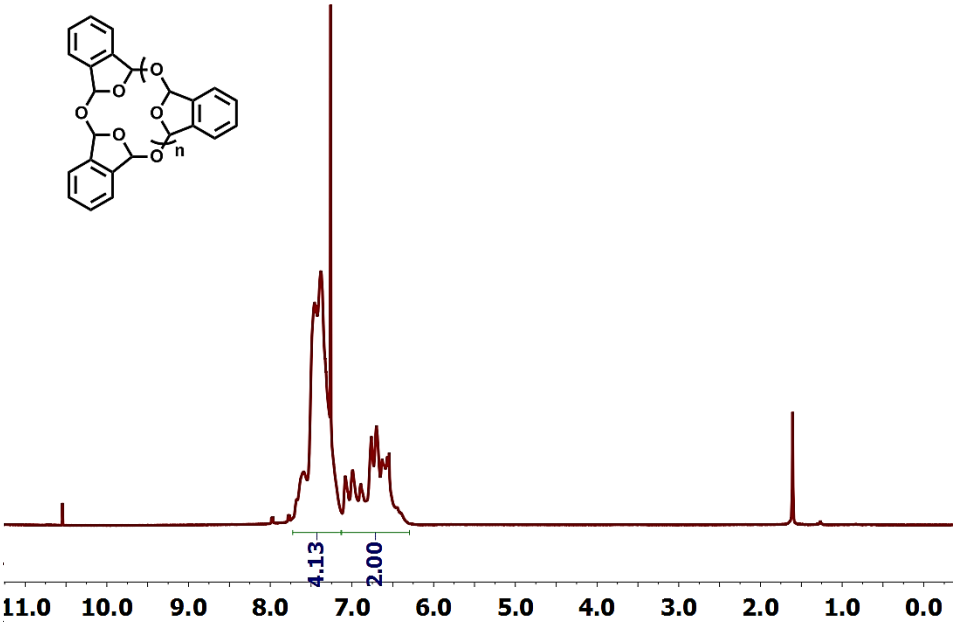

Figure 2.6 | ^{1}H NMR spectrum of cyclic PPA*: NMR spectra of M_n = 6 kDa PPA prepared by cationic polymerization in $CDCl_3$. No end-groups are observed. Additional peaks correspond to water (1.6 ppm) and residual* o*-phthalaldehyde monomer.*

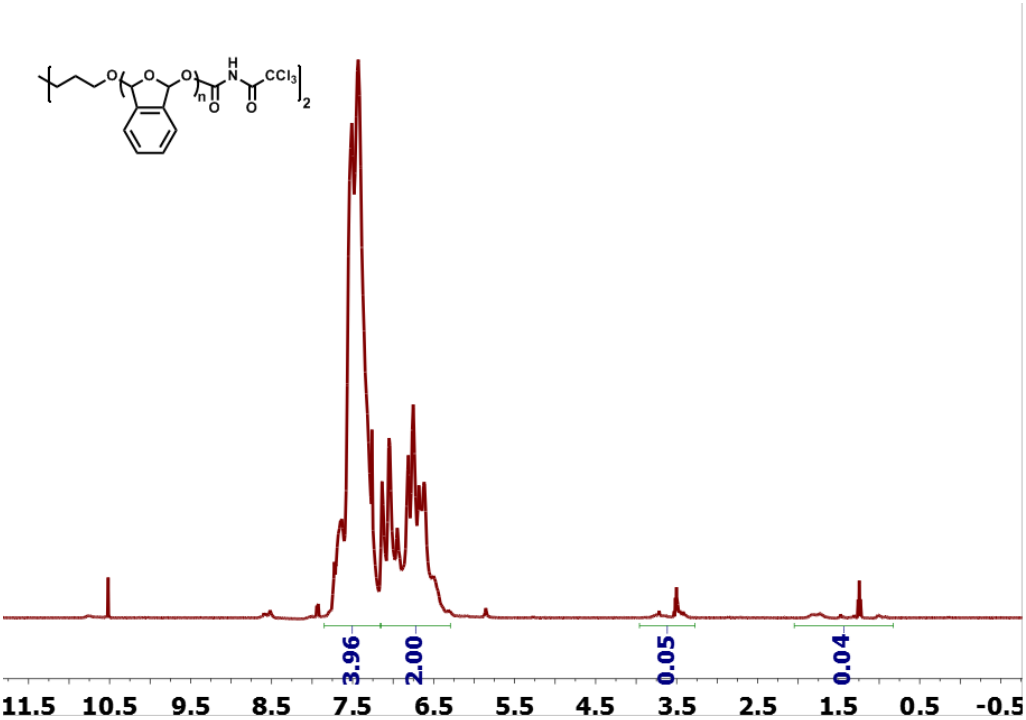

Figure 2.7 | ^{1}H NMR spectrum of linear PPA*: NMR spectra of M_n = 6 kDa PPA prepared by anionic polymerization in $CDCl_3$. Residual* o*-phthalaldehyde monomer remains even after three successive precipitations.*

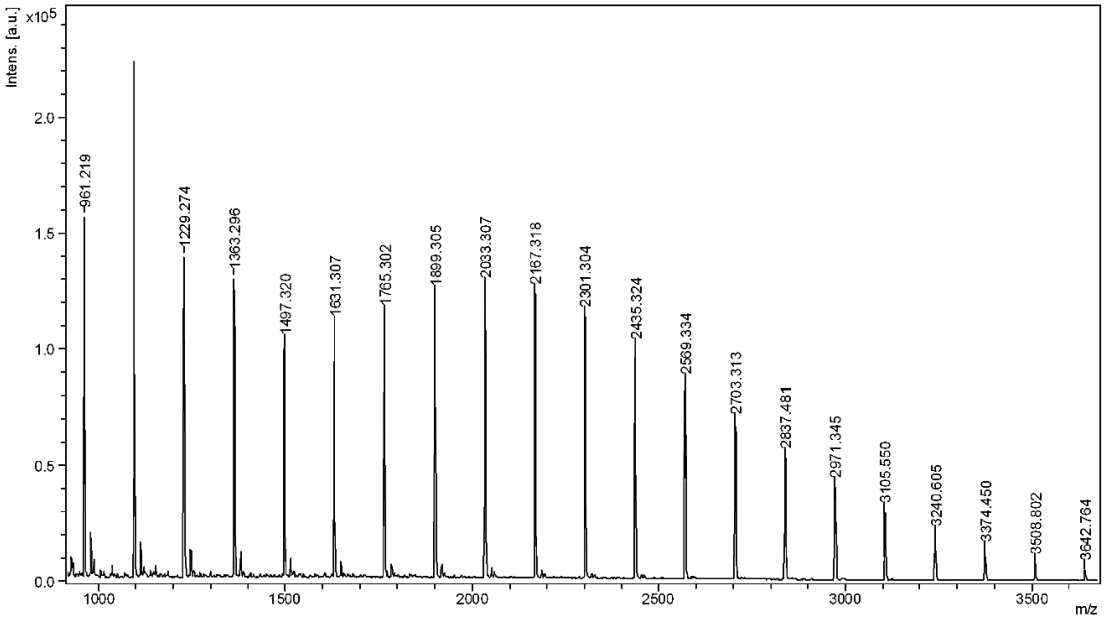

Figure 2.8 | MALDI-TOF mass spectrum of cPPA*: Peaks match sodium adduct of cPPA (GPC M_n = 2.7 kDa); minor secondary peaks match sodium and water adduct of PPA, presumably PPA with hemiacetal groups from reaction with MALDI matrix (+18 mass units).*

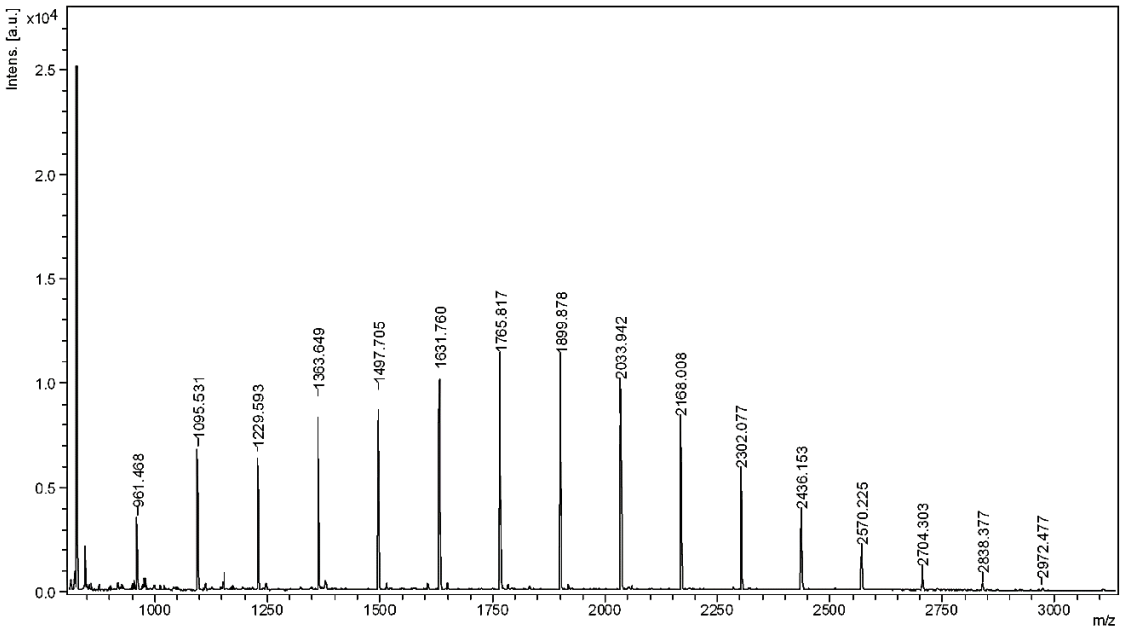

Figure 2.9 | MALDI-TOF mass spectrum of cPPA*: Peaks match sodium adduct of cPPA (GPC M_n = 25.0 kDa).*

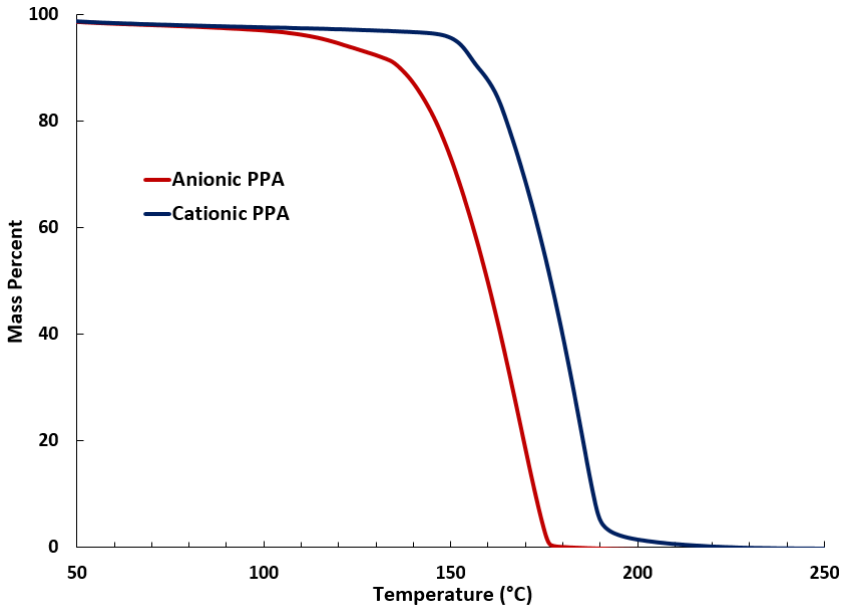

Figure 2.10 | TGA of linear and cyclic PPA*: Normalized TGA curves of representative samples of linear (red) and cyclic (blue) PPA. Molecular weight data and depolymerization temperatures are summarized in Table 2.9.*

Table 2.9 | TGA Samples. *Molecular weight and depolymerization data for linear and cyclic PPA.*

Entry	*Polymerization*	*M_n (kDa)[a]*	*M_p (kDa)[a]*	*PDI[a]*	*Onset Temp (°C)*	*Endset Temp (°C)*	*Residue at 300 °C*
1	Cationic	6.7	10.1	2.4	159	236	3.6%
2	Cationic	7.9	9.1	1.7	156	211	2.4%
3	Cationic	11.8	48.6	4.1	157	186	4.5%
4	Cationic	14.9	54.1	3.5	148	204	2.3%
5	Cationic	36.1	158	4.5	139	199	2.0%
6	Cationic	37.1	79.8	2.2	158	195	1.1%
Cationic Averages					153 ± 8 °C		2.6 ± 1.2%
7	Anionic	4.4	5.4	1.8	150	199	3.6%
8	Anionic	6.3	8.1	3.0	141	190	3.2%
9	Anionic	9.0	11.5	2.1	132	193	2.1%
10	Anionic	16.1	26.5	2.7	135	185	2.6%
11	Anionic	20.4	40.9	2.0	138	200	2.4%
12	Anionic	22.6	35.5	1.6	136	177	0.5%
Anionic Averages					139 ± 6 °C		2.4 ± 1.1%

[a]Average molecular weights and polydispersity determined by gel permeation chromatography (GPC), calibrated with monodisperse polystyrene standards.

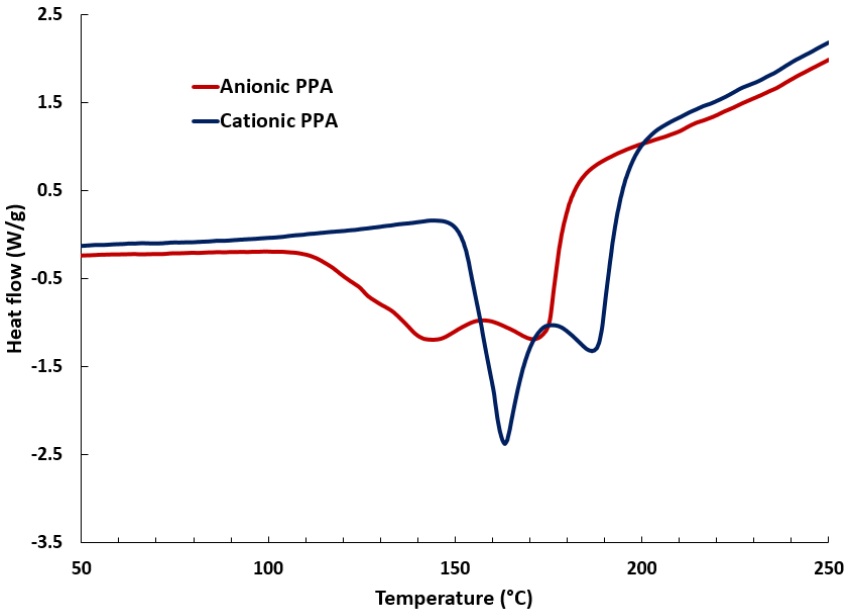

Figure 2.11 | DSC of linear and cyclic PPA*: Normalized DSC curves of representative samples of linear (blue) and cyclic (red) PPA. Molecular weight data and depolymerization temperatures are summarized in Table 2.10.*

Table 2.10 | DSC Samples*. Molecular weight and enthalpic data for linear and cyclic PPA.*

Entry	*Polymerization*	M_n *(kDa)*[a]	M_p *(kDa)*[a]	*PDI*[a]	*Enthalpy (J/g)*
1	Cationic	6.7	10.1	2.4	-540
2	Cationic	7.9	9.1	1.7	-520
3	Cationic	11.8	48.6	4.1	-540
4	Cationic	14.9	54.1	3.5	-580
5	Cationic	36.1	158	4.5	-590
6	Cationic	37.1	79.8	2.2	-520
Cationic Averages					-550 ± 30 J/g
7	Anionic	4.4	5.4	1.8	-590
8	Anionic	6.3	8.1	3.0	-580
9	Anionic	9.0	11.5	2.1	-570
10	Anionic	16.1	26.5	2.7	-530
11	Anionic	20.4	40.9	2.0	-580
12	Anionic	22.6	35.5	1.6	-520
Anionic Averages					-560 ±30 J/g

[a]Average molecular weights and polydispersity determined by gel permeation chromatography (GPC), calibrated with monodisperse polystyrene standards.

2.7 References

(1) (a) Dilauro, A. M.; Robbins, J. S.; Phillips, S. T. *Macromolecules* **2013**, 46, 2963-2968. (b) Kaitz, J. A.; Moore, J. S.; *Macromolecules* **2013**, 46, 608-612. (c) Dilauro, A. M.; Abbaspourrad, A.; Weitz, D. A.; Phillips, S. T. *Macromolecules* **2013,** 46, 3309-3313. (d) Peterson, G. I.; Larsen, M. B.; Boydston, A. J. *Macromolecules* **2012**, 45, 7317-7328.

(2) Seo, W.; Phillips, S. T. *J. Am. Chem. Soc.* **2010**, 132, 9234-9235.

(3) Coulembier, O.; Knoll, A.; Pires, D.; Gotsmann, B.; Duerig, U.; Frommer, J.; Miller, R. D.; Dubois, P.; Hedrick, J. L. *Macromolecules* **2010**, 43, 572-574.

(4) (a) Chuji, A.; Tagami, S.; Kunitake, T. *J. Polym. Sci. Part A: Polym. Chem.* **1969**, 7, 497-511. (b) Chuji, A.; Tagami, S. *Macromolecules* **1969**, 2, 414-419.

(5) (a) Willson, C. G.; Ito, H.; Frechet, J. M. J.; Tessier, T. G.; Houlihan, F. M. *J. Electrochem. Soc.* **1986**, 133, 181-187. (b) Tsuda, M.; Hata, M.; Nishida, R.; Oikawa, S. *J. Polym. Sci. Part A: Polym. Chem.* **1997**, 35, 77-89. (c) Ito, H.; Willson, C. G. *Polym. Eng. Sci.* **1983**, 23, 1012-1018. (d) Knoll, A. W.; Pires, D.; Coulembier, O.; Dubois, P.; Hedrick, J. L.; Frommer, J.; Duerig, U. *Adv. Mater.* **2010**, 22, 3361-3365.

(6) Kostler, S.; Zechner, B.; Trathnigg, B.; Fasl, H.; Kern, W.; Ribitsch, V. *J. Polym. Sci. Part A: Polym. Chem.* **2009**, 47, 1499-1509.

(7) Potisek, S. L.; Davis, D. A.; Sottos, N. R.; White, S. R.; Moore, J. S. *J. Am. Chem. Soc.* **2007**, 129, 13808-13809.

(8) (a) Jeong, W.; Shin, E. J.; Culkin, D. A.; Hedrick, J. L.; Waymouth, R. M. *J. Am. Chem. Soc.* **2009**, 131, 4884-4891. (b) Culkin, D. A.; Jeong, W.; Csihony, S.; Gomez, E. D.; Balsara, N. P.; Hedrick, J. L.; Waymouth, R. M. *Angew. Chem. Int. Ed.* **2007**, 46, 2627-2630. (c) Jeong, W.; Hedrick, J. L.; Waymouth, R. M. *J. Am. Chem. Soc.* **2007**, 129, 8414-8415. (d) Guo, L.; Zhang, D. *J. Am. Chem. Soc.* **2009**, 131, 18072-18074. (e) Guo, L.; Lahasky, S. H,; Ghale, K.; Zhang, D. *J. Am. Chem. Soc.* **2012**, 134, 9163-9171.

(9) (a) Aso, C. *Pure Appl. Chem.* **1970**, 23, 287-304. (b) Tagami, S.; Kagiyama, T.; Aso, C. *Polymer Journal* **1971**, 2, 101-108.

(10) (a) Kricheldorf, H. R. *J. Polym. Sci., Part A: Polym. Chem.* **2010**, 48, 251-284. (b) Jia, Z.; Monteiro, M. J. *J. Polym. Sci., Part A: Polym. Chem.* **2012**, 50, 2085-2097. (c) Laurent, B. A.; Grayson, S. M. *Chem. Soc. Rev.* **2009**, 38, 2202-2213. (d) Yamamoto, T.; Tezuka, Y. *Polym. Chem.* **2011**, 2, 930-1941. (e) Endo, K. *Adv. Polym. Sci.* **2008**, 217, 121-183. (f) McLeish, T. *Science* **2002**, 297, 2005-2006.

(11) (a) Wood, B. R.; Hodge, P.; Semlyen, J. A. *Polymer* **1993**, 34, 3052-3058. (b) Ruddick, C. L.; Hodge, P.; Cook, A.; McRiner, A. J. *J. Chem. Soc. Perk. Trans.* **2002**, 629-637. (c) Chisholm, M. H.; Gallucci, J. C.; Yin, H. *Proc. Natl. Acad. Sci. U. S. A.* **2006**, 103, 15315-15320.

(12) (a) Rique-Lurbet, L.; Schappacher, M.; Deffieux, A. *Macromolecules* **1994**, 27, 6318-6324. (b) Laurent, B. A.; Grayson, S. M. *J. Am. Chem. Soc.* **2006**, 128, 4238-4239. (c) Leppoittevin, B.; Perrot, X.; Masure, M.; Hemery, P. *Macromolecules* **2001**, 34, 425-429. (d) Oike, H.; Imaizumi, H.; Mouri, T.; Yoshioka, Y.; Uchibori, A.; Tezuka, Y. *J. Am. Chem. Soc.* **2000**, 122, 9592-9599. (e) Sugai, N.; Heguri, H.; Yamamoto, T.; Tezuka, Y. *J. Am. Chem. Soc.* **2011**, 133,19694-19697.

(13) (a) Bielawski, C. W.; Benitez, D.; Grubbs, R. H. *Science* **2002**, 297, 2041-2044. (b) Boydston, A. J.; Xia, Y.; Kornfield, J. A.; Gorodetskaya, I. A.; Grubbs, R. H. *J. Am. Chem. Soc.* **2008**, 130, 12775-12782. (c) Xia, Y.; Boydston, A. J.; Yao, Y.; Kornfield, J. A.; Gorodetskaya, I. A.; Spiess, H. W.; Grubbs, R. H. *J. Am. Chem. Soc.* **2009**, 131, 2670-2677. (d) Bielawski, C. W.; Benitez, D.; Grubbs, R. H. *J. Am. Chem. Soc.* **2003**, 125, 8424-8425.

(14) (a) Kricheldorf, H. R. *J. Polym. Sci. Part A: Polym. Chem.* **2004**, 42, 4723-4742. (b) Kricheldorf, H. R.; Lee, S. R. *Macromolecules* **1995**, 28, 6718-6725.

(15) Semlyen, J. A. *Cyclic Polymers*, 2nd ed.; Kluwer Academic Publishers: Dordrecht, **2000**; pp 347-384.

(16) Jacobson, H.; Stockmayer, W. H. *J. Chem. Phys.* **1950**, 18, 1600-1606.

(17) Ito, H.; Ueda, M.; Schwalm, R. *J. Vac. Sci. Technol.* **1988**, 6, 2259-2263.

(18) (a) Odian, G. *Principles of Polymerization*, 4th ed.; Wiley-Interscience: New York, **2004**. (b) Braunecker, W. A.; Matyjaszewski, K. *Prog. Polym. Sci*. **2007**, 32, 93-146.

(19) Hwang, S.-W.; Tao, H.; Kim, D.-H.; Cheng, H.; Song, J.-K.; Rill, E.; Brenckle, M. A.; Panilaitis, B.; Won, S. M.; Kim, Y.-S.; Song, Y. M.; Yu, K. J.; Ameen, A.; Li, R.; Su, Y.; Yang, M.; Kaplan, D. L.; Zakin, M. R.; Slepian, M. J.; Huang, Y.; Omenetto, F. G.; Rogers, J. A. *Science* **2012**, 337, 1640-1644.

(20) (a) Szymanski, R. S.; Kubisa, P.; Penczek, S. *Macromolecules* **1983**, 16, 1000-1008. (b) Weissermel, K.; Fischer, E.; Gutweiler, K.; Hermann, H. D.; Cherdron, H. *Angew. Chem. Int. Ed.* **1967**, 6, 526-533. (c) Hasegawa, M.; Yamamoto, K.; Shiwaku, T.; Hashimoto, T. *Macromolecules* **1990**, 23, 2629-2636.

Chapter 3: Scrambling Cyclic Homopolymer Mixtures to Produce Multi-Block and Random Cyclic Copolymers*

3.1 Abstract

The cationic polymerization of *o*-phthalaldehyde to produce macrocyclic poly(phthalaldehyde) polymers was recently discovered. Re-subjecting the cyclic polymers to the polymerization conditions led to a redistribution of the polymer to a new cyclic structure consistent with thermodynamic equilibrium. The synthesis of cyclic poly(phthalaldehyde) derivatives is now discussed, and the scrambling of distinct homopolymer mixtures to copolymers under the cationic polymerization conditions is demonstrated. Homopolymer mixtures are found to rapidly redistribute, first to multi-block cyclic copolymers. With extended reaction time, random macrocyclic copolymers are obtained. Evolution of the microstructure was monitored by NMR spectroscopy, MALDI-TOF mass spectrometry, and gel permeation chromatography (GPC). This scrambling method leads to the rapid preparation of macrocyclic copolymers of high molecular weight with variable microstructure depending on reaction times and catalyst loadings.

3.2 Introduction

Polymer scrambling and intermixing has been extensively studied in the context of dynamic covalent polymer chemistry.[1-3] Dynamic covalent polymers are unique from conventional polymers in that they consist of reversible covalent bonds and are capable of restructuring and reorganization under appropriate conditions, even after polymerization. These dynamic features enable microstructural reorganization of polymer blends for a variety of purposes such as in stimuli-responsive materials, the synthesis of complex polymer architectures, and dynamic combinatorial chemistry.[1] In this light, we were interested in the potential of low ceiling-temperature (T_c) polyacetal polymers to serve as dynamic covalent polymers,[3] utilizing their inherent reversibility when polymerization is conducted below T_c.

Low T_c polymers have also garnered significant interest in recent years for their stimuli-responsive properties and depolymerization capabilities.[4-5] One such thermodynamically unstable polymer, poly(phthalaldehyde) (PPA),[6] has found use as an acid-sensitive, radiation-sensitive, or thermally sensitive degradable film for lithography.[7] We recently reported a cationic, macrocyclic polymerization of

* Portions of this chapter have been published: Kaitz, J. A.; Diesendruck, C. E.; Moore, J. S. *Macromolecules* **2013**, 46, 8121-8128.

o-phthalaldehyde to produce cyclic PPA (cPPA).[8] The macrocyclic polymers could be re-subjected to polymerization conditions leading to a new equilibrium molecular weight distribution in accord with the repeat unit concentration. Cyclic polymers such as cPPA are of interest in their own right, but they have specifically emerged at the forefront of polymer chemistry due to their unique structural and physical properties through the topological constraint of connected chain-ends.[9] Many methods exist to construct such macrocyclic products; the Waymouth and Zhang groups in particular have pioneered zwitterionic ring-opening polymerization strategies toward the synthesis of cyclic polymers and block and gradient cyclic copolymers.[10]

We were especially intrigued, though, by the ability of cPPA to ring-open and dynamically intermix to reach a new equilibrium distribution. With this in mind, we initiated work aimed at the investigation of the microstructural consequences of polymer intermixing reactions, with the intent to develop new stimuli-responsive materials and synthesize complex new polymer architectures. In this chapter, the synthesis and scrambling of distinct cPPA homopolymer mixtures, the characterization of the resulting copolymer composition and microstructure, and the correlation of copolymer structures with scrambling conditions is discussed.

3.3 Results and Discussion

3.3.1 Cationic, Macrocyclic Homopolymerization of Phthalaldehyde Derivatives

O-phthalaldehyde derivatives with 4-bromo (B-PA) and 4-methyl (M-PA) substituents were synthesized in two steps adapted from literature procedures.[11-12] B-PA is synthesized by tetrabenzylic bromination followed by hydrolysis of 4-bromo-*o*-xylene.[11] M-PA is produced by reduction of 4-methylphthalic anhydride to the corresponding diol, followed by a Swern oxidation to give the product in high yield.[12] The homopolymerization of all three *o*-phthalaldehyde monomers was conducted with boron trifluoride etherate following our recently reported procedures (Scheme 3.1; Table 3.1, Entries 1-3).[8] The polymerization is quite rapid, giving high molecular weight cyclic polymer within two hours.

Scheme 3.1 | Cationic polymerization reaction*: Polymer collected after precipitation into methanol and washing with methanol and diethyl ether. R substituent corresponds to –H (*o*-PA), -Br (B-PA), or –CH_3 (M-PA).*

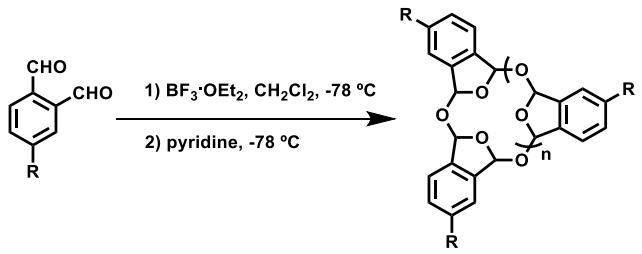

Cyclic homopolymer is obtained in near perfect purity due to the depolymerization of linear contaminants upon warming to room temperature, as confirmed by MALDI-TOF mass spectrometry. Only a single distribution of polymer structures is observed, corresponding to the sodium adduct of the various cyclic PPAs (Figure 3.1). The monomer impurity is presumably washed away in the workup. Furthermore, ^{1}H NMR spectroscopy failed to identify the presence of an end-group, as expected. The polymers were all collected as white, free-flowing solids.

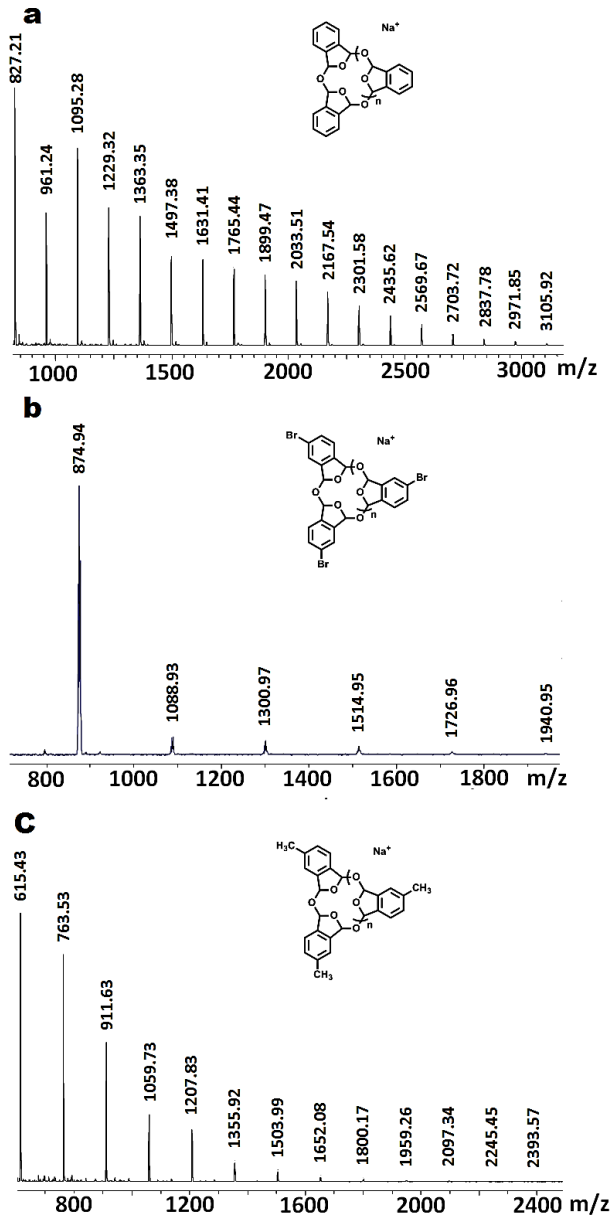

Figure 3.1 | MALDI-TOF mass spectra of cPPAs*: Peaks match sodium adduct of (a) cPPA; (b) cPBPA; and (c) cPMPA. DHB (2,5-dihydroxybenzoic acid) was used as the matrix and sodium iodide as the cationization agent.*

3.3.2 Cationic Copolymerizations of Phthalaldehyde Derivatives

Two unique methods were utilized to synthesize copolymers (See Scheme 3.2). The first, a "random" copolymerization, employed standard cationic polymerization conditions with comonomers combined in a 1:1 molar ratio (Scheme 3.2a; Table 3.1, Entries 4, 7, and 10). Although measurement of reactivity ratios is desirable, reliable methods to determine them are not available when depropagation reactions occur to a significant extent, as is the case in reversible polymerizations.[13] Nevertheless, reactivity ratios are likely close to unity due to the similarity of monomers studied,[14] so the standard copolymerization was presumed to occur in a random or close to random manner.

In a second approach, "scrambling" reactions were pursued where homopolymers were mixed in a 1:1 molar ratio and re-subjected to the polymerization conditions (Scheme 3.2b; Table 3.1, Entries 5, 6, 8, 9, 11, and 12). It was already shown that cyclic homopolymers could be dynamically ring-opened and reach an equilibrium state in the cationic polymerization conditions,[8] but true intermixing between distinct homopolymers was not attempted. We were therefore interested in comparing the scrambled copolymers to the homopolymers as well as random copolymers in an effort to verify the scrambling reaction as well as to investigate microstructure dependence on time and catalyst loading.

Scheme 3.2 | Cationic copolymerization reactions*: a) Random copolymerization; b) Scrambling copolymerization.*

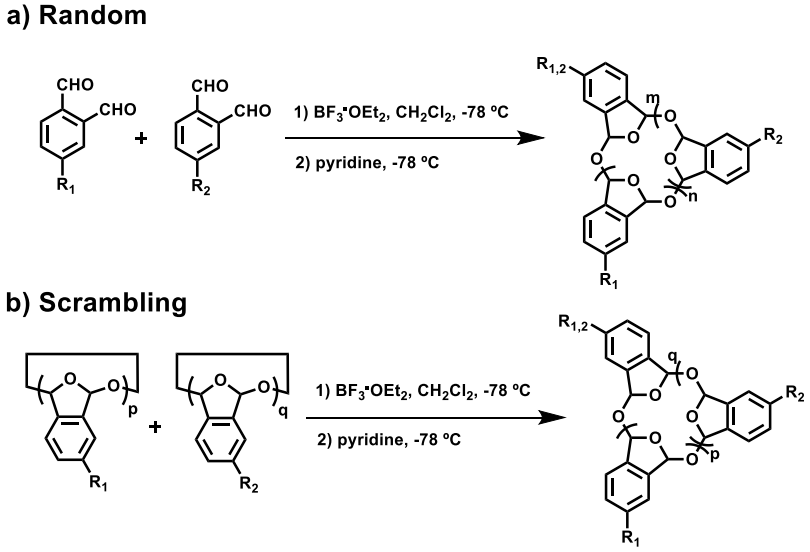

Table 3.1 | Cationic copolymerization reactions and polymers used in this study.

Entry	*Polymer*	R_1	R_2	*Reaction Type*	*Reaction Time*	$[M]^a$	$[M]_0/[I]_0$	*Yield*	M_n (kDa)^b	M_p (kDa)^b	PDI^b
1	cPPA	H	- - -	Homopolymer	2 h	0.7 M	5 / 1	97%	31.7	90.4	2.6
2	cPBPA	Br	- - -	Homopolymer	2 h	0.6 M	8 / 1	42%	2.1	5.4	2.9
3	cPMPA	CH_3	- - -	Homopolymer	2 h	0.6 M	12 / 1	54%	3.8	8.5	2.5
4	r(PPA/PBPA)	H	Br	Random	2 h	1.0 M	8 / 1	58%	8.1	14.2	1.8
5	$s(PPA/PBPA)_1$	H	Br	Scrambling	0.75 h	0.7 M	5 / 1	78%	5.9	13.8	2.3
6	$s(PPA/PBPA)_2$	H	Br	Scrambling	10 h	0.9 M	2 / 1	63%	3.6	6.5	1.9
7	r(PPA/PMPA)	H	CH_3	Random	2 h	1.0 M	8 / 1	55%	8.7	16.8	1.9
8	$s(PPA/PMPA)_1$	H	CH_3	Scrambling	0.75 h	1.0 M	6 / 1	62%	11.2	23.5	2.0
9	$s(PPA/PMPA)_2$	H	CH_3	Scrambling	10 h	1.0 M	2 / 1	51%	5.4	11.1	2.0
10	r(PBPA/PMPA)	Br	CH_3	Random	2 h	1.0 M	12 / 1	50%	2.4	4.9	2.2
11	$s(PBPA/PMPA)_1$	Br	CH_3	Scrambling	0.75 h	1.0 M	6 / 1	75%	6.6	9.9	1.7
12	$s(PBPA/PMPA)_2$	Br	CH_3	Scrambling	10 h	0.9 M	2 / 1	40%	2.6	4.7	1.8

[a]*O*-phthalaldehyde purified before use according to literature procedure.[5a] [b]Average molecular weights and polydispersity determined by gel permeation chromatography (GPC), calibrated with monodisperse polystyrene standards.

3.3.3 GPC and MALDI-TOF Characterization of Scrambled PPAs

All scrambled copolymers were characterized by GPC and compared to the homopolymer precursors. In all cases, it was readily apparent that homopolymers reshuffled to a new, monomodal distribution consistent with the expected outcome of an intermixing reaction (Figure 3.2), retaining polydispersities on the same order as, or even lower than the homopolymers. The monomodal distribution supports our previously described mechanism in which homopolymers ring-open and reach an equilibrium molecular weight distribution during polymerization.[8] The molecular weight depends on temperature and concentration, as previously demonstrated,[6a, 8] with no relation to polymerization time once equilibrium is established. GPC analysis alone, however, is not sufficient to confirm true intermixing of polymer chains rather than a simple equilibration of distinct homopolymers within the blend. MALDI-TOF mass spectrometry was therefore performed to further investigate the scrambling reaction.

MALDI-TOF mass spectrometry verified polymer scrambling to a single copolymer product. The spectra of homopolymer mixtures in a 1:1 ratio reveal two distinct series of peaks corresponding to each distinct homopolymer in the blend (Figure 3.3a-b). For homopolymer mixtures with cPBPA, cyclic hexamer is the highest molecular weight observed for cPBPA, likely due to its reduced tendency to desorb in the MALDI-TOF instrument (as seen in Figure 3.1b) in comparison to cPPA and cPMPA.

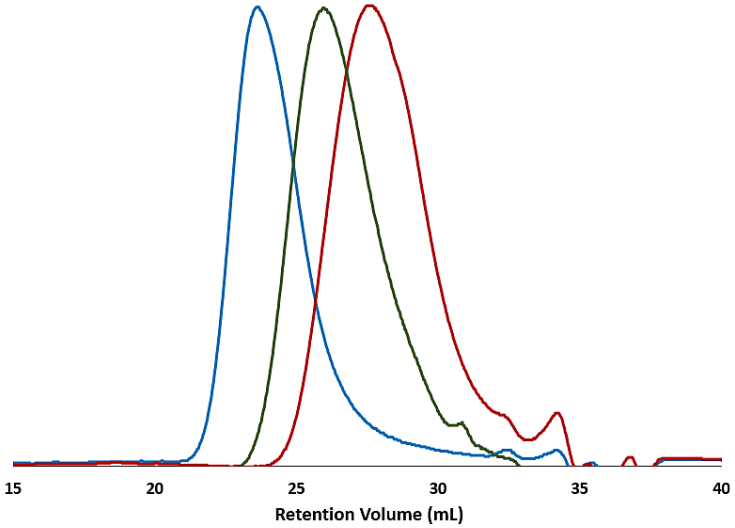

Figure 3.2 | Normalized GPC chromatograms of scrambled cPPA and cPMPA*: cPPA homopolymer (blue trace, M_p = 90.4 kDa) scrambled with cPMPA homopolymer (red trace, M_p = 8.5 kDa) for 45 minutes in cationic polymerization conditions to produce PPA/PMPA scrambled copolymer (green trace, M_p = 23.5 kDa).*

MALDI-TOF spectra of scrambled copolymers, on the other hand, show completely different patterns when compared to the homopolymer mixtures. The copolymers display complex spectra due to intermixing, confirming that scrambling truly does occur rather than the sample remaining a simple homopolymer blend (Figure 3.3c-d). As seen in Figure 3.3c, cyclic pentamer through cyclic nonamer is observed for scrambled cPPA/cPMPA copolymers. Within each cluster of oligomeric peaks, the individual spacing is 14 mass units, corresponding to a series of n-mers with an increasing number of M-PA units. For instance, Figure 3.3d shows a zoom of the seven hexamer copolymer peaks corresponding to: $cPPA_6$, $c(PPA_5 + PMPA_1)$, $c(PPA_4 + PMPA_2)$, $c(PPA_3 + PMPA_3)$, $c(PPA_2 + PMPA_4)$, $c(PPA_1 + PMPA_5)$, and $cPMPA_6$. The analogous pattern of products within each oligomer cluster qualitatively appears to approach a binomial distribution after only 45 minutes of reaction. Copolymers scrambled with cPBPA, however, do not show the fine structure observed for PPA/PMPA copolymers, likely as a result of the reduced tendency for the brominated polymers to desorb in the MALDI-TOF instrument. For those cPPA/cPBPA and cPMPA/cPBPA scrambled copolymers, cPPA and cPMPA homopolymer is still observed as the main series of peaks as well as another series of peaks from $c(PPA_{n-1} + PBPA_1)$ and $c(PMPA_{n-1} + PBPA_1)$, respectively. The presence of this second series of minor peaks confirms the incorporation of PBPA units into either homopolymer and, in conjunction with GPC analysis, verifies that polymer scrambling occurs for all copolymer combinations.

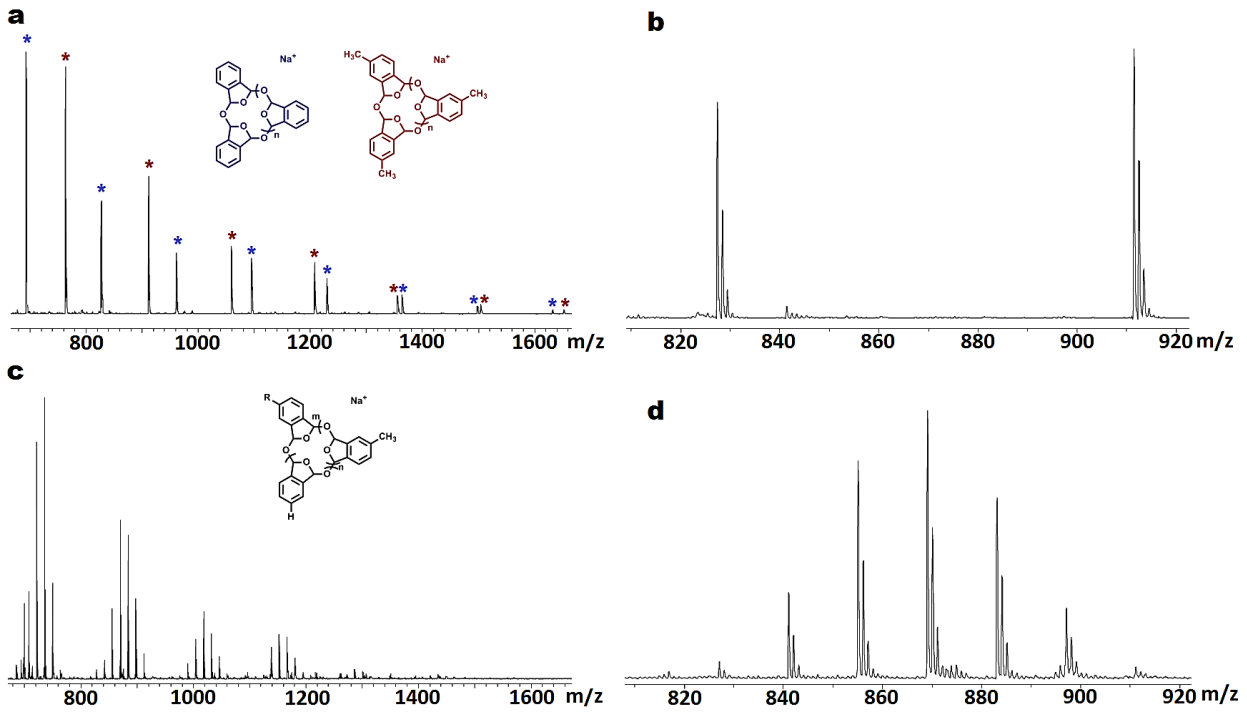

Figure 3.3 | MALDI-TOF mass spectra of blended and scrambled cPPA and cPMPA*: a) MALDI-TOF spectrum of homopolymer mix of cPPA and cPMPA in 1:1 ratio (by weight); distinct series of homopolymer peaks is observed and labeled. b) Expansion of hexamer region in homopolymer mixture; $cPPA_6$ found at 827.3 (theoretical 827.2), $cPMPA_6$ found at 911.4 (theoretical 911.3). c) MALDI-TOF spectrum of scrambled PPA/PMPA copolymer. Oligomers up to 9 repeat units are observed with a fine spacing of 14 mass units, corresponding to the mass difference between monomers and confirming copolymerization occurred. d) Expansion of hexamer region from a sample of scrambled copolymer; approximate binomial distribution of copolymers observed. Most abundant peak found at 869.1 [theoretical $c(PPA_3/PMPA_3)$ 869.3]. DHB (2,5-dihydroxybenzoic acid) was used as the matrix and sodium iodide as the cationization agent.*

3.3.4 Kinetic Investigation of cPPA and cPMPA Scrambling

A series of scrambling copolymerizations was conducted between cPPA and cPMPA to track the time evolution of polymer microstructure. Ring size equilibration was monitored by GPC, while compositional change was tracked by MALDI-TOF analysis. Scrambled cPPA/cPMPA was selected due to the ability to readily monitor copolymer composition by MALDI-TOF mass spectrometry, unlike the PBPA copolymers. Copolymerization reactions were carried out between 10 and 240 min at -78 °C. The scrambling copolymerization is extremely rapid—the GPC traces transform from a bimodal mix of homopolymers to a peak with minor shouldering after only 30 min (Figure 3.4a). A monomodal peak is observed at and beyond 45 min, and the polydispersity drops and stabilizes to a steady state of approximately two at the same time-point (Figure 3.4b).

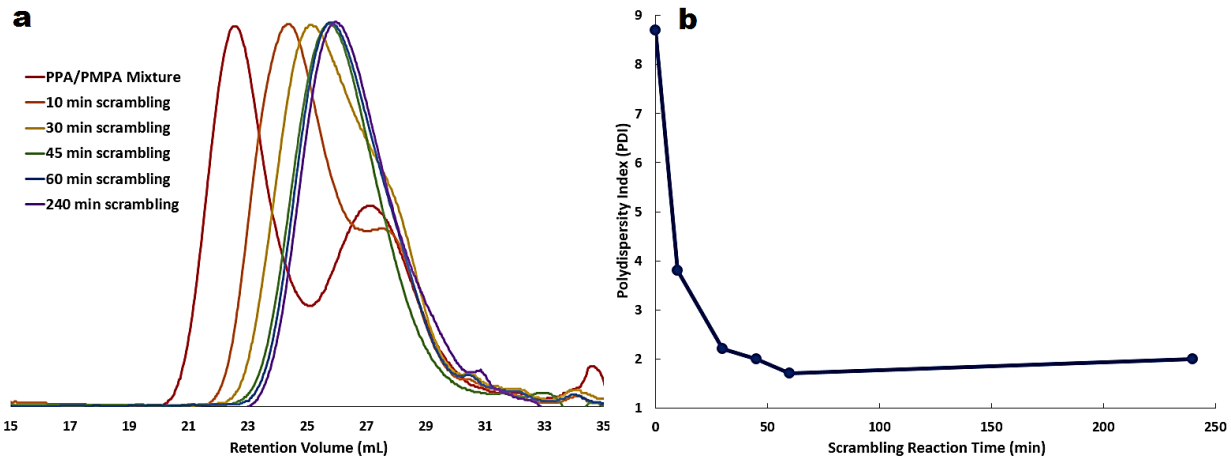

Figure 3.4 | GPC analysis of cPPA and cPMPA scrambling*: a) cPPA and cPMPA homopolymer mix (red trace) overlayed with polymer products from cPPA/cPMPA scrambling copolymerizations of various reaction times. b) Polydispersity index (PDI) of the polymer mixture as a function of time during cPPA/cPMPA scrambling copolymerization at -78 °C.*

Likewise, MALDI-TOF characterization confirmed a rapid compositional transformation from the simple cPPA/cPMPA homopolymer blend to a copolymer over the course of the scrambling reaction. Within 10 min, a full series of copolymer products is observed (Figure 3.5b), although the unreacted homopolymers remain the major product. This is consistent with the bimodal trace in the GPC as well as the substantial drop in polydispersity after 10 min, as the homopolymers begin to intermix to copolymers. After 30 min of reaction time, the copolymer products begin to stand out from the homopolymer (Figure 3.5c), but appreciable homopolymer peaks remain. A binomial distribution has not yet been reached, as the theoretical ratio of homopolymer peaks to the greatest copolymer peak for the hexamer cluster should be 1/20, which is clearly not observed. Again, this matches GPC findings at the same time-point, as the polymer product shows shouldering in the GPC traces confirming that it has not yet fully equilibrated to its final molecular weight distribution. Finally, after 45 min of scrambling, the homopolymer peaks are greatly diminished and the scrambling reaction is essentially complete (Figure 3.5d). The ratio of homopolymer to the greatest copolymer peak in the hexamer cluster qualitatively approaches that of the binomial distribution. It can be expected that all homopolymers have fully reacted by this point, and the remaining homopolymer observed has simply scrambled with identical monomer and polymer products.

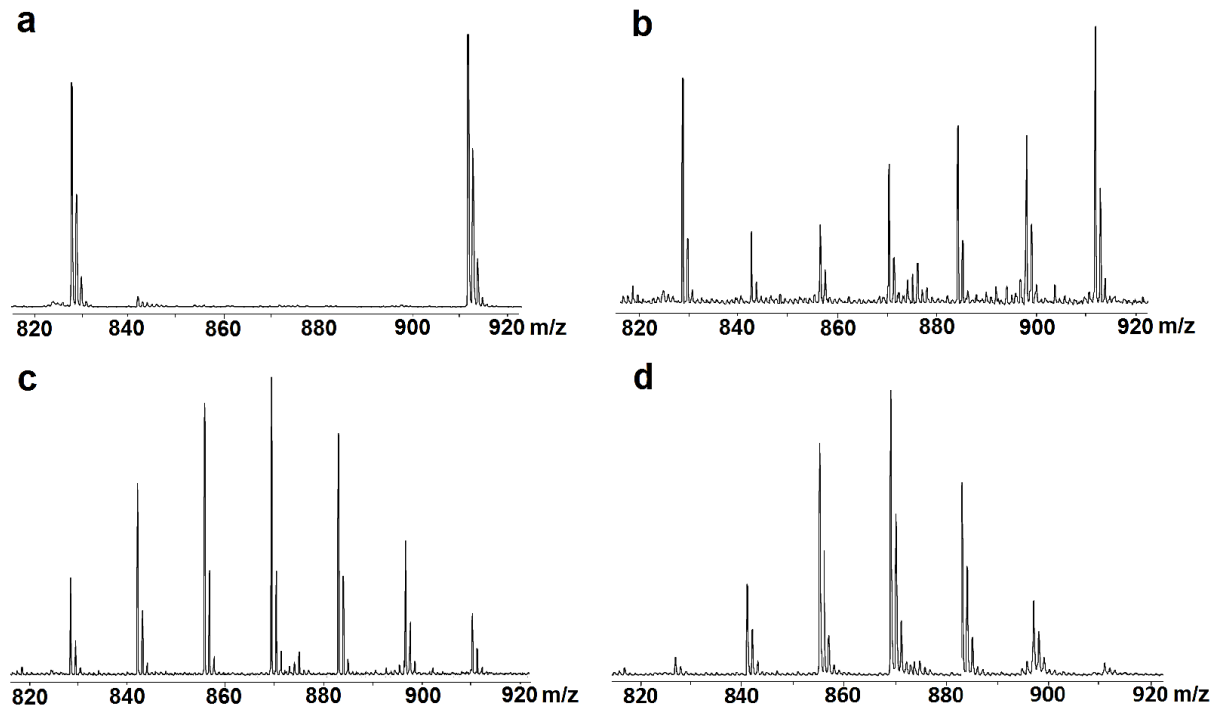

Figure 3.5 | MALDI-TOF analysis of cPPA and cPMPA scrambling, expanded on hexamer clusters*: a) MALDI-TOF spectrum of homopolymer mix of cPPA and cPMPA in 1:1 ratio (by weight); $cPPA_6$ found at 827.3 (theoretical 827.2), $cPMPA_6$ found at 911.4 (theoretical 911.3). b) MALDI-TOF spectrum of cPPA and cPMPA scrambled for 10 min. c) MALDI-TOF spectrum of cPPA and cPMPA scrambled for 30 min. d) MALDI-TOF spectrum of cPPA and cPMPA scrambled for 45 min. DHB (2,5-dihydroxybenzoic acid) was used as the matrix and sodium iodide as the cationization agent.*

3.3.5 NMR Characterization of Scrambled PPA Microstructures

^{13}C NMR spectroscopy was employed to further investigate the microstructure of all copolymers synthesized. Interestingly, the "random" copolymers displayed resonances that matched the carbons of each respective homopolymer, except at carbons in the polymer backbone and those directly adjacent to the polymer backbone. For instance, Figure 3.6a shows the shift observed in the aromatic carbons adjacent to the polymer backbone in random cPBPA/cPMPA copolymers as compared to each respective homopolymer. Both cPBPA carbon peaks shift downfield (from 140.7 ppm and 137.4 ppm to 141.0 ppm and 137.7 ppm, respectively), while the cPMPA carbons shift upfield (from 138.9 ppm and 135.8 ppm to 138.7 ppm and 135.6 ppm, respectively). While these shifts in resonance are seemingly inconsequential, the peaks of copolymers scrambled for 45 min almost entirely match the resonances of all homopolymer carbons, even those in the backbone and adjacent aromatic carbons (Figure 3.6b). Similar results are observed for both cPPA/cPBPA and cPPA/cPMPA copolymers as well (see section 3.6).

These results suggest that copolymers scrambled for short times retain a blocky microstructure. The "random" copolymer, on the other hand, shows a distinct microstructure different from either homopolymer. While it may not necessarily be perfectly random, it at least appears to be less blocky than the scrambled copolymer microstructure.

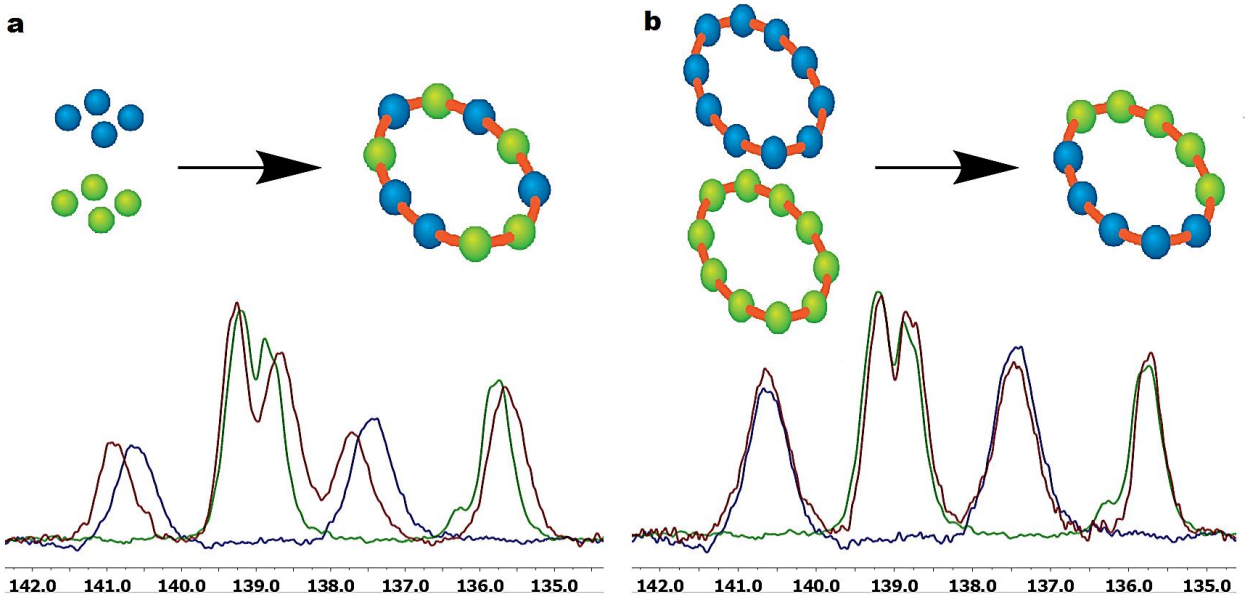

Figure 3.6 | ^{13}C NMR spectra of cPBPA/cPMPA random and scrambled copolymers*: a) PBPA/PMPA copolymer produced from "random" copolymerization reaction (red), overlayed with cPBPA (blue) and cPMPA (green) homopolymers. Shifts in resonance are observed in aromatic carbons adjacent to copolymer backbone. b) PBPA/PMPA scrambled copolymer after 45 min reaction (red), overlayed with cPBPA (blue) and cPMPA (green) homopolymers. Overlap in resonances of carbons adjacent to copolymer backbone suggests a blocky polymer microstructure. All NMR spectra collected with DMSO-d_6 solvent.*

Homopolymers were allowed to engage in scrambling reactions for up to 10 h in an attempt to further transform the copolymer microstructure. It was found that copolymers scrambled for 4 h resembled the blocky microstructure found in copolymers scrambled for 45 min. However, when the homopolymers were scrambled for 10 h with 50% catalyst loading, a unique microstructure was identified by ^{13}C NMR. The aromatic carbons adjacent to the copolymer backbone in cPBPA/cPMPA copolymers again shift in resonance (Figure 3.7), signifying that the microstructure approaches the more random structure observed in "random" copolymers. Similar observations were also made for cPPA/cPBPA and cPPA/cPMPA scrambled copolymers (see section 3.6).

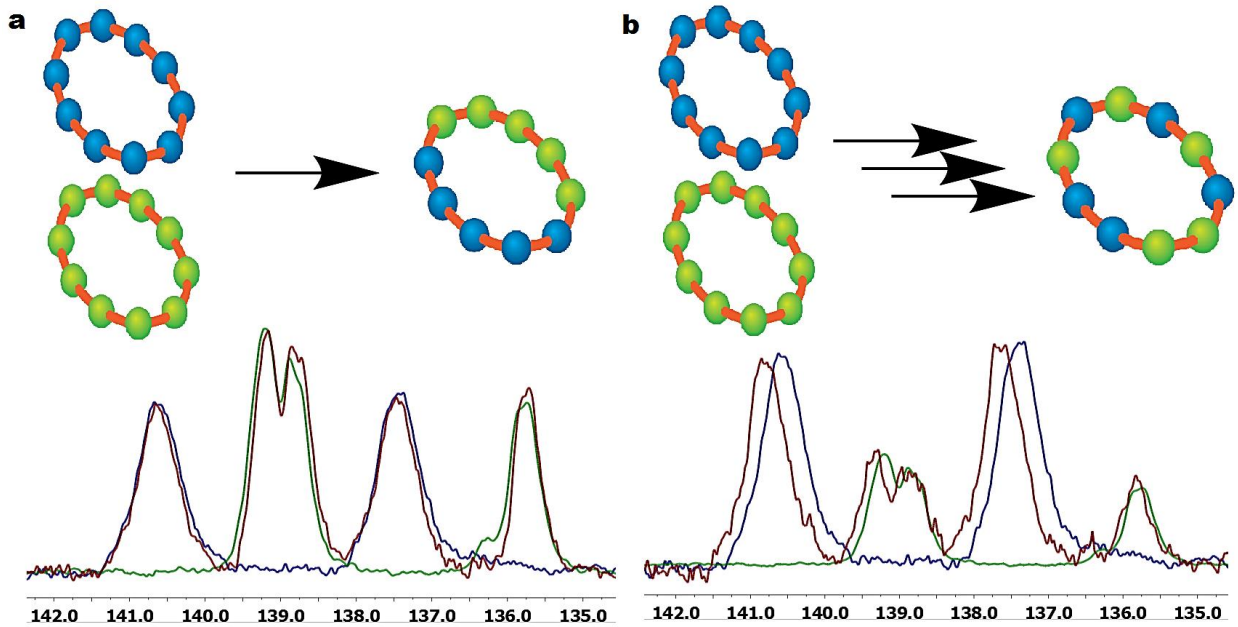

Figure 3.7 | ^{13}C NMR spectra of cPBPA/cPMPA scrambled copolymers*: a) cPBPA/cPMPA scrambled copolymer after 45 min reaction (red), overlayed with cPBPA (blue) and cPMPA (green) homopolymers to confirm blocky polymer microstructure. b) cPBPA/cPMPA scrambled copolymer after 10 h reaction (red), overlayed with cPBPA (blue) and cPMPA (green) homopolymers to illustrate changes in polymer microstructure. All NMR spectra collected with DMSO-d_6 solvent.*

It is quite valuable that a full array of copolymer structures can be obtained by this scrambling copolymerization approach; a diversity of products ranging from homopolymer, to multi-block copolymers, to completely random copolymers is possible with this technique. One could envision synthesizing a series of copolymer products with increasingly shorter block sizes (and increasingly random sequences) simply by varying the reaction time. Scrambling copolymerization reactions thus represent a unique and useful tool in polymer synthesis. In fact, the biggest limitation we face is fully characterizing these copolymers with current analytical techniques, which prevents us from knowing the true depth of this method in synthesizing complex copolymer products.

3.3.6 Scrambling Copolymerization Mechanism

On the basis of the above observations, we propose a scrambling mechanism whereby, in the presence of initiator, macrocyclic polymers open to linear polymeric species and intermix, then back-bite to form cyclic copolymer products (Scheme 3.3). The rapid formation of multi-block cyclic copolymers suggests transposition of polymer fragments rather than depolymerization to monomer followed by copolymerization. Under polymerization conditions, cyclic homopolymer (**1C**) reacts with cationic initiator

(**RX**) to form a linear cationic species (**1**), which is stable below its T_c. The linear species thus formed closes back to cyclic homopolymer by intramolecular back-biting, reacts with other linear species (not shown for clarity), or is attacked by a cyclic homopolymer (**2C**) in the mixture. Intermixing with identical cyclics (or linears) retains linear homopolymer species **1**, but scrambling with different cyclics/linears produces linear block copolymers (**3**) that cyclize to produce isolable cyclic block copolymers (**3C**). The scrambling is entropically-driven; i.e., without providing a "de-mixing" impetus such as adding a template, scrambling is irreversible. Kinetic investigations on the scrambling reaction suggest that molecular weight equilibration and intermixing to copolymer occur on similar time scales. Thus, the rate of intramolecular back-biting is on the same order as intermixing and subsequent cyclization. Once formed, cyclic block copolymers (**3C**) continue to react with initiator and linear chains to reach an equilibrium mixture of linear and cyclic random copolymer species (**4** and **4C**). As before, the scrambling process is entropically-driven, so scrambling from blocky to random copolymers is an exergonic and irreversible process.

Scheme 3.3 | Proposed mechanism of cationic scrambling copolymerization reaction.

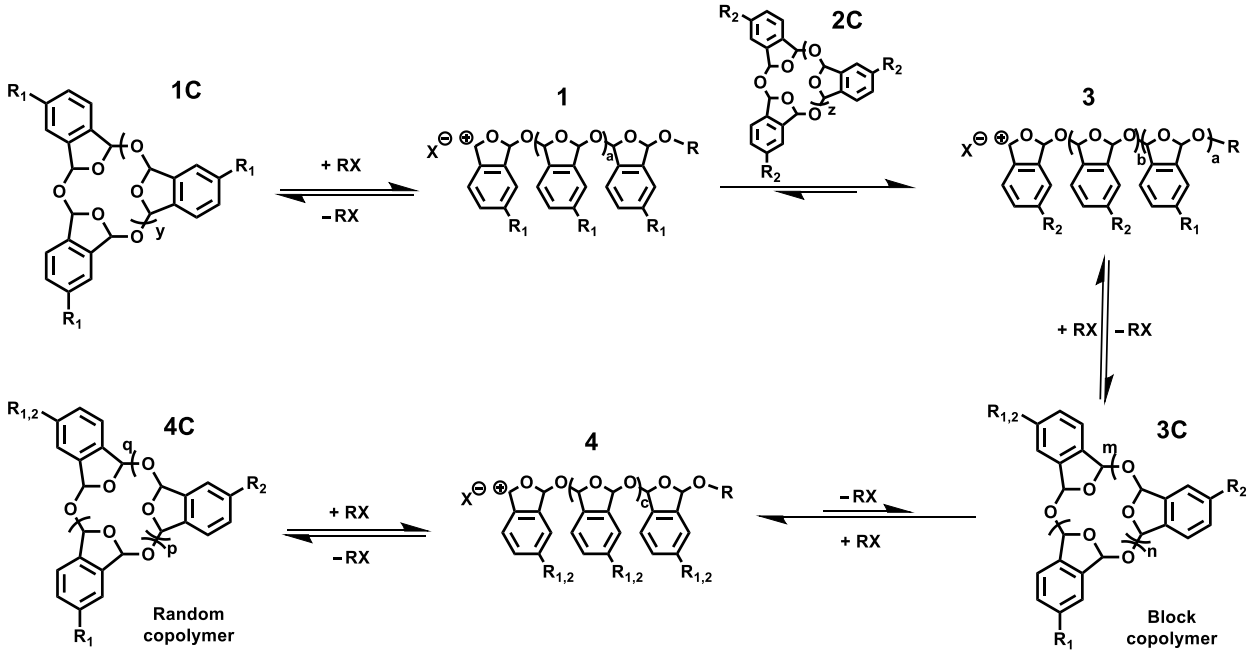

3.4 Conclusions

It was demonstrated that cyclic homopolymer mixtures could be transformed into multi-block and random cyclic copolymers through the manipulation of dynamic, reversible covalent bonds. The cationic polymerization of phthalaldehyde derivatives produces cyclic homopolymer of well-defined molecular weight; mixtures of these homopolymers are dynamically scrambled to produce a diversity of copolymer microstructures. Copolymerization was monitored and verified by GPC analysis and MALDI-TOF mass spectrometry, and ^{13}C NMR spectroscopy was used to elucidate copolymer structures. The entropically-driven scrambling technique enables easy access to a range of copolymer microstructures, from pure homopolymer to blocky and eventually random structures.

These cPPA polymers represent a new class of dynamic covalent macrocyclic polymers based on the chemically labile polyacetal motif. One could envision incorporating a template into scrambling reactions to selectively amplify specific macrocycles and obtain desired polymer products in extremely high purity. Further, the use of boron trifluoride, a relatively ubiquitous cationic initiator, introduces the potential to scramble other monomers into cPPA that are also polymerized by boron trifluoride. This may provide a quick and convenient method for the production of cyclic multi-block copolymers from other polyacetals such as polyoxymethylene or other aliphatic aldehyde polymers. Such scrambling reactions could rapidly produce a vast array of macrocyclic copolymer products that are either impossible or difficult to produce through other, more conventional routes. These matters are currently under investigation in an effort to expand the utility of the scrambling copolymerization technique.

Finally, this work exposes a significant limitation (and opportunity) in current analytical techniques. Without an effective method to probe block sizes and number of blocks in complex copolymer products, we do not know the full range of copolymer products produced by the reaction. An analytical technique capable of addressing such sequencing issues would be quite enabling in synthetic polymer chemistry, as we ultimately desire to attain control over block sizes and number of blocks in this scrambling copolymerization reaction.

3.5 Synthetic Procedures

Scheme 3.4 **|** *4-bromo phthalaldehyde synthesis.*

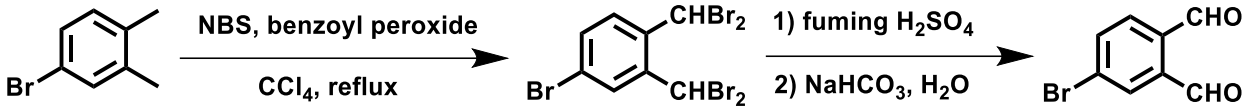

4-bromo-1,2-bisdibromomethylbenzene:

To a stirring mixture of 4-bromo-*o*-xylene (8.00 g, 43 mmol) in 105 mL CCl_4 was sequentially added N-bromo succinimide (32.00 g, 180 mmol) and benzoyl peroxide (1.00 g, 4 mmol). The mixture was heated to reflux for 14 h, then cooled to 0 °C and the precipitate filtered off and washed with diethyl ether. The solvent was removed *in vacuo*, redissolved in dichloromethane (100 mL), and washed with water (2 x 200 mL) and brine (200 mL). The organic phase was dried over $MgSO_4$ and concentrated to give a yellow solid. Recrystallization from diethyl ether and hexanes gave 4-bromo-1,2-bis-dibromomethylbenzene as a pale yellow powder (11.4 g, 53% yield). ^{1}H NMR (500 MHz, $CDCl_3$) δ 8.07 ppm (m, 2H, Ar-H), 7.64 ppm (m, 1H, Ar-H), 7.50 ppm (m, 2H, CH). LR FD-MS (*m/z*): $[C_8H_5Br_5]^+$ Found 499.8; Calculated 499.6.

4-bromophthalaldehyde:

In a flask cooled to 0 °C, 4-bromo-1,2-bisdibromomethylbenzene (5.00 g, 10 mmol) was dissolved in fuming sulfuric acid (7 mL, 140 mmol). The mixture was stirred at 0 °C for 10 min, followed by 20 min at room temperature. Then, the mixture was cooled back to 0 °C and sat. aq. $NaHCO_3$ (60 mL) was slowly added and stirred until bubbling ceased. The solution was extracted with ethyl acetate (3 x 125 mL), washed with sat. aq. $NaHCO_3$ (2 x 60 mL) and brine (100 mL), dried over $MgSO_4$ and concentrated to give a yellow residue. The residue was recrystallized from hexanes to give 4-bromophthalaldehyde as a yellow powder (1.08 g, 51% yield). ^{1}H NMR (500 MHz, $CDCl_3$) δ 10.51 ppm (s, 1H, CHO), 10.44 ppm (s, 1H, CHO), 8.09 ppm (d, 1H, Ar-H, J = 3 Hz), 7.90 ppm (dd, 1H, Ar-H, J = 3 Hz, 10 Hz), 7.84 ppm (d, 1H, Ar-H, J = 10 Hz). ^{13}C{^{1}H} NMR (125 MHz, $CDCl_3$) δ 191.3 ppm, 190.8 ppm, 136.8 ppm, 134.9 ppm, 133.9 ppm, 133.0 ppm, 132.0 ppm, 129.3 ppm. LR FD-MS (*m/z*): $[C_8H_5BrO_2]^+$ Found 212.2; Calculated 211.9.

***Scheme 3.5** | 4-methyl phthalaldehyde synthesis.*

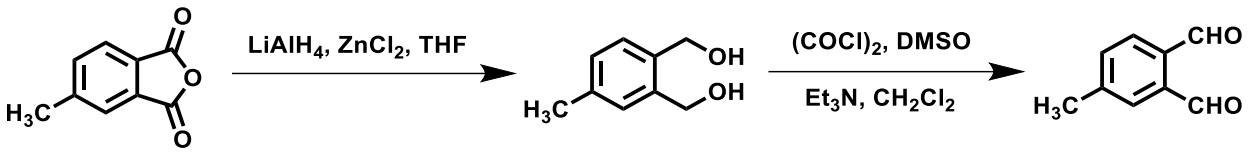

4-methyl-1,2-bishydroxymethylbenzene:

A suspension was prepared of lithium aluminum hydride (3.80 g, 100 mmol) and zinc chloride (4.10 g, 30 mmol) in 200 mL dry tetrahydrofuran. The suspension was cooled to 0 °C and 4-methyl phthalic anhydride (8.00 g, 50 mmol) in 50 mL dry tetrahydrofuran was added dropwise. The mixture was then warmed to room temperature and left stirring for 6 h. Quenching was done by dropwise addition of 30 mL ice water followed by 60 mL 2 M aq. HCl. The product was extracted into ethyl acetate (3 x 100 mL), washed with brine (2 x 200 mL), dried over $MgSO_4$ and concentrated to give a yellow oil. The crude oil was purified by flash column chromatography in 3:2 ethyl acetate:hexanes (R_f = 0.4) to give 4-methyl-1,2-bis-hydroxymethylbenzene as a white solid (2.93 g, 79%). ^{1}H NMR (500 MHz, $CDCl_3$) δ 7.20-7.09 ppm (m, 3H, Ar-H), 7.78 ppm (d, 1H, Ar-H, J = 3 Hz), 7.57 ppm (dd, 1 H, Ar-H, J = 3 Hz, 5 Hz), 4.60 ppm (s, 4H, Ar-CH_2) 3.72 ppm (br, OH) 2.34 ppm (s, 3H, CH_3). HR ESI-MS (*m/z*): $[C_9H_{12}NaO_2]^+$ Found 175.0730; Calculated 175.0735.

4-methylphthalaldehyde:

A solution of oxalyl chloride (3 mL, 35 mmol) in 100 mL dry dichloromethane was cooled to -78 °C. To the stirring solution was added DMSO (5 mL, 70 mmol) and stirring was continued 5 min. Then, 4-methyl-1,2-bishydroxymethylbenzene (1.98 g, 13 mmol) in 80 mL dry dichloromethane was added and stirring continued 20 min at -78 °C. Finally, triethylamine (21 mL, 150 mmol) was added and the mixture left 10 min at -78 °C, then warmed to room temperature and left an additional 2 h. The reaction was quenched with 150 mL 0.1 M aq. HCl, extracted into dichloromethane (3 x 70 mL), and washed with brine (200 mL). The organic phase was dried over $MgSO_4$ and concentrated to give a yellow oil. The crude oil was purified by flash column chromatography in 3:7 ethyl acetate:hexanes (R_f = 0.5) to give 4-methylphthalaldehyde as a yellow solid (1.67 g, 87%). ^{1}H NMR (500 MHz, $CDCl_3$) δ 10.56 ppm (s, 1H, CHO), 10.47 ppm (s, 1H, CHO), 7.88 ppm (d, 1H, Ar-H, J = 5 Hz), 7.78 ppm (d, 1H, Ar-H, J = 3 Hz), 7.57 ppm (dd, 1H, Ar-H, J = 3 Hz, 5 Hz), 2.52 ppm (s, 3H, CH_3). ^{13}C{^{1}H} NMR (125 MHz, $CDCl_3$) δ 192.4 ppm, 191.9 ppm, 144.8 ppm, 136.1 ppm, 134.0 ppm, 133.7 ppm, 131.4 ppm, 131.2 ppm, 21.3 ppm. LR FD-MS (*m/z*): $[C_9H_8O_2]^+$ Found 148.0; Calculated 148.1.

Scheme 3.6 **|** *General cationic homopolymerization.*

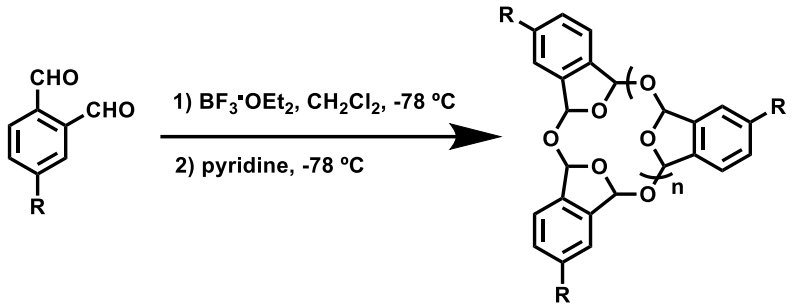

The respective phthalaldehyde monomer (2 mmol) is weighed into a Schlenk flask and dissolved in dry dichloromethane (3 mL). The solution is cooled to -78 °C and boron trifluoride etherate is added (0.02 mL, 0.16 mmol). The reaction is left stirring at -78 °C for 2 h, then pyridine (0.08 mL, 1 mmol) is added. The mixture is left stirring 2 h at -78 °C, then brought to room temperature and the polymer precipitated by pouring into methanol (100 mL). The product is collected by filtration, then further purified by dissolving in dichloromethane and re-precipitating from methanol and washing in diethyl ether.

cPPA (97% yield): ^{1}H NMR (500 MHz, DMSO-d_6) δ 7.75-7.05 ppm (br, 4H, aromatic), 7.05-6.25 ppm (br, 2H, acetal). ^{13}C{^{1}H} NMR (125 MHz, DMSO-d_6) δ 138.4 ppm, 129.6 ppm, 123.0 ppm, 105.0-101.0 ppm.

cPBPA (42% yield): ^{1}H NMR (500 MHz, DMSO-d_6) δ 8.25-7.00 ppm (br, 3H, aromatic), 7.00-6.10 ppm (br, 2H, acetal). ^{13}C{^{1}H} NMR (125 MHz, DMSO-d_6) δ 140.6 ppm, 137.4 ppm, 132.7 ppm, 126.5 ppm, 125.7 ppm, 122.8 ppm, 106.0-100.0 ppm.

cPMPA (54% yield): ^{1}H NMR (500 MHz, DMSO-d_6) δ 7.65-6.95 ppm (br, 3H, aromatic), 6.95-6.10 ppm (br, 2H, acetal), 2.45-1.75 ppm (br, 3H, CH_3). ^{13}C{^{1}H} NMR (125 MHz, DMSO-d_6) δ 139.2 ppm, 138.9 ppm, 135.8 ppm, 130.4 ppm, 123.1 ppm, 122.7 ppm, 105.5-100.3 ppm, 20.8 ppm.

Table 3.2 **|** *Homopolymer samples.*

Entry	*Polymer*	$[M]_0$	$[M]_0/[I]_0$	*Yield*	M_n *(kDa)*[a]	M_p *(kDa)*[a]	*PDI*[a]
1	cPPA	0.7 M	5 / 1	97%	31.7	90.4	2.6
2	cPBPA	0.6 M	8 / 1	42%	2.1	5.4	2.9
3	cPMPA	0.6 M	12 / 1	54%	3.8	8.5	2.5

[a]Average molecular weights and polydispersity determined by gel permeation chromatography (GPC), calibrated with monodisperse polystyrene standards.

Scheme 3.7 *| General cationic copolymerization.*

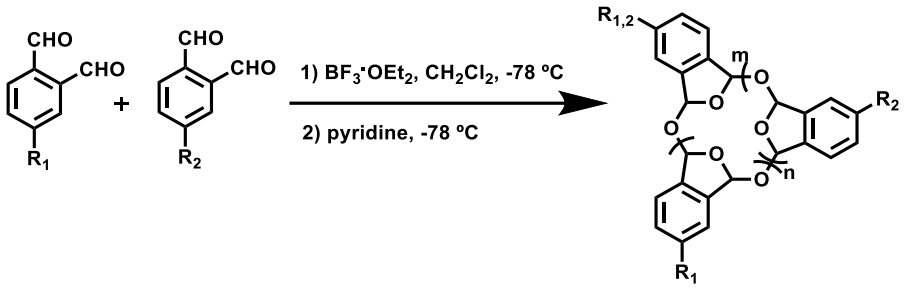

Phthalaldehyde monomer **1** (1 mmol) and phthalaldehyde monomer **2** (1 mmol) are weighed into a Schlenk flask and dissolved in dry dichloromethane (2 mL). The solution is cooled to -78 °C and boron trifluoride etherate is added (0.02 mL, 0.16 mmol). The reaction is left stirring at -78 °C for 2 h, then pyridine (0.08 mL, 1 mmol) is added. The mixture is left stirring 2 h at -78 °C, then brought to room temperature and the polymer precipitated by pouring into methanol (100 mL). The product is collected by filtration, then further purified by dissolving in dichloromethane and re-precipitating from methanol and washing in diethyl ether.

r(PPA/PBPA) (58% yield): ^{1}H NMR (500 MHz, DMSO-d_6) δ 8.30-7.05 ppm (br, 3.6H, aromatic), 7.05-6.20 ppm (br, 2H, acetal). ^{13}C{^{1}H} NMR (125 MHz, DMSO-d_6) δ 140.8 ppm, 138.3 ppm, 137.7 ppm, 132.6 ppm, 129.6 ppm, 126.5 ppm, 125.7 ppm, 123.4 ppm, 122.8 ppm, 106.0-100.2 ppm.

r(PPA/PMPA) (55% yield): ^{1}H NMR (500 MHz, DMSO-d_6) δ 7.95-7.00 ppm (br, 3.4H, aromatic), 7.00-6.15 ppm (br, 2H, acetal), 2.45-1.70 ppm (br, 1.5H, CH_3). ^{13}C{^{1}H} NMR (125 MHz, DMSO-d_6) δ 139.3 ppm, 138.9 ppm, 138.5 ppm, 135.7 ppm, 130.4 ppm, 129.6 ppm, 123.0 ppm, 106.0-100.4 ppm, 20.8 ppm.

r(PBPA/PMPA) (50% yield): ^{1}H NMR (500 MHz, DMSO-d_6) δ 8.30-7.00 ppm (br, 3H, aromatic), 7.00-6.10 ppm (br, 2H, acetal), 2.45-1.75 ppm (br, 1.8H, CH_3). ^{13}C{^{1}H} NMR (125 MHz, DMSO-d_6) δ 140.9 ppm, 139.3 ppm, 138.7 ppm, 137.7 ppm, 135.6 ppm, 132.6 ppm, 130.4 ppm, 126.5 ppm, 125.8 ppm, 122.7 ppm, 105.8-100.4 ppm, 20.9 ppm.

Table 3.3 *| Copolymer samples.*

Entry	*Polymer*	*$[M]_0$*	*$[M]_0/[I]_0$*	*Yield*	*M_n (kDa)[a]*	*M_p (kDa)[a]*	*PDI[a]*
1	r(PPA/PBPA)	1.0 M	8 / 1	58%	8.1	14.2	1.8
2	r(PPA/PMPA)	1.0 M	8 / 1	55%	8.7	16.8	1.9
3	r(PBPA/PMPA)	1.0 M	12 / 1	50%	2.4	4.9	2.2

[a]Average molecular weights and polydispersity determined by gel permeation chromatography (GPC), calibrated with monodisperse polystyrene standards.

Scheme 3.8 **|** *Polymer scrambling reactions.*

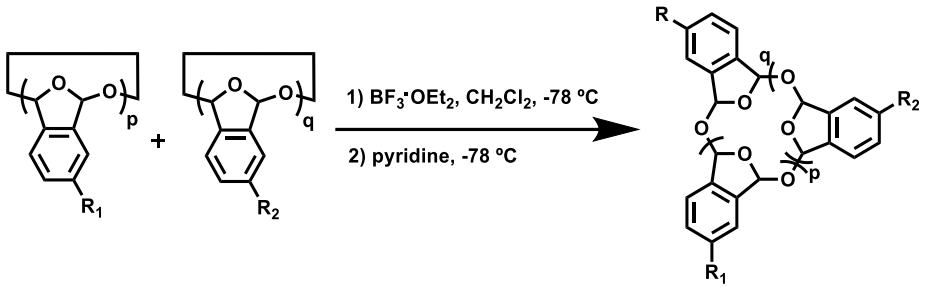

Polymer **1** (0.5 mmol monomer) and Polymer **2** (0.5 mmol monomer) are weighed into a Schlenk flask and dissolved in dichloromethane (1.5 mL). The solution is cooled to -78 °C and boron trifluoride etherate is added (0.02 mL, 0.16 mmol). The reaction is left stirring at -78 °C for 0.75-10 h, then pyridine (0.08 mL, 1 mmol) is added. The mixture is left stirring 2 h at -78 °C, then brought to room temperature and then the polymer precipitated by pouring into methanol (100 mL). The product is collected by filtration, then further purified by dissolving in dichloromethane and re-precipitating from methanol and washing in diethyl ether.

s(PPA/PBPA)$_1$ (78% yield): ^{1}H NMR (500 MHz, DMSO-d_6) δ 8.25-7.05 ppm (br, 3.5H, aromatic), 7.05-6.20 ppm (br, 2H, acetal). ^{13}C{^{1}H} NMR (125 MHz, DMSO-d_6) δ 140.7 ppm, 138.4 ppm, 137.5 ppm, 132.7 ppm, 129.6 ppm, 126.5 ppm, 125.8 ppm, 123.5 ppm, 122.9 ppm, 106.0-100.5 ppm.

s(PPA/PMPA)$_1$ (62% yield): ^{1}H NMR (500 MHz, DMSO-d_6) δ 7.85-7.00 ppm (br, 3.5H, aromatic), 7.00-6.15 ppm (br, 2H, acetal), 2.45-1.70 ppm (br, 1.2H, CH_3). ^{13}C{^{1}H} NMR (125 MHz, DMSO-d_6) δ 139.2 ppm, 138.8 ppm, 138.5 ppm, 135.8 ppm, 130.4 ppm, 129.6 ppm, 123.5 ppm, 122.9 ppm, 106.0-100.6 ppm, 20.8 ppm.

s(PBPA/PMPA)$_1$ (75% yield): ^{1}H NMR (500 MHz, DMSO-d_6) δ 8.30-7.00 ppm (br, 3H, aromatic), 7.00-6.15 ppm (br, 2H, acetal), 2.45-1.75 ppm (br, 1.5H, CH_3). ^{13}C{^{1}H} NMR (125 MHz, DMSO-d_6) δ 140.7 ppm, 139.2 ppm, 138.8 ppm, 137.5 ppm, 135.8 ppm, 132.7 ppm, 130.4 ppm, 126.5 ppm, 125.8 ppm, 122.9 ppm, 105.8-100.5 ppm, 20.8 ppm.

***Table 3.4** | Scrambled copolymer samples.*

Entry	*Copolymer*	$[M]_0$	$[M]_0/[I]_0$	*Reaction Time*	*Yield*	M_n *(kDa)*[a]	M_p *(kDa)*[a]	*PDI*[a]
1	s(PPA/PBPA)$_1$	0.7 M	5 / 1	0.75 h	78%	5.9	13.8	2.3
2	s(PPA/PBPA)$_2$	0.7 M	4 / 1	4 h	80%	5.1	8.8	2.1
3	s(PPA/PBPA)$_3$	0.9 M	2 / 1	10 h	63%	3.6	6.5	1.9
4	s(PPA/PMPA)$_1$	1.0 M	6 / 1	0.75 h	62%	11.2	23.5	2.0
5	s(PPA/PMPA)$_2$	0.7 M	5 / 1	4 h	60%	10.6	20.5	2.0
6	s(PPA/PMPA)$_3$	1.0 M	2 / 1	10 h	51%	5.4	11.1	2.0
7	s(PBPA/PMPA)$_1$	1.0 M	6 / 1	0.75 h	75%	6.6	9.9	1.7
8	s(PBPA/PMPA)$_2$	0.9 M	2 / 1	10 h	40%	2.6	4.7	1.8

[a]Average molecular weights and polydispersity determined by gel permeation chromatography (GPC), calibrated with monodisperse polystyrene standards.

***Scheme 3.9** | cPPA/cPMPA scrambling time series.*

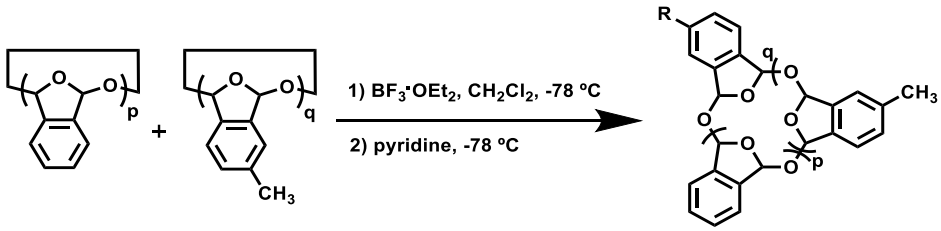

cPPA (40 mg) and cPMPA (40 mg) are weighed into a Schlenk flask and dissolved in dichloromethane (1.0 mL). The solution is cooled to -78 °C and boron trifluoride etherate is added (0.02 mL, 0.16 mmol). The reaction is left stirring at -78 °C for an allotted time, then pyridine (0.08 mL, 1 mmol) is added. The mixture is left stirring 2 h at -78 °C, then brought to room temperature and then the polymer precipitated by pouring into methanol (100 mL). The product is collected by filtration, then further purified by dissolving in dichloromethane and re-precipitating from methanol and washing in diethyl ether.

***Table 3.5** | Scrambled cPPA/cPMPA samples.*

Entry	*Reaction Time*	$[M]_0$	$[M]_0/[I]_0$	*Yield*	M_n *(kDa)*[a]	M_p *(kDa)*[a]	*PDI*[a]	*Notes*
1	0 min	- - -	- - -	- - -	14.5	125	8.7	Bimodal
2	10 min	0.6 M	4 / 1	64%	11.6	50.1	3.8	Bimodal
3	30 min	0.6 M	4 / 1	60%	13.3	33.6	2.2	Shouldering
4	45 min	1.0 M	6 / 1	62%	11.2	23.5	2.0	Monomodal
5	60 min	0.6 M	4 / 1	58%	12.5	23.2	1.7	Monomodal
6	240 min	0.7 M	5 / 1	60%	10.6	20.5	2.0	Monomodal

[a]Average molecular weights and polydispersity determined by gel permeation chromatography (GPC), calibrated with monodisperse polystyrene standards.

3.6 NMR Spectra, MALDI Spectra and ^{13}C NMR Spectral Overlays.

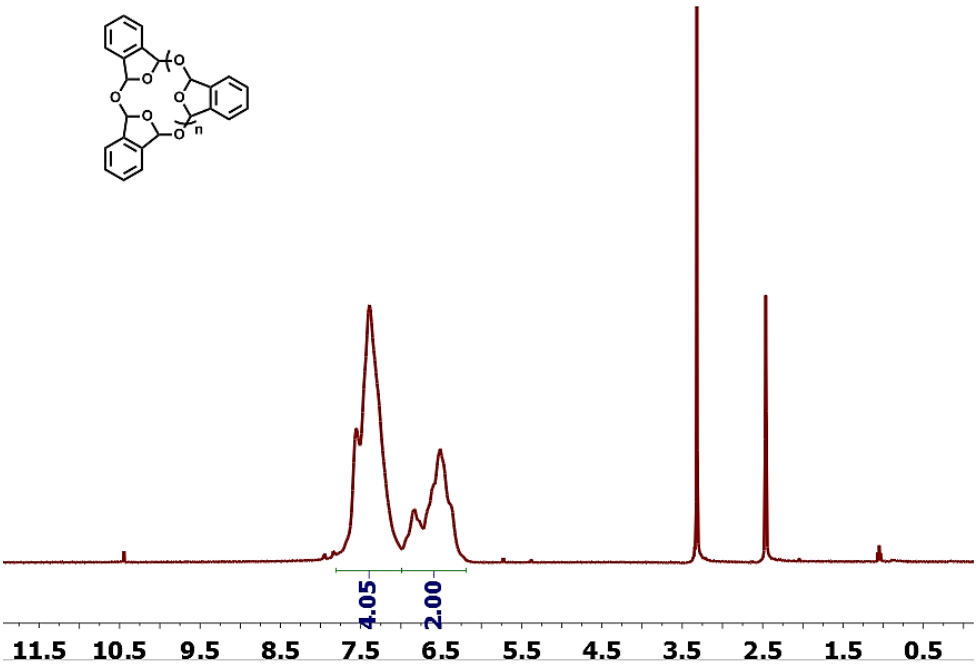

***Figure 3.8** | ^{1}H NMR spectra of cPPA in DMSO-d_6.*

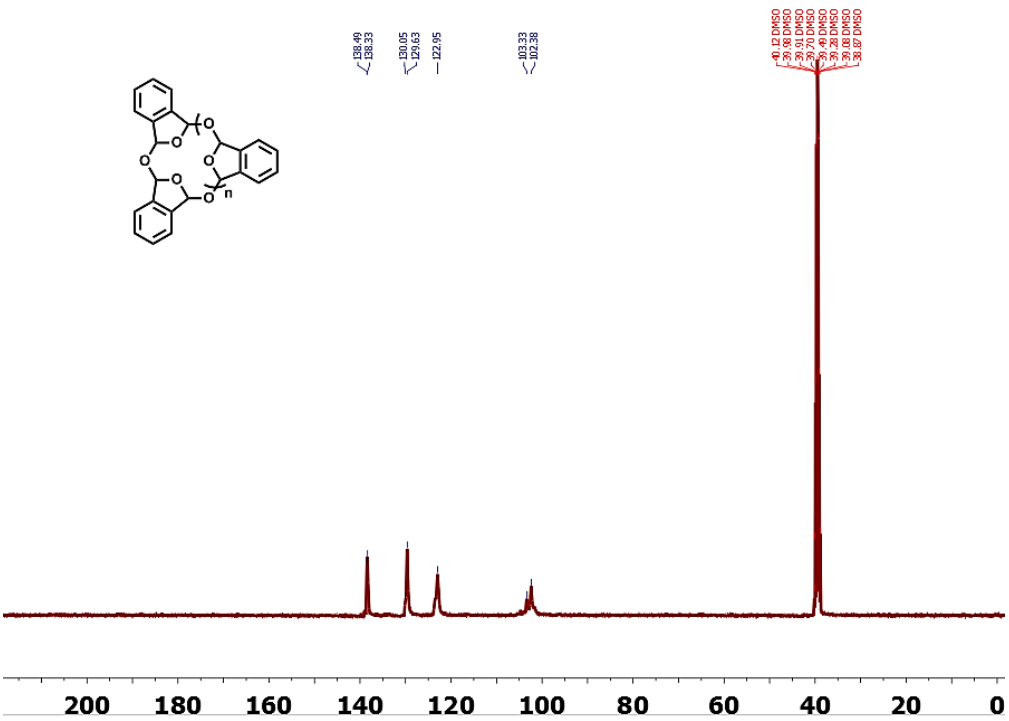

***Figure 3.9** | ^{13}C NMR spectra of cPPA in DMSO-d_6.*

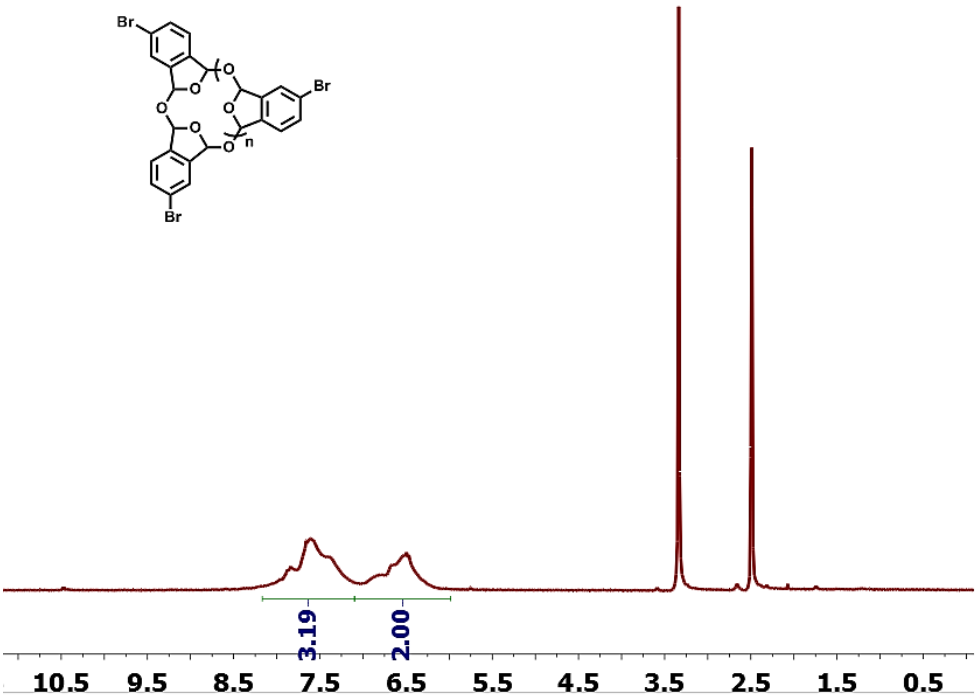

***Figure 3.10** | [1]H NMR spectra of cPBPA in DMSO-d6.*

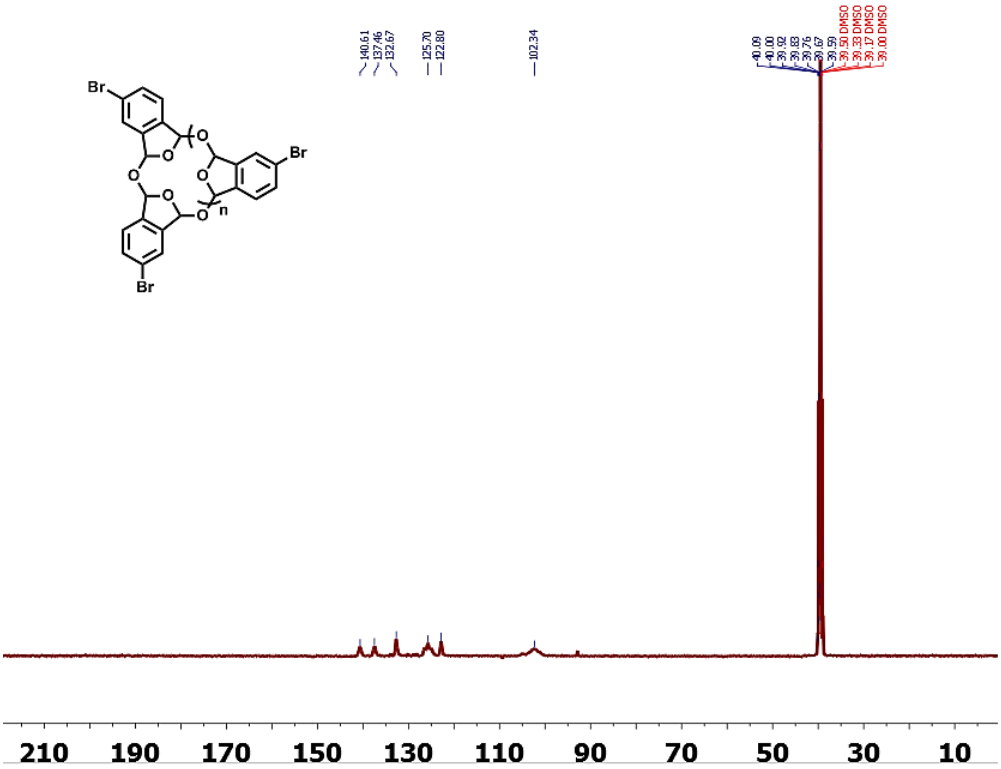

***Figure 3.11** | [13]C NMR spectra of cPBPA in DMSO-d6.*

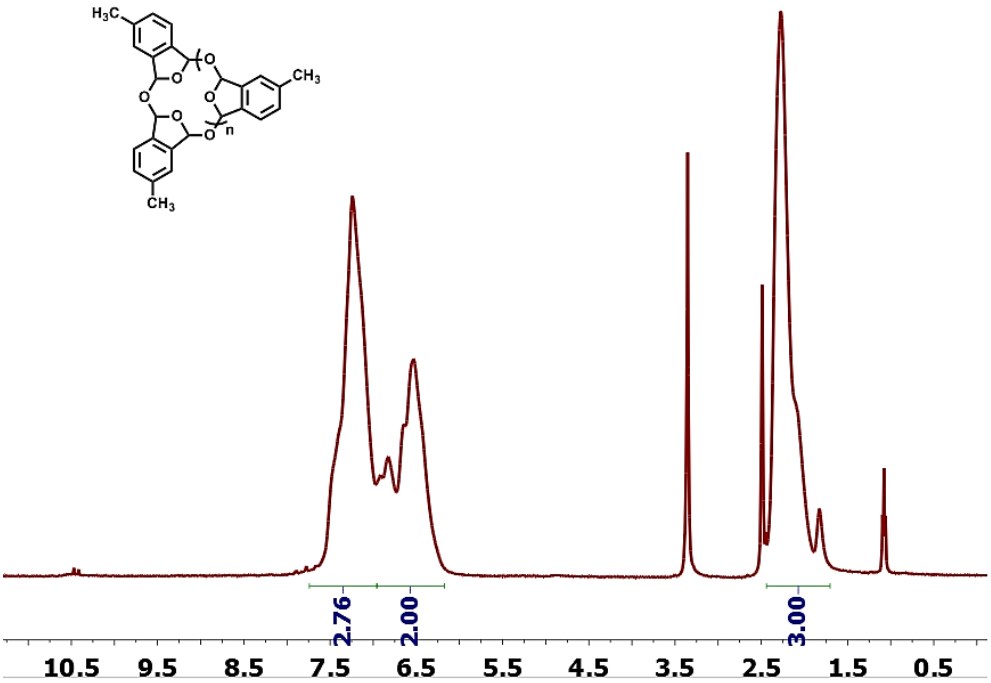

Figure 3.12 | *^{1}H NMR spectra of cPMPA in DMSO-d$_{6}$.*

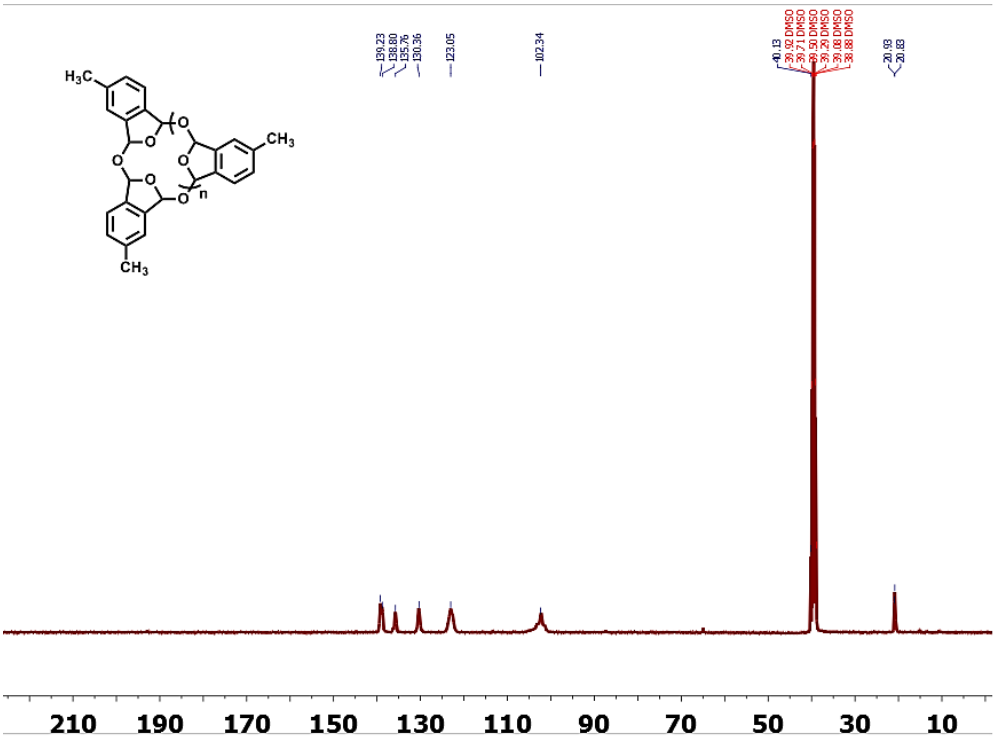

Figure 3.13 | *^{13}C NMR spectra of cPMPA in DMSO-d$_{6}$.*

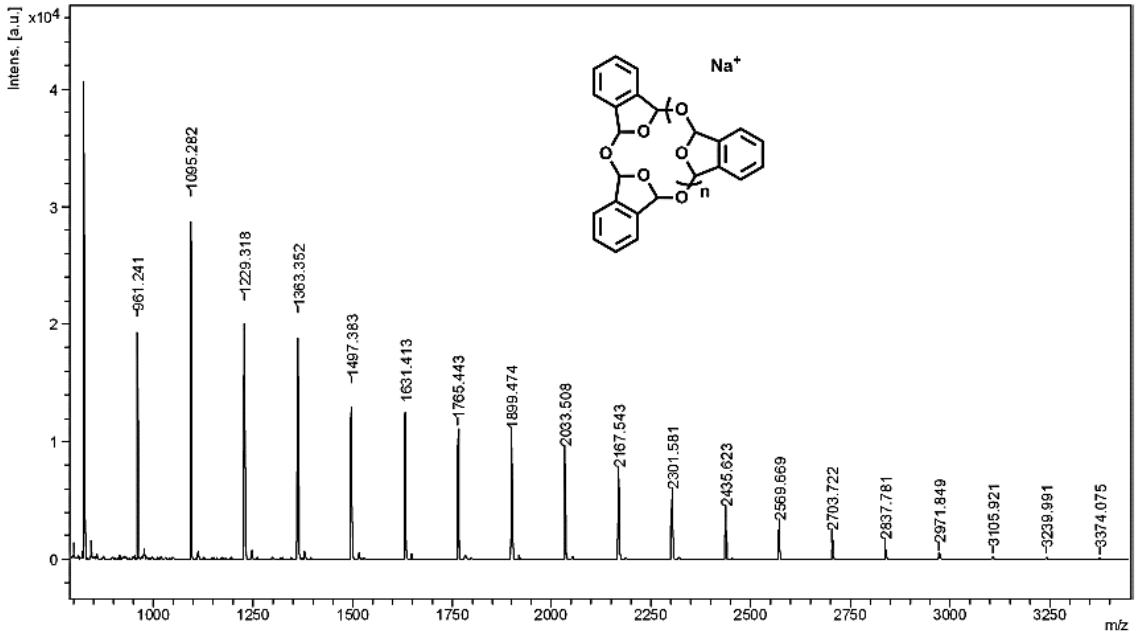

Figure 3.14 | MALDI-TOF MS spectrum of cPPA*: Peaks match sodium adduct of cPPA (Table 3.2, Entry 1). DHB (2,5-dihydroxybenzoic acid) was used as the matrix and sodium iodide as the cationization agent.*

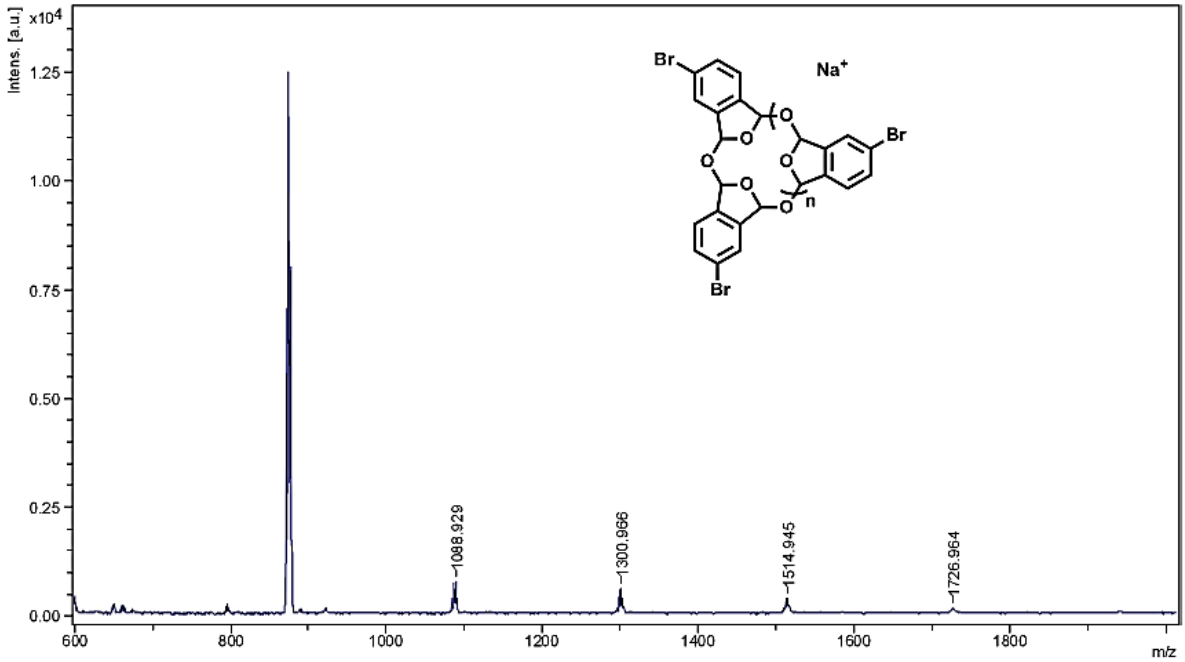

Figure 3.15 | MALDI-TOF MS spectrum of cPBPA*: Peaks match sodium adduct of cPBPA (Table 3.2, Entry 2). DHB (2,5-dihydroxybenzoic acid) was used as the matrix and sodium iodide as the cationization agent.*

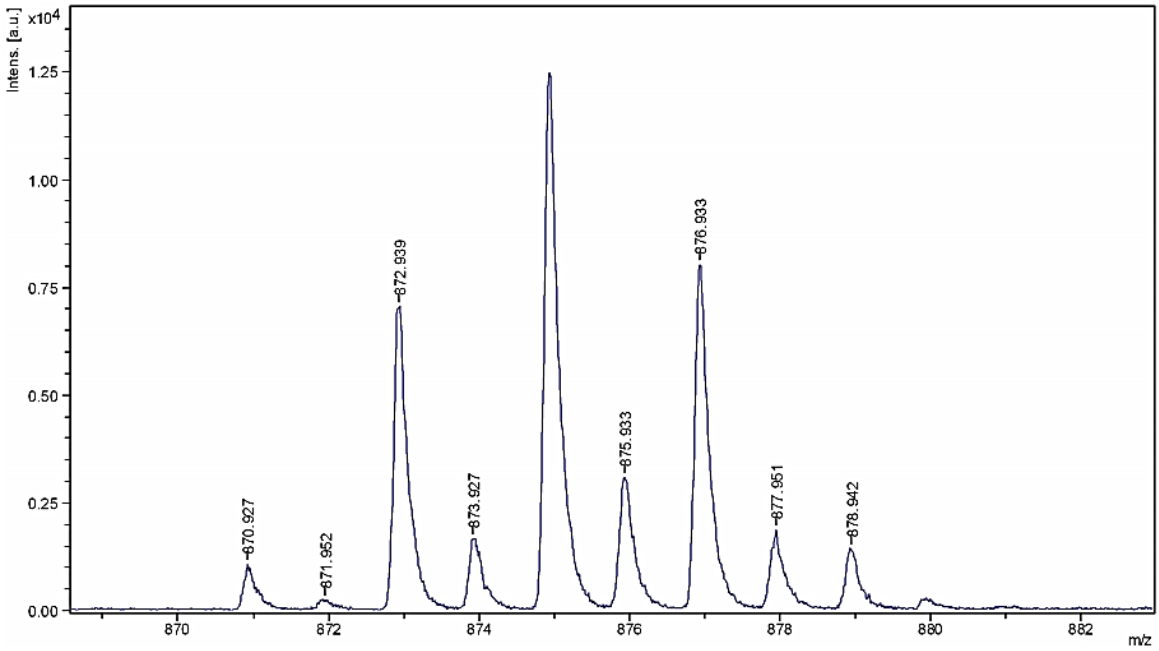

Figure 3.16 | MALDI-TOF MS spectrum of cPBPA, zoom on tetramer*: Peaks match sodium adduct of cPBPA$_4$ (Table 3.2, Entry 2), and display pattern consistent with tetrabrominated product. DHB (2,5-dihydroxybenzoic acid) was used as the matrix and sodium iodide as the cationization agent.*

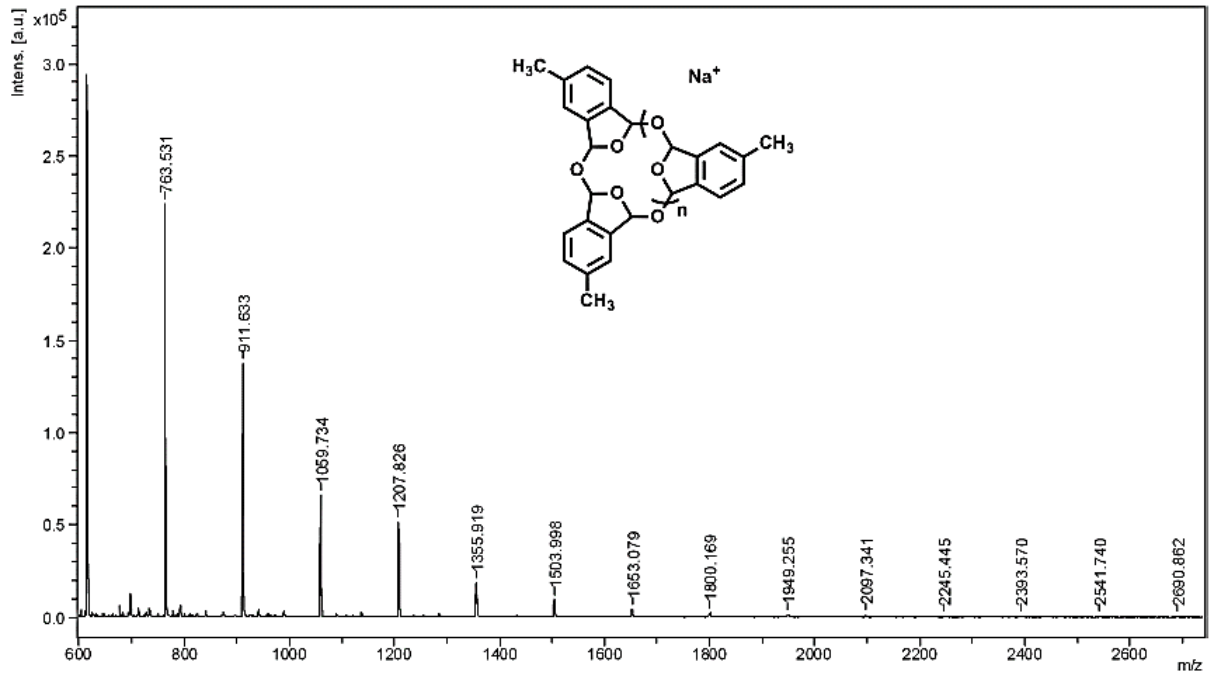

Figure 3.17 | MALDI-TOF MS spectrum of cPMPA*: Peaks match sodium adduct of cPMPA (Table 3.2, Entry 3). DHB (2,5-dihydroxybenzoic acid) was used as the matrix and sodium iodide as the cationization agent.*

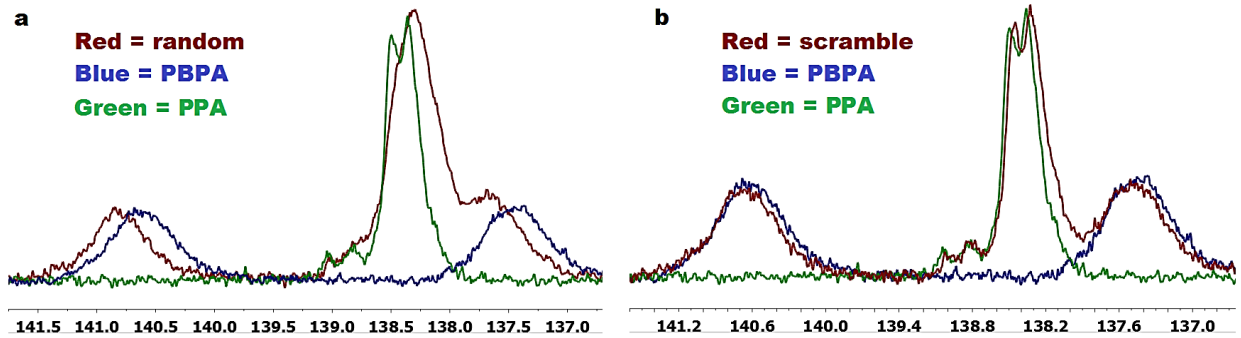

Figure 3.18 | *^{13}C NMR spectra of (a) random PPA/PBPA copolymer (red) in DMSO-d_6 overlayed with cPPA (green) and cPBPA (blue) homopolymers; and (b) scrambled PPA/PBPA copolymer (red) in DMSO-d_6 overlayed with cPPA (green) and cPBPA (blue) homopolymers.*

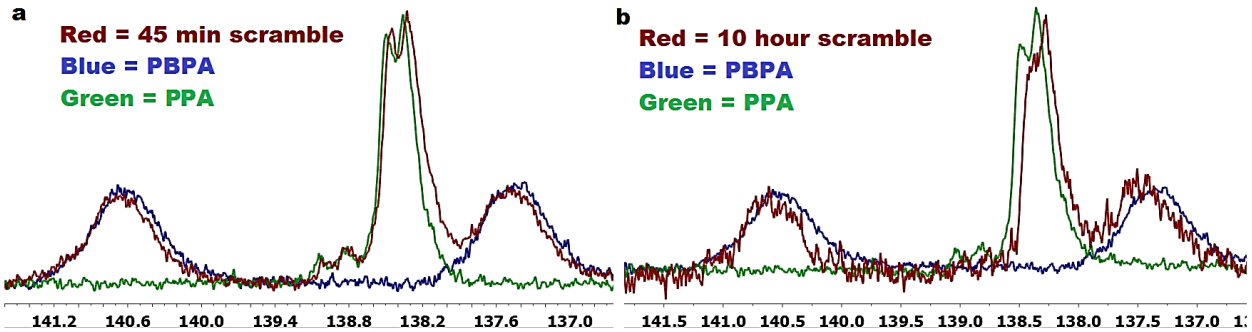

Figure 3.19 | *^{13}C NMR spectra of (a) PPA/PBPA copolymer scrambled 45 min (red) in DMSO-d_6 overlayed with cPPA (green) and cPBPA (blue) homopolymers; and (b) PPA/PBPA copolymer scrambled 10 h (red) in DMSO-d_6 overlayed with cPPA (green) and cPBPA (blue) homopolymers.*

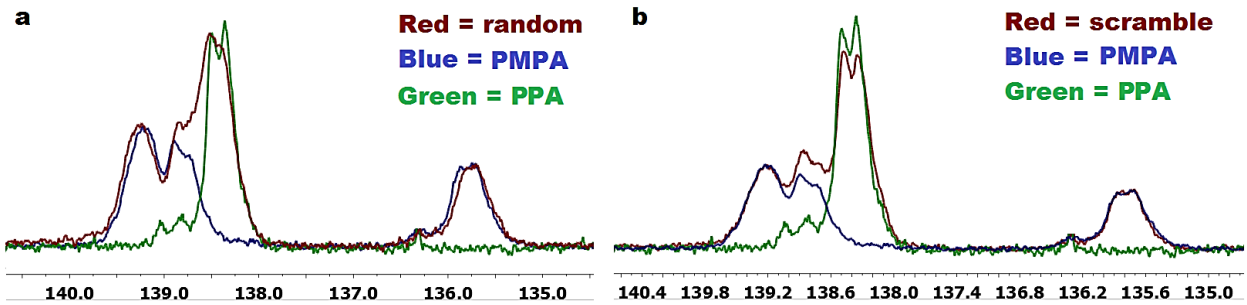

Figure 3.20 | *^{13}C NMR spectra of (a) random PPA/PMPA copolymer (red) in DMSO-d_6 overlayed with cPPA (green) and cPMPA (blue) homopolymers; and (b) scrambled PPA/PMPA copolymer (red) in DMSO-d_6 overlayed with cPPA (green) and cPMPA (blue) homopolymers.*

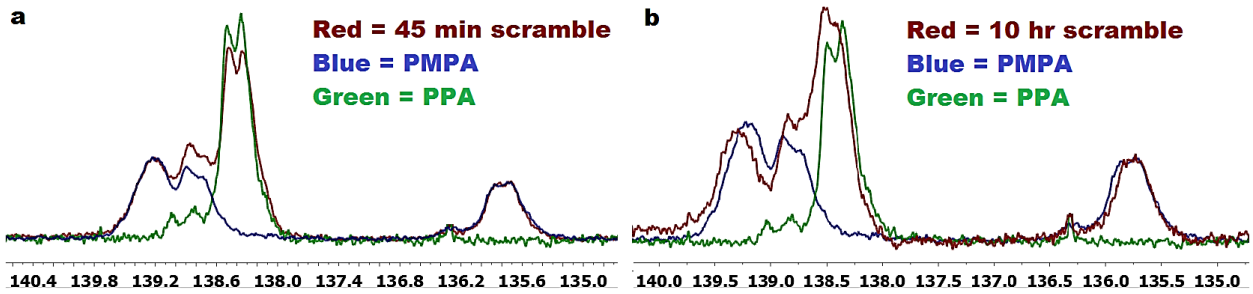

Figure 3.21 | *^{13}C NMR spectra of (a) PPA/PMPA copolymer scrambled 45 min (red) in DMSO-d_6 overlayed with cPPA (green) and cPMPA (blue) homopolymers; and (b) PPA/PMPA copolymer scrambled 10 h (red) in DMSO-d_6 overlayed with cPPA (green) and cPMPA (blue) homopolymers.*

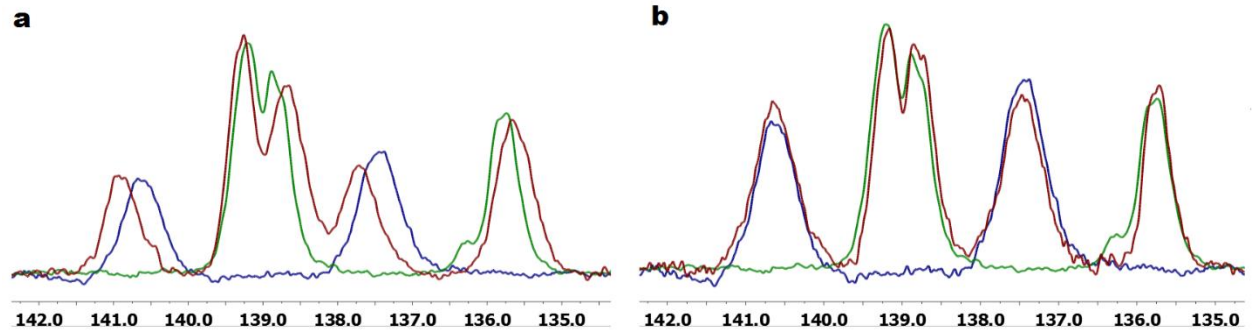

Figure 3.22 | *^{13}C NMR spectra of (a) random PBPA/PMPA copolymer (red) in DMSO-d_6 overlayed with cPMPA (green) and cPBPA (blue) homopolymers; and (b) scrambled PBPA/PMPA copolymer (red) in DMSO-d_6 overlayed with cPMPA (green) and cPBPA (blue) homopolymers.*

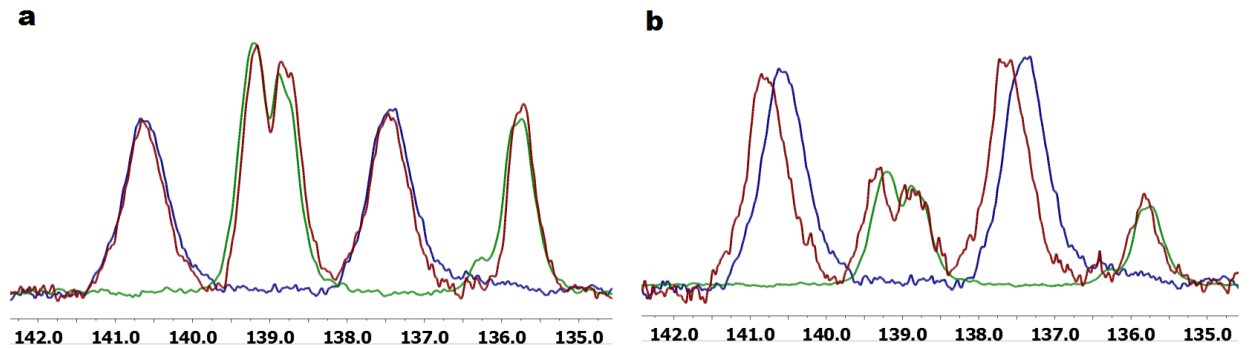

Figure 3.23 | *^{13}C NMR spectra of (a) PBPA/PMPA copolymer scrambled 45 min (red) in DMSO-d_6 overlayed with cPMPA (green) and cPBPA (blue) homopolymers; and (b) PBPA/PMPA copolymer scrambled 10 h (red) in DMSO-d_6 overlayed with cPMPA (green) and cPBPA (blue) homopolymers.*

3.7 References

(1) (a) Maeda, T.; Otsuka, H.; Takahara, A. *Prog. Polym. Sci.* **2009**, 34, 581-604. (b) Rowan, S. J.; Cantrill, S. J.; Cousins, G. R. L.; Sanders, J. K. M.; Stoddart, J. F. *Angew. Chem. Int. Ed.* **2002**, 41, 898-952. (c) Lehn, J.-M. *Prog. Polym. Sci.* **2005**, 30, 814-831.

(2) (a) Otsuka, H.; Aotani, K.; Higaki, Y.; Takahara, A. *J. Am. Chem. Soc.* **2003**, 125, 4064-4065. (b) Ono, T.; Nobori, T.; Lehn, J.-M. *Chem. Commun.* **2005**, 1522-1524. (c) Otsuka, H.; Muta, T.; Sakada, M.; Maeda, T.; Takahara, A. *Chem. Commun.* **2009**, 1073-1075.

(3) (a) Berkovich-Berger, D.; Lemcoff, N. G. *Chem. Commun.* **2008**, 1686-1688. (b) Cacciapaglia, R.; Stefano, S. D.; Mandolini, L. *J. Am. Chem. Soc.* **2005**, 127, 13666-13671. (c) Cacciapaglia, R.; Stefano, S. D.; Mandolini, L. *Chem. Eur. J.* **2006**, 12, 8566-8570.

(4) (a) Peterson, G. I.; Larsen, M. B.; Boydston, A. J. *Macromolecules* **2012**, 45, 7317-7328. (b) Esser-Kahn, A. P.; Odom, S. A.; Sottos, N. R.; White, S. R.; Moore, J. S. *Macromolecules* **2011**, 44, 5539-5553. (c) Wong, A. D.; DeWit, M. A.; Gillies, E. R. *Adv. Drug Delivery Rev.* **2012**, 64, 1031-1045. (d) Sagi, A.; Weinstain, R.; Karton, N.; Shabat, D. *J. Am. Chem. Soc.* **2008**, 130, 5434-5435. (e) DeWit, M. A.; Gillies, E. R. *J. Am. Chem. Soc.* **2009**, 131, 18327-18334. (f) Weintain, R.; Sagi, A.; Karton, N.; Shabat, D. *Chem. Eur. J.* **2008**, 14, 6857-6861. (g) Chen, E. K. Y.; McBride, R. A.; Gillies, E. R. *Macromolecules* **2012**, 45, 7364-7374. (h) Dewit, M. A.; Beaton, A.; Gillies, E. R. *J. Polym. Sci., Part A: Polym. Chem.* **2010**, 48, 3977-3985. (i) Robbins, J. S.; Schmid, K. M.; Phillips, S. T. *J. Org. Chem.* **2013**, 78, 3159-3169.

(5) (a) Seo, W.; Phillips, S. T. *J. Am. Chem. Soc.* **2010**, 132, 9234-9235. (b) Zhang, H.; Yeung, K.; Robbins, J. S.; Pavlick, R. A.; Wu, M.; Liu, R.; Sen, A.; Phillips, S. T. *Angew. Chem. Int. Ed.* **2012**, 51, 2400-2404. (c) Dilauro, A. M.; Robbins, J. S.; Phillips, S. T. *Macromolecules* **2013**, 46, 2963-2968. (d) Kaitz, J. A.; Moore, J. S.; *Macromolecules* **2013**, 46, 608-612. (e) Dilauro, A. M.; Abbaspourrad, A.; Weitz, D. A.; Phillips, S. T. *Macromolecules* **2013,** 46, 3309-3313.

(6) (a) Chuji, A.; Tagami, S.; Kunitake, T. *J. Polym. Sci. Part A: Polym. Chem.* **1969**, 7, 497-511. (b) Chuji, A.; Tagami, S. *Macromolecules* **1969**, 2, 414-419. (c) Willson, C. G.; Ito, H.; Frechet, J. M. J.; Tessier, T. G.; Houlihan, F. M. *J. Electrochem. Soc.* **1986**, 133, 181-187.

(7) (a) Tsuda, M.; Hata, M.; Nishida, R.; Oikawa, S. *J. Polym. Sci. Part A: Polym. Chem.* **1997**, 35, 77-89. (b) Ito, H.; Willson, C. G. *Polym. Eng. Sci.* **1983**, 23, 1012-1018. (c) Knoll, A. W.; Pires, D.; Coulembier, O.; Dubois, P.; Hedrick, J. L.; Frommer, J.; Duerig, U. *Adv. Mater.* **2010**, 22, 3361-3365.

(8) Kaitz, J. A.; Diesendruck, C. E.; Moore, J. S. *J. Am. Chem. Soc.* **2013**, 135, 12755-12761.

(9) (a) Kricheldorf, H. R. *J. Polym. Sci., Part A: Polym. Chem.* **2010**, 48, 251-284. (b) Jia, Z.; Monteiro, M. J. *J. Polym. Sci., Part A: Polym. Chem.* **2012**, 50, 2085-2097. (c) Laurent, B. A.; Grayson, S.

M. *Chem. Soc. Rev.* **2009**, 38, 2202-2213. (d) Yamamoto, T.; Tezuka, Y. *Polym. Chem.* **2011**, 2, 930-1941. (e) Endo, K. *Adv. Polym. Sci.* **2008**, 217, 121-183. (f) McLeish, T. *Science* **2002**, 297, 2005-2006.

(10) (a) Jeong, W.; Shin, E. J.; Culkin, D. A.; Hedrick, J. L.; Waymouth, R. M. *J. Am. Chem. Soc.* **2009**, 131, 4884-4891. (b) Culkin, D. A.; Jeong, W.; Csihony, S.; Gomez, E. D.; Balsara, N. P.; Hedrick, J. L.; Waymouth, R. M. *Angew. Chem. Int. Ed.* **2007**, 46, 2627-2630. (c) Jeong, W.; Hedrick, J. L.; Waymouth, R. M. *J. Am. Chem. Soc.* **2007**, 129, 8414-8415. (d) Shin, E. J.; Brown, H. A.; Gonzalez, S.; Jeong, W.; Hedrick, J. L.; Waymouth, R. M. *Angew. Chem. Int. Ed.* **2011**, 50, 6388-6391. (e) Guo, L.; Zhang, D. *J. Am. Chem. Soc.* **2009**, 131, 18072-18074. (f) Guo, L.; Lahasky, S. H,; Ghale, K.; Zhang, D. *J. Am. Chem. Soc.* **2012**, 134, 9163-9171.

(11) Zhu, P. C.; Wang, D.-H.; Lu, K.; Mani, N. *Sci. China Ser. B: Chem.* **2007**, 50, 249-252.

(12) Farooq, O. *Synthesis* **1994**, 1035-1036.

(13) (a) Odian, G. *Principles of Polymerization*, 4th ed.; Wiley-Interscience: New York, 2004; pp 512-518. (b) Lowry, G. G. *J. Polym. Sci.* **1960**, 42, 463-477. (c) Szymanski, R. *Makromol. Chem.* **1987**, 188, 2605-2619.

(14) (a) Frechet, J. M. J.; Matuszczak, S.; Reck, B.; Stover, H. D. H.; Willson, C. G. *Macromolecules* **1991**, 24, 1746-1754. (b) Packirisamy, S.; Hirao, A.; Nakahama, S. *J. Polym. Sci. A: Polym. Chem.* **1989**, 27, 2811-2814.

Chapter 4: Divergent Macrocyclization Mechanisms in the Cationic Polymerization of Ethyl Glyoxylate*

4.1 Abstract

The cationic polymerization of *o*-phthalaldehyde was found to generate cyclic poly(phthalaldehyde) in high yield, high molecular weight, and a high degree of cyclic purity. Given this surprising result, we pursued the cationic polymerization of ethyl glyoxylate to determine if the macrocyclization outcome is, in fact, a general trend of low ceiling temperature polyacetals. Using NMR spectroscopy, MALDI-TOF mass spectrometry, and triple detection GPC, we have uncovered divergent macrocyclization mechanisms in the cationic polymerization of ethyl glyoxylate. Back-biting is observed either via the backbone acetal or via the pendant ester to give disparate polymer products and unique polymer architectures. The favored route for cyclization is found to depend both on the monomer concentration as well as the initiating species. Understanding the underlying mechanisms of polymerization and the ability to rigorously control polymer structure has important implications for the design of new transient materials.

4.2 Introduction

Low ceiling temperature (T_c) polymers, a class of organic materials that are capable of triggered depolymerization, have generated growing interest in recent years.[1] Polyaldehydes, in particular, have been shown to possess widespread utility due to their capacity to undergo complete and rapid depolymerization on command.[2] For instance, poly(phthalaldehyde) (PPA, T_c = -40 °C)[3] has been employed in lithography[4], shape-changing materials[5], degradable thin films[6], and degradable microcapsules[7]. Recently, we investigated the cationic polymerization of *o*-phthalaldehyde and discovered that macrocyclic polymer is obtained in high yields and with high cyclic purity.[8] Given the surprising cyclic structure, we were interested in pursuing the cationic polymerization of other aldehydes to identify if the macrocyclization[9-12] phenomenon is, in fact, a general trend of low ceiling temperature polyaldehydes.

Polyethyl glyoxylate (PEtG) is a similar low ceiling temperature polyaldehyde (T_c = 37 °C) that has been prepared by anionic polymerization.[13] Ethyl glyoxylate (EtG) was selected as a suitable candidate

* Portions of this chapter have been published: Kaitz, J. A.; Diesendruck, C. E.; Moore, J. S. *Macromolecules* **2014**, 47, 3603-3607.

monomer for studies due to its lack of an α-proton, preventing elimination side reactions, and the polymer's reported good solubility in common organic solvents.[13] The anionic polymerization of methyl and ethyl glyoxylate initiated by triethylamine produces linear polymers.[13-14] The cationic polymerization of methyl glyoxylate, on the other hand, is only known to produce low molecular weight species due to inter- and intramolecular chain transfer processes.[14a] We thus set out to investigate the cationic polymerization of ethyl glyoxylate in an effort to rigorously characterize the resulting polymer structure.

4.3 Results and Discussion

4.3.1 Anionic and Cationic Polymerizations of EtG

PEtG was prepared by anionic polymerization following reported procedures using triethylamine or *n*-BuLi as initiator at -15 °C (Table 4.1).[13] The reaction is rapid, transforming from a yellow solution to a viscous, colorless mixture within minutes of adding either initiator. After 1 h reaction time, the polymer is stabilized from depolymerization by end-capping with a mixture of phenyl isocyanate and dibutyl tin dilaurate (DBTL) as catalyst.[13-14] The cationic polymerization of EtG was effected in a nearly identical manner to its anionic polymerization with a variety of Lewis acids and cationic initiators (Table 4.2). The reaction also rapidly reaches completion, but is similarly left for 1 h prior to quenching with pyridine.

Table 4.1 | *Anionic polymerization of EtG and resulting polymers used in this study.*

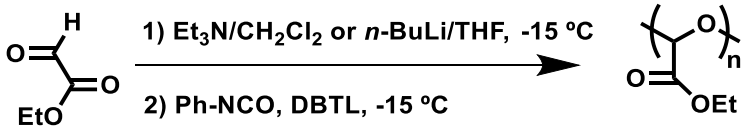

Entry	*Initiator*	*[EtG]$_0$ (M)*	*[M]$_0$/[I]$_0$*	*M_w (kDa)[a]*	*M_p (kDa)[a]*	*PDI[a]*
1	Et_3N	6	120	170	97	1.9
2	Et_3N	3	90	77	79	1.8
3	Et_3N	1	50	24	23	1.6
4	Et_3N	1	20	6.2	6.0	1.9
5	*n*-BuLi[b]	1	20	4.1	2.9	1.8

[a]Average molecular weights and polydispersity determined by gel permeation chromatography (GPC), calibrated with monodisperse polystyrene standards. [b]Reaction run in THF.

Molecular weights of PEtG polymerized by anionic initiation range from 4-170 kDa with polydispersities (PDIs) ranging from 1.6-1.9 (Table 4.1, Entries 1-5). The molecular weights track closely

with monomer-to-initiator ratios and initial monomer concentration. In contrast, the molecular weights of PEtG synthesized by cationic polymerization do not correlate with either monomer concentration or monomer-to-initiator ratios, as reported for polymethyl glyoxylate.[14a] Irrespective of concentration, initiator, or temperature[15], the cationic polymerization of EtG gives polymer products with molecular weights in the range 2-13 kDa and PDIs of 1.3-1.8 (Table 4.2, Entries 1-8).

Table 4.2 | *Cationic polymerization of EtG and resulting polymers used in this study.*

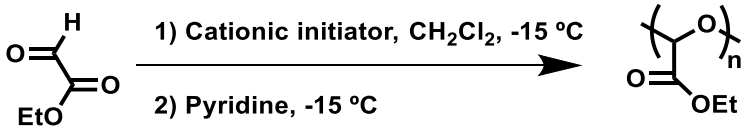

Entry	*Initiator*	*$[EtG]_0$ (M)*	*$[M]_0/[I]_0$*	*M_w (kDa)[a]*	*M_p (kDa)[a]*	*PDI[a]*	*MALDI observations (main peak series)*
1	$BF_3{\cdot}OEt_2$	10	80	3.6	3.4	1.3	Ester back-biting
2	$BF_3{\cdot}OEt_2$	6	80	5.6	4.4	1.7	Ester back-biting[b]
3	$BF_3{\cdot}OEt_2$	4	80	4.9	4.0	1.6	Main-chain back-biting[b]
4	$BF_3{\cdot}OEt_2$	2	80	5.3	4.2	1.6	Main-chain back-biting[b]
5	$SnCl_4$	9	130	5.0	4.0	1.7	Ester back-biting
6	Ph_3CBF_4	6	100	2.1	1.6	1.3	Main-chain back-biting
7	Et_3OBF_4	9	100	6.3	5.8	1.8	Main-chain back-biting[b]
8	$CH_3COCl/AlCl_3$	7	70	5.1	4.4	1.8	Ester back-biting

[a]Average molecular weights and polydispersity determined by gel permeation chromatography (GPC), calibrated with monodisperse polystyrene standards. [b]Secondary MALDI peak series observed corresponding to alternative cyclization mechanism.

4.3.2 Characterization of Polyethyl Glyoxylates

^{1}H NMR was employed to elucidate end-group structures of PEtGs synthesized by anionic and cationic polymerizations. To characterize the anionic polymerizations, the smallest sample with a molecular weight of 4 kDa was chosen for analysis (Table 4.1, Entry 5). The phenyl peaks corresponding to the urethane capping group are clearly evident in the NMR spectrum, in agreement with prior reports that document carbamate end-groups on both termini due to chain-transfer with monomer hydrate species (Figure 4.1a).[13] However, there is no evidence of any end-group structure for PEtG of corresponding molecular weight synthesized by cationic polymerization (Table 4.2, Entry 6; Figure 4.1b). The lack of a discernible end group signaled the possibility of a macrocyclic structure for PEtG, akin to the cationic polymerization of *o*-phthalaldehyde.[8]

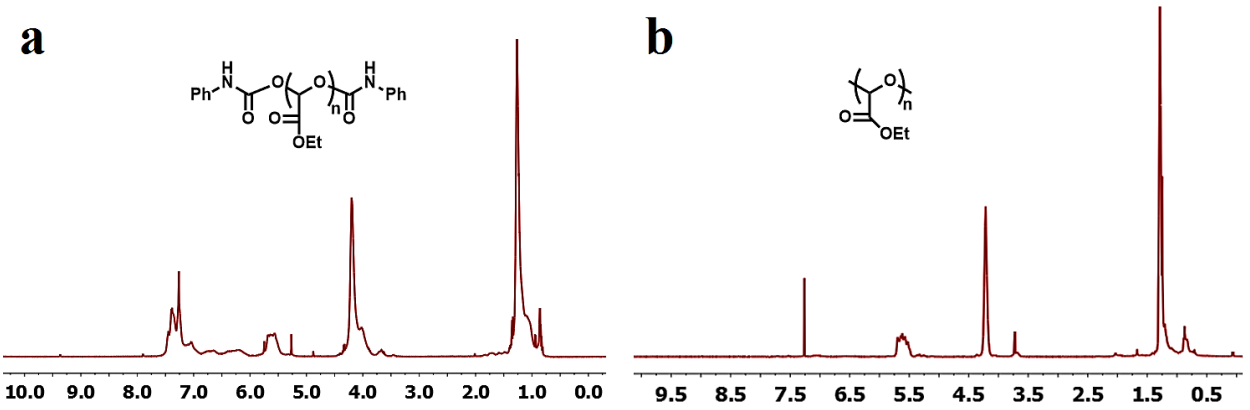

***Figure 4.1* | ^{1}H NMR characterization of PEtG in $CDCl_3$:** *PEtG prepared by (a) anionic polymerization (Table 4.1, Entry 5) and (b) cationic polymerization (Table 4.2, Entry 6). Phenyl protons consistent with end-groups are clearly observed from 6.0-7.5 ppm in the anionic polymerization of EtG. There are no readily apparent end-groups in the cationic polymerization of EtG.*

We employed two independent analytical techniques to study the polymer architecture in the cationic polymerization of EtG: MALDI-TOF mass spectrometry and triple-detection GPC. Intriguingly, mass spectra of PEtG synthesized in bulk with boron trifluoride etherate (Table 4.2, Entry 1) do not match the expected cyclic structure that corresponds to back-biting by attack of the acetal functional group. It was recognized, however, that the peak series matches perfectly with the sodium adduct of a cyclic product missing a single ethyl group (Figure 4.2a; secondary peaks correspond to cyclic product missing two ethyl groups). This major peak series is also observed in several additional samples (Table 4.2, Entries 2, 5, 8), and can be explained by intramolecular back-biting via the pendant ester of EtG followed by loss of the ethyl group to give the peak series observed.

Cyclization via the pendant ester functionality leaves the initiating species intact at the chain end. Thus, we anticipated that initiation with triphenylcarbenium tetrafluoroborate (Table 4.2, Entry 6) would generate mass spectra corresponding to an identical cyclic structure but containing triphenylmethyl end groups. Much to our surprise, the mass spectra from the resulting products perfectly matched the sodium adduct of cyclic PEtG formed by acetal main-chain back-biting (Figure 4.2b; secondary peaks correspond to cyclic product missing two ethyl groups).

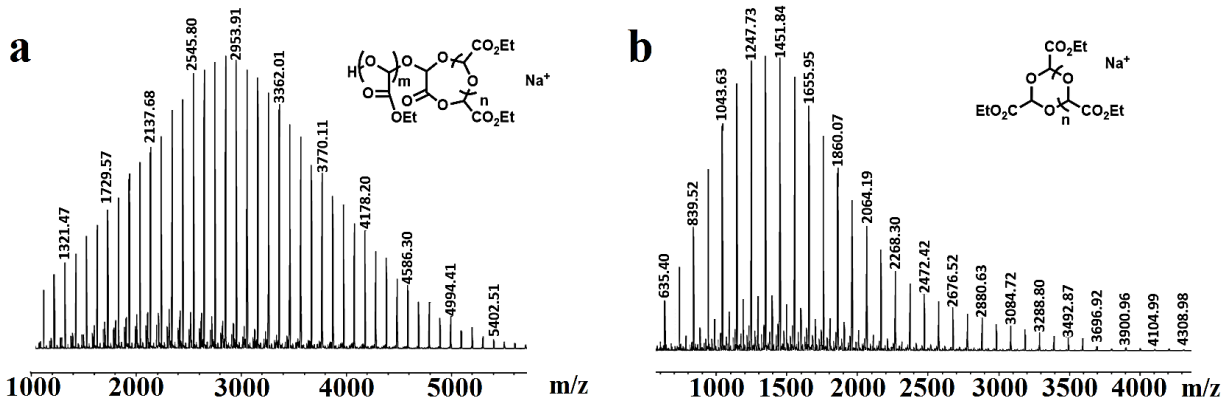

Figure 4.2 | MALDI-TOF mass spectra of PEtG: *(a) cyclized PEtG by ester back-biting (Table 4.2, Entry 1), and (b) cyclized PEtG by main-chain back-biting (Table 4.2, Entry 6). Peaks in the predominant molecular weight series match the sodium adducts of polymer structures shown. DHB (2,5-dihydroxybenzoic acid) was used as the matrix and sodium iodide as the cationization agent.*

To explain the differing mass spectra, we hypothesized two divergent cyclization mechanisms to be operative in the cationic polymerization of EtG (Scheme 4.1). At high concentrations and with Lewis acid initiators (Table 4.2, Entries 1, 2, and 5), the favored cyclization route is via the pendant ester with concomitant loss of an ethyl group (Scheme 4.1a). These reaction conditions result in rapid formation of a solid gel, and we hypothesize that solidification of the reaction mixture prevents dynamic ring-opening and equilibration to form the alterative macrocyclic product. In fact, diluting the reaction mixture from 10 M to 2 M to solubilize the polymer product prior to quenching affords a mixture of both macrocyclic products, the same outcome observed when the reaction is run at 2 M. The macrocyclization phenomenon is thus dynamic; the final polymer structure can be altered by changing reaction conditions prior to catalyst quenching, much like the cationic polymerization of *o*-phthalaldehyde.[8]

On the other hand, at lower concentrations or with carbocationic initiators (Table 4.2, Entries 3, 4, 6, 7), gelation does not occur and back-biting via the acetal main-chain oxygen is observed (Scheme 4.1b). For these cases, reaction conditions actually dictate whether end-to-end macrocyclization or statistical back-biting to form the cyclic product is favored. At low EtG concentrations with Lewis acidic initiators, the polymerization equilibrates to a statistical distribution with both polymer structures evidenced in the MALDI-TOF spectra, with the main-chain back-biting product slightly predominating. For carbocationic initiators, the main-chain back-biting is favored to a significantly greater extent, suggesting that end-to-end macrocyclization is the major cyclization pathway due to the increased nucleophilicity of backbone acetal oxygens near the electron-donating chain-end. The divergent cyclization pathway is thus dependent on both initiator and concentration.

Scheme 4.1 | Proposed macrocyclization mechanisms in the cationic polymerization of EtG. *Cyclization occurs via (a) pendant ester groups, or (b) the acetal backbone oxygen to generate two unique cyclic structures. "R" corresponds to either the initiating species or polymer chains bound with initiating species at the end-group.*

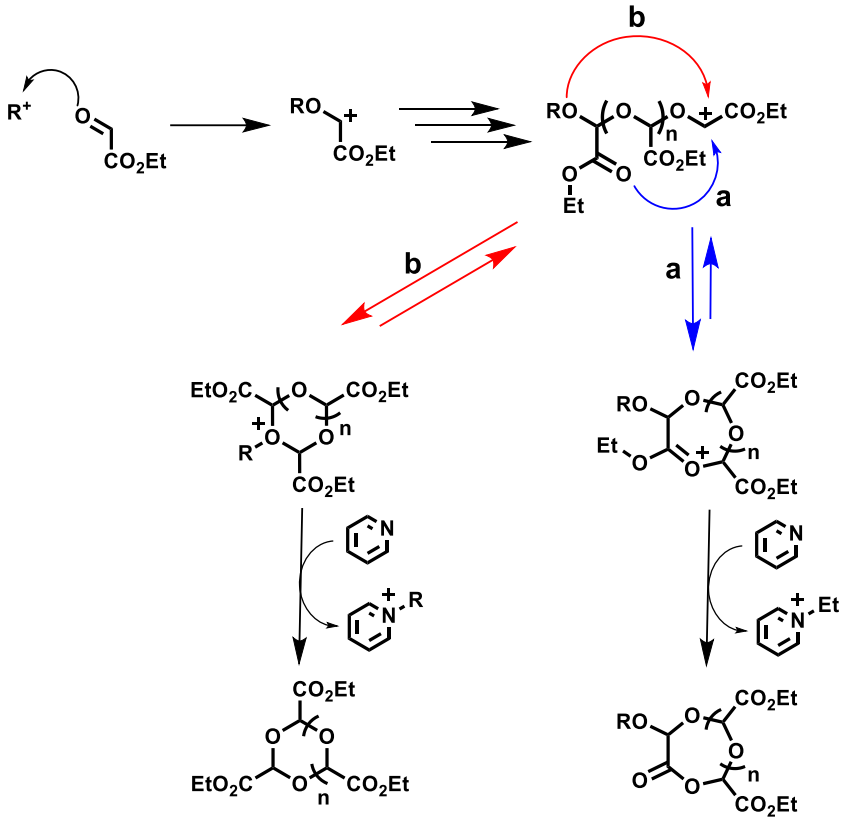

4.3.3 Evidence for Macrocyclization Mechanisms

Given the proposed divergent cyclization mechanisms, the cationic polymerization can produce two unique PEtG architectures. For main-chain back-biting products, the structure is perfectly cyclic. However, polymer products generated by ester back-biting may make lariat shapes due to non-terminal ester back-biting, or even more complex structures due to multiple ring-opening and re-cyclization events. In fact, a peak series is observed in several mass spectra corresponding to the loss of two ethyl groups, which could occur from either ester back-biting followed by ring-opening and re-cyclization at a different location or intermolecular termination events, generating an exquisitely complex polymer product.

Triple-detection GPC was employed to explore the solution behavior of the various polymer architectures. Owing to differences in hydrodynamic volume, cyclic polymers have lower intrinsic viscosities (η) than linear polymers at identical molecular weights,[9] and we hypothesized that lariat shapes (or a more complex cyclic structure) may have hydrodynamic characteristics intermediary to linear and

cyclic samples. The results are shown in Figure 4.3, with η plotted against absolute molecular weight for each reaction mechanism. Polymers prepared by cationic polymerization were injected at high concentrations in order to compare high molecular weight chains, which present less error in their light-scattering data. The η ratio of cyclic to linear PEtG is 0.7, indicative of its macrocyclic structure,[8a, 9] and both cyclic and linear present a similar slope. The more complex lariat structure, on the other hand, has viscosities in between that of cyclic or linear PEtG at all molecular weights plotted. Interestingly, the slope of the ester back-biting PEtG sample differs from the linear and cyclic polymers, reflecting its unique architecture. The small slope observed in the lariat structure closely resembles that of single-chain polymer nanoparticles, indicating a higher number of back-biting reactions with increasing molecular weight.[16]

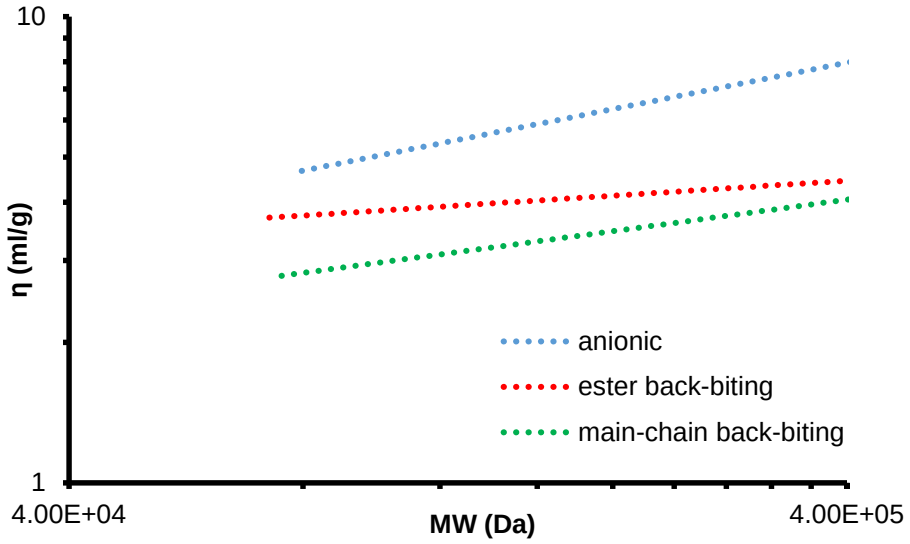

Figure 4.3 | Mark-Houwink-Sakurada plot of PEtG architectures in THF: *linear PEtG (blue), cyclic PEtG (green), and lariat PEtG (red). The intrinsic viscosity ratio of cyclic to linear PEtG is 0.7, indicative of a cyclic structure. Lariat PEtG has an intermediary intrinsic viscosity and a different slope in comparison to linear and cyclic polymers, consistent with a unique architecture.*

Since the lariat PEtGs were expected to contain at least a single hydroxyl terminus, we tested for this possibility by end-capping the polymers in an analogous manner to that for the anionic polymerization. The cationic polymerization was initiated by boron trifluoride and quenched with pyridine (identical conditions to Table 4.2, Entry 2). Following quenching, phenyl isocyanate and the DBTL catalyst were added to the reaction mixture. MALDI-TOF MS and NMR spectroscopy confirm the unambiguous incorporation of the phenyl group into the polymer at a composition consistent with end groups. Also of significance is the difference in thermal stability between the various polymer architectures. Heating at 10 °C/min in a nitrogen atmosphere, the linear and cyclic PEtGs are stable up to approximately 200 °C and

230 °C, respectively. The lariat product, on the other hand, begins degrading just above room temperature due to its unprotected hydroxyl end-group, consistent with the degradation of uncapped linear polymer at temperatures below 100 °C.[13a] After end-capping with phenyl isocyanate, though, the lariat polymers display stability up to temperatures approaching 150 °C (Figure 4.4).

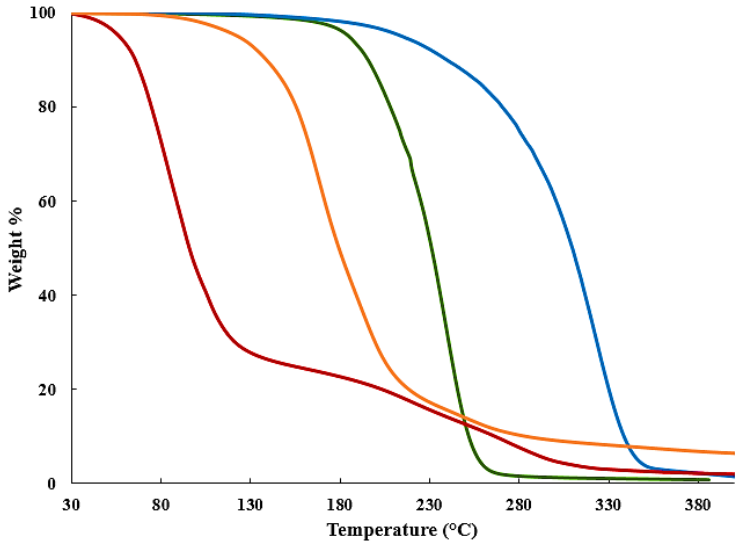

Figure 4.4 | Thermal gravimetric analysis of PEtG architectures: *(a) linear (green), (b) cyclic (blue), (c) lariat (red), and (d) end-capped lariat (orange) PEtGs. Polymers are heated at 10 °C/min under a nitrogen atmosphere. Different polymer structures each display differing thermal stability, with cyclic PEtG showing the greatest stability and uncapped lariat PEtG showing the least.*

We sought to address why different initiators yield different polymer architectures. We surmised that at high concentration, the electronics of the initiating species determine the cyclization route. With Lewis acids, which readily react with trace water or monomer hydrate species present in solution[13], the initiator is a proton. Alternatively, the carbocationic initiators remain on chain ends and act as electron-donating groups, pushing electron density into the acetal backbone and favoring main-chain back-biting.

To test this hypothesis, the cationic polymerization was initiated instead by an electron-withdrawing carbocation, the acylium ion formed by reaction of acetyl chloride with aluminum chloride (Table 4.2, Entry 8). Ester back-biting should be favored in this case, which is precisely what was observed by MALDI-TOF MS. The two main mass spectrum peaks correspond to ester back-biting with an H- end group (from H^+ initiation after reaction with trace water or monomer hydrate) and ester back-biting with an acyl end group, as expected. Furthermore, a peak corresponding to an acyl end-group was observed by NMR, confirming that the cyclization mechanism is determined by the electronics of the initiating species. To test for the possibility of acetyl chloride reacting as an end-capping reagent similar to phenyl isocyanate, as described above, we ran a control reaction where the polymerization was initiated by boron trifluoride

(identical conditions to Table 4.2, Entry 2), followed by quenching with pyridine and an attempted end-capping with acetyl chloride. MALDI-TOF MS demonstrated that the acetyl group is not incorporated at the polymer chain-end in this case, confirming that the acetyl end-group is generated via initiation and not end-capping.

4.4 Conclusions

In conclusion, we studied the cationic polymerization of EtG and showed it generates cyclic and lariat shaped polymer of low molecular weight. The molecular weight does not correlate to theoretical values due to significant transfer reactions from intramolecular cyclization. Two divergent routes for cyclization were identified, either via main-chain back-biting or pendant ester back-biting to give the different polymer architectures. The favored route for cyclization was found to depend both on the monomer concentration as well as the electronics of the initiating species.

Understanding the underlying mechanisms of polymerization and the ability to rigorously control polymer structure has important implications toward the design of new materials. As demonstrated, the different polymer architectures display unique physical properties, differing in terms of thermal stabilities, hydrodynamic radii, and intrinsic viscosities. Manipulation of polymer architecture is thus a useful tool in materials design, and additional strategies toward the rational development of complex architectures are needed. These results will prove instructive in the future development of transient materials.

4.5 Synthetic Procedures

Scheme 4.2 **|** *General anionic polymerization of ethyl glyoxylate.*

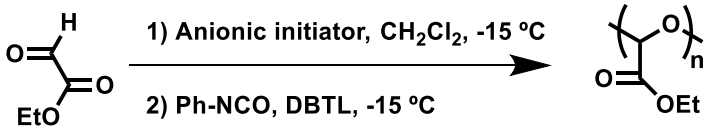

Distilled ethyl glyoxylate (EtG, 1.0 mL, 10 mmol) is added to a Schlenk flask and dissolved in dichloromethane (9 mL). The solution is cooled to -15 °C and triethylamine is added (0.03 mL, 0.2 mmol). The reaction turns colorless and viscous within minutes. After 1 h at -15 °C, phenyl isocyanate (0.15 mL, 1.4 mmol) and dibutyl tin dilaurate (0.02 mL, 0.03 mmol) are added. The mixture is left stirring and allowed to warm to room temperature overnight (~18 hours). The polymer is then precipitated into *n*-pentane (100

mL) and collected as a gummy white solid (0.95 g, 92%). ^{1}H NMR (500 MHz, $CDCl_3$) δ 7.50-6.10 ppm (br, phenyl), 5.75-5.45 ppm (br, 1H, acetal), 4.30-4.05 ppm (br, 2H, -OCH_2-), 1.35-1.15 ppm (br, 3H, CH_3). ^{13}C{^{1}H} NMR (125 MHz, $CDCl_3$) δ 166.5-165.0 ppm, 130.0-127.5 ppm, 94.5-91.0 ppm, 62.3 ppm, 14.1 ppm.

Table 4.3 *| Anionic polymerization reactions.*

Entry	*Initiator*	*[EtG]$_0$ (M)*	*[M]$_0$/[I]$_0$*	*M_w (kDa)[a]*	*M_p (kDa)[a]*	*PDI[a]*
1	Et_3N	6	120	170	97	1.9
2	Et_3N	3	90	77	79	1.8
3	Et_3N	1	50	24	23	1.6
4	Et_3N	1	20	6.2	6.0	1.9
5	*n*-BuLi[b]	1	20	4.1	2.9	1.8

[a]Average molecular weights and polydispersity determined by gel permeation chromatography (GPC), calibrated with monodisperse polystyrene standards. [b]Reaction run in THF.

Scheme 4.3 *| General cationic polymerization of ethyl glyoxylate.*

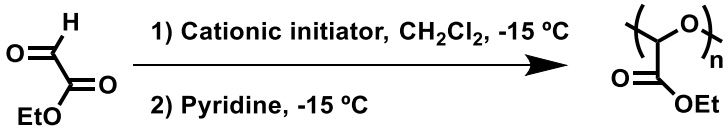

Distilled ethyl glyoxylate (EtG, 2.0 mL, 20 mmol) is added to a Schlenk flask and dissolved in dichloromethane (1.5 mL). The solution is cooled to -15 °C and boron trifluoride etherate is added (0.03 mL, 0.24 mmol). The reaction turns colorless and viscous within minutes. After 1 h at -15 °C, pyridine (0.08 mL, 1.0 mmol) is added. The mixture is left for 2 h and then warmed to room temperature. The polymer is then precipitated into n-pentane (100 mL), and the separated material collected as a colorless oil (1.7 g, 83%). ^{1}H NMR (500 MHz, $CDCl_3$) δ 5.75-5.45 ppm (br, 1H, acetal), 4.30-4.05 ppm (br, 2H, -OCH_2), 1.35-1.15 ppm (br, 3H, -CH_3). ^{13}C{^{1}H} NMR (125 MHz, $CDCl_3$) δ 166.5-165.0 ppm, 94.5-91.0 ppm, 62.3 ppm, 14.1 ppm.

The procedure with solid initiators (Ph_3CBF_4, Et_3OBF_4, and $AlCl_3$) is identical to the above, except initiators are weighed and dissolved in a minimal amount of dichloromethane in a glovebox prior to addition.

Reactions were repeated with the identical procedure at two alternative temperatures, -78 °C (M_w < 1 kDa) and 25 °C (M_w = 2.9 kDa). Furthermore, the procedure was repeated with toluene as solvent in place of dichloromethane (M_w = 3.5 kDa).

Table 4.4 | *Cationic polymerization reactions.*

Entry	*Initiator*	*[EtG]$_0$ (M)*	*[M]$_0$/[I]$_0$*	*M_w (kDa)*[a]	*M_p (kDa)*[a]	*PDI*[a]	*MALDI observations (main peak series)*
1	$BF_3{\cdot}OEt_2$	10	80	3.6	3.4	1.3	Ester back-biting
2	$BF_3{\cdot}OEt_2$	6	80	5.6	4.4	1.7	Ester back-biting[b]
3	$BF_3{\cdot}OEt_2$	4	80	4.9	4.0	1.6	Main-chain back-biting[b]
4	$BF_3{\cdot}OEt_2$	2	80	5.3	4.2	1.6	Main-chain back-biting[b]
5	$SnCl_4$	9	130	5.0	4.0	1.7	Ester back-biting
6	Ph_3CBF_4	6	100	2.1	1.6	1.3	Main-chain back-biting
7	Et_3OBF_4	9	100	6.3	5.8	1.8	Main-chain back-biting[b]
8	$CH_3COCl/AlCl_3$	7	70	5.1	4.4	1.8	Ester back-biting

[a]Average molecular weights and polydispersity determined by gel permeation chromatography (GPC), calibrated with monodisperse polystyrene standards. [b]Secondary MALDI peak series observed corresponding to alternative cyclization mechanism.

Scheme 4.4 | *Cationic polymerization of ethyl glyoxylate with end-capping.*

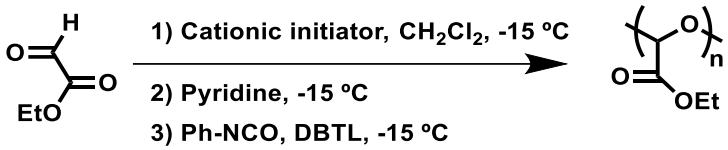

Distilled ethyl glyoxylate (EtG, 2.0 mL, 20 mmol) is added to a Schlenk flask and dissolved in dichloromethane (1.0 mL). The solution is cooled to -15 °C and boron trifluoride etherate is added (0.03 mL, 0.2 mmol). The reaction turns colorless and viscous within minutes. After 1 h at -15 °C, pyridine (0.08 mL, 1.0 mmol) is added, followed by phenyl isocyanate (0.09 mL, 0.8 mmol) and dibutyl tin dilaurate (0.02 mL, 0.03 mmol). The mixture is left stirring and then allowed to warm to room temperature overnight (~18 hours). The polymer is then precipitated into n-pentane (100 mL) and collected as a yellow oil (1.6 g, 79%). ^{1}H NMR (500 MHz, $CDCl_3$) δ 7.50-6.10 ppm (br, phenyl), 5.75-5.45 ppm (br, 1H, acetal), 4.30-4.05 ppm (br, 2H, -OCH_2-), 1.35-1.15 ppm (br, 3H, -CH_3). $^{13}C\{^1H\}$ NMR (125 MHz, $CDCl_3$) δ 166.5-165.0 ppm, 130.0-127.5 ppm, 94.5-91.0 ppm, 62.3 ppm, 14.1 ppm.

Table 4.5 | *End-capped cationic polymerization reactions.*

Entry	*Initiator*	*[EtG]$_0$ (M)*	*[M]$_0$/[I]$_0$*	*M_w (kDa)*[a]	*M_p (kDa)*[a]	*PDI*[a]	*MALDI observations (main peak series)*
1	$BF_3{\cdot}OEt_2$	7	80	4.0	3.6	1.5	Ester back-biting

[a]Average molecular weights and polydispersity determined by gel permeation chromatography (GPC), calibrated with monodisperse polystyrene standards.

Scheme 4.5 **|** *Varying initiator concentration in the cationic polymerization of ethyl glyoxylate.*

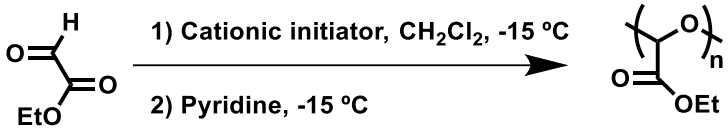

Distilled ethyl glyoxylate (EtG, 1.0 mL, 10 mmol) is added to a Schlenk flask and dissolved in dichloromethane (0.6 mL). The solution is cooled to -15 °C and boron trifluoride etherate is added (0.01-0.20 mL, 0.08-1.6 mmol). With low initiator concentrations, the reaction remains stirring for at least 15 min, but with high initiator loadings, the reaction turns colorless and stirring is halted within seconds. After 1 h, pyridine (0.05-0.30 mL, 0.6-3.7 mmol) is added. The mixture is left for 2 h and then warmed to room temperature. The polymer is then precipitated into n-pentane (100 mL), and the separated material is collected as a colorless oil (64-80% yields).

Table 4.6 **|** *Cationic polymerization reactions.*

Entry	*Initiator*	*$[EtG]_0$ (M)*	*$[M]_0/[I]_0$*	*M_w (kDa)[a]*	*M_p (kDa)[a]*	*PDI[a]*	*MALDI observations (main peak series)*
1	$BF_3{\cdot}OEt_2$	6	120	2.6	0.9	2.8	Main-chain back-biting[b]
2	$BF_3{\cdot}OEt_2$	6	80	5.6	4.4	1.7	Ester back-biting[b]
3	$BF_3{\cdot}OEt_2$	6	20	10.9	11.4	2.6	Main-chain back-biting[b]
4	$BF_3{\cdot}OEt_2$	6	12	13.6	10.8	1.4	Main-chain back-biting[b]
5	$BF_3{\cdot}OEt_2$	6	6	13.0	10.2	1.6	Ester back-biting[b]

[a]Average molecular weights and polydispersity determined by gel permeation chromatography (GPC), calibrated with monodisperse polystyrene standards. [b]Secondary MALDI peak series observed corresponding to alternative cyclization mechanism.

Scheme 4.6 **|** *Testing dynamic nature of cationic polymerization of ethyl glyoxylate.*

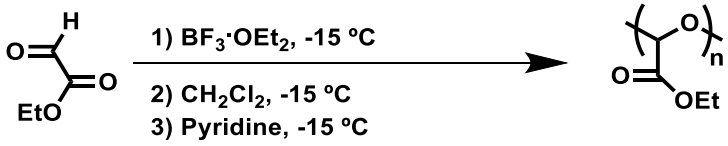

Distilled ethyl glyoxylate (EtG, 1.0 mL, 10 mmol) is added to a Schlenk flask. The solution is cooled to -15 °C and boron trifluoride etherate is added (0.10 mL, 0.8 mmol). The reaction turns colorless and stirring is halted within seconds. After 1 h, dichloromethane (4 mL) is added, and the mixture left another 2 h at -15 °C. The solid gel takes 1 h to dissolve, and is left an additional 1 h to react at the new concentration. Then, pyridine (0.20 mL, 2.5 mmol) is added. The mixture is left stirring for 2 h and warmed to room

temperature. The polymer is then precipitated into n-pentane (100 mL), and the separated material collected as an opaque oil (0.57 g, 55% yield).

***Table 4.7** | Cationic initiated polymerization reactions.*

Entry	*Initiator*	*$[EtG]_0$ (M)*	*$[M]_0/[I]_0$*	*M_w (kDa)[a]*	*M_p (kDa)[a]*	*PDI[a]*	*MALDI observations (main peak series)*
1	$BF_3{\cdot}OEt_2$	10 M → 2 M	12	10.4	8.7	1.3	Main-chain back-biting[b]

[a]Average molecular weights and polydispersity determined by gel permeation chromatography (GPC), calibrated with monodisperse polystyrene standards. [b]Secondary MALDI peak series observed corresponding to alternative cyclization mechanism.

4.6 NMR and MALDI Spectra

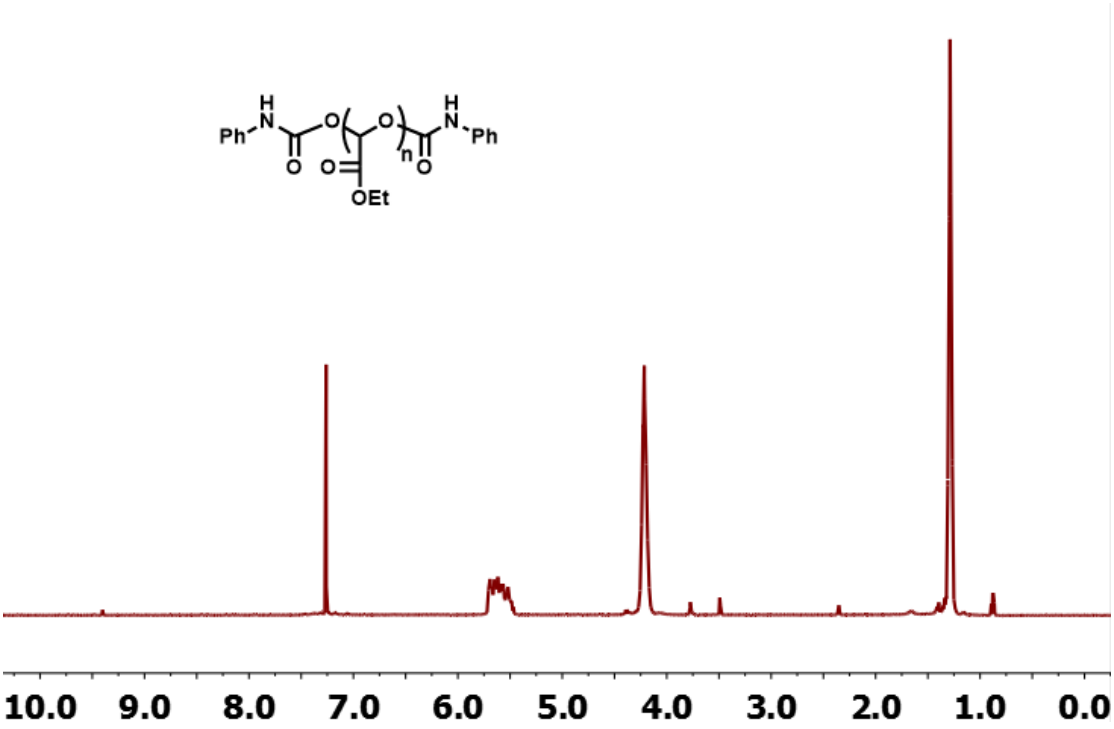

***Figure 4.5 | ^{1}H NMR spectrum of anionic initiated PEtG**: NMR spectrum of M_n = 43 kDa PEtG (Table 4.3, Entry 2) prepared by anionic polymerization in $CDCl_3$.*

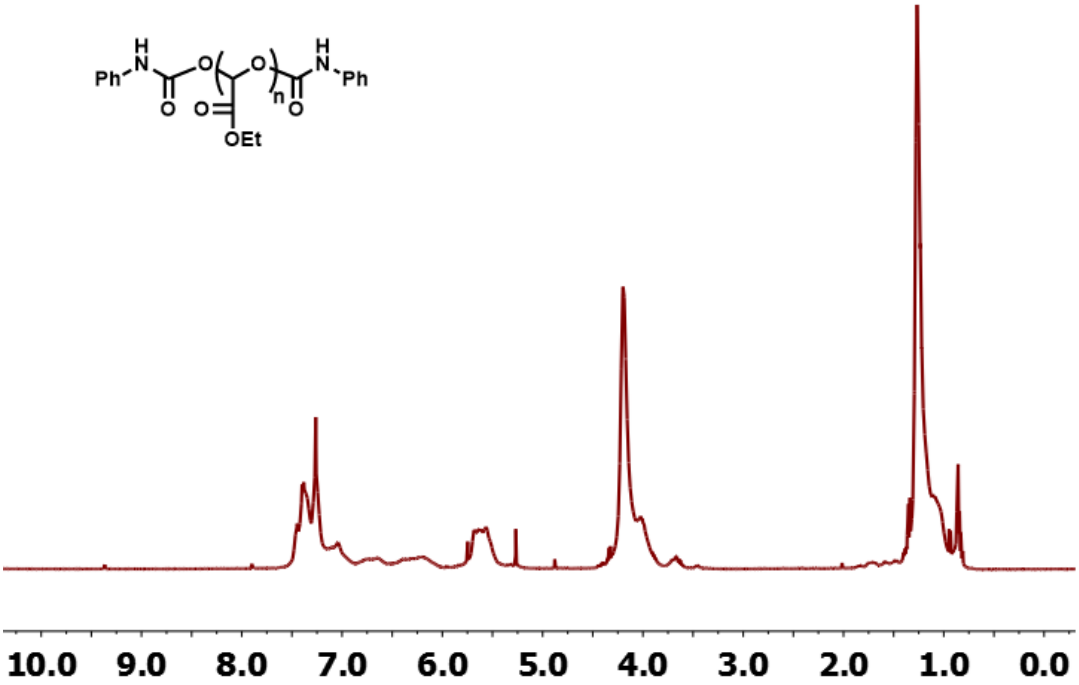

***Figure 4.6 | ^{1}H NMR spectrum of anionic initiated PEtG**: NMR spectrum of M_n = 2.3 kDa PEtG (Table 4.3, Entry 5) prepared by anionic polymerization in $CDCl_3$. Phenyl groups are observed, consistent with the capping reaction.*

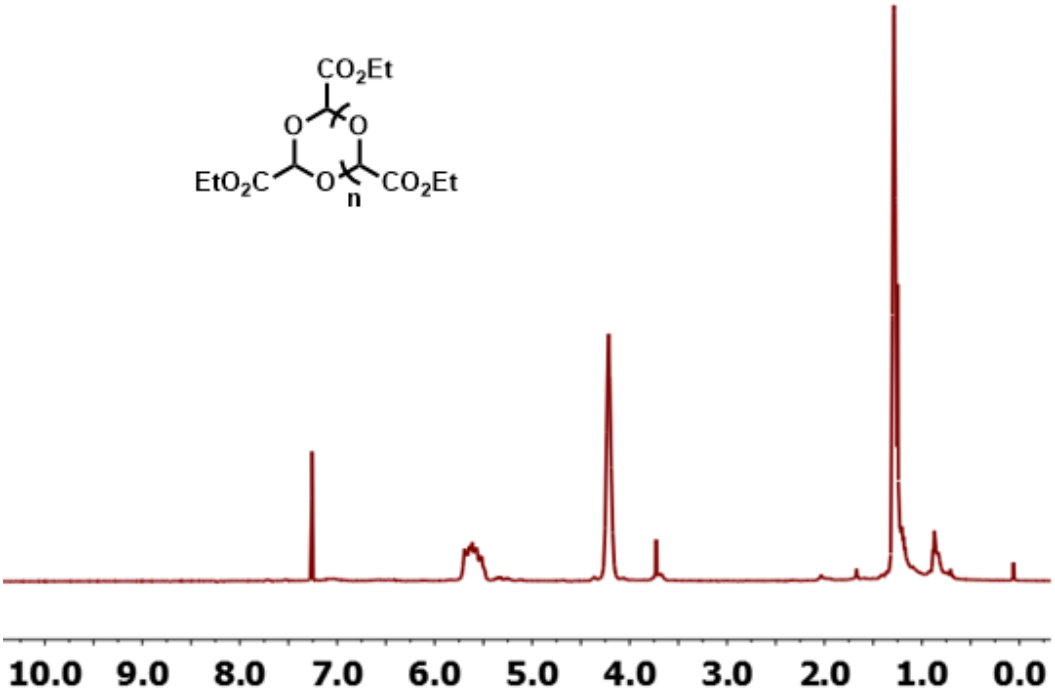

***Figure 4.7 | ^{1}H NMR spectrum of cyclic PEtG**: NMR spectrum of M_w = 2.1 kDa PEtG (Table 4.4, Entry 6) prepared by cationic polymerization with triphenylcarbenium tetrafluoroborate initiation in $CDCl_3$. End groups are not discernible.*

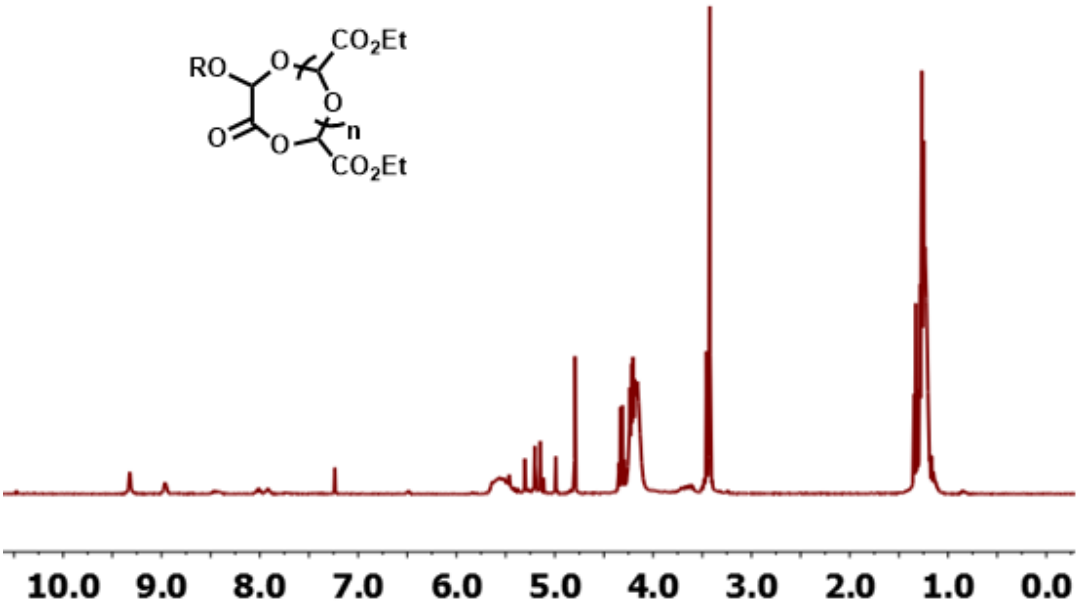

***Figure 4.8 | ^{1}H NMR spectrum of lariat PEtG**: NMR spectrum of M_w = 3.6 kDa PEtG (Table 4.4, Entry 1) prepared by cationic polymerization with boron trifluoride etherate initiation in $CDCl_3$. Spectrum displays additional peaks corresponding to partial depolymerization from uncapped hemiacetal chain ends and residual pyridinium salts.*

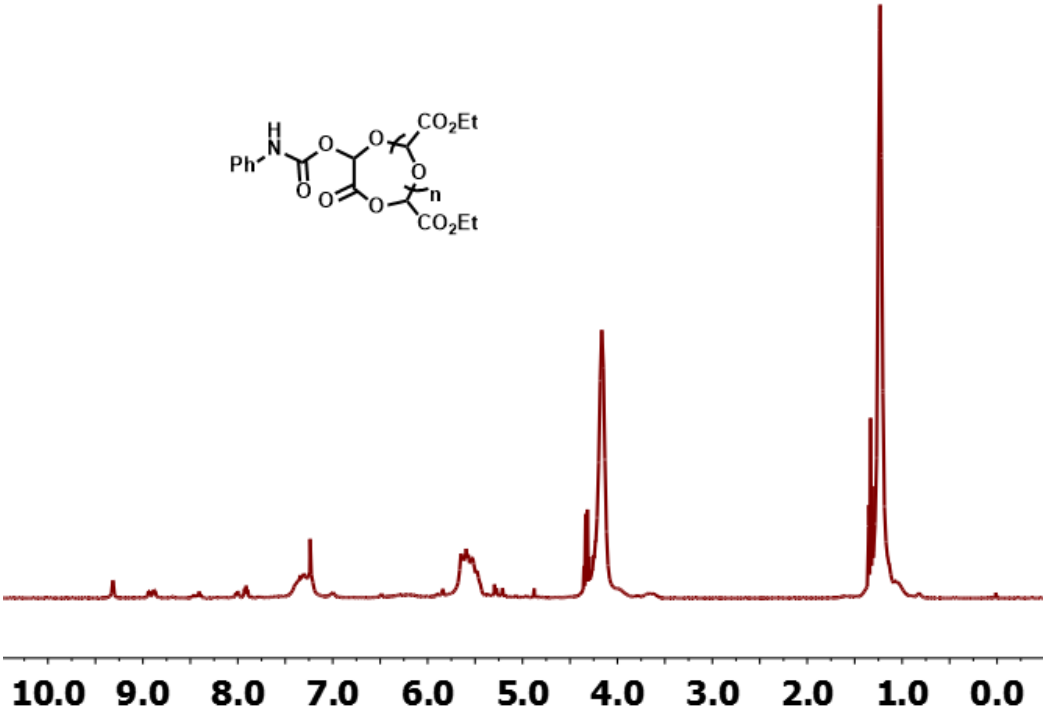

***Figure 4.9 | ^{1}H NMR spectrum of end-capped lariat PEtG**: NMR spectrum in $CDCl_3$ of M_w = 4.0 kDa PEtG (Table 4.5, Entry 1) prepared by cationic polymerization with boron trifluoride etherate initiation and phenyl isocyanate end-capping. Partial depolymerization and residual pyridinium salts can be seen, as in Figure S7, but majority of polymer is end-capped and phenyl end-group is observed.*

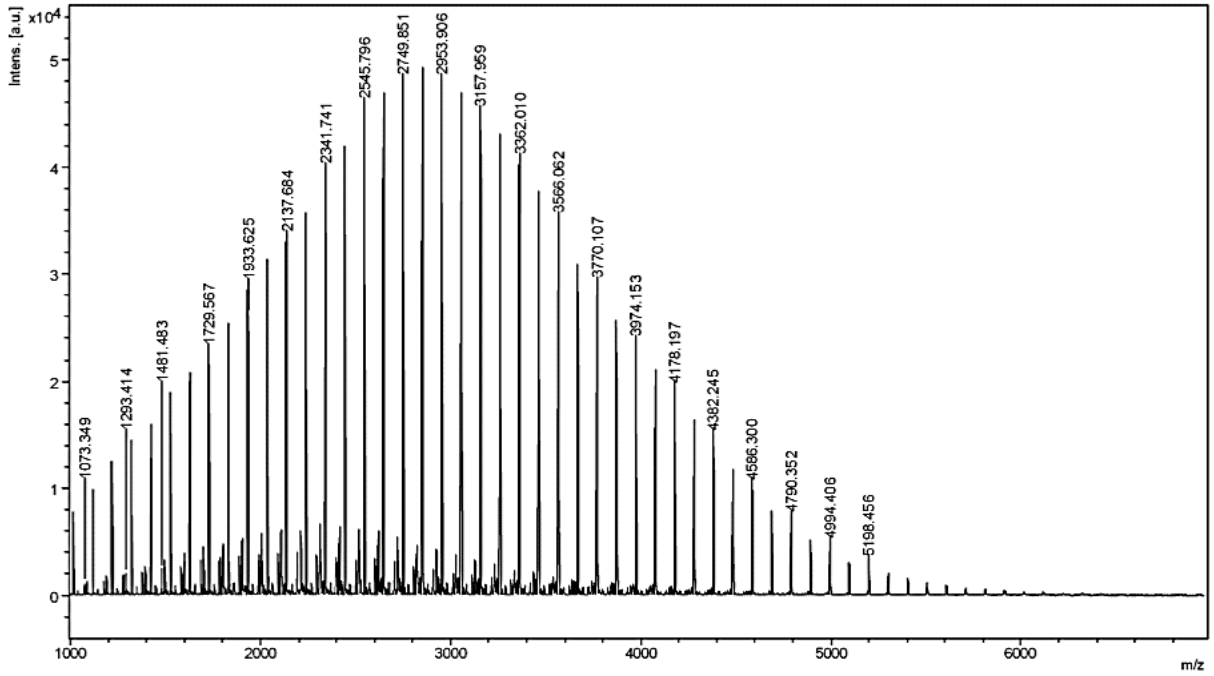

Figure 4.10 | MALDI-TOF mass spectrum of lariat PEtG*: Spectrum of PEtG polymerized with boron trifluoride etherate at 10 M (Table 4.4, Entry 1, GPC M_w = 3.6 kDa). Peaks match sodium adduct of cyclic PEtG missing a single ethyl group (ester back-biting cyclization). Minor secondary peaks match sodium adduct of cyclic PEtG missing two ethyl groups (double ester back-biting series).*

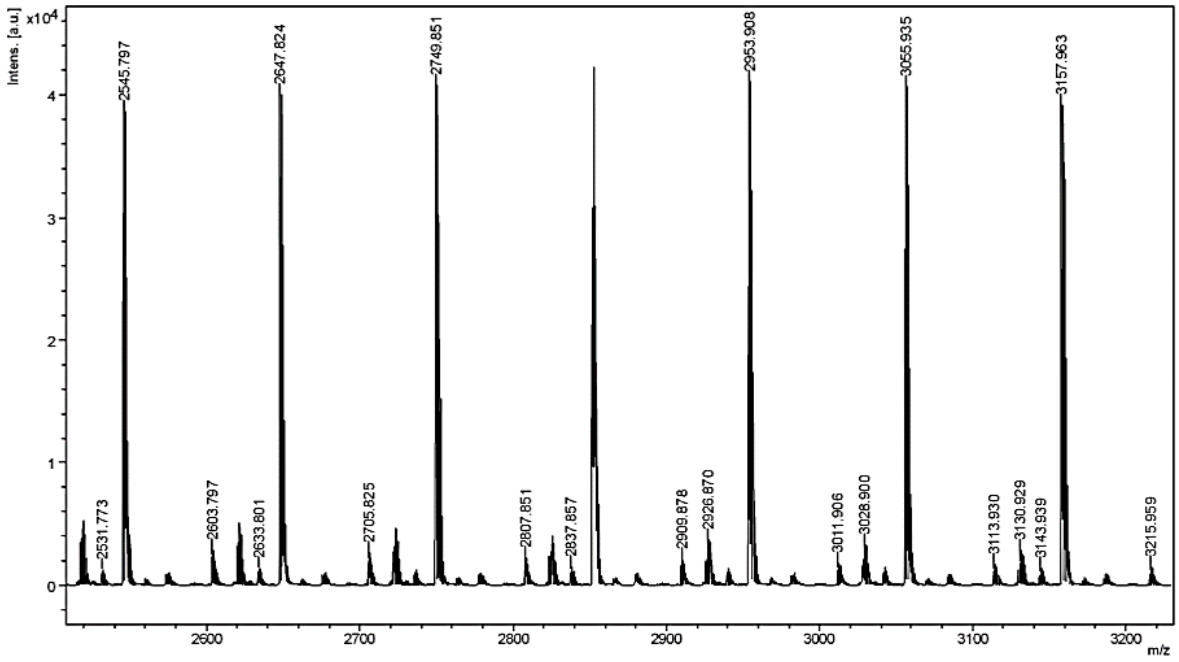

Figure 4.11 | MALDI-TOF mass spectrum of lariat PEtG*: Expansion of mass spectrum of PEtG polymerized with boron trifluoride etherate at 10 M (Table 4.4, Entry 1, GPC M_w = 3.6 kDa). Peaks match sodium adduct of cyclic PEtG missing a single ethyl group (ester back-biting cyclization).*

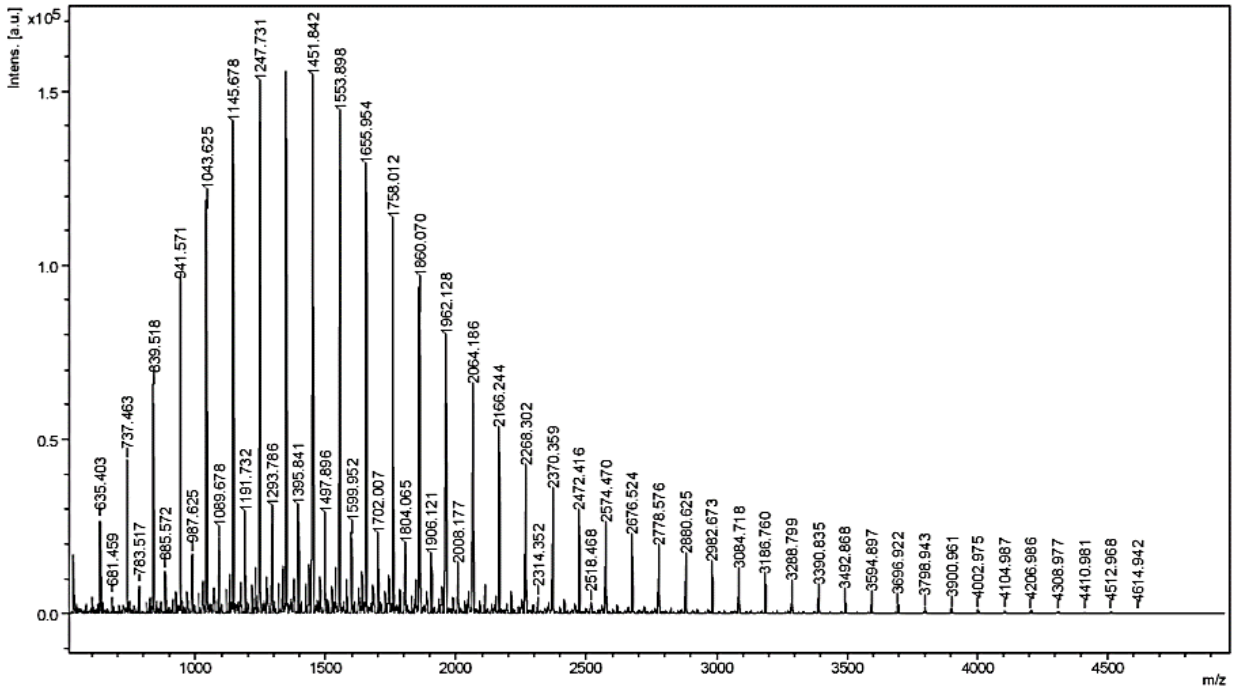

Figure 4.12 | MALDI-TOF mass spectrum of cyclic PEtG*: Spectrum of PEtG polymerized with Ph_3CBF_4 (Table 4.4, Entry 6, GPC M_w = 2.1 kDa). Peaks match sodium adduct of cyclic PEtG (main-chain back-biting cyclization). Minor secondary peaks match sodium adduct of cyclic PEtG missing two ethyl groups (double ester back-biting series).*

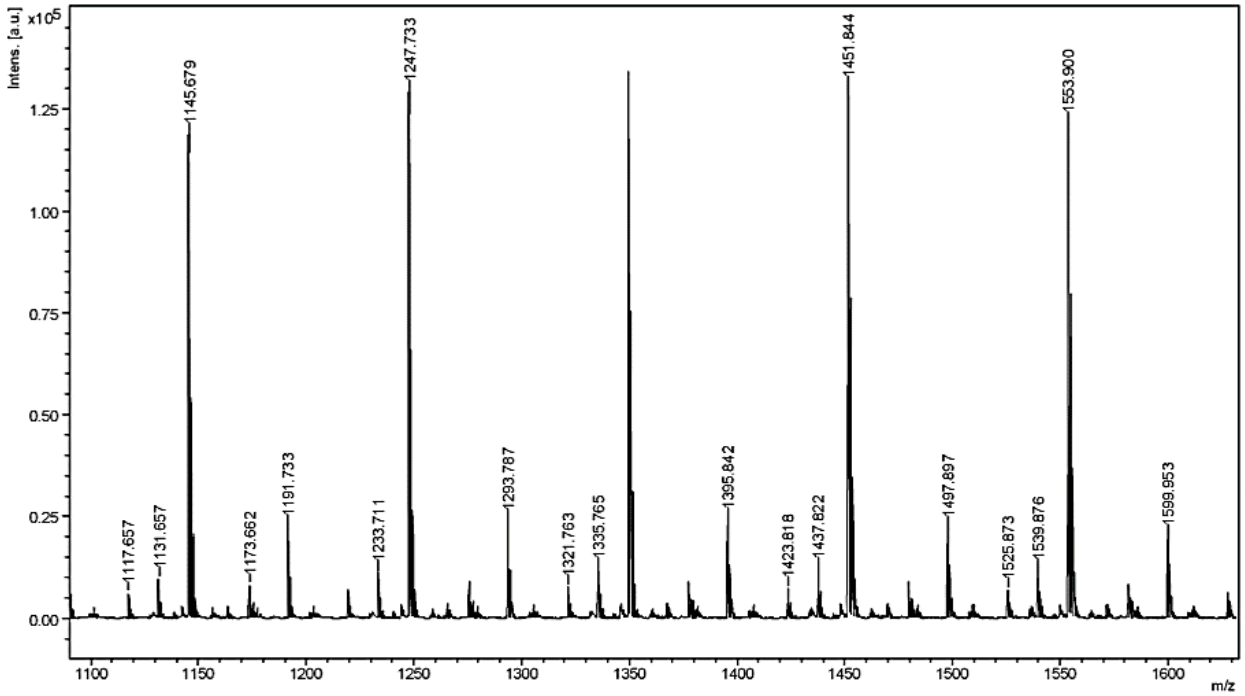

Figure 4.13 | MALDI-TOF mass spectrum of cyclic PEtG*: Expansion of spectrum of PEtG polymerized with Ph_3CBF_4 (Table 4.4, Entry 6, GPC M_w = 2.1 kDa). Peaks match sodium adduct of cyclic PEtG (main-chain back-biting cyclization).*

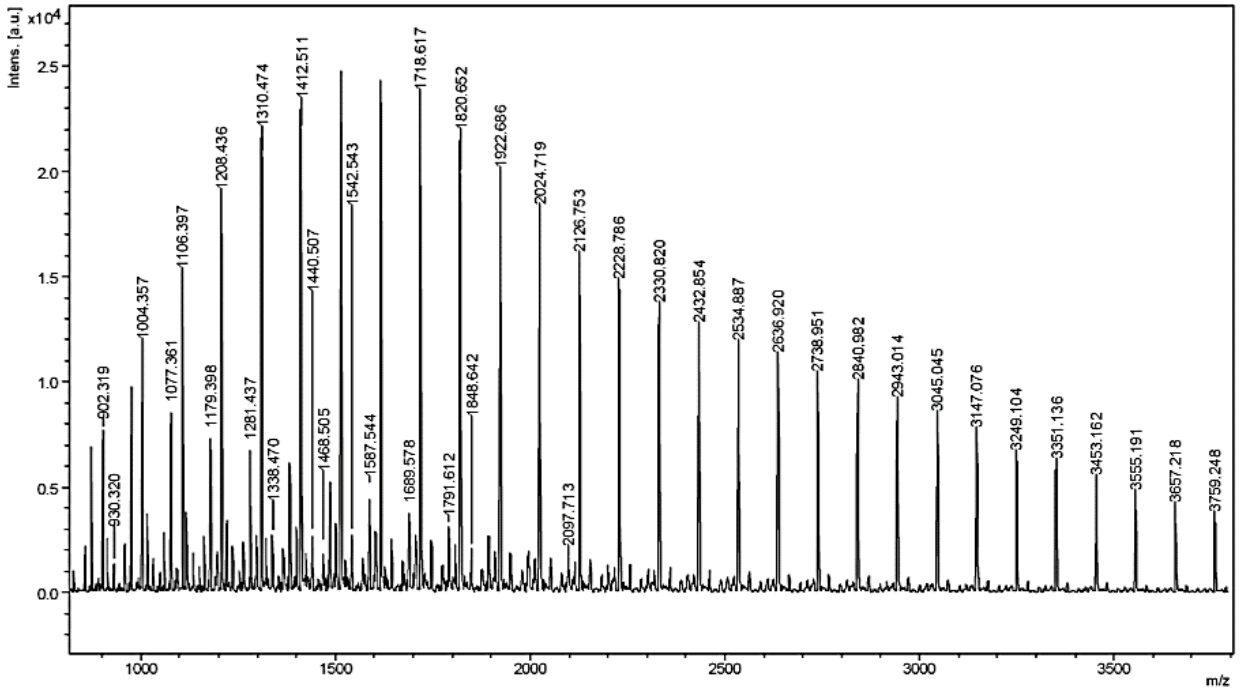

Figure 4.14 | MALDI-TOF mass spectrum of end-capped lariat PEtG*: Spectrum of PEtG polymerized by boron trifluoride etherate with phenyl isocyanate end-caps (Table 4.5, Entry 1, GPC M_w = 4.0 kDa). Peaks match sodium adduct of cyclic PEtG missing two ethyl groups plus phenyl isocyanate end-group (double ester back-biting cyclization with end-capping).*

4.7 References

(1) (a) Peterson, G. I.; Larsen, M. B.; Boydston, A. J. *Macromolecules* **2012**, 45, 7317-7328. (b) Esser-Kahn, A. P.; Odom, S. A.; Sottos, N. R.; White, S. R.; Moore, J. S. *Macromolecules* **2011**, 44, 5539-5553. (c) Wong, A. D.; DeWit, M. A.; Gillies, E. R. *Adv. Drug Delivery Rev.* **2012**, 64, 1031-1045. (d) Sagi, A.; Weinstain, R.; Karton, N.; Shabat, D. *J. Am. Chem. Soc.* **2008**, 130, 5434-5435.

(2) (a) Vogl, O. *J. Polym. Sci., Part A: Polym. Chem.* **2000**, 38, 2293-2299. (b) Kostler, S. *Polym. Int.* **2012**, 61, 1221-1227.

(3) (a) Chuji, A.; Tagami, S.; Kunitake, T. *J. Polym. Sci. Part A: Polym. Chem.* **1969**, 7, 497-511. (b) Chuji, A.; Tagami, S. *Macromolecules* **1969**, 2, 414-419. (c) Willson, C. G.; Ito, H.; Frechet, J. M. J.; Tessier, T. G.; Houlihan, F. M. *J. Electrochem. Soc.* **1986**, 133, 181-187. (d) Tsuda, M.; Hata, M.; Nishida, R.; Oikawa, S. *J. Polym. Sci. Part A: Polym. Chem.* **1997**, 35, 77-89.

(4) (a) Ito, H.; Willson, C. G. *Polym. Eng. Sci.* **1983**, 23, 1012-1018. (b) Knoll, A. W.; Pires, D.; Coulembier, O.; Dubois, P.; Hedrick, J. L.; Frommer, J.; Duerig, U. *Adv. Mater.* **2010**, 22, 3361-

3365. (c) Coulembier, O.; Knoll, A.; Pires, D.; Gotsmann, B.; Duerig, U.; Frommer, J.; Miller, R. D.; Dubois, P.; Hedrick, J. L. *Macromolecules* **2010**, 43, 572-574.

(5) (a) Seo, W.; Phillips, S. T. *J. Am. Chem. Soc.* **2010**, 132, 9234-9235. (b) Dilauro, A. M.; Robbins, J. S.; Phillips, S. T. *Macromolecules* **2013**, 46, 2963-2968. (c) Kaitz, J. A.; Moore, J. S. *Macromolecules* **2013**, 46, 608-612. (d) Kaitz, J. A.; Possanza, C. M.; Song, Y.; Diesendruck, C. E.; Spiering, A. J. H.; Meijer, E. W.; Moore, J. S. *Polym. Chem.* **2014**, 5, 3788-3794.

(6) DiLauro, A. M.; Zhang, H.; Baker, M. S.; Wong, F.; Sen, A.; Phillips, S. T. *Macromolecules* **2013**, 46, 7257-7265.

(7) Dilauro, A. M.; Abbaspourrad, A.; Weitz, D. A.; Phillips, S. T. *Macromolecules* **2013,** 46, 3309-3313.

(8) (a) Kaitz, J. A.; Diesendruck, C. E.; Moore, J. S. *J. Am. Chem. Soc.* **2013**, 135, 12755-12761. (b) Kaitz, J. A.; Diesendruck, C. E.; Moore, J. S. *Macromolecules* **2013**, 46, 8121-8128.

(9) (a) Semlyen, J. A. *Cyclic Polymers*, 2nd ed.; Kluwer Academic Publishers: Dordrecht, **2000**; pp 347-384. (b) Kricheldorf, H. R. *J. Polym. Sci., Part A: Polym. Chem.* **2010**, 48, 251-284. (c) Jia, Z.; Monteiro, M. J. *J. Polym. Sci., Part A: Polym. Chem.* **2012**, 50, 2085-2097. (d) Laurent, B. A.; Grayson, S. M. *Chem. Soc. Rev.* **2009**, 38, 2202-2213. (e) Yamamoto, T.; Tezuka, Y. *Polym. Chem.* **2011**, 2, 930-1941. (f) Endo, K. *Adv. Polym. Sci.* **2008**, 217, 121-183.

(10) (a) Jeong, W.; Shin, E. J.; Culkin, D. A.; Hedrick, J. L.; Waymouth, R. M. *J. Am. Chem. Soc.* **2009**, 131, 4884-4891. (b) Culkin, D. A.; Jeong, W.; Csihony, S.; Gomez, E. D.; Balsara, N. P.; Hedrick, J. L.; Waymouth, R. M. *Angew. Chem. Int. Ed.* **2007**, 46, 2627-2630. (c) Jeong, W.; Hedrick, J. L.; Waymouth, R. M. *J. Am. Chem. Soc.* **2007**, 129, 8414-8415. (d) Shin, E. J.; Brown, H. A.; Gonzalez, S.; Jeong, W.; Hedrick, J. L.; Waymouth, R. M. *Angew. Chem. Int. Ed.* **2011**, 50, 6388-6391. (e) Guo, L.; Zhang, D. *J. Am. Chem. Soc.* **2009**, 131, 18072-18074. (f) Guo, L.; Lahasky, S. H,; Ghale, K.; Zhang, D. *J. Am. Chem. Soc.* **2012**, 134, 9163-9171.

(11) (a) Rique-Lurbet, L.; Schappacher, M.; Deffieux, A. *Macromolecules* **1994**, 27, 6318-6324. (b) Laurent, B. A.; Grayson, S. M. *J. Am. Chem. Soc.* **2006**, 128, 4238-4239. (c) Leppoittevin, B.; Perrot, X.; Masure, M.; Hemery, P. *Macromolecules* **2001**, 34, 425-429. (d) Oike, H.; Imaizumi, H.; Mouri, T.; Yoshioka, Y.; Uchibori, A.; Tezuka, Y. *J. Am. Chem. Soc.* **2000**, 122, 9592-9599. (e) Sugai, N.; Heguri, H.; Yamamoto, T.; Tezuka, Y. *J. Am. Chem. Soc.* **2011**, 133,19694-19697.

(12) (a) Bielawski, C. W.; Benitez, D.; Grubbs, R. H. *Science* **2002**, 297, 2041-2044. (b) Boydston, A. J.; Xia, Y.; Kornfield, J. A.; Gorodetskaya, I. A.; Grubbs, R. H. *J. Am. Chem. Soc.* **2008**, 130, 12775-12782. (c) Xia, Y.; Boydston, A. J.; Yao, Y.; Kornfield, J. A.; Gorodetskaya, I. A.; Spiess, H. W.; Grubbs, R. H. *J. Am. Chem. Soc.* **2009**, 131, 2670-2677. (d) Bielawski, C. W.; Benitez, D.; Grubbs, R. H. *J. Am. Chem. Soc.* **2003**, 125, 8424-8425.

(13) (a) Burel, F.; Rossignol, L.; Pontvianne, P.; Hartman, J.; Couesnon, N.; Bunel, C. *e-Polymers* **2003**, 3, 407-411. (b) Belloncle, B.; Burel, F.; Oulyadi, H.; Bunel, C. *Polym. Degr. Stab.* **2008**, 93, 1151-1157.

(14) (a) Vairon, J. P.; Muller, E.; Bunel, C. *Macromol. Symp.* **1994**, 85, 307-312. (b) Brachais, C. H.; Huguet, J.; Bunel C. *Polymer*, **1997**, 38, 4959-4964. (c) Brachais, C. H.; Duclos, R.; Vaugelade, C.; Huguet, J.; Capelle-Hue, M.-L.; Bunel, C. *Int. J. Pharm.* **1998**, 169, 23-31. (d) Basko, M.; Kubisa, P.; Penczek, S.; Moreau, M.; Vairon, J. P. *Macromolecules* **2000**, 33, 294-302. (e) Basko, M.; Kubisa, P. *Macromolecules* **2002**, 35, 8948-8953.

(15) The polymerization temperature is -15 °C for all polymer samples included in Table 4.2. Polymerizations were also conducted at -78 °C and room temperature, generating the same low molecular weight species as observed in the -15 °C reaction.

(16) (a) He, J.; Tremblay, L.; Lacellea, S.; Zhao, Y. *Soft Matter* **2011**, 7, 2380-2386. (b) Beck, J. B.; Killops, K. L.; Kang, T.; Sivanandan, K.; Bayles, A.; Mackay, M. E.; Wooley, K. L.; Hawker, C. J. *Macromolecules* **2009**, 42, 5629–5635.

Chapter 5: Cationic Copolymerization of *o*-Phthalaldehyde and Ethyl Glyoxylate: Cyclic Macromolecules with Alternating Sequence and Tunable Thermal Properties*

5.1 Abstract

Aldehyde polymers have gained attention in recent decades as a class of stimuli-responsive materials capable of rapid, triggered depolymerization to monomer. Exploitation of the most prominent polyaldehydes for various solid-state applications, however, is limited by poor thermal and mechanical properties of the materials. To address these limitations, we pursued the copolymerization of ethyl glyoxylate, precursor to tacky polymers, with o-phthalaldehyde, precursor to brittle materials. Using NMR spectroscopy and MALDI-TOF mass spectrometry, we have discovered the surprising tendency of these sequences to alternate, resulting in alternating cyclic copolymers in certain feed ratios. We also report the ability to tailor the thermal properties of the solid copolymers by varying copolymer composition, enabling the selective tuning of copolymer glass transition and degradation temperatures to meet application demands. We envision that this copolymer system, which blends the properties of the tacky and brittle homopolymers, will find use as depolymerizable polyaldehydes for solid-state applications.

5.2 Introduction

Aldehyde polymers have emerged in recent years as a class of stimuli-responsive polymers, generating interest due to their low ceiling temperatures (T_c), which endow them with the capacity to undergo triggered depolymerization.[1] Much like other self-immolative polymers,[2-3] this class of polymers is prized due to their ability to respond immediately and specifically to fleeting stimuli with an amplified output. Low T_c aldehyde polymers have already found use in a variety of applications. For instance, poly(phthalaldehyde) (PPA, T_c = -40 °C)[4] has been employed in lithography,[5] shape-changing materials,[6] as a degradable thin film,[7] and as a shell wall material for degradable microcapsules.[8] However, PPA is limited in solid-state applications due to its brittle nature. From our own experience, unplasticized PPA

* Portions of this chapter have been published: Kaitz, J. A.; Moore, J. S. *Macromolecules* **2014**, 47, 5509-5513.

films are prone to cracking and suffer from poor mechanical toughness, even though molecular weights can exceed 250 kDa.

Polyethyl glyoxylate (PEtG) is a similar low ceiling temperature polyaldehyde (T_c = 37 °C) that has been reported in the literature.[9] Both PEtG and its counterpart polymethyl glyoxylate (PMeG, T_c = 26 °C) are reported as soft materials with glass transition temperatures (T_g) near or below room temperature.[9-10] Pioneering work on the cationic copolymerization of methyl glyoxylate with cyclic acetals produced thermally stable polyacetals that were further modified for use as functional materials.[11] However, the thermal properties of the copolymers were not fully investigated.

In order to employ depolymerizable aldehyde polymers in solid-state applications without the need for plasticization, we set out to copolymerize *o*-phthalaldehyde (OPA, precursor to brittle PPA) with ethyl glyoxylate (EtG, precursor to tacky PEtG). The goal was to provide a suitable material with an intermediate T_g between those of the homopolymers. The present chapter discusses the synthesis and complete solution and solid-state characterization of the resulting PPA/PEtG copolymers.

5.3 Results and Discussion

5.3.1 Cationic Copolymerization of OPA and EtG and Chemical Characterization of 1:1 Copolymer

PPA/PEtG copolymers were prepared by a cationic polymerization initiated by boron trifluoride etherate at -78 °C (Scheme 5.1). The cationic homopolymerization of both OPA and EtG monomers has been studied extensively by our group and served as the basis for conditions for the copolymerization reaction.[12] The solution polymerization transforms from a yellow to a colorless mixture within ten minutes, but is left for two hours to fully equilibrate. Finally, excess pyridine is added to quench the Lewis acid initiator, and the polymer is collected by precipitation into methanol and n-pentane.

Scheme 5.1 | *Copolymerization reaction of* o-*phthalaldehyde and ethyl glyoxylate*.

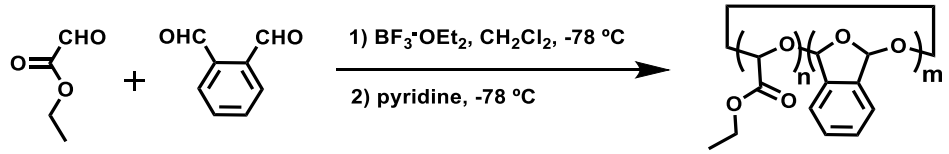

Copolymers starting from 1:1 monomer feed ratios were initially prepared for analysis. Qualitatively, it was apparent that the copolymer differed from either homopolymer, as it was collected as a white, sticky solid. Molecular weights of the copolymer ranged from M_w = 11-15 kDa (two repititions, degree of polymerization *ca*. 90-130), with polydispersities of *ca*. 1.8-2.2.

^{1}H and ^{13}C NMR spectroscopy were employed to determine copolymer compositions and investigate copolymer microstructure, respectively. Polyacetal backbone protons corresponding to EtG (δ = 5.3-6.1 ppm) or OPA (δ = 6.3-7.1 ppm) units are resolved in the copolymers, enabling accurate calculation of copolymer composition (see section 5.6). The copolymer composition of PPA/PEtG starting from 1:1 monomer feed ratios was determined to be 53/47 PPA/PEtG, averaged from the two runs. That this value is quite close to the monomer feed ratios suggested that the copolymerization successfully incorporates both monomers with similar reactivity.

Intriguingly, ^{13}C NMR spectra of the copolymers suggest that a microstructure entirely distinct from either homopolymer is produced in the copolymerization reaction. When copolymer spectra are compared to either homopolymer ^{13}C NMR spectra, a noticeable shift in resonance for all of the peaks is observed, with carbons assigned to the polymer backbone and adjacent to the polymer backbone demonstrating the largest shifts (Figure 5.1). Shifts in resonance are not unexpected for random copolymers,[12b] but most surprising was that acetal carbons from EtG (δ = 90-94 ppm) collapse to a single resonance and ester carbons (δ = 164-166 ppm) collapse to a single peak at 167 ppm, downfield from PEtG homopolymer peaks. In fact, ester peaks corresponding to EtG-EtG diads are not observed at all in the copolymer spectra, suggesting that the sequence is exclusively composed of EtG residues flanked on both sides by OPA units. OPA backbone (δ = 102-105 ppm) and adjacent carbons (δ = 138-140 ppm) likewise shift upfield, corroborating the possibility of an alternating copolymer sequence.

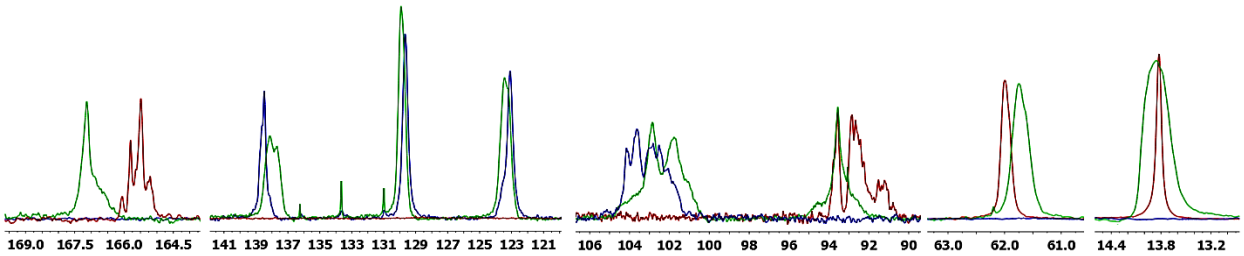

Figure 5.1 | ^{13}C NMR spectra of poly(phthalaldehyde-co-ethyl glyoxylate) copolymer*: PPA/PEtG copolymer produced from copolymerization reaction with 1:1 monomer feed ratio (green), overlaid with PEtG (red) and PPA (blue) homopolymers. Shifts in resonance are observed most prominently for backbone and adjacent carbons for PPA and PEtG units, suggesting a microstructure distinct from either homopolymer. All NMR spectra collected in $CDCl_3$ solvent.*

To further investigate the possibility of an alternating copolymer, MALDI-TOF mass spectrometry was utilized to probe the copolymer microstructure. An immediate pattern was recognized in the mass spectra thus obtained, which showed far fewer peaks than what would be expected for a true random copolymer.[12b] The major peaks correspond to cyclic copolymers with a 1:1 composition of EtG and OPA,

and the main peak series of 236 mass units correlates to the sum of both monomer units (Figure 5.2, red arrows). Furthermore, two major secondary peaks are observed, which are identified as being an additional OPA or EtG monomer unit added to the main peak series (Figure 5.2, blue and green arrows). Taken collectively with NMR data, these results suggest that the PPA/PEtG thus formed is a near-perfect alternating cyclic copolymer. To the best of our knowledge, this is the first example of such a macrocyclic alternating copolymer.

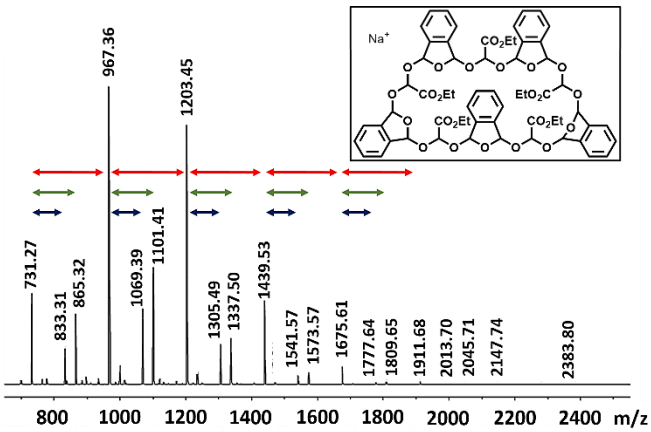

Figure 5.2 | MALDI-TOF mass spectra of poly(phthalaldehyde-co-ethyl glyoxylate) copolymer*: Main repeat series (red arrows) corresponds to sodium adduct of cyclic structure containing both monomer units; secondary peaks observed corresponding to main repeat series plus ethyl glyoxylate monomer (blue arrows) or o-phthalaldehyde monomer (green arrows). Inset structure corresponds to cyclic alternating decamer (theoretical m/z = 1203.33; observed m/z = 1203.45; error = 0.01%). DHB (2,5-dihydroxybenzoic acid) was used as the matrix and sodium iodide as the cationization agent.*

5.3.2 Investigation of Alternating Tendency in PPA/PEtG Copolymers

To further elucidate the alternating behavior of PPA/PEtG copolymers, a full series of copolymers with varying monomer feed ratios was prepared by cationic copolymerization under identical conditions. Copolymerization conditions and copolymer properties are summarized in Table 5.1, with all copolymers prepared in duplicate. It is noteworthy that as the ratio of EtG in comonomer feeds increases, the molecular weight and yield of copolymers drop substantially. This is attributed to significant transfer reactions that occur in the cationic polymerization of EtG, as well as poor precipitation of the low molecular weight and thermally unstable polymers produced at high EtG feeds.[12c]

Table 5.1 | PPA/PEtG copolymerization reactions and polymers used in this study.

Entry	*$[OPA]_0$ (M)*	*$[EtG]_0$ (M)*	*$[OPA]_0$/ $[EtG]_0$*	*$[M]_0/[I]_0$*	*Yield (%)*	*M_w (kDa)[a]*	*M_p (kDa)[a]*	*PDI[a]*	*% OPA in copolymer[b]*	*% EtG in copolymer[b]*	*T_g (°C)[c]*
1	1.0	- - -	- - -	30 / 1	92	320	255	2.4	100	0	- - -
2	0.8	0.2	4 / 1	26 / 1	85	19.6	21.6	2.7	73	27	129
3	0.6	0.4	3 / 2	26 / 1	78	15.4	18.2	2.6	61	39	100
4	0.5	0.5	1 / 1	26 / 1	76	15.1	15.8	2.2	53	47	97
5	0.4	0.6	2 / 3	26 / 1	73	14.5	14.3	2.0	50	50	84
6	0.2	0.8	1 / 4	26 / 1	48[d]	8.3	6.8	2.5	38	62	40
7	- - -	5.0[e]	- - -	60 / 1	57[d]	1.4	1.3	1.2	0	100	-19

[a]Average molecular weights and polydispersity determined by gel permeation chromatography (GPC), calibrated with monodisperse polystyrene standards. [b]Determined by ^{1}H NMR integrations (average of 2 runs). [c]Determined by DSC, average of 2 runs. [d]Product does not readily precipitate from n-pentane so yield data unreliable. [e]EtG polymerization at 1.0 M results in multi-modal GPC traces due to intermolecular termination events.[12c]

As with copolymers prepared from 1:1 monomer feed ratios, copolymer compositions were readily calculated from ^{1}H NMR integrations of acetal protons. Copolymer compositions deviate significantly from the 1:1 PPA/PEtG ratio that would be expected for a strictly alternating copolymer. However, when copolymer composition is plotted against comonomer feed, there is a noticeable preference toward alternation in the copolymers (Figure 5.3). At low EtG feeds, the copolymers deviate slightly from an ideal random copolymer and have a greater incorporation of EtG than in the feed. ^{13}C NMR resonances for EtG residues are comparable to those observed for 1:1 copolymers, indicating that EtG units are not incorporated sequentially into the copolymer but are rather flanked by OPA units or stretches. At high EtG feeds, there is an even more pronounced tendency for alternation, with the copolymer composition again strongly deviating toward what would be expected for an alternating copolymer. Incredibly, in the case of 4:1 EtG/OPA feed, ^{13}C NMR peaks corresponding to EtG-EtG diads are finally observed alongside the EtG-OPA peaks. While these results reveal that the PPA/PEtG copolymers are not strictly alternating copolymers, they do apparently have an alternating tendency at suitable monomer ratios. In fact, between 50% and 60% EtG feeds, the slope in the composition plot is nearly zero, and MALDI-TOF mass spectra corroborate that these copolymers display mostly alternating macrocyclic structures in this range (see section 5.6).

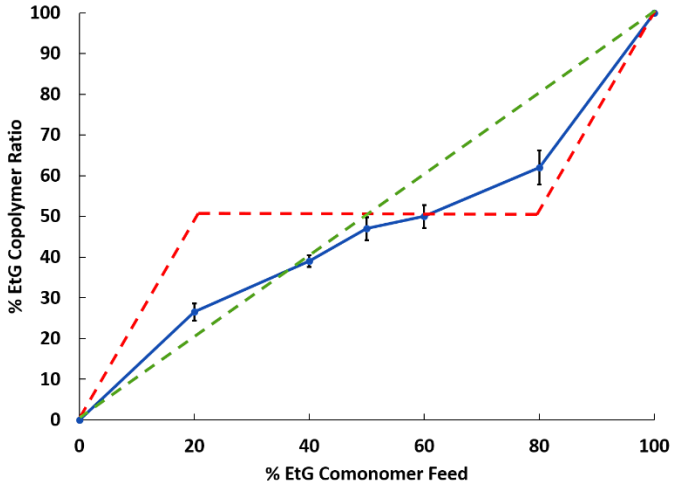

Figure 5.3 | Copolymer composition plot for poly(phthalaldehyde-co-ethyl glyoxylate) copolymers*: Percent EtG incorporation into copolymer plotted versus EtG monomer feed ratios (blue, averaged from two runs). Overlaid dashed lines correspond to theoretical composition plots for ideal random copolymer (green) and true alternating copolymer (red). Two regions are observed for PPA/PEtG copolymers; at low EtG ratios, EtG fully incorporated into copolymer and flanked by OPA units; at high EtG ratios, partially alternating copolymer is observed. Copolymer ratios are determined by* ^{1}*H NMR integrations of polyacetal backbone protons.*

To explain the alternating behavior, we anticipated the potential involvement of both electronic and steric factors. It was already suggested that there is a similar alternating tendency in the copolymerization of methyl glyoxylate with cyclic acetals due to steric repulsion between bulky glyoxylate units.[11] This is likely also a strong driver in the copolymerization of EtG and OPA. However, we reasoned that there could also be an electronic preference for alternation in this system. It is known that alternating copolymers are produced in the copolymerization of electron-rich and electron-poor monomers due to the pre-coordination of monomers to form charge-transfer complexes, as in the case of styrene copolymerization with electron-poor olefins.[13] To investigate possible pre-coordination, ^{1}H NMR spectra of both monomers were collected individually as well as mixed together in a 1:1 ratio in different solvents. In chloroform and dichloromethane, both non-polar solvents, shifts in resonance for both monomers were observed ranging from δ = 0.01-0.05 ppm when mixed. On the other hand, in polar aprotic solvents such as DMSO, shifts are not observed between the monomers individually and when mixed (δ < 0.01 ppm), suggesting that non-covalent complexation is impeded in disruptive solvents. The results thus indicate that a combination of both electronic and steric factors promote the alternating tendency observed in PPA/PEtG copolymers.

5.3.3 Thermal Characterization of PPA/PEtG Copolymers

Thermal characterization of the solid copolymers was investigated. Dynamic scanning calorimetry (DSC) was performed in duplicate to determine copolymer glass transition temperatures (T_g), and thermal gravimetric analysis (TGA) was performed to identify copolymer degradation temperatures (T_d). The thermal properties are summarized in Figure 5.4.

As expected, based on the soft, sticky nature of the PPA/PEtG copolymers that were prepared, the T_g of all copolymers was lower than that of PPA homopolymer. In fact, no T_g is observed for PPA as the polymer degrades before evidence of any transition. The T_g of the tacky PEtG homopolymer is -19 °C,[14] and T_g's of PPA/PEtG copolymers range from 40 °C for 62% EtG incorporation to 129 °C for 27% EtG incorporation. A linear trend is observed when T_g is plotted versus copolymer composition, where increasing OPA incorporation causes a concomitant increase in T_g (Figure 5.4, blue trace).[15] Based on this trendline, a virtual T_g was calculated for PPA to be 184 °C, higher than its T_d, and in agreement with the lack of experimental observation of the transition.

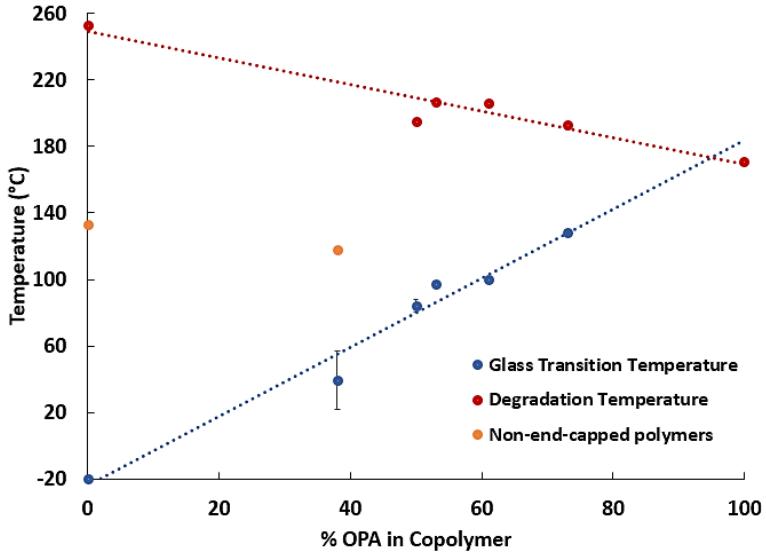

Figure 5.4 | Thermal characterization of poly(phthalaldehyde-co-ethyl glyoxylate) copolymers*: Glass transition temperature (*T_g*, blue, average of two runs) and degradation temperature (*T_d*, red) plotted against OPA copolymer ratio. Trendlines intersect at PPA/PEtG copolymer ratio of 95/5, suggesting that above this ratio, degradation occurs before observation of* T_g*. Virtual* T_g *calculated for PPA homopolymer is 184 °C. Degradation temperature for end-capped PEtG homopolymer prepared by anionic polymerization used because cationic polymerization yields thermally unstable oligomers.*

An inverse relationship is observed for T_d's, as increasing OPA incorporation results in decreasing T_d in an almost linear fashion (Figure 5.4, red trace). As we have previously shown, PEtG prepared by cationic polymerization results in thermally unstable, low molecular weight lariat polymer structures.[12c]

Thus, an end-capped PEtG sample prepared by anionic polymerization was employed to determine an accurate T_d for PEtG.[14] Like the PEtG homopolymer, PPA/PEtG copolymers with 62% EtG incorporation also demonstrated thermal instability likely due to an analogous transfer reaction to produce lariat species, so these polymers were excluded from the trendline. With increasing OPA incorporation in the PPA/PEtG copolymers, the T_d drops to ~200 °C, and finally down to 170 °C for PPA homopolymer. The T_g and T_d trendlines intersect at a copolymer ratio of 95/5 PPA/PEtG, suggesting that degradation will be observed before appearance of a T_g for all copolymers with that ratio or more of OPA units in the chain.

5.4 Conclusions:

The PPA/PEtG copolymers disclosed here represent a new, potentially important polyaldehyde family of depolymerizable materials that we anticipate will find use in solid-state applications. The copolymers are not strictly alternating but show alternating tendency at suitable monomer ratios based on NMR spectroscopic and MALDI-TOF mass spectrometry findings. To the best of our knowledge, the copolymers based on 1:1 comonomer feeds represent the first example of an alternating macrocyclic copolymer. Significantly, it is possible to tailor the T_g of PPA/PEtG copolymers by varying comonomer ratios; as the percent incorporation of OPA increases, the T_g likewise increases in a linear fashion. On the other hand, with increasing OPA incorporation into the copolymers, thermal stability decreases to the point that degradation occurs before a T_g is observed, as is the case in PPA homopolymer.

One could envision lowering T_g further to form even softer depolymerizable materials by incorporating alternative, bulkier glyoxylate monomers with various ester substituents.[16] The incorporation of the ester functional group into these polyacetal copolymers additionally permits their functionalization for advanced applications, as has been demonstrated by amide formation in polymethyl glyoxylate copolymers.[11b] PPA/PEtG copolymers thus represent a new class of soft, depolymerizable polymers that open avenues for further research. For our own purposes, the copolymers will be employed in the preparation of films with improved properties compared to those of brittle PPA homopolymer.

5.5 Synthetic Procedures

Scheme 5.2 | *General cationic polymerizations of ethyl glyoxylate and o-phthalaldehyde.*

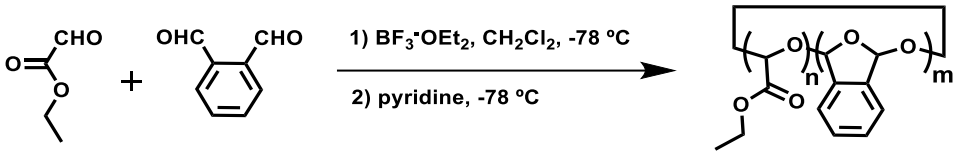

In a glovebox, purified *o*-phthalaldehyde (540 mg, 4.0 mmol) is weighed into a Schlenk flask and dissolved in dichloromethane (8 mL). The solution is removed from the glovebox and charged with distilled ethyl glyoxylate (0.40 mL, 4.0 mmol). The solution is cooled to -78 °C and boron trifluoride etherate is added (0.04 mL, 0.32 mmol). The reaction turns colorless within minutes, but is left stirring at -78 °C for 2 h. Then, pyridine (0.10 mL, 1.2 mmol) is added. The mixture is left stirring at -78 °C for 2 h and then warmed to room temperature. The polymer is precipitated by pouring into methanol (100 mL) and adding *n*-pentane until solid particles coagulate (~20-100 mL).

Table 5.2 | *PPA/PEtG copolymerization reactions and polymers used in this study.*

Entry	*$[OPA]_0$ (M)*	*$[EtG]_0$ (M)*	*$[OPA]_0/[EtG]_0$*	*$[M]_0/[I]_0$*	*Yield (%)*	*M_w (kDa)[a]*	*M_p (kDa)[a]*	*PDI[a]*	*Physical Appearance*
1	1.0	- - -	- - -	30 / 1	92	320	255	2.4	White brittle solid
2	0.8	0.2	4 / 1	26 / 1	85	19.6	21.6	2.7	White powder
3	0.6	0.4	3 / 2	26 / 1	78	15.4	18.2	2.6	White tacky solid
4	0.5	0.5	1 / 1	26 / 1	76	15.1	15.8	2.2	White tacky solid
5	0.4	0.6	2 / 3	26 / 1	73	14.5	14.3	2.0	White tacky solid
6	0.2	0.8	1 / 4	26 / 1	48[b]	8.3	6.8	2.5	Gummy semi-solid
7	- - -	5.0	- - -	60 / 1	57[b]	1.4	1.3	1.2	Colorless viscous oil

[a]Average molecular weights and polydispersity determined by gel permeation chromatography (GPC), calibrated with monodisperse polystyrene standards. [b]Product does not readily precipitate from n-pentane so yield data unreliable.

Table 5.3 | *PPA/PEtG copolymerization results.*

Entry	*Monomer Feed Ratio (OPA/EtG)*	*Copolymer Ratio Run 1 (OPA/EtG)[a]*	*Copolymer Ratio Run 2 (OPA/EtG)[a]*	*T_g (°C) (Run 1)[b]*	*T_g (°C) (Run 2)[b]*	*T_d (°C)[c]*
1	1 / 0	100 / 0	100 / 0	None	None	171
2	4 / 1	75 / 25	72 / 28	129.5	127.5	193
3	3 / 2	62 / 38	61 / 39	100.1	99.5	206
4	1 / 1	51 / 49	56 / 44	98.7	96.0	207
5	2 / 3	48 / 52	52 / 48	81.3	87.0	195
6	1 / 4	41 / 59	35 / 65	27.4	52.2	118[e]
7[d]	0 / 1	0 / 100	0 / 100	-19.4	-19.6	133[e]

[a]Determined by ^{1}H NMR integrations. [b]Determined by DSC. [c]Determined by TGA. [d]PEtG homopolymer prepared by cationic polymerization. [e]Thermally unstable species show immediate drop in mass on warming. TGA results not indicative of degradation temperature for end-capped polymers.

5.6 NMR Spectra and ^{13}C NMR and MALDI Spectral Overlays

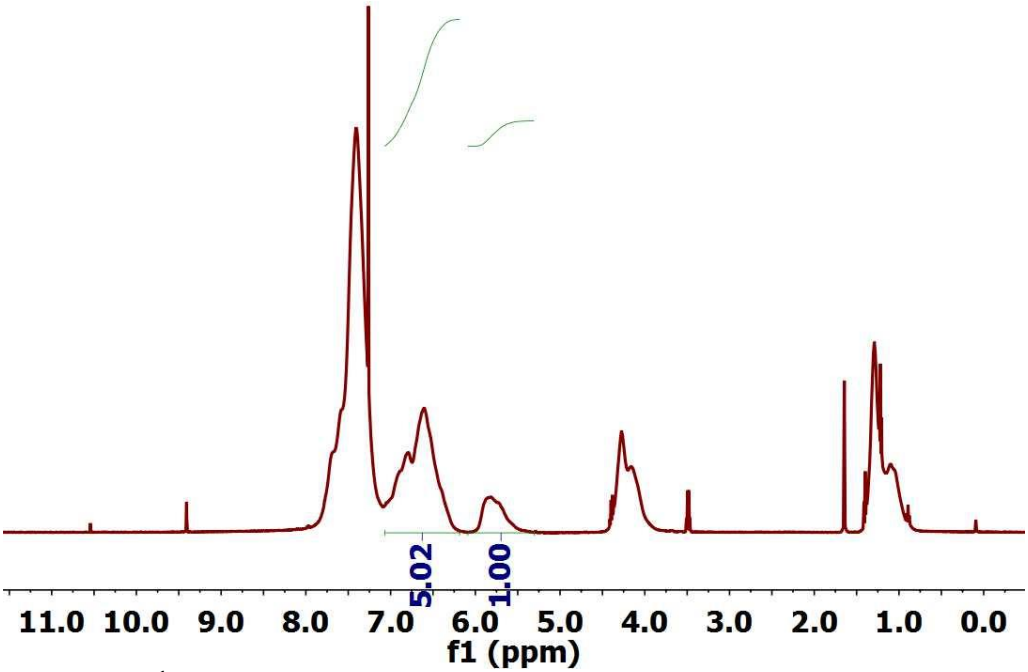

Figure 5.5 | ^{1}H NMR spectrum of PPA/PEtG copolymer*: NMR spectrum of M_w = 19.6 kDa PPA/PEtG (Table 5.2, Entry 2) prepared by cationic polymerization in $CDCl_3$. Starting comonomer feed: 4/1 OPA/EtG; copolymer ratio: 72/28 PPA/PEtG.*

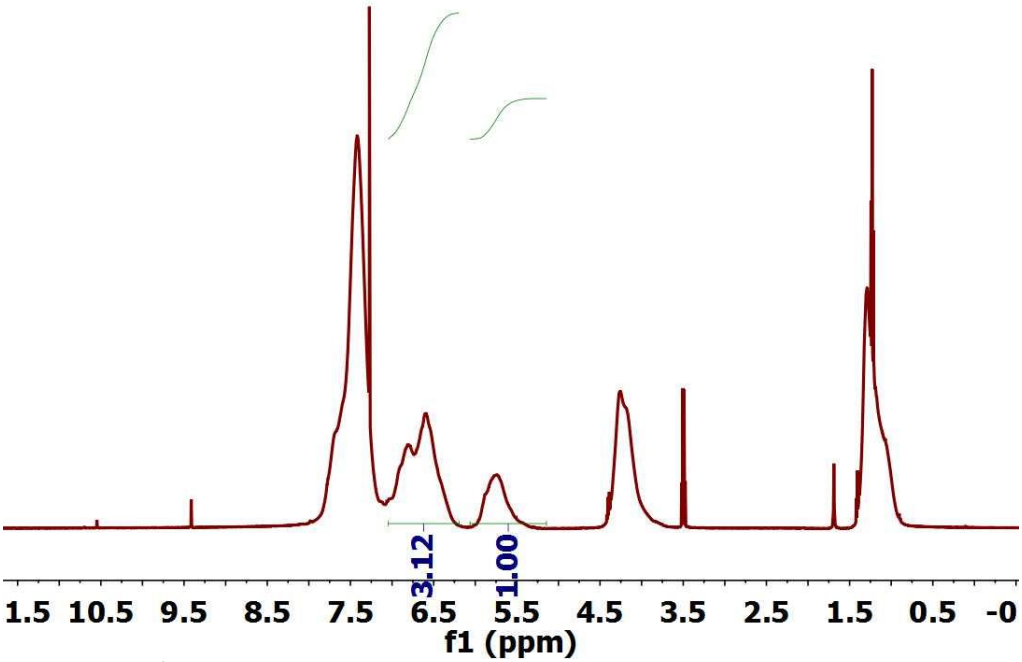

Figure 5.6 | ^{1}H NMR spectrum of PPA/PEtG copolymer*: NMR spectrum of M_w = 15.4 kDa PPA/PEtG (Table 5.2, Entry 3) prepared by cationic polymerization in $CDCl_3$. Starting comonomer feed: 3/2 OPA/EtG; copolymer ratio: 61/39 PPA/PEtG.*

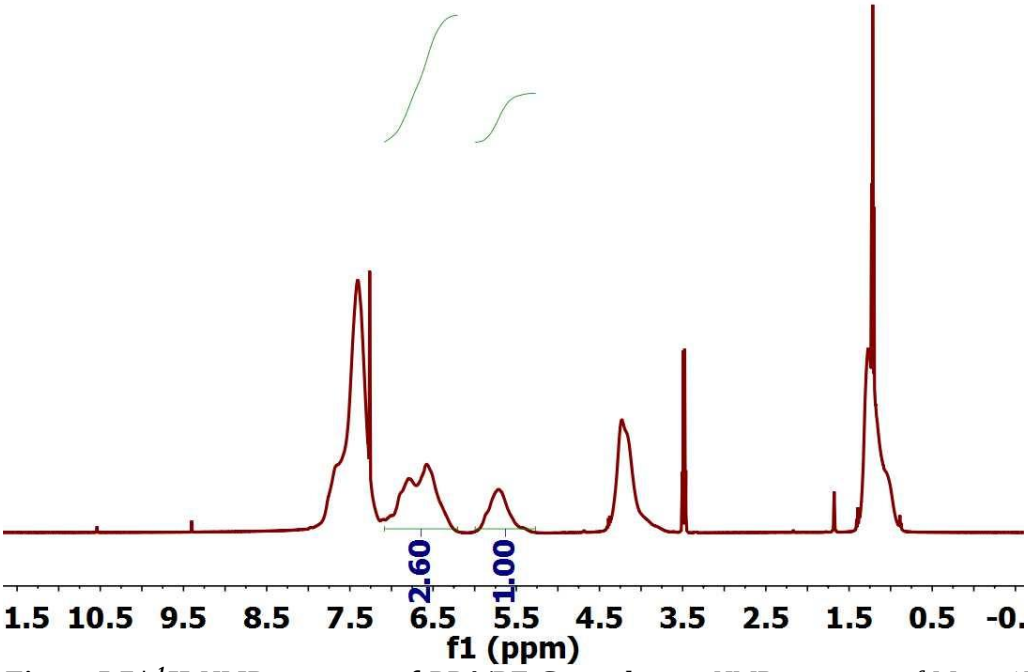

Figure 5.7 | ^{1}H NMR spectrum of PPA/PEtG copolymer*: NMR spectrum of M_w = 15.1 kDa PPA/PEtG (Table 5.2, Entry 4) prepared by cationic polymerization in $CDCl_3$. Starting comonomer feed: 1/1 OPA/EtG; copolymer ratio: 56/44 PPA/PEtG.*

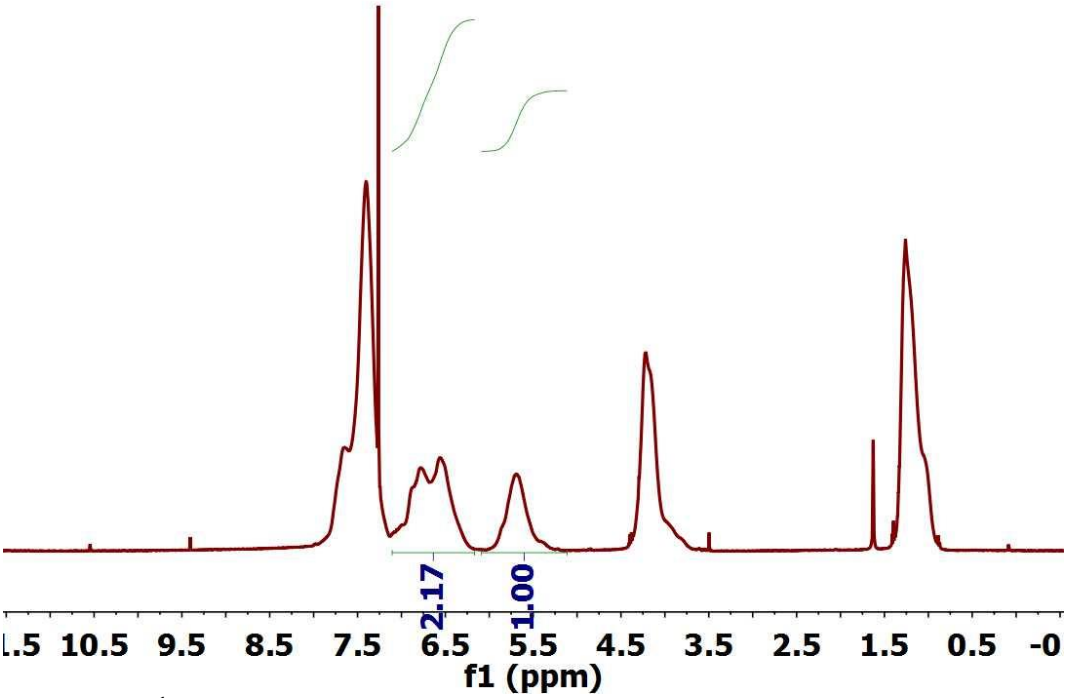

Figure 5.8 | ^{1}H NMR spectrum of PPA/PEtG copolymer*: NMR spectrum of M_w = 14.5 kDa PPA/PEtG (Table 5.2, Entry 5) prepared by cationic polymerization in $CDCl_3$. Starting comonomer feed: 2/3 OPA/EtG; copolymer ratio: 52/48 PPA/PEtG.*

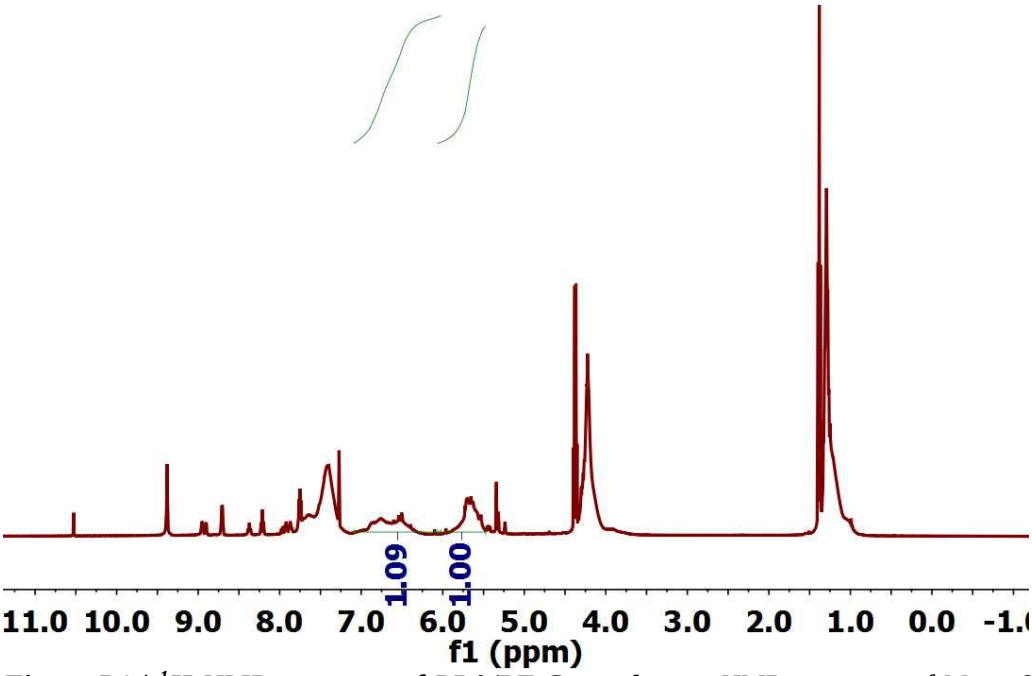

Figure 5.9 | ^{1}H NMR spectrum of PPA/PEtG copolymer*: NMR spectrum of M_w = 8.3 kDa PPA/PEtG (Table 5.2, Entry 6) prepared by cationic polymerization in $CDCl_3$. Starting comonomer feed: 1/4 OPA/EtG; copolymer ratio: 35/65 PPA/PEtG. Partial depolymerization and presence of pyridinium salts are observed for thermally unstable, non-end-capped sample.*

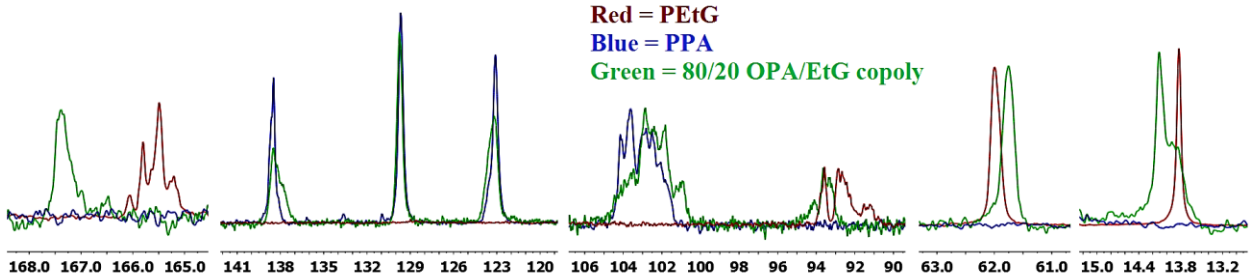

Figure 5.10 | ^{13}C NMR spectrum overlays of PPA, PEtG, and PPA/PEtG copolymer*: NMR spectrum in $CDCl_3$ of PPA/PEtG copolymer (Table 5.2, Entry 2, green), overlayed with PPA homopolymer (blue) and PEtG homopolymer (red). Peak shifts are clearly observed for EtG resonances in copolymer, attributed to EtG units flanked by OPA residues.*

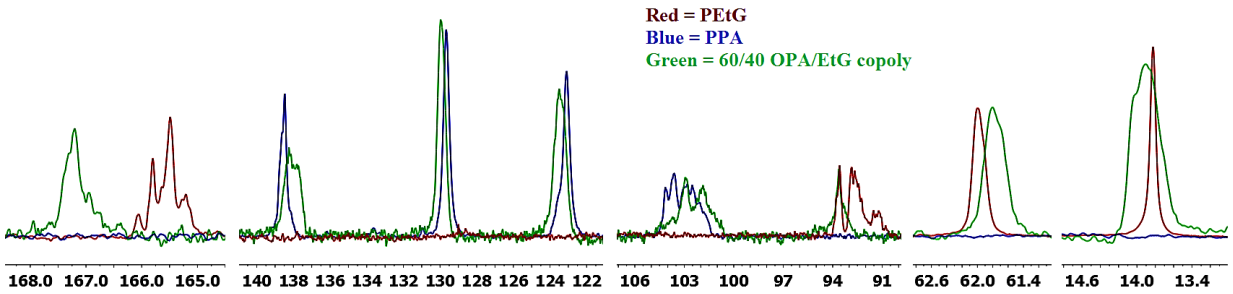

Figure 5.11 | ^{13}C NMR spectrum overlays of PPA, PEtG, and PPA/PEtG copolymer*: NMR spectrum in $CDCl_3$ of PPA/PEtG copolymer (Table 5.2, Entry 3, green), overlayed with PPA homopolymer (blue) and PEtG homopolymer (red). Peak shifts are clearly observed for EtG resonances in copolymer, attributed to EtG units flanked by OPA residues.*

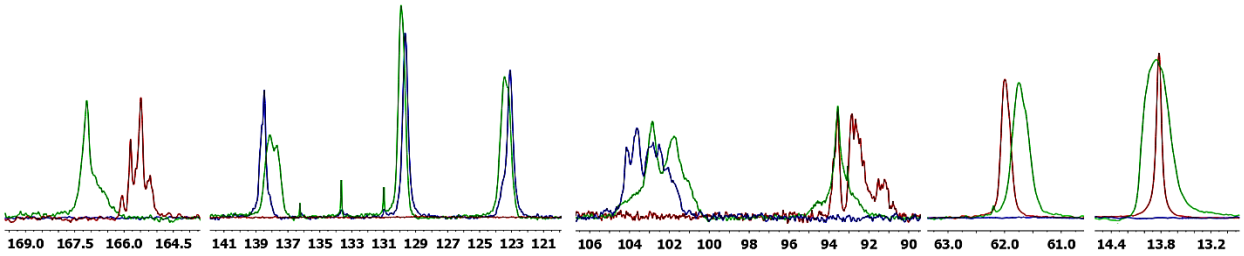

Figure 5.12 | ^{13}C NMR spectrum overlays of PPA, PEtG, and PPA/PEtG copolymer*: NMR spectrum in $CDCl_3$ of PPA/PEtG copolymer (Table 5.2, Entry 4, green), overlayed with PPA homopolymer (blue) and PEtG homopolymer (red). Peak shifts are clearly observed for EtG resonances in copolymer, attributed to EtG units flanked by OPA residues.*

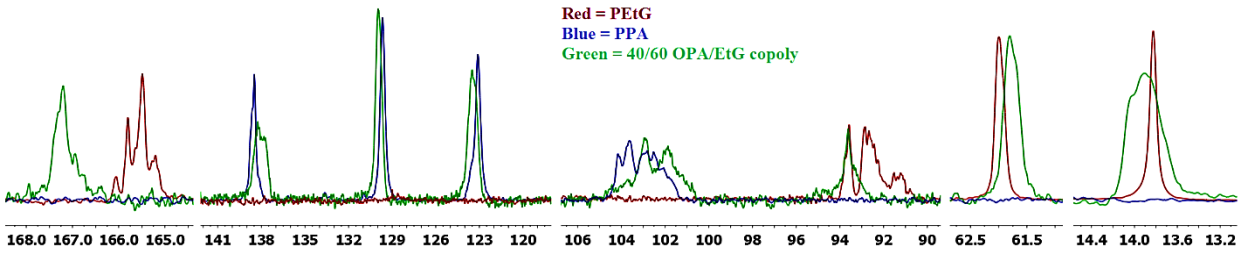

Figure 5.13 | ^{13}C NMR spectrum overlays of PPA, PEtG, and PPA/PEtG copolymer*: NMR spectrum in $CDCl_3$ of PPA/PEtG copolymer (Table 5.2, Entry 5, green), overlayed with PPA homopolymer (blue) and PEtG homopolymer (red). Peak shifts are clearly observed for EtG resonances in copolymer, attributed to EtG units flanked by OPA residues.*

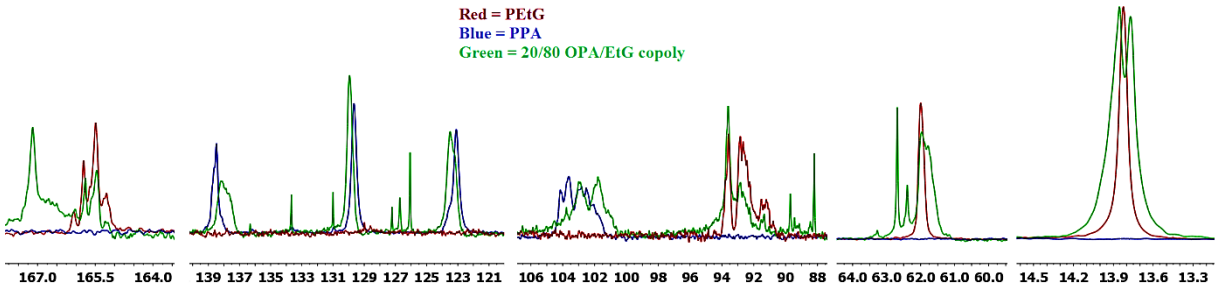

Figure 5.14 | ^{13}C NMR spectrum overlays of PPA, PEtG, and PPA/PEtG copolymer*: NMR spectrum in $CDCl_3$ of PPA/PEtG copolymer (Table 5.2, Entry 6, green), overlayed with PPA homopolymer (blue) and PEtG homopolymer (red). Peak shifts are clearly observed for EtG resonances in copolymer, attributed to EtG units flanked by OPA residues. Peaks correlating to PEtG homopolymer also appear in this copolymer, attributed to successive EtG residues in copolymer.*

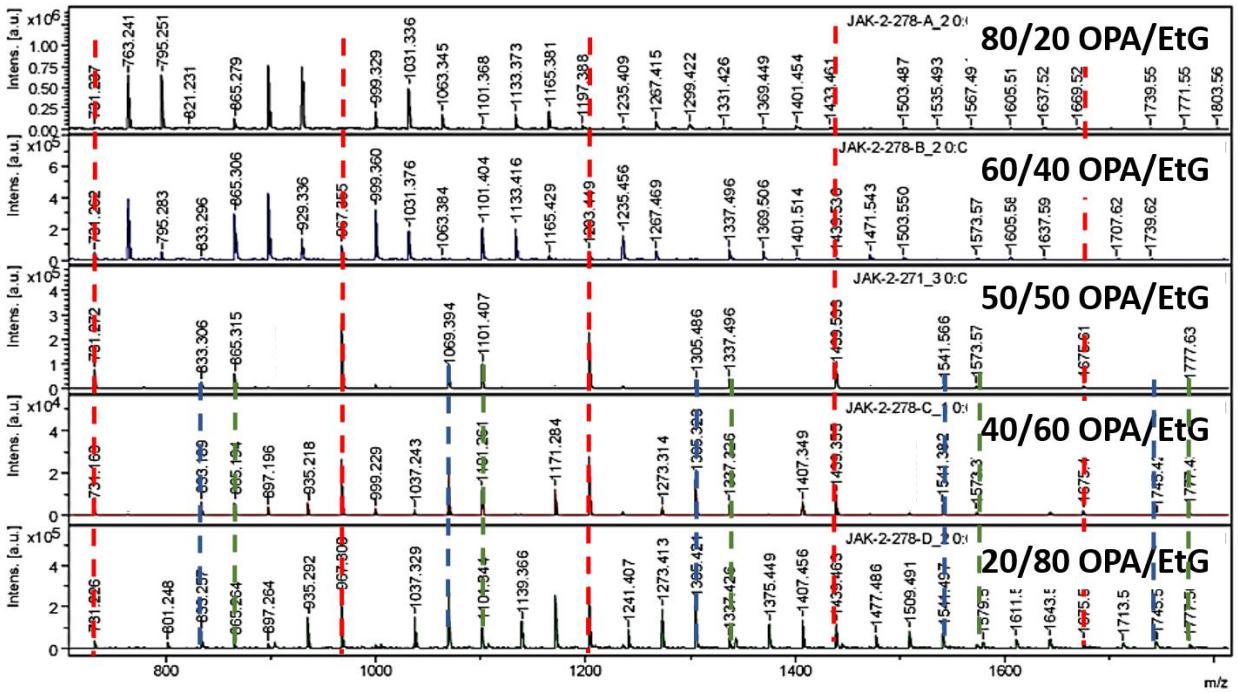

Figure 5.15 | MALDI-TOF mass spectra overlays of PPA/PEtG copolymers: *Dashed lines correspond to potential alternating cyclic copolymer peaks (red), and alternating copolymer plus EtG (blue) or OPA (green). At high OPA or EtG feeds, full series of copolymer peaks is observed. However, for copolymers with 40-50/50-60 OPA/EtG feeds, main peaks correspond to potential alternating cyclic copolymers and other copolymer peaks are diminished or not observed.*

5.7 References

(1) (a) Vogl, O. *J. Polym. Sci., Part A: Polym. Chem.* **2000**, 38, 2293-2299. (b) Kostler, S. *Polym. Int.* **2012**, 61, 1221-1227.

(2) (a) Peterson, G. I.; Larsen, M. B.; Boydston, A. J. *Macromolecules* **2012**, 45, 7317-7328. (b) Phillips, S. T.; DiLauro, A. M. *ACS Macro Lett.* **2014**, 2, 298-304. (c) Esser-Kahn, A. P.; Odom, S. A.; Sottos, N. R.; White, S. R.; Moore, J. S. *Macromolecules* **2011**, 44, 5539-5553. (d) Wong, A. D.; DeWit, M. A.; Gillies, E. R. *Adv. Drug Delivery Rev.* **2012**, 64, 1031-1045. (e) Sagi, A.; Weinstain, R.; Karton, N.; Shabat, D. *J. Am. Chem. Soc.* **2008**, 130, 5434-5435.

(3) (a) DeWit, M. A.; Gillies, E. R. *J. Am. Chem. Soc.* **2009**, 131, 18327-18334. (b) Weintain, R.; Sagi, A.; Karton, N.; Shabat, D. *Chem. Eur. J.* **2008**, 14, 6857-6861. (c) Chen, E. K. Y.; McBride, R. A.; Gillies, E. R. *Macromolecules* **2012**, 45, 7364-7374. (d) Dewit, M. A.; Beaton, A.; Gillies, E. R. *J. Polym. Sci., Part A: Polym. Chem.* **2010**, 48, 3977-3985. (e) Robbins, J. S.; Schmid, K. M.; Phillips, S. T. *J. Org. Chem.* **2013**, 78, 3159-3169.

(4) (a) Chuji, A.; Tagami, S.; Kunitake, T. *J. Polym. Sci., Part A: Polym. Chem.* **1969**, 7, 497-511. (b) Chuji, A.; Tagami, S. *Macromolecules* **1969**, 2, 414-419. (c) Willson, C. G.; Ito, H.; Frechet, J. M. J.; Tessier, T. G.; Houlihan, F. M. *J. Electrochem. Soc.* **1986**, 133, 181-187. (d) Tsuda, M.; Hata, M.; Nishida, R.; Oikawa, S. *J. Polym. Sci., Part A: Polym. Chem.* **1997**, 35, 77-89.

(5) (a) Ito, H.; Willson, C. G. *Polym. Eng. Sci.* **1983**, 23, 1012-1018. (b) Knoll, A. W.; Pires, D.; Coulembier, O.; Dubois, P.; Hedrick, J. L.; Frommer, J.; Duerig, U. *Adv. Mater.* **2010**, 22, 3361-3365. (c) Coulembier, O.; Knoll, A.; Pires, D.; Gotsmann, B.; Duerig, U.; Frommer, J.; Miller, R. D.; Dubois, P.; Hedrick, J. L. *Macromolecules* **2010**, 43, 572-574.

(6) (a) Seo, W.; Phillips, S. T. *J. Am. Chem. Soc.* **2010**, 132, 9234-9235. (b) Dilauro, A. M.; Robbins, J. S.; Phillips, S. T. *Macromolecules* **2013**, 46, 2963-2968. (c) Kaitz, J. A.; Moore, J. S. *Macromolecules* **2013**, 46, 608-612. (d) Kaitz, J. A.; Possanza, C. M.; Song, Y.; Diesendruck, C. E.; Spiering, A. J. H.; Meijer, E. W.; Moore, J. S. *Polym. Chem.* **2014**, 5, 3788-3794.

(7) DiLauro, A. M.; Zhang, H.; Baker, M. S.; Wong, F.; Sen, A.; Phillips, S. T. *Macromolecules* **2013**, 46, 7257-7265.

(8) Dilauro, A. M.; Abbaspourrad, A.; Weitz, D. A.; Phillips, S. T. *Macromolecules* **2013,** 46, 3309-3313.

(9) (a) Burel, F.; Rossignol, L.; Pontvianne, P.; Hartman, J.; Couesnon, N.; Bunel, C. *e-Polym.* **2003**, 3, 407-411. (b) Belloncle, B.; Burel, F.; Oulyadi, H.; Bunel, C. *Polym. Degrad. Stab.* **2008**, 93, 1151-1157.

(10) (a) Vairon, J. P.; Muller, E.; Bunel, C. *Macromol. Symp.* **1994**, 85, 307-312. (b) Brachais, C. H.; Huguet, J.; Bunel C. *Polymer* **1997**, 38, 4959-4964. (c) Brachais, C. H.; Duclos, R.; Vaugelade, C.; Huguet, J.; Capelle-Hue, M.-L.; Bunel, C. *Int. J. Pharm.* **1998**, 169, 23-31.

(11) (a) Basko, M.; Kubisa, P.; Penczek, S.; Moreau, M.; Vairon, J. P. *Macromolecules* **2000**, 33, 294-302. (b) Basko, M.; Kubisa, P. *Macromolecules* **2002**, 35, 8948-8953.

(12) (a) Kaitz, J. A.; Diesendruck, C. E.; Moore, J. S. *J. Am. Chem. Soc.* **2013**, 135, 12755-12761. (b) Kaitz, J. A.; Diesendruck, C. E.; Moore, J. S. *Macromolecules* **2013**, 46, 8121-8128. (c) Kaitz, J. A.; Diesendruck, C. E.; Moore, J. S. *Macromolecules* **2014**, 47, 3603-3607.

(13) (a) Chen, G.-Q.; Wu, Z.-Q.; Wu, J.-R.; Li, Z.-C.; Li, F.-M. *Macromolecules* **2000**, 33, 232-234. (b) Lutz, J.-F.; Kirci, B.; Matyjaszewski, K. *Macromolecules* **2003**, 36, 3136-3145. (c) Saegusa, T. *Makromol. Chem.* **1979**, 3, 157-176.

(14) An anionic, end-capped sample of PEtG homopolymer was prepared for proper thermal characterization of T_d because cationic polymerization yields thermally unstable oligomers. The T_g of this stabilized polymer, which has M_w = 77 kDa, is -1.5 °C.

(15) Glass transition temperatures versus copolymer composition have been shown to have both linear and non-linear relationships depending on comonomers. (a) Wood, L. A. *J. Polym. Sci., Part A: Polym. Chem.* **1958**, 28, 319-330. (b) Penzel, E.; Rieger, J.; Schneider, H. A. *Polymer* **1997**, 38, 325-337.

(16) Fan, B.; Trant, J. F.; Wong, A. D.; Gillies, E. R. *J. Am. Chem. Soc.* **2014**, 136, 10116-10123.

Chapter 6: Functional Phthalaldehyde Polymers by Copolymerization with Substituted Benzaldehydes*

6.1 Abstract

End-capped poly(phthalaldehyde) (PPA) is a well studied depolymerizable polymer that has attracted interest due to its ease of synthesis and rapid depolymerization. PPA is limited, however, in the type of macromolecular, cross-linked architectures accessible, as functionalizable phthalaldehyde derivatives are not commercially available and their synthesis is cumbersome. To this end, a general route toward phthalaldehyde-benzaldehyde copolymers was developed, as benzaldehyde comonomers with various pendant functionalities are readily available. It was found that copolymers are synthesized by an anionic polymerization of phthalaldehyde and electron-deficient benzaldehydes. The comonomer reactivities are shown to be sensitive to the benzaldehyde electronics; the relative reactivities of phthalaldehyde-benzaldehyde comonomer pairs strongly correlate with the Hammett values of the benzaldehyde monomers. These copolymers are then further modified to yield cross-linked, acid-degradable polymer networks in just a two-step sequence. This work highlights the functionalization of depolymerizable polymers by incorporating substituted benzaldehydes into PPA and the subsequent development of polymer networks capable of triggered degradation.

6.2 Introduction

Stimuli-responsive, depolymerizable polymers have garnered significant interest in recent years.[1] By virtue of being above the polymer's ceiling temperature yet kinetically stabilized by end-capping, depolymerizable polymers are a unique class of materials in that they are capable of complete and spontaneous head-to-tail depolymerization after triggering.[1-2] These polymers harness a single chemical or physical signaling event to initiate a depolymerization cascade that reverts an entire polymer chain to monomers or other small molecule analogs. Advantages of depolymerizable polymers in stimuli-responsive applications include their high sensitivity to sensory input, the broad range of specific triggering moieties that are readily incorporated into polymer chains, and the inherent signal amplification that accompanies their depolymerization.

* Portions of this chapter have been published: Kaitz, J. A.; Moore, J. S. *Macromolecules* **2013**, 46, 608-612.

Poly(phthalaldehyde) (PPA) is one such polymer with a ceiling temperature around -40 °C.[3] Since the first PPA syntheses in the 1960s, it has primarily been used as an acid-, radiation-, or heat-sensitive degradable film for lithography.[4] It was recently demonstrated that by end-capping with specific triggering moieties, a head-to-tail depolymerization cascade is selectively initiated in the presence of specific chemical reagents.[5] Relative to other depolymerizable polymers, PPA benefits from its ease of synthesis[4c] and rapid and complete degradation. However, the system is limited in the type of macromolecular architectures accessible, as functionalizable phthalaldehyde derivatives are not commercially available and their synthesis is cumbersome. To this end, a general route to phthalaldehyde-benzaldehyde copolymers was developed, as benzaldehyde comonomers with various pendant functionalities are commercially available and easily synthesized. These copolymers have only been briefly mentioned in the literature, rigorous chemical characterization has not been reported, and no systematic studies have been undertaken.[6] The present chapter discusses the synthesis, characterization, and functionalization of such copolymers.

6.3 Results and Discussion

6.3.1 Phthalaldehyde-Benzaldehyde Copolymerization

Homopolymerization of aromatic aldehydes other than *o*-phthalaldehyde (OPA) is known to be difficult, and only a few reports even discuss copolymerizing benzaldehyde (BA) with other monomers.[3a, 6-7] This difficulty is a thermodynamic phenomenon. The ceiling temperature of PPA is significantly higher than that of poly(BA) because it possesses two aldehydes that form a stable five-membered ring repeat unit, making the polymerization considerably more exothermic than BA. The entropic cost of BA polymerization therefore overrides its more modest enthalpic gain and drives the ceiling temperature below accessible levels. By comparing the enthalpies of reaction for forming the dimethyl acetals of OPA and BA, a ceiling temperature of -190 ºC was estimated for poly(BA) (calculations by T1 Thermochemical Recipes on Spartan V10.0).

Experimental and computational data have established an equilibrium shift to hydrate formation for the reaction of electron-deficient BAs with water.[8] The more exothermic nature of electron-deficient BA hydration compared to their electron-rich BA counterparts suggests the higher polymerizability of the former. To probe this hypothesis, initial efforts focused on the copolymerization of 4-nitro BA with OPA, but only PPA homopolymer was obtained with either anionic or cationic initiating systems. It was discovered, however, that BAs with multiple electron-withdrawing substituents, all of which have Hammett parameters greater than that of a single para-nitro group (0.78, See Table 6.1), underwent copolymerization.[9]

Table 6.1 | *Synthesis of poly(phthalaldehyde-*co*-benzaldehyde) copolymers and corresponding benzaldehyde monomers used in this study.*

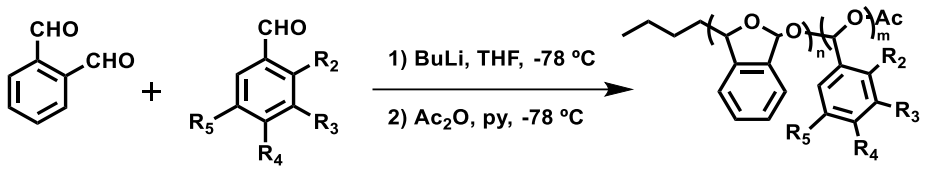

Benzaldehyde Monomer	*R_2*	*R_3*	*R_4*	*R_5*	*Hammett Value*[a]
2-DNBA	NO_2	H	NO_2	H	1.56
3-DNBA	H	NO_2	H	NO_2	1.42
NFBA	NO_2	H	CF_3	H	1.32
BNBA	H	Br	H	NO_2	1.10
DFBA	CF_3	H	CF_3	H	1.08
NIPA	H	NO_2	H	CHO	1.06
CNBA	H	NO_2	Cl	H	0.94

[a]Para Hammett values used for *ortho*-substituents, per literature precedence.[9]

For each BA monomer, a series of polymerizations initiated by *n*-BuLi with molar feed ratios of OPA/BA ranging from 9/1 to 3/2 was run in triplicate. The copolymers were fully characterized by NMR and GPC (also TGA and DSC on selected series). Molecular weights (M_n) ranged from 4-6 kDa with PDIs of 1.1-1.4 (degree of polymerization *ca*. 25-40). Copolymer ratios were readily calculated by ^{1}H NMR spectroscopy since peaks corresponding to BA were resolved from OPA due to the electron-deficient nature of each BA comonomer used. The BA protons are found at δ = 8.0-8.9 ppm while the OPA protons are found at δ = 7.05-7.75 ppm. Other peaks correspond to backbone protons, initiator, and acetate end-cap (Figure 6.1 and Section 6.6).

Reactivity ratios for copolymer systems in which both monomers reversibly add to the chain end are difficult to compute and rely on a large number of assumptions and unknown parameters.[10] This difficulty is a result of the multiple unique depolymerization reactions that occur on the growing chain end, each having its own depropagation rate coefficient (Scheme 6.1). Given this complexity, a simple experimental parameter, the incorporation ratio, was devised to describe the poly(phthalaldehyde-*co*-benzaldehyde) system. The incorporation ratio is defined as the slope of the line obtained by plotting copolymer composition against comonomer feed ratio for each BA monomer (Figure 6.2a). It simply corresponds to the fraction of BA that is actually incorporated into the copolymer. At low conversion, for example, an incorporation ratio of one would indicate equal reactivity between OPA and BA. However, even the most electron-deficient BA exhibits a slope below one, signifying that OPA is more thermodynamically favorable to polymerize than any of the BA monomers.

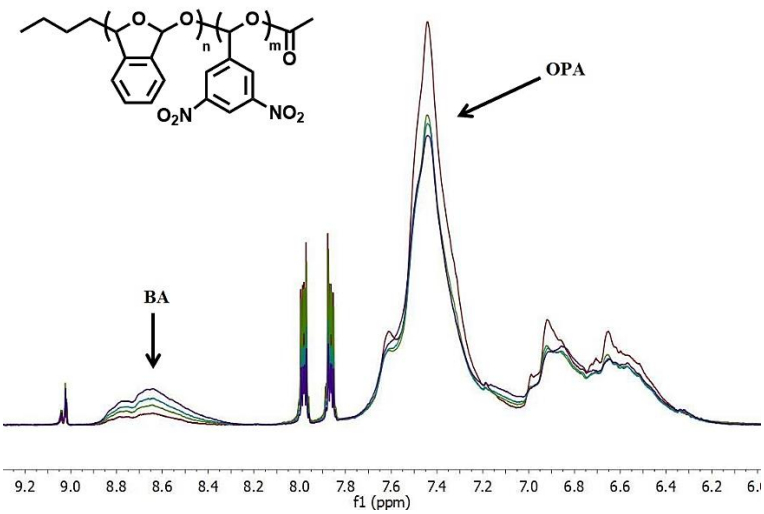

Figure 6.1 *| Representative ^{1}H NMR spectra of a series of poly(phthalaldehyde-*co*-3,5-dinitrobenzaldehyde) copolymers in DMSO-d_6. Integrated areas correspond to copolymer ratios of (OPA/BA): 95/5 (red), 89/11 (green), 85/15 (blue), and 81/19 (purple). Sharp peaks correspond to residual monomer.*

Scheme 6.1 *| Kinetic reaction scheme for anionic copolymerization with monomers A and B both capable of depolymerization.*

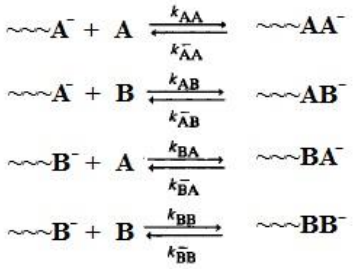

A strong correlation exists between incorporation ratio and the electron-deficiency of the BA; BAs with larger Hammett values have larger incorporation ratios (Figure 6.2b). The x-intercept, 0.92, corresponds to the Hammett value at which the incorporation ratio is zero, indicating that the BA does not copolymerize. Below this threshold, BA is not reactive in the polymerization conditions, matching the experimental finding that 4-nitro-BA did not polymerize. In order to examine OPA reactivity, the Kelen-Tudos model was applied to give a rough estimation of reactivity ratios.[11] A clear pattern emerged from these data as well, as the reactivity ratio for OPA climbs monotonically as the BA comonomer approaches the Hammett value threshold for copolymerization (Figure 6.2c). This result effectively indicates that as the BA becomes less electron-deficient, OPA preferentially forms homopolymer, in agreement with experimental observations.

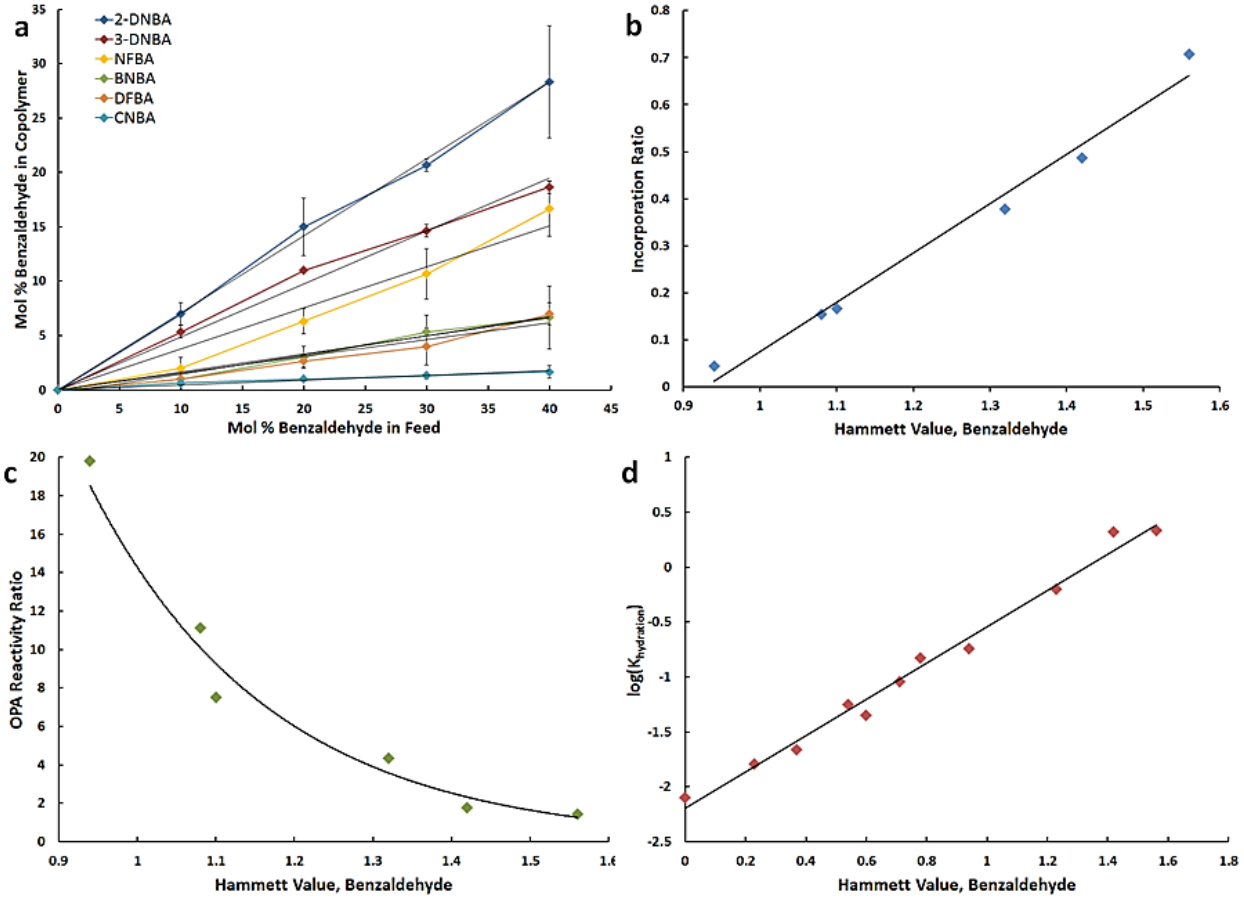

Figure 6.2 | Reactivity studies on PPA-BA copolymers. *(a) Experimental copolymer compositions in relation to comonomer feed ratio, where the slope is the incorporation ratio; (b) the incorporation ratio plotted against the Hammett values of benzaldehyde monomers (line of best fit: y=1.05x-0.97, R^2=0.98); (c) approximate reactivity ratio of phthalaldehyde plotted against the Hammett value of the benzaldehyde comonomer (see text for details); (d) log of $K_{hydration}$ plotted against the Hammett values of various benzaldehydes (line of best fit: y=1.65x-2.19, R^2=0.99; $K_{hydration}$ values obtained from literature*[8, 12-13]*).*

To compare these findings to literature precedent, the well studied hydration of substituted BAs was employed as a model reaction for the polymerization (Scheme 6.2).[8, 12-13] BA comonomer uptake correlates to the established trend that stronger electron-withdrawing substituents make hydrate formation more favorable, as evidenced by the relationship between Hammett value and the equilibrium of hydration for substituted BAs (Figure 6.2d). The aforementioned polymerization threshold for BA corresponds to a $K_{hydration}$ value of 0.22, which is an order of magnitude lower than the $K_{hydration}$ for OPA.[12] Even the most highly electron-deficient BA studied in this work exhibits a $K_{hydration}$ value lower than that of OPA, corroborating the incorporation ratio below one.

Scheme 6.2 **|** *Benzaldehyde hydration model reaction.*

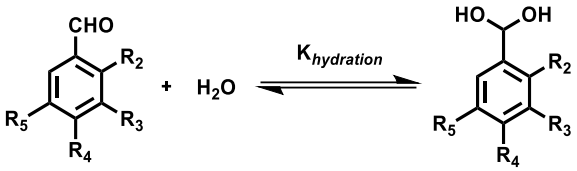

A bifunctional aldehyde monomer was conceived to test the validity of the Hammett value threshold. Isophthalaldehyde (Hammett value 0.35) was found to be unreactive in the *n*-BuLi-initiated polymerization. However, 5-nitroisophthalaldehyde (NIPA) should theoretically polymerize due to its Hammett value (1.06) when regarded as a disubstituted BA. Interestingly, the monomer would not be expected to act as cross-linker because the Hammett value drops below the polymerization threshold (0.76)[14] after the first aldehyde adds to the polymer. As expected, copolymerization of OPA and NIPA yielded linear PPA-BA copolymer with pendant aldehyde groups (Figure 6.5).

6.3.2 Functionalization of Phthalaldehyde-Benzaldehyde Copolymers

The utility of these phthalaldehyde-benzaldehyde copolymers was probed by executing several post-polymerization modification reactions to further functionalize the BA component. Unfortunately, nitro group reduction, which would have provided a reactive aniline amino group, was not achieved with either PPA-2-DNBA or PPA-3-DNBA copolymers due to polymer degradation or limited reactivity toward heterogeneous hydrogenation catalysts. Several cross-coupling reactions, on the other hand, proceeded in moderate yield (Scheme 6.3). Stille couplings successfully vinylated poly(phthalaldehyde-*co*-3-bromo-5-nitrobenzaldehyde) (**1**) with 48% polymer recovery and 93% coupling conversion (Polymer **2**). Sonogashira coupling reactions on the same copolymer affixed trimethylsilyl acetylene to the copolymer with 40% recovery and 62% coupling conversion (Polymer **3**). Polymer vinylation opens avenues for radical- or photo-mediated cross-linking, while alkyne coupling enables "click" functionalization via copper-catalyzed alkyne-azide cycloaddition.

Scheme 6.3 **|** *Functionalization reactions performed on PPA-BNBA copolymers (**1**). Both acetyl and trichloroacetyl isocyanate end-caps (X) were utilized to end-cap the copolymers.*

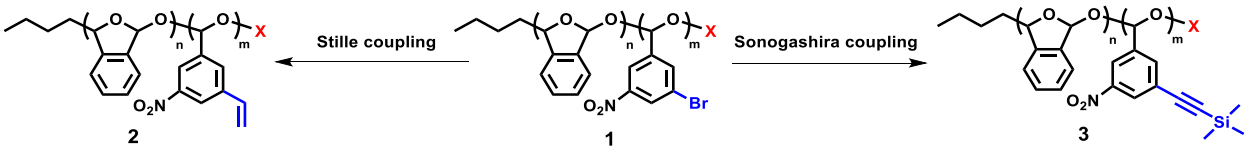

NIPA copolymers containing a reactive pendant aldehyde (**4**) were found to be an even more versatile choice for functionalization (Scheme 6.4). Polymer was recovered in high yields after Wittig reactions with various phosphonium salts (60%, Polymer **5**), imine formation occurred with amines and diamines (82% yield, Polymer **6**), and sodium borohydride-mediated reduction afforded the corresponding alcohol (68% yield, Polymer **7**). Reduction to hydroxy-functionalized polymer (**7**) permitted further modification of the polymers. For instance, isocyanate reagents were coupled to the polymers in nearly quantitative yields (Polymers **8-10**), and polylactide (PLA) was grafted to the copolymers via anionic ring-opening polymerization of lactide with a phosphazene base catalyst (Polymer **11**).[15] Notably, even though the copolymer molecular weights were relatively low, cross-linking of **7** was achieved by reaction with a multi-functional isocyanate reagent, poly[(phenyl isocyanate)-*co*-formaldehyde], and annealing the mixture at 80 ºC overnight (Polymer **10**). The resulting yellow, insoluble film was analyzed by IR spectroscopy and solid state NMR spectroscopy, both of which confirmed the formation of carbamate groups in the cross-linking reaction.

Scheme 6.4 *| Functionalization reactions performed on PPA-NIPA copolymers (**4**) and hydroxylated analog (**7**). Both acetyl and trichloroacetyl isocyanate end-caps (X) were utilized to end-cap the copolymers.*

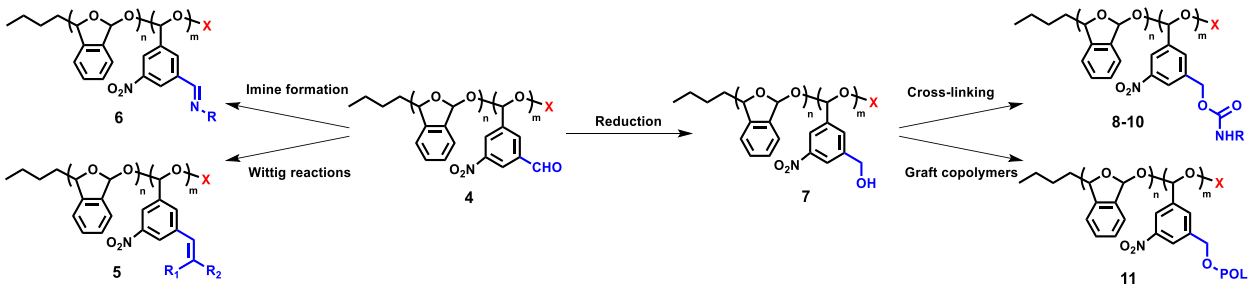

To evaluate the degradability of cross-linked PPA, the polymer network was exposed to acid in order to hydrolyze the acetal main-chain linkages and trigger complete depolymerization. Cross-linked PPA was ground into a powder, suspended in chloroform, and mixed with one drop of deuterium chloride. Within seconds, the insoluble suspension transformed to a yellow solution, which was identified as majority OPA and other small molecule impurities, presumably the coupling products between the BA comonomer and the isocyanate reagent (Figure 6.3). Importantly, this result demonstrates that cross-linked PPA polymers are still susceptible to triggered depolymerization. Robust covalent networks can therefore be constructed and deconstructed in response to an external stimulus.

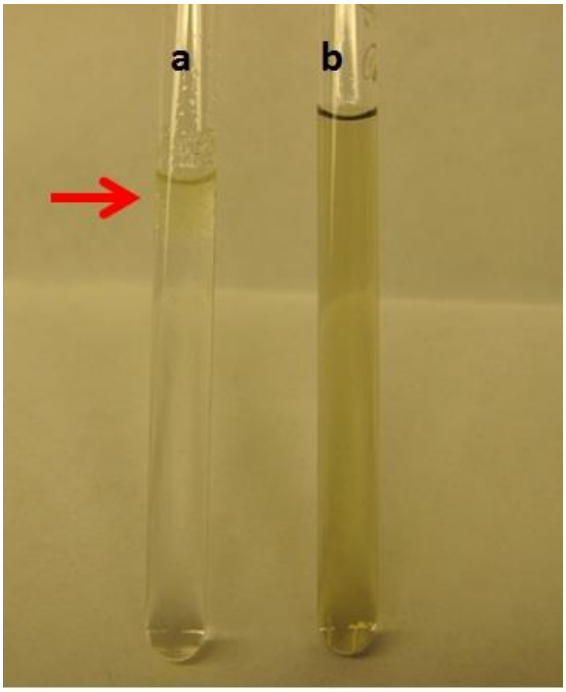

Figure 6.3 | *(a) Insoluble cross-linked PPA network suspended in chloroform, red arrow points to insoluble powderized polymer, and (b) degraded polymer network after addition of one drop deuterium chloride.*

6.4 Conclusions

Phthalaldehyde-benzaldehyde copolymers were prepared and shown to present a convenient route toward functionalizable, stimuli-responsive, depolymerizable polymers. In just two steps, it is possible to synthesize copolymers with specific end-caps, then install reactive functional groups into those copolymers by post-polymerization modification reactions. A new parameter, the incorporation ratio, was established and verified to predict the composition of these equilibrium copolymers. Cross-linking reactions and graft copolymerizations were performed on the copolymers to demonstrate their utilities toward developing of depolymerizable nanostructures of higher order. These materials may pave the way to new triggerable, depolymerizable architectures such as microcapsules, which will be explored in further work.

6.5 Synthetic Procedures

Scheme 6.5 | *General copolymerization initiated by* n-*BuLi.*

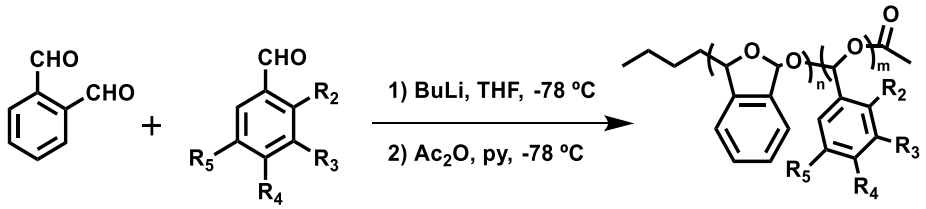

To a Schlenk flask were added *o*-phthalaldehyde (1.8-3.0 mmol) and the benzaldehyde comonomer (0.0-1.2 mmol). The solids were dissolved in THF (5 mL) and the solution cooled to -78 °C. Then, 1.6 M *n*-BuLi in hexanes (0.08 mL, 0.13 mmol) was added and the reaction mixture stirred at -78 °C for 8 h. Acetic anhydride (0.14 mL, 1.5 mmol) and pyridine (0.12 mL, 1.5 mmol) were then added and the mixture stirred overnight at -78 °C. The polymer was precipitated in methanol and washed in methanol and diethyl ether. If necessary, the polymers were further purified by dissolving in dichloromethane and re-precipitating into methanol. The white solid powders were characterized by GPC (for molecular weight and polydispersity; eluent = THF) and NMR spectroscopy. ^{1}H NMR (500 MHz, DMSO-d_6) δ 8.90-8.00 (b, 3H, benzaldehyde), 7.75-7.05 (b, 4H, phthalaldehyde), 7.05-6.25 (b, acetal), 2.15-2.00 (b, acetate), 1.55-1.15 (b, initiator), 0.90-0.60 (b, initiator).

Table 6.2 | *Data for copolymer samples with 2,4-dinitrobenzaldehyde (2-DNBA, Hammett value 1.56).*

Feed Ratio (OPA/BA)	*Copolymer Composition (Series 1)*	*Copolymer Composition (Series 2)*	*Copolymer Composition (Series 3)*	*Average Yield*	*M_n (kDa)*[a]	*PDI*[a]
90/10	93/7	94/6	92/8	54%	4.7	1.2
80/20	82/18	87/13	86/14	48%	4.6	1.2
70/30	80/20	79/21	79/21	17%	3.9	1.2
60/40	73/27	76/24	66/34	11%	3.7	1.1

[a]Average molecular weights and polydispersity determined by gel permeation chromatography (GPC), calibrated with monodisperse polystyrene standards.

***Table 6.3** | Data for copolymer samples with 3,5-dinitrobenzaldehyde (3-DNBA, Hammett value 1.42).*

Feed Ratio (OPA/BA)	*Copolymer Composition (Series 1)*	*Copolymer Composition (Series 2)*	*Copolymer Composition (Series 3)*	*Average Yield*	*M_n (kDa)[a]*	*PDI[a]*
90/10	94/6	95/5	95/5	46%	4.9	1.2
80/20	89/11	89/11	89/11	45%	4.7	1.2
70/30	85/15	85/15	86/14	31%	4.4	1.1
60/40	81/19	81/19	82/18	19%	4.0	1.1

[a]Average molecular weights and polydispersity determined by gel permeation chromatography (GPC), calibrated with monodisperse polystyrene standards.

***Table 6.4** | Copolymers with 2-nitro-4-trifluoromethylbenzaldehyde (NFBA, Hammett value 1.32).*

Feed Ratio (OPA/BA)	*Copolymer Composition (Series 1)*	*Copolymer Composition (Series 2)*	*Copolymer Composition (Series 3)*	*Average Yield*	*M_n (kDa)[a]*	*PDI[a]*
90/10	98/2	99/1	97/3	43%	5.7	1.3
80/20	93/7	95/5	93/7	32%	4.8	1.2
70/30	88/12	92/8	88/12	17%	4.7	1.2
60/40	86/14	81/19	83/17	4%	4.6	1.1

[a]Average molecular weights and polydispersity determined by gel permeation chromatography (GPC), calibrated with monodisperse polystyrene standards.

***Table 6.5** | Data for copolymers with 3-bromo-5-nitrobenzaldehyde (BNBA, Hammett value 1.10).*

Feed Ratio (OPA/BA)	*Copolymer Composition (Series 1)*	*Copolymer Composition (Series 2)*	*Copolymer Composition (Series 3)*	*Average Yield*	*M_n (kDa)[a]*	*PDI[a]*
90/10	98/2	100/0	99/1	41%	5.0	1.3
80/20	96/4	97/3	98/2	36%	4.5	1.2
70/30	93/7	95/5	96/4	24%	4.6	1.2
60/40	90/10	95/5	95/5	13%	4.0	1.2

[a]Average molecular weights and polydispersity determined by gel permeation chromatography (GPC), calibrated with monodisperse polystyrene standards.

***Table 6.6** | Copolymers with 2,4-bis(trifluoromethyl)benzaldehyde (DFBA, Hammett value 1.08).*

Feed Ratio (OPA/BA)	*Copolymer Composition (Series 1)*	*Copolymer Composition (Series 2)*	*Copolymer Composition (Series 3)*	*Average Yield*	*M_n (kDa)[a]*	*PDI[a]*
90/10	99/1	99/1	99/1	48%	5.2	1.3
80/20	97/3	98/2	97/3	24%	4.6	1.2
70/30	95/5	98/2	95/5	16%	4.4	1.2
60/40	93/7	94/6	92/8	2%	3.9	1.2

[a]Average molecular weights and polydispersity determined by gel permeation chromatography (GPC), calibrated with monodisperse polystyrene standards.

***Table 6.7** | Data for copolymers with 4-chloro-3-nitrobenzaldehyde (CNBA, Hammett value 0.94).*

Feed Ratio (OPA/BA)	*Copolymer Composition (Series 1)*	*Copolymer Composition (Series 2)*	*Copolymer Composition (Series 3)*	*Average Yield*	*M_n (kDa)[a]*	*PDI[a]*
90/10	99.5/0.5	99.5/0.5	99.5/0.5	46%	5.0	1.2
80/20	99/1	99/1	99/1	32%	4.4	1.2
70/30	98.5/1.5	98.5/1.5	99/1	22%	4.2	1.2
60/40	98/2	99/1	98/2	16%	4.0	1.2

[a]Average molecular weights and polydispersity determined by gel permeation chromatography (GPC), calibrated with monodisperse polystyrene standards.

***Scheme 6.6** | Oligomers for end-group analysis.*

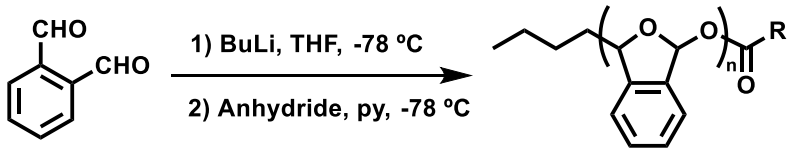

O-phthalaldehyde (0.50 g, 3.7 mmol) was dissolved in THF (5 mL) and cooled to -78 °C. Then, 1.6 M *n*-BuLi in hexanes (0.30 mL, 0.48 mmol) was added and the reaction mixture stirred at -78 °C for 4 h. Acetic anhydride (0.18 mL, 1.9 mmol) or methacrylic anhydride (0.28 mL, 1.9 mmol) and pyridine (0.15 mL, 1.9 mmol) were then added, and the mixture stirred for 3 hours at -78 °C before it was warmed to room temperature. The polymer was precipitated in methanol and washed in methanol and diethyl ether. The polymers were purified by twice dissolving in dichloromethane and re-precipitating into methanol. The white solid powders were characterized by GPC (for molecular weight and polydispersity) and NMR spectroscopy.

Acetate: ^{1}H NMR (500 MHz, $CDCl_3$) δ 7.80-7.18 (b, Ar-H), 7.18-6.35 (b, -O-CH-O-), 5.60-5.51 (b, -CH_2-CH-O-), 5.36-5.27 (b, -CH_2-CH-O-), 2.28-2.11 (b, $COCH_3$), 2.10-1.35 (b, -CH_2-), 1.13-0.83 (b, -CH_3). ^{13}C{^{1}H} NMR (500 MHz, $CDCl_3$) δ 170.5 ppm, 143.1 ppm, 138.7 ppm, 137.4 ppm, 129.7 ppm, 127.7 ppm, 123.1 ppm, 120.9 ppm, 101.5-104.3 ppm, 99.4 ppm, 84.4 ppm, 82.9 ppm, 37.5 ppm, 35.0 ppm, 27.8 ppm, 27.0 ppm, 22.7 ppm, 21.2 ppm, 14.0 ppm. GPC (THF, RI): M_n = 2.1 kDa, PDI = 1.1.

Methacrylate: ^{1}H NMR (500 MHz, $CDCl_3$) δ 7.80-7.18 (b, Ar-H), 7.18-6.35 (b, -O-CH-O-), 6.29-6.11 (b, =CH), 5.76-5.61 (b, =CH), 5.60-5.51 (b, -CH_2-CH-O-), 5.37-5.27 (b, -CH_2-CH-O-), 2.08-1.99 (b, -C-CH_3), 1.99-1.31 (b, -CH_2-), 1.07-0.82 (b, CH_3-). ^{13}C{^{1}H} NMR (500 MHz, $CDCl_3$) δ 166.7 ppm, 143.2 ppm, 138.5 ppm, 137.5 ppm, 135.8 ppm, 129.8 ppm, 127.7 ppm, 126.8 ppm, 123.1 ppm, 120.9 ppm, 101.5-104.7 ppm, 99.7 ppm, 84.3 ppm, 82.8 ppm, 37.5 ppm, 35.0 ppm, 27.8 ppm, 27.0 ppm, 22.7 ppm, 18.1 ppm, 14.0 ppm. GPC (THF, RI): M_n = 2.1 kDa, PDI = 1.1.

***Scheme 6.7** | Copolymerization of phthalaldehyde and 5-nitroisophthalaldehyde (**4**).*

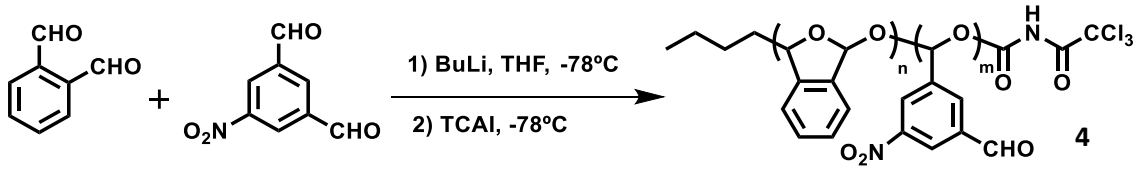

To a Schlenk flask were added *o*-phthalaldehyde (0.68 g, 5.1 mmol) and 5-nitroisophthalaldehyde (0.38 g, 2.1 mmol). The solids were dissolved in THF (10 mL), and the solution cooled to -78 °C. Then, 1.6 M *n*-BuLi in hexanes (0.17 mL, 0.27 mmol) was added and the reaction mixture stirred at -78 °C for 10 h. Trichloroacetyl isocyanate (0.10 mL, 0.8 mmol) was then added and the mixture stirred overnight at -78 °C. The polymer was precipitated in methanol and washed in methanol and diethyl ether (0.65 g yield, 61%). The white solid powder **4** was characterized by GPC (for molecular weight and polydispersity) and NMR spectroscopy. ^{1}H NMR (500 MHz, DMSO-d_6) δ 10.25-9.75 (b, 1H, aldehyde), 8.80-8.15 (b, 3H, benzaldehyde), 7.75-7.05 (b, 4H, phthalaldehyde), 7.05-6.25 (b, acetal), 1.95-1.15 (b, initiator), 0.90-0.60 (b, initiator). ^{13}C{^{1}H} NMR (500 MHz, $CDCl_3$) δ 192.2 ppm, 148.3 ppm, 138.5 ppm, 135.9 ppm, 133.5 ppm, 130.8 ppm, 129.6 ppm, 127.9 ppm, 126.8 ppm, 123.0 ppm, 105.0-100.5 ppm, 22.3 ppm. GPC (THF, RI): M_n = 4.6 kDa, PDI = 1.3.

Scheme 6.8 | *Sonogashira Coupling: poly(phthalaldehyde-*co*-3-nitro-5-trimethylsilylalkynyl-benzaldehyde) (Polymer **3**).*

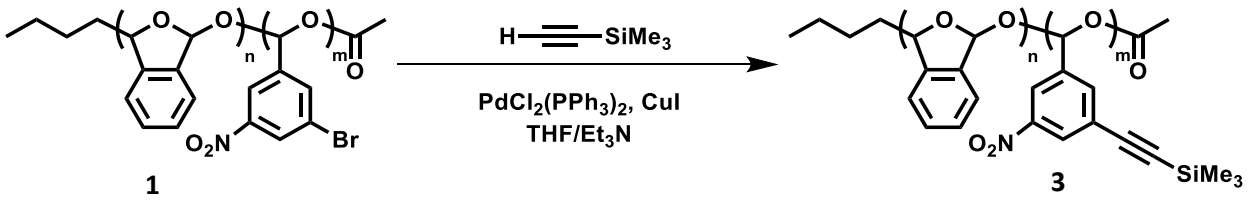

To a 20-mL flask were added bis(triphenylphosphine)palladium(II) dichloride (1.1 mg, 1.6 µmol), copper(I) iodide (0.4 mg, 2.1 µmol), poly(phthalaldehyde-*co*-3-bromo-5-nitrobenzaldehyde) (**1**, 62.0 mg, 94/6 molar ratio, 25 µmol bromide), and trimethylsilylacetylene (0.04 mL, 0.28 mmol). The reagents were dissolved in a mixture of THF (2.5 mL) and triethylamine (2.5 mL) and heated to 70 °C for 4 h. The mixture was then cooled to room temperature, and the polymer was precipitated by pouring into methanol (100 mL). The polymer was washed in methanol and diethyl ether and collected in 25.0 mg yield (40% recovery, 62% coupling conversion). The gray solid powder **3** was characterized by GPC (for molecular weight and polydispersity) and NMR spectroscopy. ^{1}H NMR (500 MHz, DMSO-d_6) δ 8.50-8.00 (b, 3H, benzaldehyde), 7.75-7.05 (b, 4H, phthalaldehyde), 7.05-6.25 (b, acetal), 2.15-2.00 (b, acetate) 1.55-1.15 (b, initiator), 0.90-0.60 (b, initiator), 0.35-0.05 (b, trimethylsilyl). GPC (THF, RI): M_n = 5.1 kDa, PDI = 1.1.

Scheme 6.9 | *Stille Coupling: poly(phthalaldehyde-*co*-3-nitro-5-vinylbenzaldehyde) (Polymer **2**).*

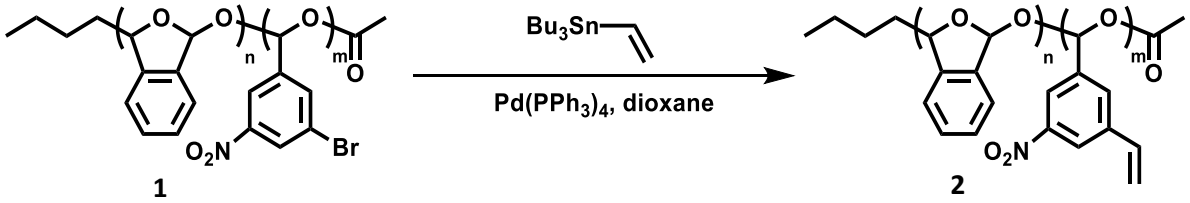

To a 20-mL flask were added tetrakis(triphenylphosphine)palladium(0) (2.2 mg, 1.9 µmol), tributyl(vinyl)tin (12.0 mg, 38 µmol), and poly(phthalaldehyde-*co*-3-bromo-5-nitrobenzaldehyde) (**1**, 60.1 mg, 94/6 molar ratio, 21 µmol bromide). The reagents were dissolved in 1,4-dioxane (5 mL), and the mixture was heated to 80 °C for 2 h. The mixture was then cooled to room temperature, and the polymer was precipitated by pouring into methanol (100 mL). The polymer was washed in methanol and diethyl ether and collected in 29.0 mg yield (48% recovery, 93% coupling conversion). The off-white solid powder **2** was characterized by GPC (for molecular weight and polydispersity) and NMR spectroscopy. ^{1}H NMR (500 MHz, DMSO-d_6) δ 8.50-8.00 (b, 3H, benzaldehyde), 7.75-7.05 (b, 4H, phthalaldehyde), 7.05-6.25 (b, acetal), 6.10-5.85 (b, vinyl), 5.50-5.15 (b, vinyl), 2.15-2.00 (b, acetate), 1.55-1.15 (b, initiator), 0.90-0.60 (b, initiator). GPC (THF, RI): M_n = 5.5 kDa, PDI = 1.2.

Scheme 6.10 **|** *Aldehyde reduction: poly(phthalaldehyde-*co*-3-hydroxymethyl-5-nitrobenzaldehyde) (Polymer **7**).*

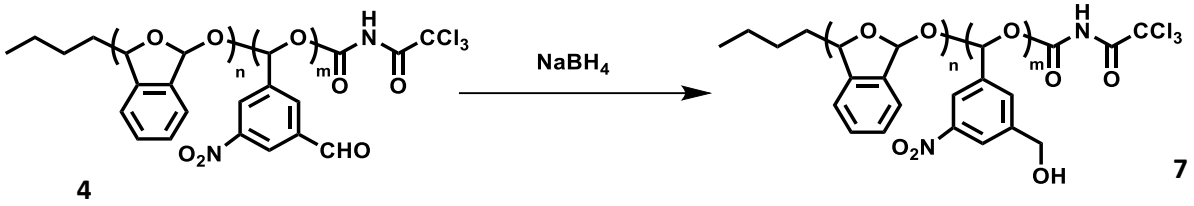

To a 20-mL flask were added sodium borohydride (3.0 mg, 79 μmol) and poly(phthalaldehyde-*co*-5-nitroisophthalaldehyde) (**4**, 104.7 mg, 92/8 molar ratio, 61 μmol aldehyde). The reagents were dissolved in a mixture of dichloromethane (4 mL) and methanol (1 mL), and the reaction contents were stirred at room temperature for 1 h. The polymer was precipitated by pouring into methanol (100 mL), washed in methanol and diethyl ether, and collected in 71.0 mg yield (68% recovery, quantitative reduction). The white solid powder **7** was characterized by GPC (for molecular weight and polydispersity) and NMR spectroscopy. ^{1}H NMR (500 MHz, DMSO-d_6) δ 8.40-7.80 (b, benzaldehyde), 7.75-7.05 (b, phthalaldehyde), 7.05-6.25 (b, acetal), 5.65-5.45 (b, hydroxyl), 4.70-4.40 (b, benzyl) 1.55-1.15 (b, initiator), 0.90-0.60 (b, initiator). ^{13}C{^{1}H} NMR (500 MHz, $CDCl_3$) δ 143.4 ppm, 140.9 ppm, 138.5 ppm, 131.0 ppm, 129.7 ppm, 127.6 ppm, 123.0 ppm, 121.2 ppm, 120.8 ppm, 105.0-100.5 ppm, 62.9 ppm, 22.3 ppm. GPC (THF, RI): M_n = 4.5 kDa, PDI = 1.2.

Scheme 6.11 **|** *Wittig Reaction (Polymer **5**).*

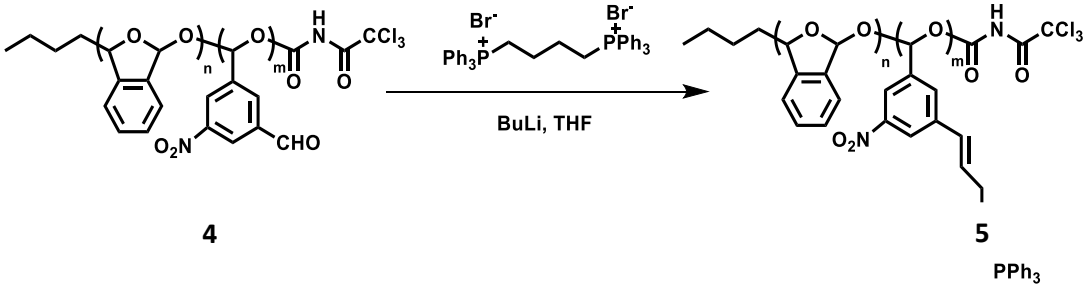

To a 20-mL flask were added tetramethylene bis(triphenylphosphonium bromide) (22.6 mg, 31 μmol) and poly(phthalaldehyde-*co*-5-nitroisophthalaldehyde) (**4**, 103.5 mg, 92/8 molar ratio, 60 μmol aldehyde). The reagents were dissolved in THF (2.5 mL), and 1.6 M *n*-BuLi in hexanes was added (0.06 mL, 96 μmol). The mixture was stirred at room temperature overnight, and the polymer was precipitated by pouring into methanol (100 mL). The polymer was washed in excess methanol and diethyl ether and collected in 62.0 mg yield (60%). The yellow solid powder **5** was characterized by GPC (for molecular weight and polydispersity) and NMR spectroscopy. ^{1}H NMR (500 MHz, DMSO-d_6) δ 8.70-7.90 (b, benzaldehyde),

7.87 (b, $Ph_3P=O$), 7.75 (b, $Ph_3P=O$), 7.70-7.05 (b, phthalaldehyde), 7.05-6.25 (b, acetal), 5.75-5.50 (b, -C=CH-), 4.70-4.40 (b, benzyl), 3.70-3.55 (b, -C=C-CH_2-), 2.00-1.55 (b, -CH_2-) 1.55-1.15 (b, initiator), 0.90-0.60 (b, initiator). GPC (THF, RI): M_n = 6.1 kDa, PDI = 1.7.

Scheme 6.12 | *Imine Formation (Polymer **6**).*

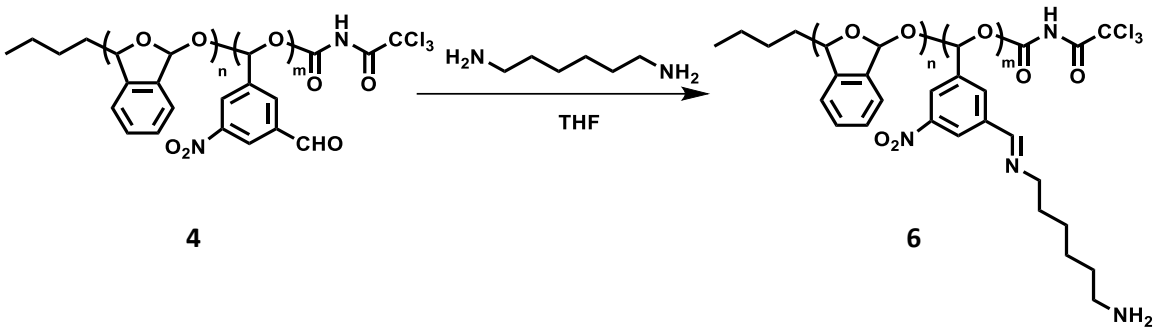

To a 20-mL flask were added hexamethylene diamine (4.0 mg, 34 μmol) and poly(phthalaldehyde-*co*-5-nitroisophthalaldehyde) (**4**, 103.3 mg, 92/8 molar ratio, 60 μmol aldehyde). The reagents were dissolved in a mixture of N-methyl pyrrolidone (2 mL) and hexamethyl phosphoramide (1 mL), and the reaction contents were stirred 7 h at room temperature. The polymer was precipitated by pouring into methanol (100 mL), washed in excess methanol and diethyl ether, and collected in 85.0 mg yield (82% recovery). The pink solid powder **7** was characterized by GPC (for molecular weight and polydispersity) and NMR spectroscopy. ^{1}H NMR (500 MHz, DMSO-d_6) δ 8.70-8.10 (b, benzaldehyde), 7.75-7.05 (b, phthalaldehyde), 7.05-6.25 (b, acetal), 3.90-3.35 (b, =N-CH_2-), 2.15-1.55 (b, -CH_2-), 1.55-1.15 (b, initiator), 0.90-0.60 (b, initiator). GPC (THF, RI): M_n = 5.7 kDa, PDI = 1.6.

Scheme 6.13 | *Reaction with methylene diphenyl diisocyanate (Polymer **8**).*

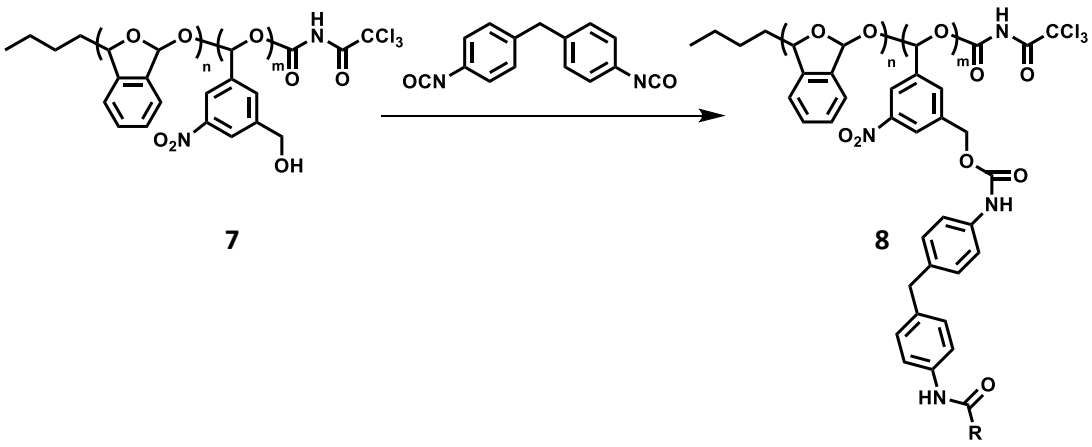

To a 20-mL flask were added 4,4'-methylene diphenyl diisocyanate (4.1 mg, 16 µmol) and poly(phthalaldehyde-*co*-3-hydroxymethyl-5-nitrobenzaldehyde) (**7**, 51.6 mg, 92/8 molar ratio, 30 µmol alcohol). The reagents were dissolved in dichloromethane (1.5 mL) and stirred at room temperature for 6 h. The solvent was slowly evaporated and the residue was heated to 80 ºC overnight. The residue was dissolved in dichloromethane, and the polymer was precipitated by pouring into methanol (100 mL). The polymer was washed in excess methanol and diethyl ether and collected in 31.0 mg yield (60% recovery, quantitative conversion). The white solid powder **8** was characterized by GPC (for molecular weight and polydispersity) and NMR spectroscopy. ^{1}H NMR (500 MHz, DMSO-d_6) δ 9.90-9.50 (b, NH) 8.40-7.80 (b, benzaldehyde), 7.75-7.05 (b, phthalaldehyde), 7.05-6.25 (b, acetal), 5.65-5.45 (b, hydroxyl), 4.70-4.35 (b, benzyl), 3.90-3.65 (b, methylene), 3.65-3.55 (b, NH_2), 1.55-1.15 (b, initiator), 0.90-0.60 (b, initiator). GPC (THF, RI): M_n = 5.5 kDa, PDI = 1.6.

Scheme 6.14 **|** *Reaction with toluene diisocyanate (Polymer **9**).*

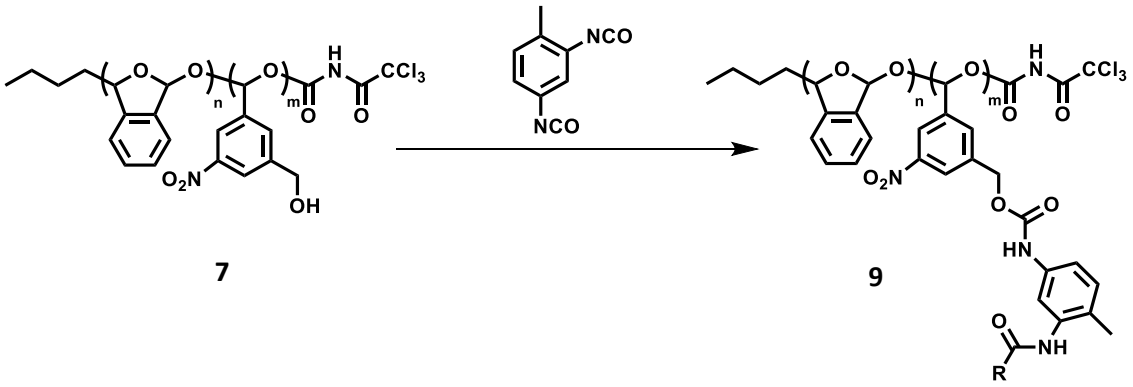

To a 20-mL flask were added 2,4-diisocyanato-1-methyl-benzene (19.9 mg, 0.11 mmol) and poly(phthalaldehyde-*co*-3-hydroxymethyl-5-nitrobenzaldehyde) (**7**, 66.2 mg, 92/8 molar ratio, 38 µmol alcohol). The reagents were dissolved in THF (1 mL) and warmed to 40 ºC for 5 h. The solvent was slowly evaporated and the residue was heated to 80 ºC overnight. The residue was dissolved in dichloromethane, and the polymer was precipitated by pouring into methanol (100 mL). The polymer was washed in excess methanol and diethyl ether and collected in 75.0 mg yield (quantitative recovery and conversion). The white solid powder **9** was characterized by GPC (for molecular weight and polydispersity) and NMR spectroscopy. ^{1}H NMR (500 MHz, DMSO-d_6) δ 10.15-9.45 (b, NH) 8.40-7.80 (b, benzaldehyde), 7.75-7.05 (b, phthalaldehyde), 7.05-6.25 (b, acetal), 5.50-4.90 (b, benzyl), 3.70-3.50 (b, NH_2), 2.40-1.85 (b, -CH_3), 1.55-1.15 (b, initiator), 0.90-0.60 (b, initiator). GPC (THF, RI): M_n = 4.7 kDa, PDI = 36.7.

Scheme 6.15 **|** *Cross-linking of poly(phthalaldehyde-*co*-3-hydroxymethyl-5-nitrobenzaldehyde) (Polymer **10**).*

To a 20-mL flask were added poly[(phenyl isocyanate)-*co*-formaldehyde] (avg. M_n 400, 3.2 isocyanate groups/molecule, 6.0 mg, 15 µmol) and poly(phthalaldehyde-*co*-3-hydroxymethyl-5-nitrobenzaldehyde) (**7**, 65.0 mg, 92/8 molar ratio, 38 µmol alcohol). The reagents were dissolved in THF (1 mL) and warmed to 40 ºC for 5 h. The solvent was slowly evaporated and the residue was heated to 80 ºC overnight. The resulting insoluble yellow film (**10**) was grinded into a powder and washed with methanol and dichloromethane, leaving 34 mg insoluble solid (52% recovery). The solid was characterized by CP-MAS ^{13}C NMR spectroscopy. ^{13}C NMR (500 MHz) δ 161-152 ppm, 152-147 ppm, 145-136 ppm, 136-128 ppm, 128-116 ppm, 115-99 ppm, 72-64 ppm, 19-14 ppm.

Scheme 6.16 **|** *Cross-linked PPA-BA copolymer degradation.*

10 mg of cross-linked PPA-BA copolymer (**10**) was suspended in $CDCl_3$ (1 mL). One drop of deuterium chloride (35 wt. % in D_2O) was added to the suspension, which immediately became a homogeneous yellow solution. The mixture was directly analyzed by NMR spectroscopy and ESI-MS. ^{1}H NMR (500 MHz, $CDCl_3$) δ 10.54 (2H, s, CHO), 7.98 (2H, dd, Ar-H), 7.78 (2H, dd, Ar-H). ^{13}C{^{1}H} NMR (500 MHz, $CDCl_3$) δ 192.3 ppm, 136.4 ppm, 133.7 ppm, 131.1 ppm. HR ESI-MS (m/z): calcd for $C_8H_7O_2$ $[M+H]^+$, 135.0446; found 135.0452.

Scheme 6.17 **|** *Graft copolymerization: poly(phthalaldehyde-*co*-3-hydroxymethyl-5-nitrobenzaldehyde-*graft*-poly lactic acid) (Polymer **11**).*

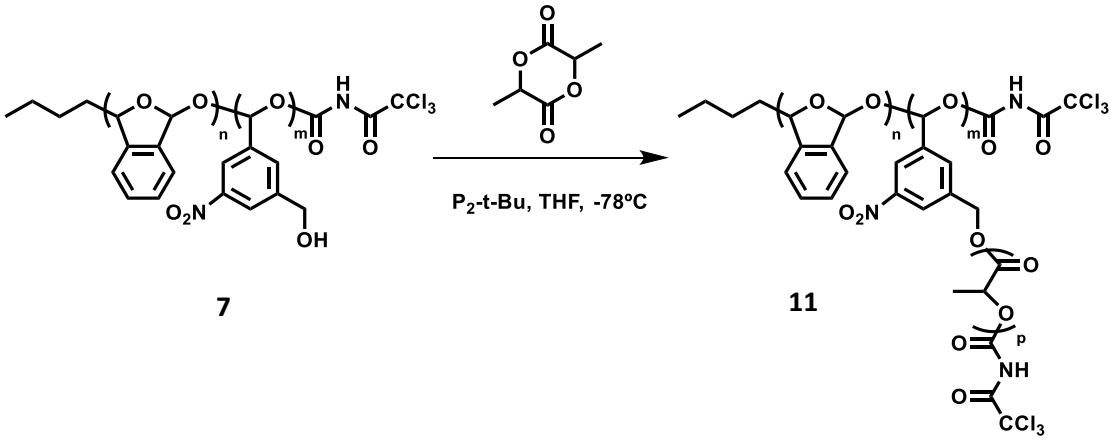

To a Schlenk flask were added poly(phthalaldehyde-*co*-3-hydroxy-5-nitrobenzaldehyde) (**7**, 30.0 mg, 92/8 molar ratio, 17 µmol alcohol) and lactide (90-280 mg, 0.6-1.9 mmol). The solids were dissolved in THF (8 mL) and cooled to -78 °C. P_2-t-Bu phosphazene base (2.0 M in THF, 10 µL, 20 µmol) was added to initiate polymerization. The reaction mixture was stirred at -78 °C for 3 h, then quenched with trichloroacetyl isocyanate (0.08 mL, 0.8 mmol) and left to stir for another 1 h at -78 °C. The mixture was then brought to room temperature, and the polymer was precipitated in methanol. The polymer was washed in excess methanol and collected in quantitative yield as a white solid. Polymer **11** was characterized by TGA and NMR spectroscopy. ^{1}H NMR (500 MHz, $CDCl_3$) δ 7.70-7.10 (b, phthalaldehyde), 7.10-6.20 (b, acetal), 5.30-5.00 (b, 1H, -CH-), 1.65-1.50 (b, 3H, -CH_3).

6.6 NMR Spectra

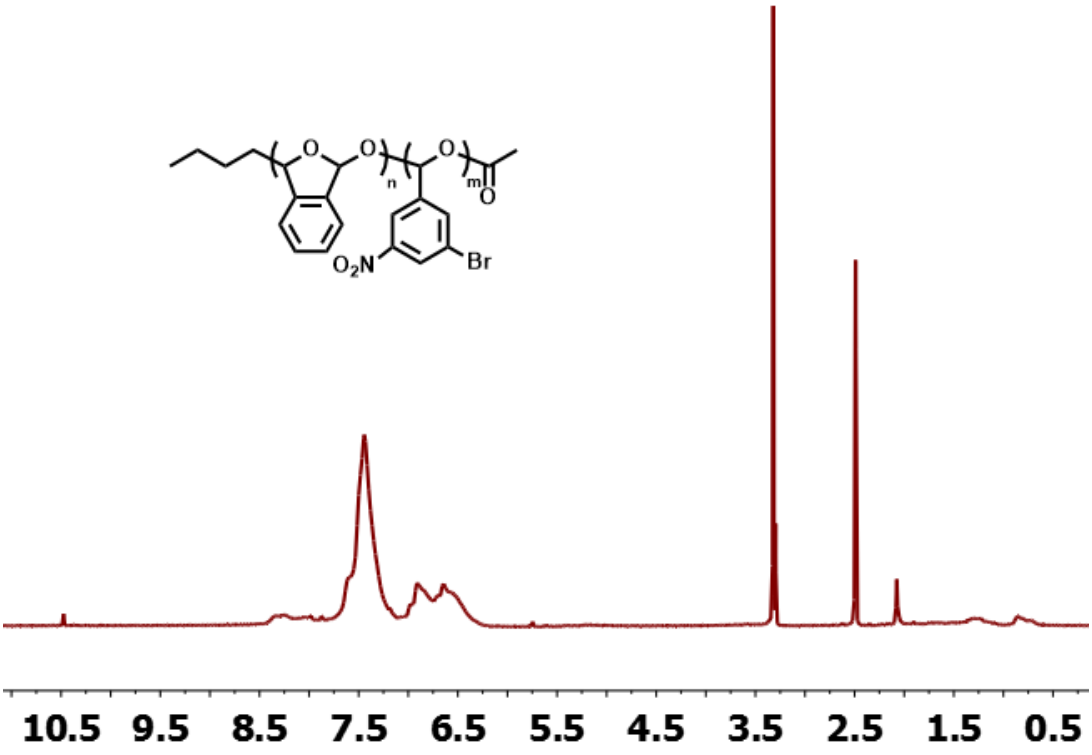

***Figure 6.4** | ^{1}H NMR spectrum of poly(phthalaldehyde-*co*-3-bromo-5-nitrobenzaldehyde) (Polymer **1**) in DMSO-d_6.*

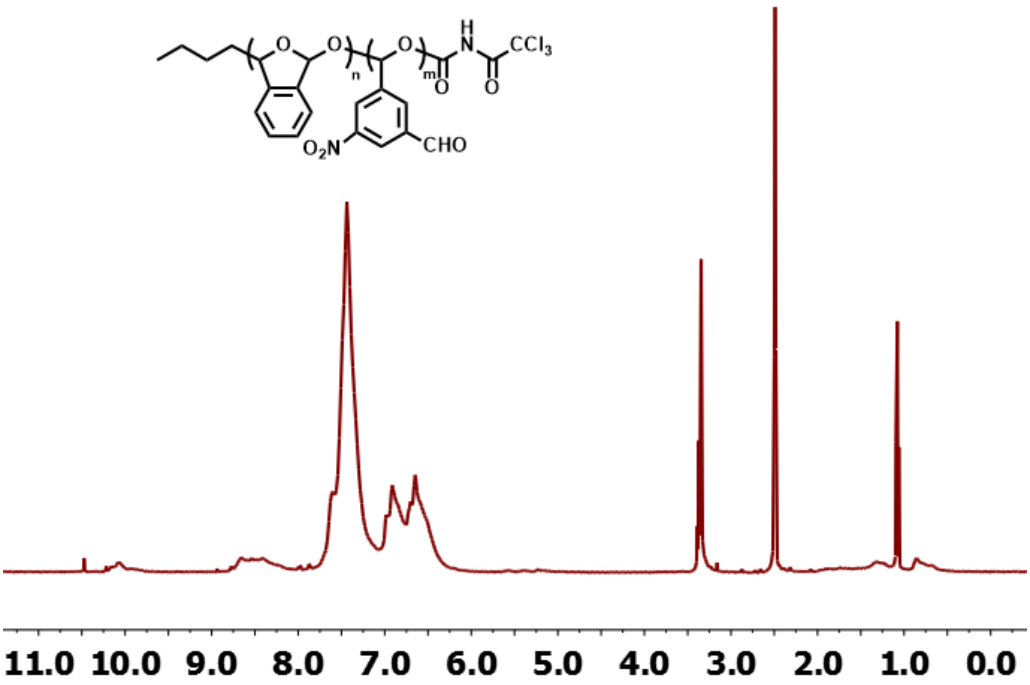

Figure 6.5 *| ^{1}H NMR spectrum of poly(phthalaldehyde-co-5-nitroisophthalaldehyde) (Polymer **4**) in DMSO-d_6.*

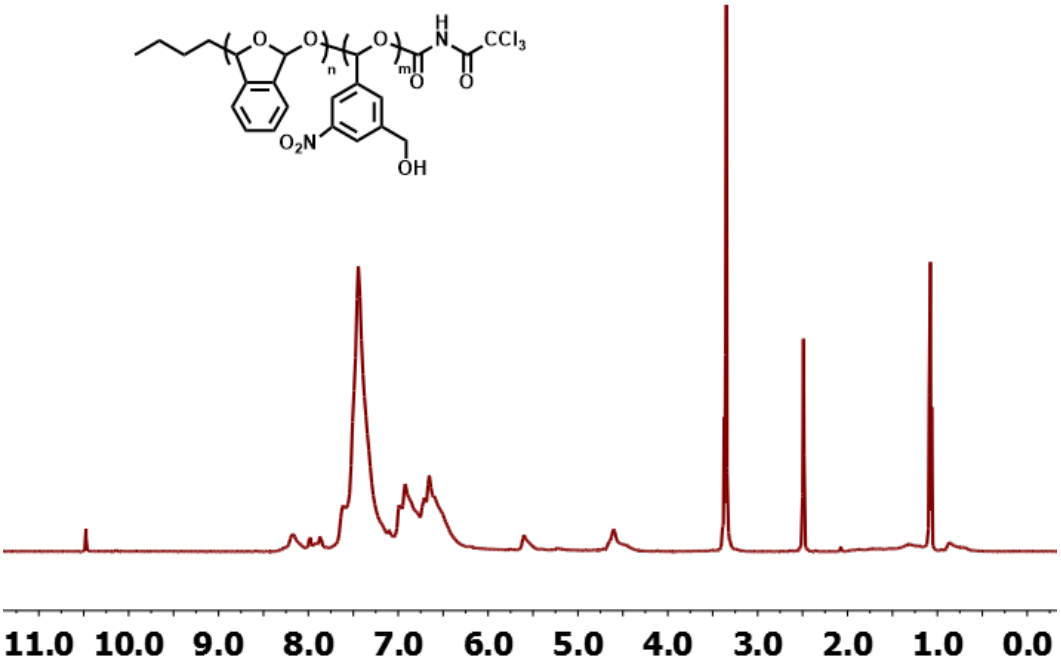

Figure 6.6 *| ^{1}H NMR spectrum of poly(phthalaldehyde-co-3-hydroxy-5-nitrobenzaldehyde) (Polymer **7**) in DMSO-d_6.*

6.7 References

(1) (a) Peterson, G. I.; Larsen, M. B.; Boydston, A. J. *Macromolecules* **2012**, 45, 7317-7328. (b) Esser-Kahn, A. P.; Odom, S. A.; Sottos, N. R.; White, S. R.; Moore, J. S. *Macromolecules* **2011**, 44, 5539-5553. (c) DeWit, M. A.; Nazemi, A.; Karamdoust, S.; Beaton, A.; Gillies, E. R. *ACS Symposium Series* **2011**, 1066, 9-21. (d) Wong, A. D.; DeWit, M. A.; Gillies, E. R. *Adv. Drug Delivery Rev.* **2012**, 64, 1031-1045.

(2) (a) Sagi, A.; Weinstain, R.; Karton, N.; Shabat, D. *J. Am. Chem. Soc.* **2008**, 130, 5434-5435. (b) DeWit, M. A.; Gillies, E. R. *J. Am. Chem. Soc.* **2009**, 131, 18327-18334. (c) Esser-Kahn, A. P.; Sottos, N. R.; White, S. R.; Moore, J. S. *J. Am. Chem. Soc.* **2010**, 132, 10266-10268. (d) Weintain, R.; Sagi, A.; Karton, N.; Shabat, D. *Chem. Eur. J.* **2008**, 14, 6857-6861. (e) Chen, E. K. Y.; McBride, R. A.; Gillies, E. R. *Macromolecules* **2012**, 45, 7364-7374.

(3) (a) Chuji, A.; Tagami, S.; Kunitake, T. *J. Polym. Sci., Part A: Polym. Chem.* **1969**, 7, 497-511. (b) Chuji, A.; Tagami, S. *Macromolecules* **1969**, 2, 414-419.

(4) (a) Tsuda, M.; Hata, M.; Nishida, R.; Oikawa, S. *J. Polym. Sci., Part A: Polym. Chem.* **1997**, 35, 77-89. (b) Ito, H.; Willson, C. G. *Polym. Eng. Sci.* **1983**, 23, 1012-1018. (c) Coulembier, O.; Knoll, A.; Pires, D.; Gotsmann, B.; Duerig, U.; Frommer, J.; Miller, R. D.; Dubois, P.; Hedrick, J. L. *Macromolecules* **2010**, 43, 572-574.

(5) Seo, W.; Phillips, S. T. *J. Am. Chem. Soc.* **2010**, 132, 9234-9235.

(6) Coady, D. J.; Duerig, U. T.; Frommer, J. E.; Fukushima, K.; Hedrick, J. L.; Knoll, A. W. *U.S. Pat. US 2012/0082944 A1*, **2012**.

(7) (a) Stampa, G. B., *Macromolecules* **1969**, 2, 203-206. (b) Raff, R.; Cook, J. L.; Ettling, B. V. *J. Polym. Sci., Part A: Polym. Chem.* **1965**, 3, 3511-3517. (c) Ishido, Y.; Aburaki, R.; Kanaoka, S.; Aoshima, S. *Macromolecules* **2010**, 43, 3141-3144. (d) Ishido, Y.; Aburaki, R.; Kanaoka, S.; Aoshima, S. *J. Polym. Sci., Part A: Polym. Chem.* **2010**, 48, 1838-1843.

(8) Guthrie, J. P. *J. Am. Chem. Soc.* **2000**, 122, 5529-5538.

(9) Many ortho-substituted BAs are commercially available. Hammett values for ortho-substituents were estimated by using the value of the substituent in the para position. See: (a) Hammett, L. P. *J. Am. Chem. Soc.* **1937**, 59, 96-103. (b) Jaffé, H. H. *Chem. Rev.* **1953**, 53, 191-261. (c) Charton, M. *Can. J. Chem.* **1960**, 38, 2493-2499. (d) Tribble, M. T.; Traynham, J. G. *J. Am. Chem. Soc.* **1969**, 91, 379-388.

(10) (a) Odian, G. *Principles of Polymerization*, 4th ed.; Wiley-Interscience: New York, 2004; pp 512-518. (b) Lowry, G. G. *J. Polym. Sci.* **1960**, 42, 463-477. (c) Szymanski, R. *Makromol. Chem.* **1987**, 188, 2605-2619.

(11) Kelen, T.; Tudos, F. *J. Macromol. Sci. Chem.* **1975**, A9, 1-27.

(12) (a) Bowden, K.; El-Kaissi, F. A.; Nadvi, N. S. *J. Chem. Soc. Perk. Trans. 2* **1979**, 642-645. (b) McDonald, R. S.; Martin, E. V. *Can. J. Chem.* **1979**, 57, 506-516.

(13) (a) Greenzaid, P. *J. Org. Chem.* **1973**, 38, 3164-3167. (b) McClelland, R. A.; Coe, M. *J. Am. Chem. Soc.* **1983**, 105, 2718-2725. (c) Bell, R. P.; Sorenson, P. E. *J. Chem. Soc. Perk. Trans. 2* **1976**, 1594-1598.

(14) Hansch, C.; Leo, A.; Taft, R. W. *Chem. Rev.* **1991**, 91, 165-195.

(15) (a) Boileau, S.; Illy, N. *Prog. Polym. Sci*. **2011**, 36, 1132-1151. (b) Zhang, L.; Nederberg, F.; Messman, J. M.; Pratt, R. C.; Hedrick, J. L.; Wade, C. G. *J. Am. Chem. Soc.* **2007**, 129, 12610-12611.

Chapter 7: Depolymerizable, Adaptive Supramolecular Polymer Nanoparticles and Networks*

7.1 Abstract

Incorporation of supramolecular cross-linking motifs into low-ceiling temperature (T_c) polymers allows for the possibility of remendable polymeric networks and nanoparticles whose structure and chemical backbones can be dynamically modified or depolymerized as desired. In this chapter, we demonstrate the synthesis of phthalaldehyde-benzaldehyde copolymers bearing a pendant dimerizing 2-ureido-pyrimidinone (UPy) motif. The UPy moiety promotes single-chain polymeric nanoparticle formation through non-covalent cross-linking at intermediate concentrations and results in reversible polymer network formation at high concentrations. Furthermore, due to the low T_c polymer backbone within such macromolecules, the materials depolymerize to monomer under appropriate conditions. We envision that the synthesis of such depolymerizable, adaptive supramolecular polymeric materials may find use in materials capable of self-healing and remodeling as well as in triggered release applications or the development of nanoporous structures.

7.2 Introduction

Stimuli-responsive materials that utilize reversible and dynamic supramolecular interactions have generated strong interest in recent years.[1] These materials acquire their unique properties from non-covalent interactions and have promise in self-healing applications.[2] Moreover, they have been employed for the controlled formation of single-chain polymeric architectures.[3] The quadruple hydrogen-bond dimerizing 2-ureido-pyrimidinone (UPy) motif has been introduced toward the synthesis of robust supramolecular polymers and nanoparticles.[4] The UPy motif, which dimerizes by a self-complementary DDAA (donor-donor-acceptor-acceptor) hydrogen bonding array, exhibits a dimerization constant greater than 10^7 M^{-1} in chloroform at room temperature.[4c] Due to its ease of synthesis as well as its strong affinity for non-covalent cross-linking, the UPy motif has been incorporated into polymers either at the chain-end or as a pendant functionality to form stable yet reversible non-covalent cross-links and facilitate the formation of various architectures and nanostructures.[4]

* Portions of this chapter have been published: Kaitz, J. A.; Possanza, C. M.; Song, Y.; Diesendruck, C. E.; Spiering, A. J. H.; Meijer, E. W.; Moore, J. S. *Polym. Chem.* **2014**, 5, 3788-3794.

Low ceiling temperature (T_c) polymers have likewise garnered significant interest in recent years, being attractive materials for triggered release, lithography, and degradable nanostructures.[5-7] By virtue of being above the polymer's ceiling temperature, yet kinetically stabilized from depolymerization by end-capping, these polymers represent a unique class of materials capable of rapid and complete head-to-tail depolymerization upon removal of the end-cap.[6] Poly(phthalaldehyde) (PPA) is one such low T_c polymer that has been extensively studied due to its ease of synthesis and fast, complete depolymerization upon triggering.[7] We recently demonstrated the copolymerization of phthalaldehyde with various substituted benzaldehydes toward the preparation of more complex, depolymerizable nanostructures.[8a] We have also demonstrated the ability to dynamically modify backbone polyacetal linkages within the PPA backbone under cationic polymerization conditions.[8b-c]

Using these synthetic methods, we sought to make materials which combine the dynamic, reversible nature of supramolecular interactions and the stimuli-responsive capabilities of low T_c polymers. To the best of our knowledge, there are no examples incorporating supramolecular cross-linking units into depolymerizable polymers toward the development of dynamic polymer nanoparticles or networks. Here we report the synthesis of phthalaldehyde-benzaldehyde copolymers modified with pendant UPy dimerizing functionalities, the characterization of the resulting morphologies, and the demonstration of their dynamic reversibility and triggered depolymerization.

7.3 Results and Discussion

7.3.1 Phthalaldehyde Copolymer Synthesis and Functionalization with Supramolecular Cross-Linker

Anionic copolymerization of *o*-phthalaldehyde with a substituted benzaldehyde monomer, 5-nitroisophthalaldehyde (NIPA), was carried out in order to prepare a PPA that could be further functionalized with a supramolecular cross-linking motif (Scheme 7.1). UPy-functionalized benzaldehyde could not be copolymerized directly with *o*-phthalaldehyde, as the copolymerization requires strongly electron-withdrawing substituents for incorporation of the benzaldehyde comonomer.[8a] To prepare polymers of suitably high molecular weight, the copolymerization was initiated by 1,6-hexanediol in conjunction with phosphazene base P_2-*t*-Bu, per literature precedent.[7i] The copolymerization yielded PPA-NIPA (**1**) random copolymers in three hours with a degree of polymerization of ca. 110 and 8% incorporation of the NIPA monomer, as determined by ^{1}H NMR. At this molecular weight and composition, we expect an average of 8 to 9 UPy units per chain, assuming near quantitative conversion of each step of post-polymerization modification. The pendant aldehyde of the PPA-NIPA copolymer was then quantitatively reduced to a benzylic alcohol by reaction with sodium borohydride, affording PPA-HMNB

polymer (**2**, HMNB = 3-hydroxymethyl-5-nitrobenzaldehyde) in high yield. A slight increase in molecular weight and a decrease in polydispersity were observed in this polymer, which was attributed to the removal of low molecular weight species after repeated precipitations (see Table 7.1).

Finally, PPA-HMNB was functionalized with the 2-ureido-pyrimidinone (UPy) motif by reaction with an isocyanate terminated UPy.[4e] Due to the high sensitivity of PPA polymers toward acid, 1,4-diazabicyclo[2.2.2]octane (DABCO) was employed as a catalyst rather than the tin (II) catalysts typically used in the reaction.[9] The PPA-UPy (**3**) polymers thus produced show characteristic peaks in the ^{1}H NMR spectrum corresponding to the three hydrogen-bonded protons in UPy at δ 10.2 ppm, 11.8 ppm, and 13.1 ppm (Figure 7.1). Molecular weights and yields of polymers used in this study are summarized in Table 7.1.

Scheme 7.1 | Synthesis of UPy-functionalized PPA polymers. *Polymer yields and molecular weights are summarized in Table 7.1.*

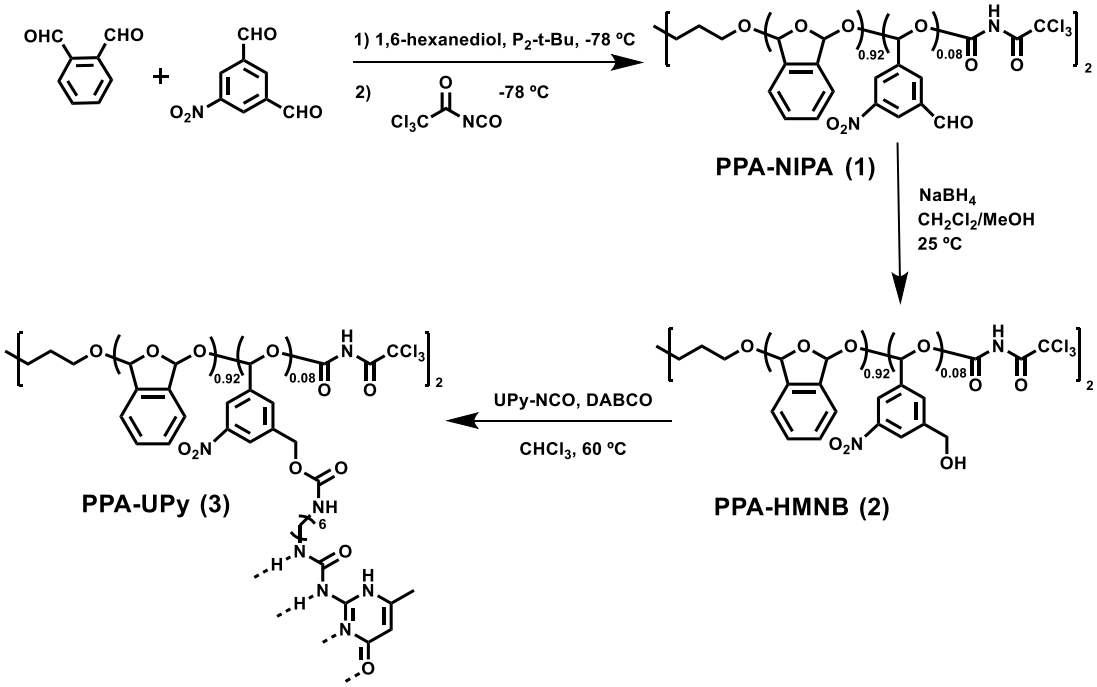

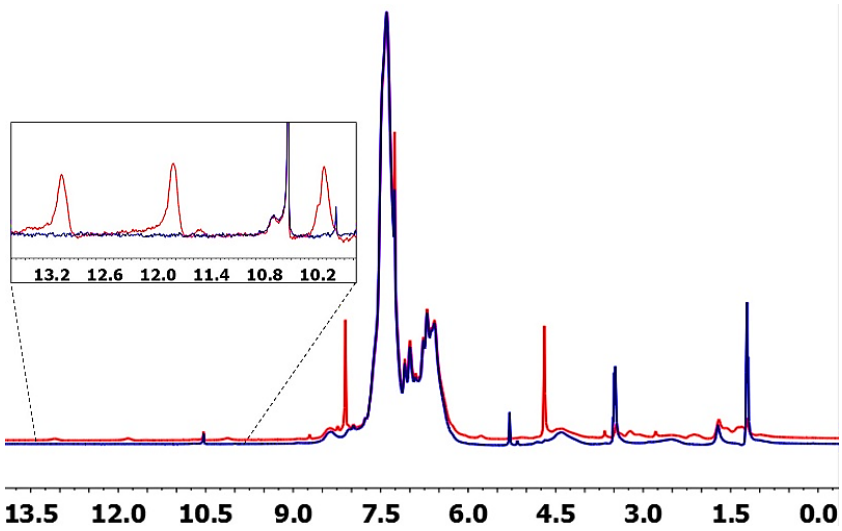

Figure 7.1 | NMR characterization of polymers in chloroform*: PPA-HMNB (Polymer 2, blue trace) overlayed with PPA-UPy (Polymer 3, red trace). Characteristic hydrogen-bonded protons corresponding to UPy are observed at δ 10.2, 11.8, and 13.1 ppm.*

Table 7.1 | Characterization data for Polymers 1-3.[a]

Polymer	*Name*	*Yield*	M_n *(kDa)*[b]	M_w *(kDa)*[b]	*PDI*[b]	R_h *(nm)*[c]
1	PPA-NIPA	68%	13.5	20.0	1.49	- - -
2	PPA-HMNB	72%	15.7	21.0	1.34	5.9
3	PPA-UPy	85%	15.3	20.1	1.31	4.9

[a]*o*-Phthalaldehyde purified before use according to literature procedure.[7i] [b]Average molecular weights and polydispersity determined by gel permeation chromatography (GPC), calibrated with monodisperse polystyrene standards. [c]Hydrodynamic radius determined by dynamic light scattering.

7.3.2 Characterization of Supramolecular Single-Chain Polymeric Nanoparticles

In order to investigate PPA-UPy intramolecular folding into well-defined polymeric nanoparticles, triple-detector GPC, dynamic light scattering (DLS), and atomic force microscopy (AFM) characterization techniques were utilized. It has previously been demonstrated that at low concentration, UPy functionalized polymers undergo reversible intramolecular folding to form single-chain polymeric nanoparticles (SCPNs).[4] To investigate this phenomenon in PPA-UPy polymers, the polymers were injected onto a triple-detector GPC at 9 mg/mL in THF. A slight increase in retention time was observed for PPA-UPy compared to PPA-HMNB when comparing the raw chromatograms, indicative of a decreased hydrodynamic radius and a more compact structure (Figure 7.2a). Even more significant, when absolute molecular weights of the two polymers are plotted versus retention time, PPA-UPy gives a greater retention time than PPA-HMNB at all molecular weights (Figure 7.2b). Again, this suggests a collapse in hydrodynamic radius consistent

with intramolecular association to produce PPA SCPNs. Interestingly, the polymer M_n absolute values increase from 20.8 kDa to 22.4 kDa after functionalization of PPA-HMNB with UPy, consistent with covalent functionalization of between five and six UPy units per polymer chain (corresponding to a 63% incorporation of UPy). Dynamic light scattering analysis confirmed this decrease in hydrodynamic radius, as the particles shrank from number-weighted average radii of 5.9 nm to 4.9 nm after functionalization with UPy. The observed 17% decrease in hydrodynamic radius is consistent with previous findings for intramolecular folding of SCPNs in THF.[3e,4e]

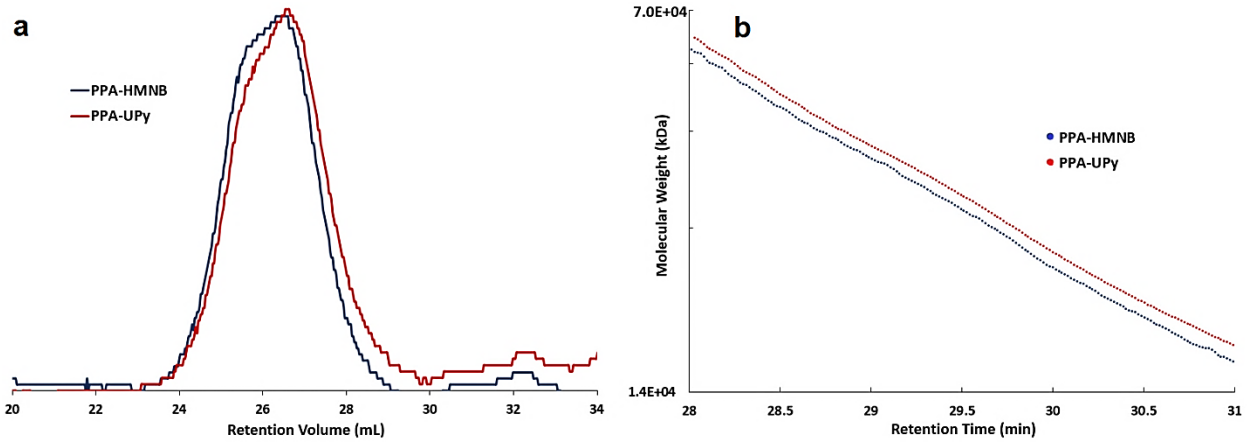

Figure 7.2 | Triple-detection GPC characterization of polymers*: (a) Normalized GPC chromatograms of PPA-HMNB (Polymer 2, blue trace) overlayed with PPA-UPy (Polymer 3, red trace) in THF at 1 mg/mL. (b) Triple detector plot of absolute molecular weight versus retention time for PPA-HMNB (Polymer 2, blue trace) and PPA-UPy (Polymer 3, red trace) in THF at 9 mg/mL. Both plots reveal longer retention times for PPA-UPy, suggesting a smaller hydrodynamic radius due to intramolecular UPy dimerization.*

In order to further characterize the SCPNs, we utilized AFM to visualize their size, morphology, and dispersity. Samples were prepared by casting extremely dilute solutions (0.1 µg/mL in THF) on freshly cleaved mica and allowing them to air dry under ambient conditions. The low concentration is critical to minimize nanoparticle aggregation.[4d] The micrographs demonstrate that the PPA SCPNs exhibit a spherical/round morphology and display a monodisperse distribution, as expected (Figure 7.3). The particle heights were found to be 4.2 nm on average, with an average diameter of 46.5 nm. Assuming a half-ellipsoid geometry of nanoparticles under AFM conditions[4d], the radius of unflattened nanoparticle spheres is calculated to be about 16.5 nm. That this radius does not correlate well with DLS results is not surprising, as SCPN radii extracted from AFM images are known to yield larger values than expected.[3f] The AFM images, however, serve to qualitatively corroborate GPC and DLS analytical techniques and confirm the presence of monodisperse, spherical SCPNs.

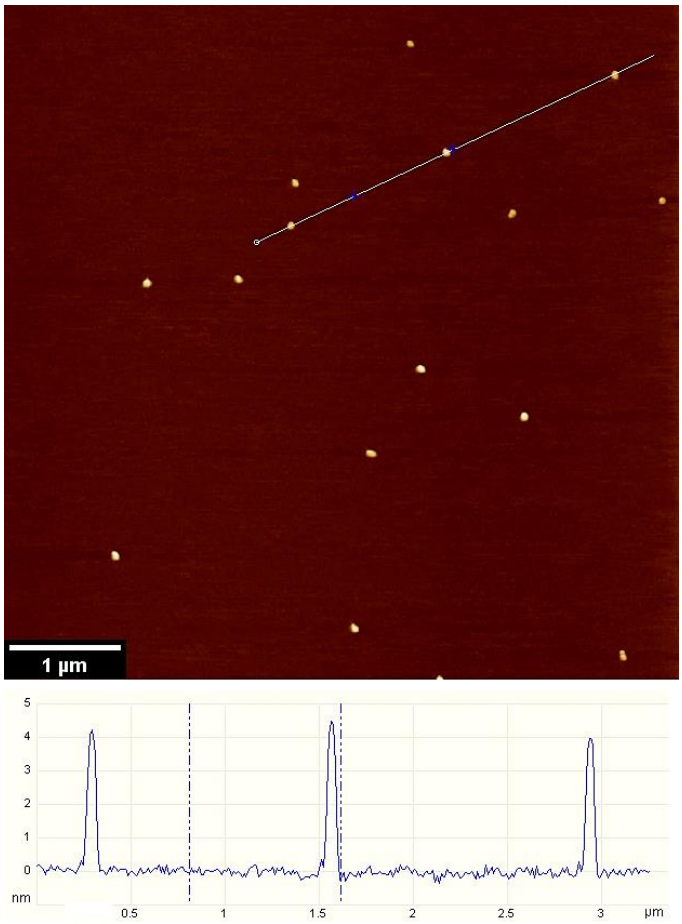

Figure 7.3 | AFM micrograph of single-chain polymeric nanoparticles*: PPA-UPy (Polymer 3) nanoparticles on mica, casted from a 0.1 µg/mL solution in THF. Nanoparticles are spherical and monodisperse, with heights of approximately 4 nm and average diameters of 46 nm.*

7.3.3 Dynamic Reconstitution of Low T_c Polymeric Nanostructures and Polymer Network Formation

The utility of PPA as the polymer scaffold was probed by exploring the depolymerization and reconstitution of PPA SCPNs. PPA is known to depolymerize when exposed to acid or chemical reagents appropriate to the end-group structure.[7] Further, we have shown that PPA can be subjected to cationic initiators in appropriate conditions and the molecular weight and architecture of the polymer backbone is dynamically modified.[8] With this knowledge at hand, we exposed PPA-UPy to the Lewis acid boron trifluoride etherate at room temperature. As expected, immediate depolymerization to monomer was observed and confirmed by NMR (Scheme 7.2c-d; Figure 7.4). Triggered depolymerization of polymeric nanoparticles provides a simple approach toward the development of nanoporous structures, where pore size is defined by nanoparticle size and number of pores is determined by the concentration of nanoparticles in solution.[10]

Scheme 7.2 | Supramolecular polymer reconstitution and depolymerization*: a) $BF_3{\cdot}OEt_2$, CH_2Cl_2, -78 °C; b) Pyridine, -78 °C. c) $BF_3{\cdot}OEt_2$, CH_2Cl_2, 25 °C; d) Pyridine, 25 °C. X represents pendant ureidopyrimidinone functionality.*

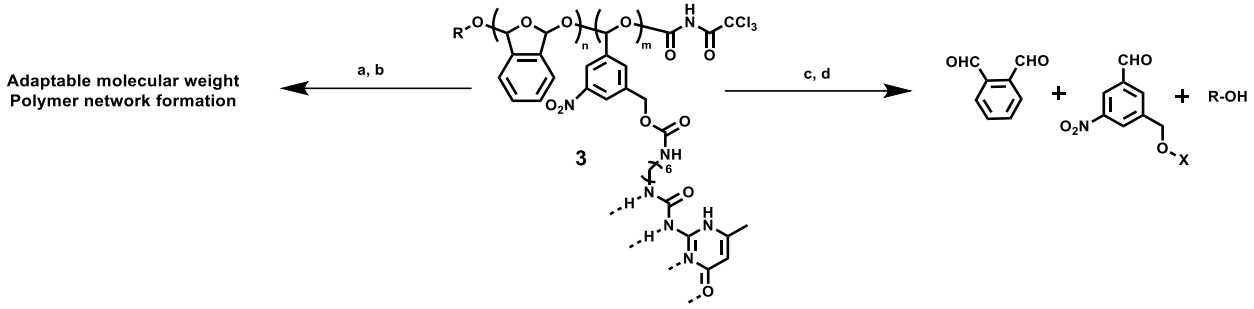

In order to test the reconstitution of the PPA nanoparticle backbone, PPA-UPy was exposed to boron trifluoride etherate at -78 °C (Scheme 7.2a-b), a temperature below the PPA T_c (ca. -40 °C).[7a] When the reaction is conducted at low concentration, i.e., below 0.7 M with respect to polymer repeat units, a shift toward lower molecular weight is observed in the GPC (Figure 7.4). The molecular weight of the product is tuned by varying the initial concentration, as previously demonstrated.[8b] Interestingly, this process makes it possible to dynamically modify supramolecular polymers to achieve desired molecular weights, even after their initial formation. These unique polymers can therefore be reversibly tuned by two chemically orthogonal methods; both the UPy cross-linker as well as the PPA backbone itself can be dynamically controlled.

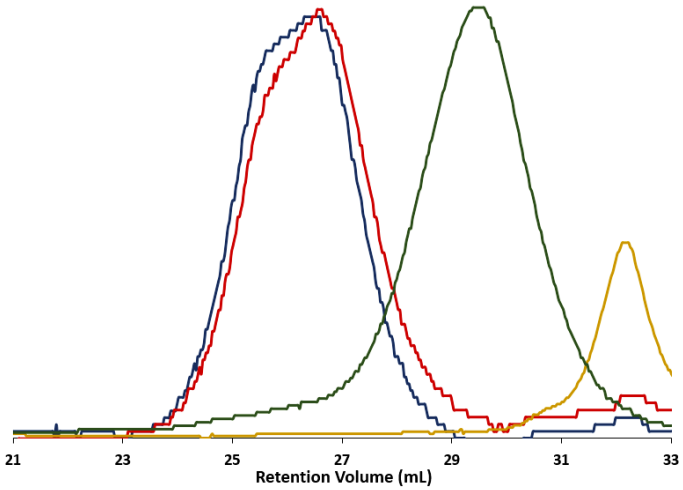

Figure 7.4 | GPC chromatograms of polymer reconstitution and depolymerization reactions*: GPC traces of PPA-HMNB (Polymer 2, blue trace), PPA-UPy (Polymer 3, red trace), PPA-UPy reconstituted to lower molecular weight (green trace), and after depolymerization (yellow trace). The peak at 32 mL corresponds to remainder small molecule in the void volume.*

Remarkably, an insoluble supramolecular polymer network is formed when PPA-UPy is subjected to reconstitution at high concentration, i.e., greater than 1.0 M. The white solid thus collected swelled but remained insoluble in typical solvents for PPA, specifically chloroform, dichloromethane, THF, and dimethyl sulfoxide. When reconstitution at high concentration is attempted on PPA-HMNB, however, the polymer remains soluble throughout the reaction, confirming that the supramolecular UPy cross-linker promotes polymer network formation. Figure 7.5 demonstrates triggered degradation of these supramolecular polymer networks. The cross-linked samples were initially swollen in deuterated chloroform, remaining insoluble opaque gels (Figure 7.5a). A drop of trifluoroacetic acid (TFA), which can hydrolyze the backbone acetal linkages, was then added to a single sample, and the polymer sample immediately shrunk in size, completely disappearing within 2 min (Figure 7.5b-c, right). The solution was collected and analyzed by NMR, confirming depolymerization to monomer. The control sample, on the other hand, remains unchanged (Figure 7.5b-c, left). This experiment demonstrates that supramolecular PPA networks are not only easily constructed, but unlike typical thermosets, this cross-linked polymer is rapidly deconstructed in response to an external stimulus.

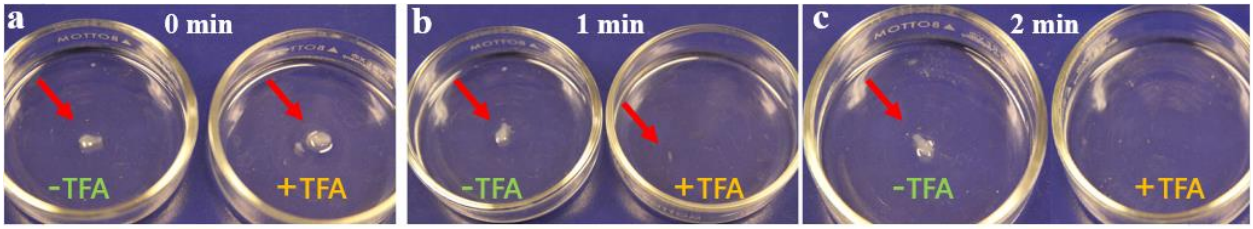

***Figure 7.5 | Supramolecular PPA-UPy Network and Triggered Depolymerization of Polymer Backbones**: (a) Image of PPA-UPy polymer networks suspended in $CDCl_3$ before addition of trifluoroacetic acid (TFA); (b) Image of PPA-UPy polymer network after one minute exposure to TFA (right) and without exposure to TFA (left); and (c) Image of fully depolymerized PPA-UPy network after two minute exposure to acid (right) and without exposure to acid (left).*

7.4 Conclusions

The results presented here serve as an initial foray into combining reversible supramolecular cross-linking reagents with dynamic low T_c polymers. Supramolecular PPA-UPy polymers were prepared by taking advantage of a previously reported phthalaldehyde-benzaldehyde copolymerization approach. The PPA-UPy polymers exhibit two distinct levels of control, as both the UPy dimerizing motif and the PPA backbone are capable of dynamic reorganization. The supramolecular cross-linker was shown to permit the preparation of both single-chain polymeric nanoparticles as well as degradable polymer networks. The polymer nanoparticles were then reconstituted to various molecular weights, and the polymer networks were shown to depolymerize by reaction with an external signal. We envision a wide range of applications

for such polymers, from the development of nanoporous structures to potential self-healing materials that are also fully recyclable and capable of structural remodeling.

7.5 Synthetic Procedures

***Scheme 7.3** | Synthesis of PPA-NIPA (Polymer **1**).*

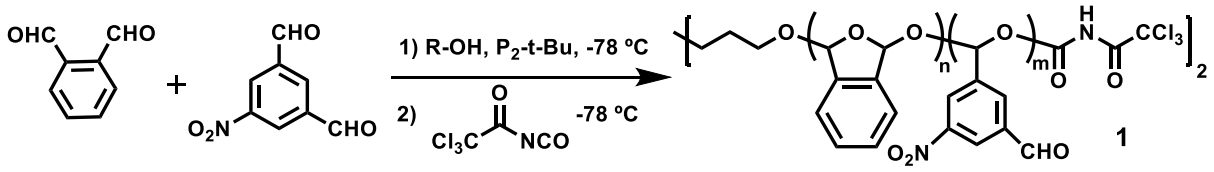

In a glovebox, purified *o*-PA (2.62 g, 19.5 mmol) and 5-nitroisophthalaldehyde[11] (1.01 g, 5.6 mmol) were weighed into a Schlenk flask and dissolved in THF (35 mL). The solution was removed from the glovebox and degassed by three freeze-pump-thaw cycles. Then, 1,6-hexanediol in THF (0.80 mL of a 0.03 M solution, 24 μmol) was added, and the solution stirred 2 minutes then cooled to -78 °C. Finally, P_2-t-Bu phosphazene base in THF (0.05 mL of a 2.0 M solution, 100 μmol) was added to initiate polymerization. The reaction was left stirring at -78 °C for 3 h, then the polymer end-capped by adding trichloroacetyl isocyanate (0.65 mL, 5.5 mmol) and allowing the mixture to stir an additional 2 h at -78 °C. The reaction mixture was then brought to room temperature and polymer precipitated by pouring into methanol (100 mL) and collected by filtration. Polymer **1** was further purified by dissolving in dichloromethane and re-precipitating from methanol and washed in diethyl ether (2.46 g, 68%). ^{1}H NMR (500 MHz, DMSO-d_6) δ 10.25-9.75 (b, 1H, aldehyde), 8.80-8.15 (b, 3H, benzaldehyde), 7.75-7.05 (b, 4H, phthalaldehyde), 7.05-6.25 (b, acetal). GPC (THF, RI): M_n = 13.5 kDa, PDI = 1.49.

***Scheme 7.4** | Synthesis of PPA-HMNB (Polymer **2**).*

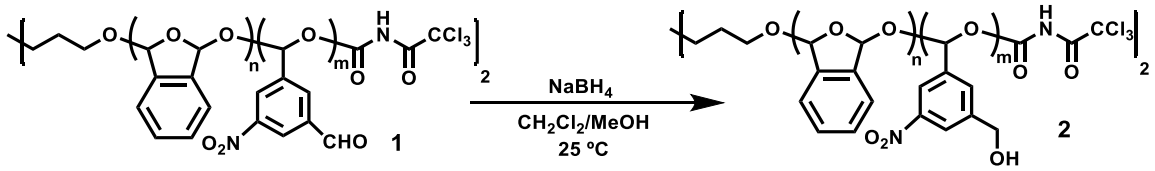

To a Schlenk flask were added 2.41 g PPA-NIPA (Polymer **1**, 1.4 mmol –CHO) and sodium borohydride (0.10 g, 2.6 mmol). The solids were dissolved in dichloromethane (40 mL) and methanol (8 mL), and the reaction mixture left stirring 1 h at room temperature. Polymer **2** was then precipitated into excess methanol (200 mL) and washed in methanol and diethyl ether (1.74 g, 72%). ^{1}H NMR (500 MHz, DMSO-d_6) δ 8.45-

7.75 (b, 3H, benzaldehyde), 7.75-7.05 (b, 4H, phthalaldehyde), 7.05-6.25 (b, acetal), 5.70-5.40 (b, CH_2-O*H*), 4.75-4.25 (b, -C*H*$_2$-OH). GPC (THF, RI): M_n = 15.7 kDa, PDI = 1.34.

Scheme 7.5 | *Synthesis of PPA-UPy (Polymer **3**).*

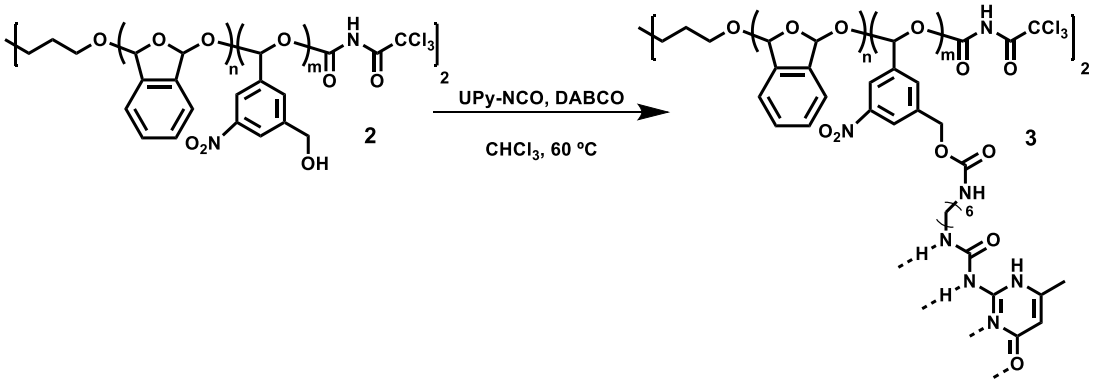

In a glovebox, PPA-HMNB (Polymer **2**, 0.20 g, 88 μmol –OH) and 1-(6-isocyanatohexyl)-3-(6-methyl-4-oxo-1,4-dihydro-pyrimidin-2-yl)urea[1c] (UPy-NCO, 28 mg, 95 μmol) were weighed into a Schlenk flask and dissolved in chloroform (60 mL, neutralized by stirring over K_2CO_3). To this solution was added 1,4-diazabicyclo[2.2.2]octane (DABCO, 0.65 mL of a 8.8 mM solution, 6 μmol) and the flask was closed and warmed to 60 °C overnight (18 hours). After overnight reaction, 1,6-hexanediamine (50 mg) was added to quench the PPA-UPy and the mixture filtered and concentrated in vacuo. The residue was dissolved in dichloromethane (20 mL) and filtered, then precipitated into methanol (150 mL) and washed in methanol and diethyl ether (0.17 g, 85%). ^{1}H NMR (500 MHz, $CDCl_3$) δ 13.3-12.9 (b, NH), 12.0-11.7 (b, NH), 10.3-9.9 (b, NH), 8.50-7.75 (b, 3H, benzaldehyde), 7.75-7.05 (b, 4H, phthalaldehyde), 7.05-6.25 (b, acetal), 4.75-4.00 (b, -C*H*$_2$-O), 4.00-0.50 (b, aliphatic –C*H*$_2$-). GPC (THF, RI): M_n = 15.3 kDa, PDI = 1.31.

Scheme 7.6 | *Depolymerization of PPA-UPy.*

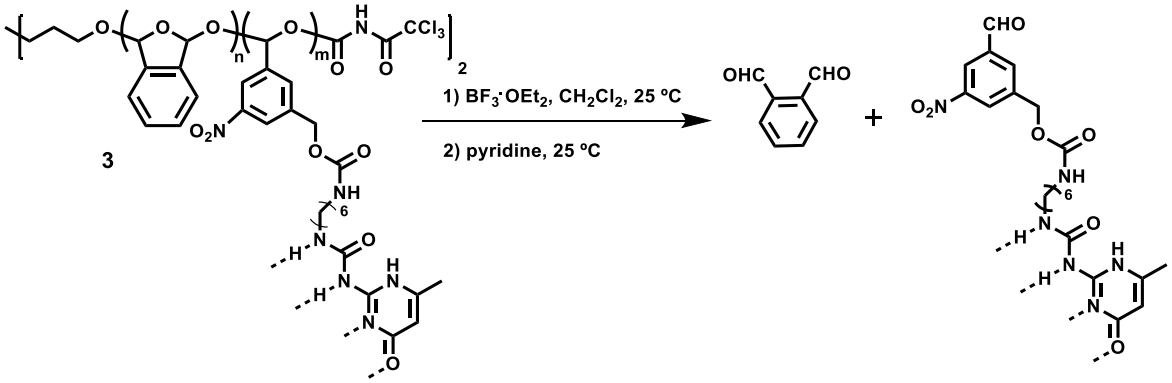

In a Schlenk flask, PPA-UPy (Polymer **3**, 40 mg) was dissolved in dichloromethane (0.4 mL). To the solution was added boron trifluoride etherate (1 drop, ~0.04 mmol) and the reaction mixture stirred for 5 min at room temperature, turning deep yellow immediately. To the mixture was then added pyridine (0.10 mL, 1.2 mmol) and left stirring 2 h. The reaction mixture was concentrated in vacuo and collected as a yellow oil, identified as majority *o*-PA by ^{1}H NMR spectroscopy. ^{1}H NMR (500 MHz, $CDCl_3$) δ 10.54 (s, 2H, CHO), 7.98 (q, 2H, Ar-H), 7.78 (q, 2H, Ar-H). GPC (THF, RI): No polymer.

Scheme 7.7 **|** *Reconstitution of PPA-UPy.*

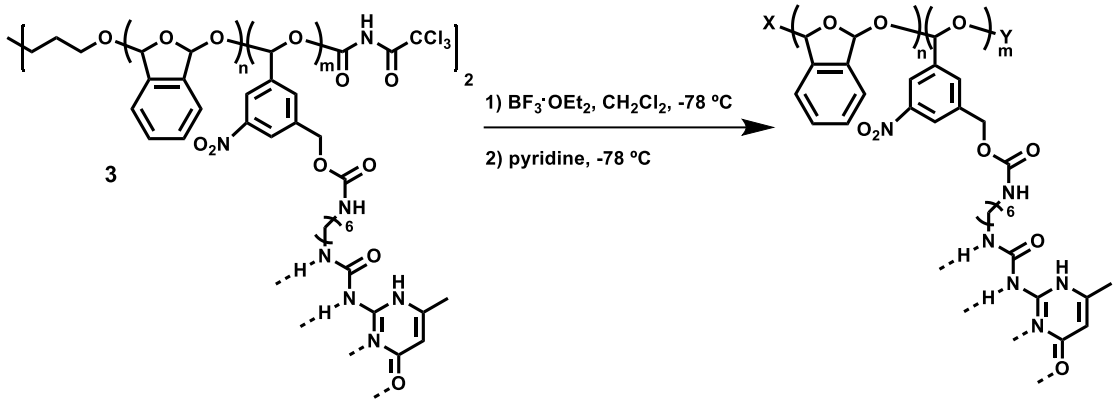

In a Schlenk flask, PPA-UPy (Polymer **3**, 40 mg) was dissolved in dichloromethane (0.4 mL). The solution was cooled to -78 °C, and boron trifluoride etherate (1 drop, ~0.04 mmol) was added. The reaction mixture was stirred for 2 h at -78 °C, then quenched by adding pyridine (0.10 mL, 1.2 mmol) and left stirring 2 h. The solution was then warmed to room temperature and polymer collected by precipitation into methanol (50 mL) and washing in methanol and diethyl ether (30 mg, 75%). GPC (THF, RI): M_n = 2.5 kDa, PDI = 2.00.

Scheme 7.8 **|** *Formation of PPA-UPy Supramolecular Networks.*

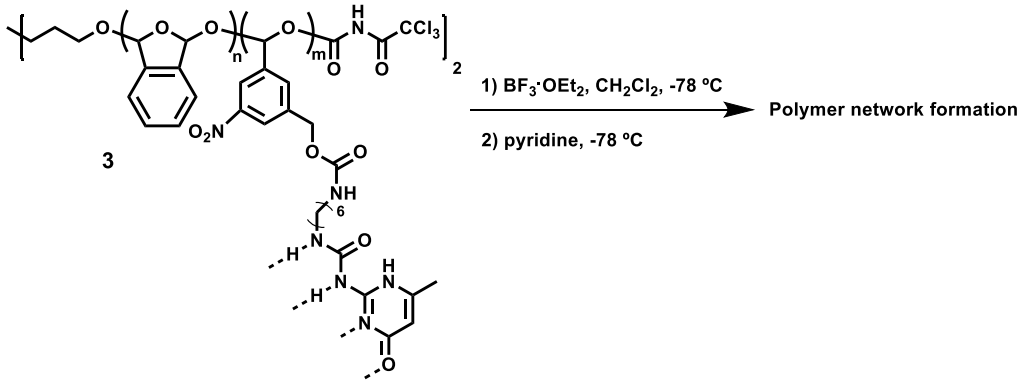

In a Schlenk flask, PPA-UPy (Polymer **3**, 70 mg) was dissolved in dichloromethane (0.4 mL). The solution was cooled to -78 °C, and boron trifluoride etherate (0.01 mL, 0.08 mmol) was added. The reaction mixture gels almost immediately, but was left for 2 h at -78 °C before quenching with pyridine (0.10 mL, 1.2 mmol) and left stirring 2 h. The solution was brought to room temperature and the resulting solid polymer was washed in excess methanol and diethyl ether (71 mg, quantitative recovery). The white solid was insoluble in chloroform, dichloromethane, THF, and dimethyl sulfoxide (all good solvents for PPA-UPy).

As a control reaction, the above procedure was repeated with PPA-HMNB (Polymer **2**, 70 mg in 0.4 mL dichloromethane). The reaction mixture remains soluble and colorless, and the polymer was collected as a white powder (34 mg, 49% yield). The polymer is soluble in all typical solvents for PPA. GPC (THF, RI): M_n = 2.0 kDa, PDI = 1.80.

Scheme 7.9 | *Depolymerization of PPA-UPy Supramolecular Networks (Figure 7.5).*

Cross-linked PPA-UPy (10-20 mg) was suspended in $CDCl_3$ (~3 mL) in a small glass dish, turning to an opaque gel. To the suspension was added three drops trifluoroacetic acid. The solid sample shrank in size immediately and disappeared completely within 2 min. The solution was collected for analysis and identified as majority *o*-PA monomer by ^{1}H NMR spectroscopy. ^{1}H NMR (500 MHz, $CDCl_3$) δ 10.54 (s, 2H, CHO), 7.98 (q, 2H, Ar-H), 7.78 (q, 2H, Ar-H).

7.6 NMR Spectra

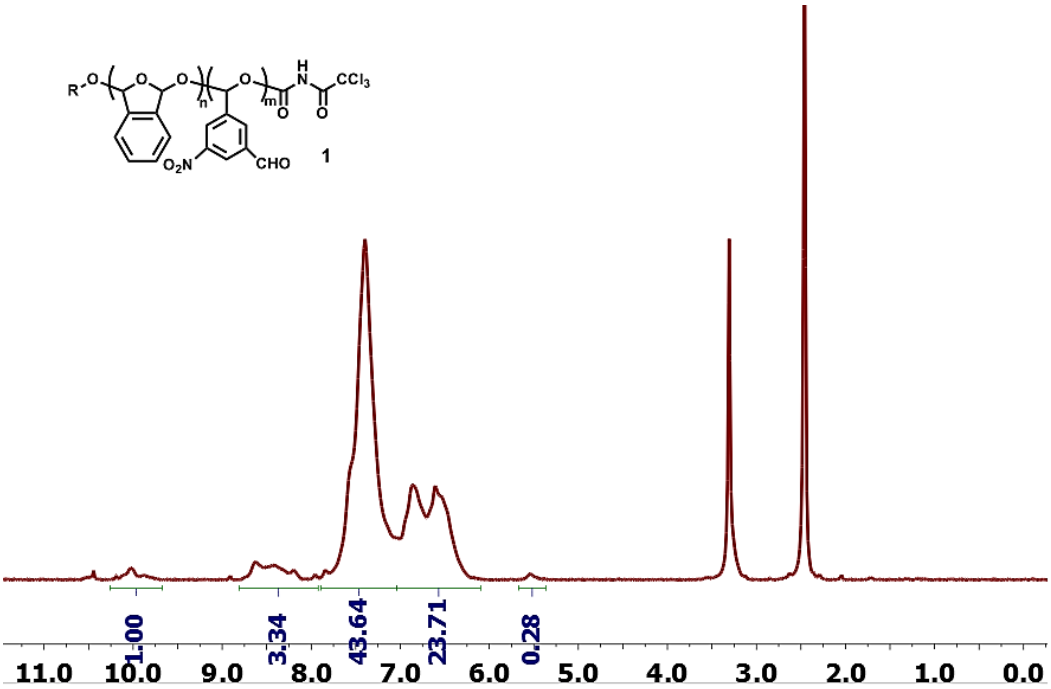

Figure 7.6 | ^{1}H NMR spectrum of PPA-NIPA*: NMR spectrum of M_n = 13.5 kDa PPA-NIPA (Polymer **1**) in DMSO-*d_6*. Additional peak corresponds to water.*

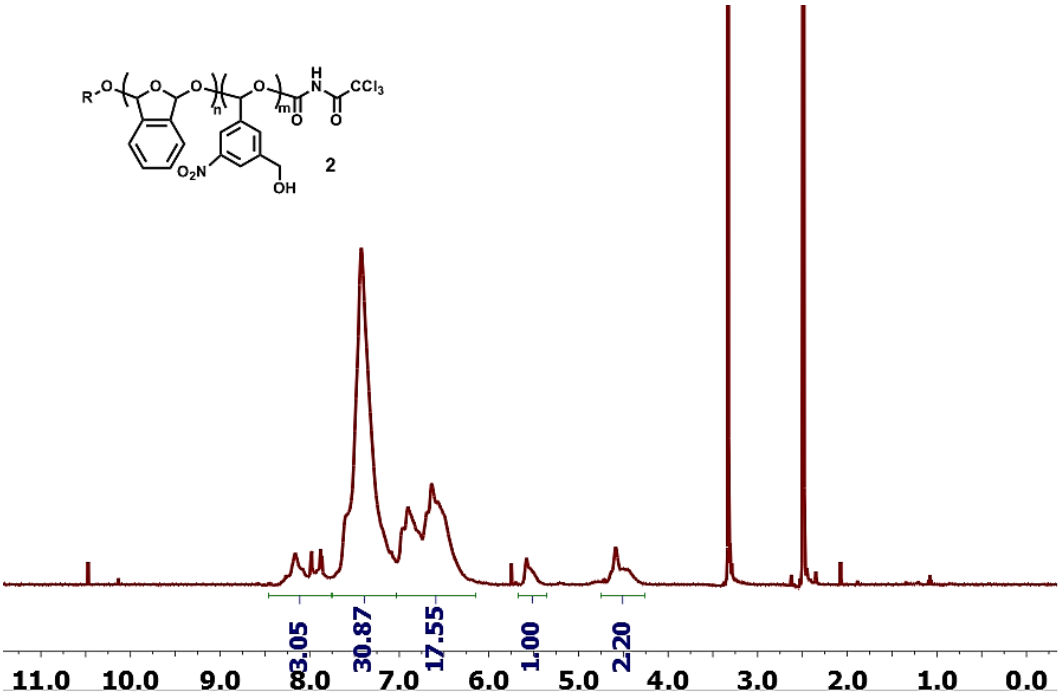

Figure 7.7 | ^{1}H NMR spectrum of PPA-HMNB*: NMR spectrum of M_n = 15.7 kDa PPA-HMNB (Polymer **2**) in DMSO-*d_6*. Additional peaks correspond to monomer and solvent.*

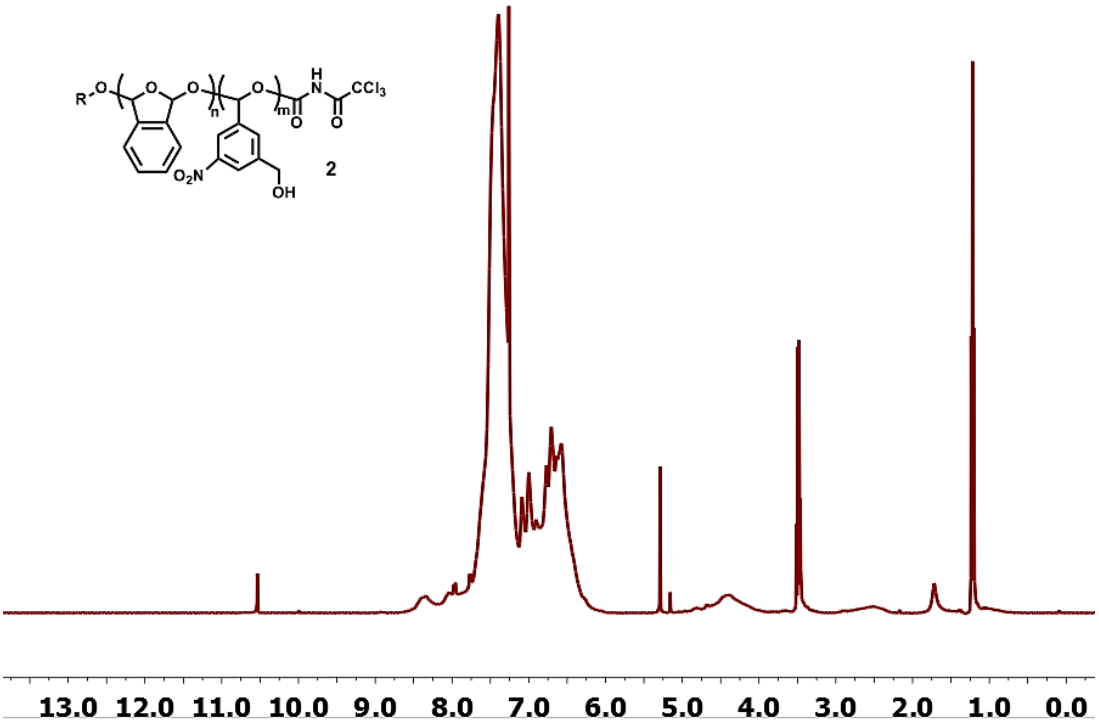

Figure 7.8 | ^{1}H NMR spectrum of PPA-HMNB*: NMR spectrum of M_n = 15.7 kDa PPA-HMNB (Polymer **2**) in $CDCl_3$. Additional peaks correspond to monomer and solvent.*

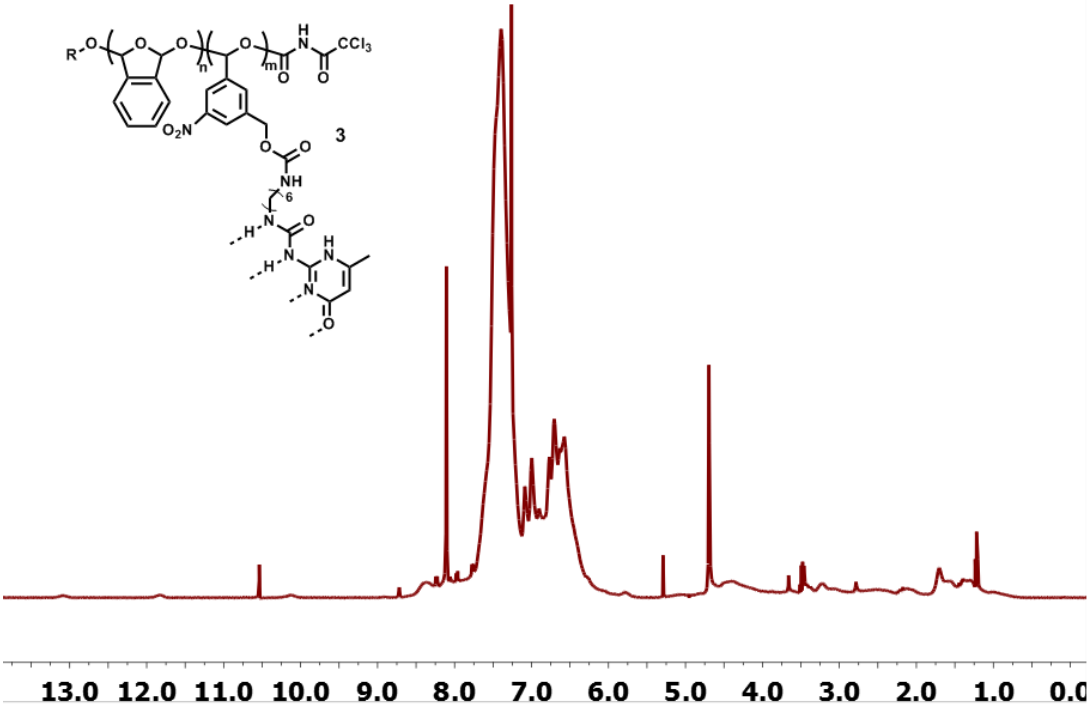

Figure 7.9 | ^{1}H NMR spectrum of PPA-UPy*: NMR spectrum of M_n = 15.3 kDa PPA-UPy (Polymer **3**) in $CDCl_3$. Additional peaks correspond to monomer and solvent.*

7.7 References

(1) (a) Brunsveld, L.; Folmer, B. J. B.; Meijer, E. W.; Sijbesma, R. P. *Chem. Rev.* **2001**, 101, 4071-4098. (b) Aida, T.; Meijer, E. W.; Stupp, S. I. *Science* **2012**, 335, 813-817. (c) Folmer, B. J. B.; Sijbesma, R. P.; van der Rijt, J. A. J.; Meijer, E. W. *Adv. Mater.* **2000**, 12, 874-878. (d) Sijbesma, R. P.; Meijer, E. W. *Chem. Commun.* **2003**, 5-16. (e) De Greef, T. F. A.; Smulders, M. M. J.; Wolffs, M.; Schenning, A. P. H. J.; Sijbesma, R. P.; Meijer, E. W. *Chem. Rev.* **2009**, 109, 5687-5754.

(2) (a) Hart, L. R.; Harries, J. L.; Greenland, B. W.; Colquhoun, H. M.; Hayes, W. *Polym. Chem.* **2013**, 4, 4860-4870. (b) Burnworth, M.; Tang, L.; Kumpfer, J. R.; Duncan, A. J.; Beyer, F. L.; Fiore, G. L.; Rowan, S. J.; Weder, C. *Nature* **2011**, 472, 334-337. (c) Cordier, P.; Tournilhac, F.; Soulie-Ziakovic, C.; Leibler, L. *Nature* **2008**, 451, 977-980. (d) Chen, Y.; Kushner, A. M.; Williams, G. A.; Guan, Z. *Nat. Chem.* **2012**, 4, 467-472. (e) Hentschel, J.; Kushner, A. M.; Ziller, J.; Guan, Z. *Angew. Chem. Int. Ed.* **2012**, 51, 10561-10565. (f) Burattini, S.; Greenland, B. W.; Merino, D. H.; Weng, W.; Seppala, J.; Colquhoun, H. M.; Hayes, W.; Mackay, M. E.; Hamley, I. W.; Rowan, S. J. *J. Am. Chem. Soc.* **2010**, 132, 12051-12058.

(3) (a) Ouchi, M.; Badi, N.; Lutz, J.-F.; Sawamoto, M. *Nat. Chem.* **2011**, 3, 917-924. (b) Altintas, O.; Barner-Kowollik, C. *Macromol. Rapid. Commun.* **2012**, 33, 958-971. (c) Seo, M.; Beck, B. J.; Paulusse, J. M. J.; Hawker, C.; Kim, S. Y. *Macromolecules*, **2008**, 41, 6413-6418. (d) Altintas, O.; Lejeune, E.; Gerstel, P.; Barner-Kowollik, C. *Polym. Chem.* **2012**, 3, 640-651. (e) Mavila, S.; Diesendruck, C. E.; Linde, S.; Amir, L.; Shikler, R.; Lemcoff, N. G. *Angew. Chem. Int. Ed.* **2013**, 52, 5767-5770. (f) Altintas, O.; Willenbacher, J.; Wuest, K. N. R.; Oehlenschlager, K. K.; Krolla-Sidenstein, P.; Gliemann, H.; Barner-Kowollik, C. *Macromolecules* **2013**, 46, 8092-8101.

(4) (a) Sijbesma, R. P.; Beijer, F. H.; Brunsveld, L.; Folmer, B. J. B.; Hirschberg, J. H. K. K.; Lange, R. F. M.; Lowe, J. K. L.; Meijer, E. W. *Science* **1997**, 278, 1601-1604. (b) Beijer, F. H.; Sijbesma, R. P.; Kooijman, H.; Spek, A. L.; Meijer, E. W. *J. Am. Chem. Soc.* **1998**, 120, 6761-6769. (c) Sontjens, S. H. M.; Sijbesma, R. P.; van Genderen, M. H. P.; Meijer, E. W. *J. Am. Chem. Soc.* **2000**, 122, 7487-7493. (d) Foster, E. J.; Berda, E. B.; Meijer, E. W. *J. Am. Chem. Soc.* **2009**, 131, 6964-6966. (e) Stals, P. J. M.; Gillissen, M. A. J.; Nicolay, R.; Palmans, A. R. A.; Meijer, E. W. *Polym. Chem.* **2013**, 4, 2584-2597. (f) Berda, E. B.; Foster, E. J.; Meijer, E. W. *Macromolecules* **2010**, 43, 1430-1437. (g) Hosono, N.; Gillissen, M. A. J.; Li, Y.; Sheiko, S. S.; Palmans, A. R. A.; Meijer, E. W. *J. Am. Chem. Soc.* **2013**, 135, 501-510.

(5) (a) Peterson, G. I.; Larsen, M. B.; Boydston, A. J. *Macromolecules* **2012**, 45, 7317-7328. (b) Esser-Kahn, A. P.; Odom, S. A.; Sottos, N. R.; White, S. R.; Moore, J. S. *Macromolecules* **2011**, 44,

5539-5553. (c) Wong, A. D.; DeWit, M. A.; Gillies, E. R. *Adv. Drug Delivery Rev.* **2012**, 64, 1031-1045.

(6) (a) Sagi, A.; Weinstain, R.; Karton, N.; Shabat, D. *J. Am. Chem. Soc.* **2008**, 130, 5434-5435. (b) Weintain, R.; Sagi, A.; Karton, N.; Shabat, D. *Chem. Eur. J.* **2008**, 14, 6857-6861. (c) DeWit, M. A.; Gillies, E. R. *J. Am. Chem. Soc.* **2009**, 131, 18327-18334. (d) Chen, E. K. Y.; McBride, R. A.; Gillies, E. R. *Macromolecules* **2012**, 45, 7364-7374. (e) Dewit, M. A.; Beaton, A.; Gillies, E. R. *J. Polym. Sci., Part A: Polym. Chem.* **2010**, 48, 3977-3985. (f) McBride, R. A.; Gillies, E. R. *Macromolecules* **2013**, 46, 5157-5166. (g) Robbins, J. S.; Schmid, K. M.; Phillips, S. T. *J. Org. Chem.* **2013**, 78, 3159-3169. (h) Olah, M. G.; Robbins, J. S.; Baker, M. S.; Phillips, S. T. *Macromolecules* **2013**, 46, 5924-5928. (i) Wang, W.; Alexander, C. *Angew. Chem. Int. Ed.* **2008**, 47, 7804-7806. (j) Esser-Kahn, A. P.; Sottos, N. R.; White, S. R.; Moore, J. S. *J. Am. Chem. Soc.* **2010**, 132, 10266-10268.

(7) (a) Chuji, A.; Tagami, S.; Kunitake, T. *J. Polym. Sci., Part A: Polym. Chem.* **1969**, 7, 497-511. (b) Chuji, A.; Tagami, S. *Macromolecules* **1969**, 2, 414-419. (c) Willson, C. G.; Ito, H.; Frechet, J. M. J.; Tessier, T. G.; Houlihan, F. M. *J. Electrochem. Soc.* **1986**, 133, 181-187. (d) Ito, H.; Willson, C. G. *Polym. Eng. Sci.* **1983**, 23, 1012-1018. (e) Coulembier, O.; Knoll, A.; Pires, D.; Gotsmann, B.; Duerig, U.; Frommer, J.; Miller, R. D.; Dubois, P.; Hedrick, J. L. *Macromolecules* **2010**, 43, 572-574. (f) Knoll, A. W.; Pires, D.; Coulembier, O.; Dubois, P.; Hedrick, J. L.; Frommer, J.; Duerig, U. *Adv. Mater.* **2010**, 22, 3361-3365. (g) Seo, W.; Phillips, S. T. *J. Am. Chem. Soc.* **2010**, 132, 9234-9235 (h) Zhang, H.; Yeung, K.; Robbins, J. S.; Pavlick, R. A.; Wu, M.; Liu, R.; Sen, A.; Phillips, S. T. *Angew. Chem. Int. Ed.* **2012**, 51, 2400-2404. (i) Dilauro, A. M.; Robbins, J. S.; Phillips, S. T. *Macromolecules* **2013**, 46, 2963-2968. (j) Dilauro, A. M.; Abbaspourrad, A.; Weitz, D. A.; Phillips, S. T. *Macromolecules* **2013,** 46, 3309-3313.

(8) (a) Kaitz, J. A.; Moore, J. S.; *Macromolecules* **2013**, 46, 608-612. (b) Kaitz, J. A.; Diesendruck, C. E.; Moore, J. S. *J. Am. Chem. Soc.* **2013**, 135, 12755-12761. (c) Kaitz, J. A.; Diesendruck, C. E.; Moore, J. S. *Macromolecules* **2013**, 46, 8121-8128.

(9) Smith, H. A. *J. Appl. Polym. Sci.* **1963**, 7, 85-95.

(10) (a) Hou, X.; Guo, W.; Jiang, L. *Chem. Soc. Rev.* **2011**, 40, 2385-2401. (b) Fan, J.-B.; Huang, C.; Jiang, L.; Wang, S. *J. Mater. Chem. B* **2013**, 1, 2222-2235. (c) Dekker, C. *Nat. Nanotech.* **2007**, 2, 209-215.

(11) Company, A.; Gomez, L.; Mas-Balleste, R.; Korendovych, I. V.; Ribas, X.; Poater, A.; Parella, T.; Fontrodona, X.; Benet-Buchholz, J.; Sola, M.; Que, L.; Rybak-Akimova, E. V.; Costas, M. *Inorg. Chem.* **2007**, 46, 4997-5012.

Chapter 8: Efforts toward Recyclable, Sustainable Depolymerizable Polyesters

8.1 Abstract

With increasing awareness of the environmental burden of plastic production and disposal, there is an emerging interest in the identification of polymeric materials that can be produced from renewable resources and which can efficiently biodegrade to benign byproducts. Depolymerizable polymers prepared from biobased monomers would represent an advantageous route to achieve eco-friendly, recyclable and sustainable materials due to their ability to undergo triggered depolymerization on command to unzip directly to monomer. Experiments were therefore initiated with the aim of developing a novel depolymerizable polyester based on bioavailable lactone monomers. Attempts to polymerize a dimethyl substituted δ-valerolactone monomer were unsuccessful owing to an extremely low ceiling temperature for the monomer, as elucidated by computational studies. Computational studies were further employed to identify potential candidate monomers for such a depolymerizable polyester system, which, if successful, would signal a key advance in the development of green, recyclable, and sustainable polymeric materials.

8.2 Introduction

The field of sustainable and green materials has notably emerged in the literature in recent years.[1] Recognition of the growing environmental and economic burdens of producing and disposing of conventional plastics has increased significantly in the past decade.[1-2] Continued exploitation of fossil fuel resources for plastic production and further clogging of landfills with non-biodegradable plastic waste is simply unsustainable in the long term. We are only now becoming fully aware of the true impact of plastic life cycles on the environment, and researchers have thus begun to devote significant resources toward the production of environmentally friendly, sustainable, and degradable materials.

Two main hallmarks have taken shape in the field of green materials chemistry: first, a shift toward developing sustainable, biorenewable building blocks from which to prepare materials; and second, a focus on degradable materials that break down to benign products and thereby reduce waste buildup.[1-2] In terms of sustainable starting materials, there has been an emphasis to shift material resource infrastructure away from finite fossil fuel feedstocks and toward bioavailable and biorenewable products.[3-4] For example, several research groups have initiated projects to prepare and study aliphatic polyesters based on bioderived lactone monomers.[1b] Several novel monomers and polymers have been synthesized from bioavailable

carvone and menthol precursors, and current efforts are focused on achieving favorable mechanical properties akin to commodity plastics with these new sustainable materials.[4] Amazingly, the Zhang and Hillmyer groups have even demonstrated the ability to engineer bacteria to directly manufacture lactone monomers, which could be copolymerized with lactide to produce mechanically robust materials.[3c]

The second major research effort in green materials chemistry aims to reduce waste by preparing biodegradable and recyclable materials.[2] A wide variety of materials have been prepared and studied with triggered degradation mechanisms based on photo-triggering, acid-sensitivity, or susceptibility to hydrolysis.[5] The Miller group, in fact, has shown that incorporating acetal functionality into polyesters via acetal metathesis polymerization yields polyesteracetals that degrade at enhanced rates compared to analogous polyesters without the acetal functionality.[5c-d] While autonomic degradation into benign byproducts is of course desirable, it would be more efficient to directly recycle materials back into monomers on command.

Advanced green materials will surely merge both research strategies and utilize sustainable monomers that are not only capable of biodegradation, but can also be recycled and reused. We hypothesize that depolymerizable polymers based on renewable monomers could serve this purpose. One could envision preparing a low ceiling temperature (T_c) polymer with sustainable and eco-friendly monomer units, which would be capable of triggered depolymerization to regenerate monomer for reuse. Depolymerizable polymers have advantages compared to typical degradable materials in that they revert to monomer on depolymerization rather than alternative small molecule products that need further refinement to convert to monomer. Further, numerous triggering events could be employed to effect the unzipping reaction to recycle monomer on demand. Finally, the depolymerization process is extremely rapid compared to degradation so material recycling can be achieved rapidly on demand. For all of these reasons, we initiated a project geared toward identifying potential low T_c polymers based on biorenewable monomers, and to prepare and study these eco-friendly, sustainable, depolymerizable polymers.

8.3 Results and Discussion

8.3.1 Identification of Monomer Target

The first aim was to identify a bioderived monomer that would conceivably have a T_c at or below room temperature. Lactone monomers were initially targeted due to the breadth of literature concerning their preparation and polymerization, as well as their known bioavailability.[1, 3-4] Intriguingly, it was discovered that substituents in 4- and 6- positions in δ-valerolactones lower the enthalpy of polymerization

to be considerably less exothermic, resulting in a decreased T_c for such polyesters compared to the parent polymer (Scheme 8.1, Table 8.1).[3] For example, unsubstituted poly(δ-valerolactone) is known to have a moderately high T_c of 150 °C (Table 8.1, Entry 1).[3a] However, incorporating a 4-methyl or 6-pentyl substituent in the lactone markedly decreased the polymer T_c to 27 °C and 44 °C, respectively (Table 8.1, Entries 2-3).[3b-c]

It was suggested that, while the entropies of polymerization are not as significantly affected, the basis for this decreased enthalpy of polymerization is less ring-strain in the substituted monomers. We therefore reasoned that further decreasing the ring-strain in the lactone monomer would yield polymers with T_c's below room temperature, as desired. Based on this rationale, we theorized that incorporating 4- and 6-methyl substituents in the lactone would generate the desired depolymerizable polyester material (Scheme 8.1, Table 8.1, Entry 4).[6] In support this hypothesis, it was demonstrated computationally that the 4-methyl, 6-methyl, and *cis*-4,6-dimethyl-δ-valerolactones all adopt the same half-chair conformation as their most stable conformer.[7]

Scheme 8.1 | *Hypothesized depolymerizable, sustainable polyesters.*

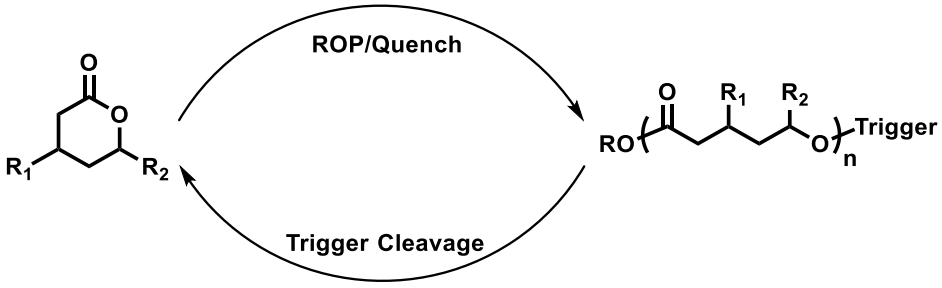

Table 8.1 | Thermodynamic data for substituted δ-valerolactone monomers.

Entry	*R_1*	*R_2*	*ΔH (kJ/mol)*	*ΔS (J/mol K)*	*T_c (°C)[a]*
1[b]	H	H	-27.4	-65	150
2[c]	CH_3	H	-13.8	-46	27
3[d]	H	C_5H_{11}	-17.1	-54	44
4[e]	CH_3	CH_3	- - -	- - -	- - -

[a]At 1 M. [b]Ref 3a. [c]Ref 3c. [d]Ref 3b. [e]This work.

8.3.2 Synthesis and Ring-Opening Polymerization of 4,6-dimethyl-δ-valerolactone

The targeted 4,6-dimethyl-δ-valerolactone monomer was prepared in a single step from a commercially available precursor (Scheme 8.2). Briefly, 4,6-dimethyl-α-pyrone was reduced by catalytic hydrogenation and the monomer was purified by vacuum distillation to yield a viscous, colorless liquid.[8]

As expected for heterogeneous hydrogenation conditions, ^{1}H NMR characterization of the product revealed the presence of almost exclusively the *cis* isomer.[8b-c]

Scheme 8.2 | *Two-step synthetic route to poly(4,6-dimethyl-δ-valerolactone).*

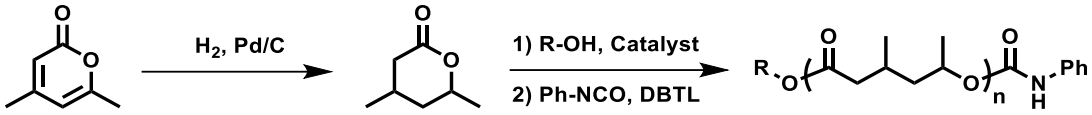

With the monomer in hand, efforts shifted to preparing the polyester via either anionic or cationic ring-opening polymerizations (Scheme 8.2).[9] Anionic ring-opening polymerizations were conducted either in bulk (~8 M monomer) or in dichloromethane, and were initiated by a combination of 1,6-hexanediol and triazabicyclodecene. Cationic ring-opening polymerizations followed the same general procedure, but were instead initiated by a combination of 1,6-hexanediol and diethylzinc.

Initial polymerization attempts over a range of concentrations, temperatures, and monomer-to-initiator ratios did not successfully furnish polymer, so additional steps were taken to purify the monomer. It was already known that ring-opening polymerizations can be extremely sensitive to impurities, so a more rigorous monomer purification protocol was undertaken, per literature precedent.[3c] In short, the monomer was dried overnight over calcium hydride, followed by two successive vacuum distillations to obtain rigorously purified 4,6-dimethyl-δ-valerolactone.

Attempted polymerization of the purified monomer still did not generate any appreciable quantity of polymer. It was hypothesized that the potentially low T_c of the polymer was preventing polymerization, so polymerizations were attempted in bulk at 0 °C (the monomer freezes at temperatures below 0 °C). Even in bulk at low temperature, monomer was recovered in quantitative yield with no evidence of any polymer for either anionic or cationic ring-opening polymerizations. As a control to test reagent efficacy, identical polymerizations were set up with lactide as monomer. Poly(lactide) was recovered in good yields, confirming catalyst and initiator purity.

8.3.3 Computational Studies and Identification of Candidate Lactone Monomers

The reluctance of 4,6-dimethyl-δ-valerolactone to polymerize was probed computationally. The insertion of methyl acetate into the lactone was employed as a model reaction for propagation to estimate an enthalpy of polymerization, as was previously done to model the polymerization of 1,3-dioxolan-4-one and γ-butyrolactone (Scheme 8.3).[5d] With an estimation of the enthalpy of polymerization, it is possible to calculate an approximate T_c for the monomer by assuming an entropy of polymerization similar to

analogous lactones. Thus, the corresponding heats of formation for various substituted δ-valerolactones, the ring-opened products, and methyl acetate were calculated by the T1 thermochemical recipe computational method, and the results are summarized in Table 8.2.

Scheme 8.3 | *Model reaction for lactone ring-opening polymerization for computational studies.*

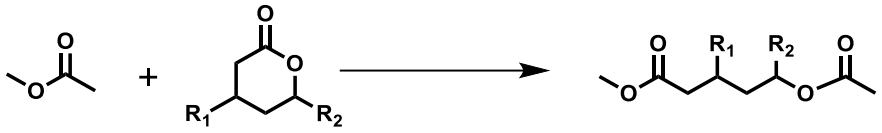

Table 8.2 | Computational data for substituted δ-valerolactone monomers.

Entry	R_1	R_2	*ΔH (kJ/mol), calc.*[a]	*ΔH (kJ/mol), cal.*[b]	*ΔH (kJ/mol), expt.*[c]	T_c *(°C)*[d] *calc.*	T_c *(°C) expt.*[c]
1	H	H	-10.8	-27.5	-27.4	220	150
2	CH_3	H	21.8	-14.8	-13.8	0	27
3	H	CH_3	18.5	-16.1	-17.1	20	44
4	CH_3	CH_3	38.3	-8.3	- - -	-120	- - -
5	*t*-Bu	H	52.5	-2.8	- - -	-220	- - -
6	H	*t*-Bu	21.3	-15.0	- - -	0	- - -
7	OCH_3	CH_3	21.5	-14.9	- - -	0	- - -

[a]Calculated by T1 thermochemical recipe computational method. [b]After normalization based on calibration curve. [c]See Table 8.1. [d]At 1 M, with ΔS = 55 J/mol K (average of known values) and ΔH determined by calibration.

As seen in Table 8.2, some enthalpies are estimated to be endothermic, which would make the polymerization thermodynamically impossible. This is not entirely unexpected for such an oversimplified model reaction. Importantly, though, the computation accurately predicts the order of enthalpies for known monomers, with δ-valerolactone, 4-methyl-δ-valerolactone, and 6-methyl-δ-valerolactone displaying the proper order of calculated ΔH_p's (Entries 1-3). Undeterred, a calibration curve was constructed using the three known data points for the enthalpy of polymerization and the calculated values from the model reaction (Figure 8.1). Incredibly, the calibration curve is quite linear and with a high correlation coefficient, suggesting that interpretation of the data in the manner is not unreasonable. In fact, the computed enthalpies of polymerization are in close agreement with known values, and estimated T_c's by this method are gratifyingly accurate, even when using an average entropy of polymerization in such estimates rather than the known values (Table 8.2, Entries 1-3).

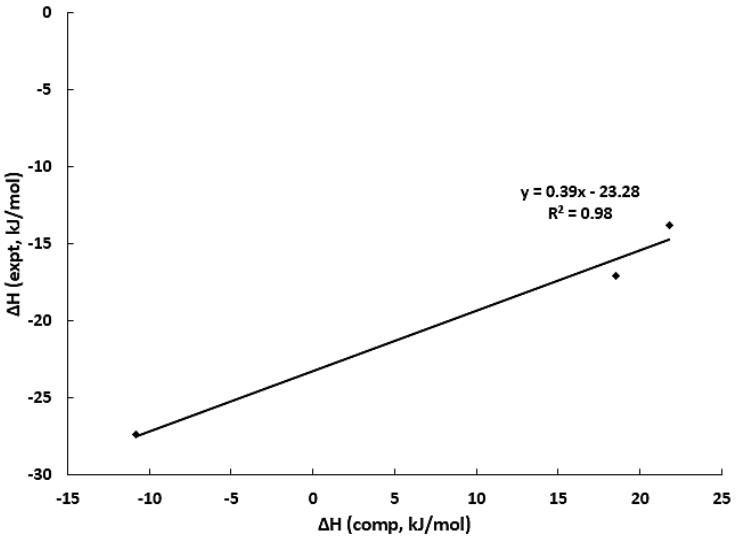

***Figure 8.1** | Calibration curve for determining ΔH_p computationally for various lactones.*

With this apparent validation of the computational method (and a recognition of its potential limitations in accuracy), the method was applied to the 4,6-dimethyl-δ-valerolactone monomer (Table 8.2, Entry 4). Not surprisingly, it was found that this lactone has a significantly reduced exotherm of polymerization of -8.3 kJ/mol, likely owing to the further decrease in ring-strain with double substitution. The T_c is calculated to be approximately -120 °C, explaining the apparent reluctance to polymerize. In fact, the T_c for this monomer in bulk is estimated as -50 °C (at 8 M), well below its freezing point. The equilibrium monomer concentration at 0 °C can be estimated to be substantially greater than 8 M, again corroborating the monomer's inability to polymerize.

An effort was undertaken to identify other potential monomer candidates using this computational method. Two monomers with *tert*-butyl substituents in either the 4- or 6-position were evaluated because it was hypothesized that the bulky substituent may further attenuate lactone ring-strain, and 4-methoxy-6-methyl-δ-valerolactone was also assessed because of its ease of preparation from the parent pyrone, which is commercially available (4-methoxy-6-methyl-2H-pyran-2-one).[10] Several other substituted 2-pyrone starting materials are commercially available, and could be considered in further iterations.

As anticipated, *tert*-butyl substitution does significantly modulate the enthalpy of ring-opening. In the 4-position, the enthalpy of polymerization is estimated to be -2.8 kJ/mol, having a T_c of approximately -220 °C (Table 8.2, Entry 5), far below what would be considered a viable monomer candidate. The 6-*tert*-butyl substituted lactone, on the other hand, has an apparent T_c close to 0 °C, in a range that merits further consideration (Table 8.2, Entry 6). Likewise, 4-methoxy-6-methyl-δ-valerolactone has an estimated T_c close to 0 °C (Table 8.2, Entry 7). Since these values are only rough estimates, it would certainly be of value to prepare the corresponding candidate monomers (depicted in Scheme 8.4) and assess their viability

to serve as eco-friendly, sustainable, and depolymerizable polyester systems. Such efforts are currently underway.

Scheme 8.4 **|** *Lactone monomer candidates based on computational analysis.*

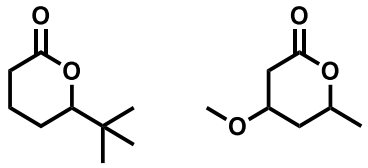

8.4 Conclusions

In this chapter, the groundwork was laid for the development of a green, depolymerizable polymeric system. A candidate monomer, 4,6-dimethyl-δ-valerolactone, was prepared and its polymerizability assessed, but it was discovered that polymerization was thermodynamically unfavorable under feasible experimental conditions. To evaluate other candidate monomers, a computational method was devised where the ring-opening of lactones by insertion of methyl acetate was used to model a ring-opening polymerization. This method identified two additional monomer candidates, one of which can be prepared in a single step from commercially available starting materials, as viable candidate monomers for further exploration. If successful, this type of sustainable, recyclable, depolymerizable polyester would signal a key advance in the development of green materials.

8.5 Synthetic Procedures

Scheme 8.5 **|** *4,6-dimethyl-δ-valerolactone synthesis.*

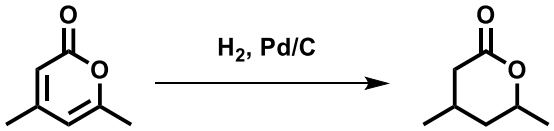

In a round-bottom flask, palladium on carbon (10% Pd, 0.51 g, 0.5 mmol Pd) and 4,6-dimethyl-α-pyrone (2.10 g, 17 mmol) are thoroughly degassed under nitrogen. The solids are then dissolved in a 2:1 mixture of diethyl ether:methanol (60 mL) and the flask is equipped with hydrogen from four filled balloons. The mixture is left stirring overnight at room temperature, then the catalyst is filtered off and the crude product concentrated to a yellow oil. The oil is stirred over CaH_2 for 24 h, then filtered and distilled twice under

vacuum (0.15 Torr, 60 °C). The distillate is collected as a viscous, colorless liquid (1.61 g, 73%, ρ = 1.08 g/mL). ^{1}H NMR (500 MHz, $CDCl_3$) δ 4.40 ppm (m, 1H, -CH-), 2.65 ppm (dd, 1H, -CH_2-), 2.12-2.00 ppm (m, 2H, -CH- & -CH_2-), 1.96 ppm (m, 1H, -CH_2-), 1.91 ppm (dd, 1H, -CH_2-), 1.35 ppm (d, 3H, CH_3), 1.01 ppm (d, 3H, CH_3). ^{13}C{^{1}H} NMR (500 MHz, $CDCl_3$) δ 171.7 ppm, 77.2 ppm, 39.0 ppm, 38.0 ppm, 27.0 ppm, 22.1 ppm, 21.8 ppm. HR EI-MS (m/z): calcd for $C_7H_{12}O_2$ $[M]^+$, 128.0837; found 128.0838.

Scheme 8.6 | *Anionic ring opening polymerization of 4,6-dimethyl-δ-valerolactone.*

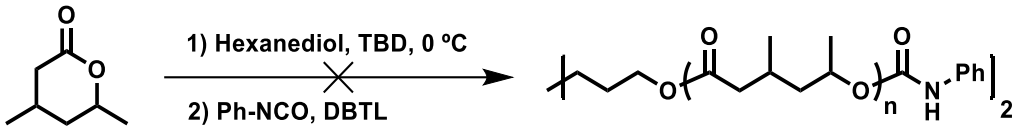

In a glovebox, 4,6-dimethyl-δ-valerolactone (0.50 g, 3.9 mmol) and 1,6-hexanediol (6 mg, 0.05 mmol, 2.5 mol% -OH) are weighed into a 20-mL vial. Then, triazabicyclodecene (TBD, 14 mg, 0.1 mmol) is added and the vial rapidly sealed, removed from the glovebox, and cooled to 0 °C. The polymerization reaction is left stirring at 0 °C for 6 h. Then, phenyl isocyanate (0.05 mL, 0.5 mmol) and dibutyl tin dilaurate (DBTL, 0.01 mL, 0.02 mmol) are added, and the reaction mixture is allowed to warm to room temperature overnight. The resulting mixture is dried overnight on vacuum and analyzed directly by GPC and NMR spectroscopy. The analytical results confirm the mixture is majority monomer. GPC (THF, RI): No polymer.

Scheme 8.7 | *Cationic ring opening polymerization of 4,6-dimethyl-δ-valerolactone.*

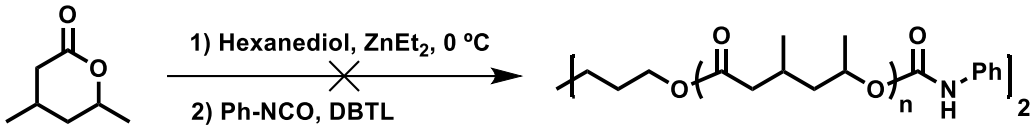

In a glovebox, 4,6-dimethyl-δ-valerolactone (0.50 g, 3.9 mmol) and 1,6-hexanediol (6 mg, 0.05 mmol, 2.5 mol% -OH) are weighed into a 20-mL vial. Then, diethylzinc (15 µL, 0.15 mmol) is added and the vial rapidly sealed, removed from the glovebox, and cooled to 0 °C. The polymerization reaction is left stirring at 0 °C for 6 h. Then, phenyl isocyanate (0.05 mL, 0.5 mmol) and dibutyl tin dilaurate (DBTL, 0.01 mL, 0.02 mmol) are added, and the reaction mixture is allowed to warm to room temperature overnight. The resulting mixture is dried overnight on vacuum and analyzed directly by GPC and NMR spectroscopy. The analytical results confirm the mixture is majority monomer. GPC (THF, RI): No polymer.

8.6 Computational Results

Scheme 8.8 | *Model reaction for lactone ring-opening polymerization.*

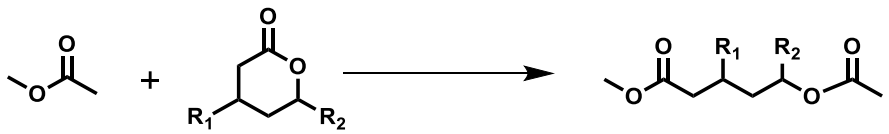

Table 8.3 | Computational data for substituted δ-valerolactone monomers.[a]

Entry	*R_1*	*R_2*	*H_f (kJ/mol), methyl acetate*	*H_f (kJ/mol), lactone*	*H_f (kJ/mol), di-ester*	*ΔH (kJ/mol), calc.*	*ΔH (kJ/mol), cal.*[b]	*T_c (°C) expt.*[c]
1	H	H	-408.28	-378.82	-797.90	-10.8	-27.5	220
2	CH_3	H	-408.28	-409.52	-796.02	21.8	-14.8	0
3	H	CH_3	-408.28	-419.05	-808.85	18.5	-16.1	20
4	CH_3	CH_3	-408.28	-449.59	-819.53	38.3	-8.3	-120
5	*t*-Bu	H	-408.28	-480.77	-836.55	52.5	-2.8	-220
6	H	*t*-Bu	-408.28	-496.73	-883.70	21.3	-15.0	0
7	OCH_3	CH_3	-408.28	-553.57	-940.32	21.5	-14.9	0

[a]Calculated by T1 thermochemical recipe computational method. [b]After normalization based on calibration curve. [c]At 1 M, with ΔS = 55 J/mol K (average of known values) and ΔH determined by calibration.

8.7 References

(1) (a) Miller, S. A.; *ACS Macro Lett.* **2013**, 2, 550-554. (b) Hillmyer, M. A.; Tolman, W. B. *Acc. Chem. Res.* **2014**, 47, 2390-2396. (c) Yao, K.; Tang, C. *Macromolecules* **2013**, 46, 1689-1712. (d) Ragauskas, A. J.; Williams, C. K.; Davison, B. H.; Britovsek, G.; Cairney, J.; Eckert, C. A.; Frederick, Jr., W. J.; Hallett, J. P.; Leak, D. J.; Liotta, C. L.; Mielenz, J. R.; Murphy, R.; Templer, R.; Tschaplinski, T. *Science* **2006**, 311, 484-489. (e) Mulhaupt, R.; *Macromol. Chem. Phys.* **2013**, 214, 159-174. (f) Gandini, A. *Macromolecules* **2008**, 41, 9491-9504. (g) Bayer, I. S.; Puyol, S. G.; Heredia-Guerrero, J. A.; Ceseracciu, L.; Pignatelli, F.; Ruffilli, R.; Cingolani, R.; Athanassiou, A. *Macromolecules* **2014**, 47, 5135-5143.

(2) (a) Mudhoo, A.; Mohhe, R.; Unmar, G. D.; Sharma, S. K. *RSC Green. Chem. Ser.* **2011**, 12, 332-364. (b) Ikada, Y.; Tsuji, H. *Macromol. Rapid Commun.* **2000**, 21, 117-132. (c) Gross, R. A.; Kalra, B. *Science* **2002**, 297, 803-807. (d) Song, J. H.; Murphy, R. J.; Narayan, R.; Davies, G. B. H. *Philos. Trans. R. Soc. B* **2009**, 364, 2127-2139.

(3) (a) Duda, A.; Kowalski, A. "Thermodynamics and kinetics of ring-opening polymerizations," in *Handbook of Ring-Opening Polymerization*. Wiley-VCH: Weinheim, **2009**; p. 1-51. (b) Martello,

M. T.; Burns, A.; Hillmyer, M. A. *ACS Macro Lett.* **2012**, 1, 131-135. (c) Xiong, M.; Schneiderman, D. K.; Bates, F. S.; Hillmyer, M. A.; Zhang, K. *Proc. Natl. Acad. Sci., U.S.A* **2014**, 111, 8357-8362.

(4) (a) Neitzel, A. E.; Peterson, M. A.; Kokkoli, E.; Hillmyer, M. A. *ACS Macro Lett.* **2014**, 3, 1156-1160. (b) Lowe, J. R.; Martello, M. T.; Tolman, W. B.; Hillmyer, M. A. *Polym. Chem.* **2011**, 2, 702-708. (c) Knight, S. C.; Schaller, C. P.; Tolman, W. B.; Hillmyer, M. A. *RSC Adv.* **2013**, 3, 20399-20404. (d) Wanamaker, C. L.; O'Leary, L. E.; Lynd, N. A.; Hillmyer, M. A.; Tolman, W. B. *Biomacromolecules* **2007**, 8, 3634-3640. (e) Wanamaker, C. L.; Bluemle, M. J.; Pitet, L. M.; O'Leary, L. E.; Tolman, W. B.; Hillmyer, M. A. *Biomacromolecules* **2009**, 10, 2904-2911.

(5) (a) Rajendran, S.; Raghunathan, R.; Hevus, I.; Krishnan, R.; Ugrinov, A.; Sibi, M. P.; Webster, D. C.; Sivaguru, J. *Angew. Chem. Int. Ed.* **2014**, 53, 1-6. (b) Garcia, J. M.; Jones, G. O.; Virwani, K.; McCloskey, B. D.; Boday, D. J.; Huurne, G. M.; Horn, H. W.; Coady, D. J.; Bintaleb, A. M.; Alabdulrahman, A. M. S.; Alsewailem, F.; Almegren, H. A. A.; Hedrick, J. L. *Science* **2014**, 344, 732-735. (c) Pemba, A. G.; Flores, J. A.; Miller, S. A. *Green Chem.* **2013**, 15, 325-329. (d) Martin, R. T.; Camargo, L. P.; Miller, S. A. *Green Chem.* **2014**, 16, 1768-1773.

(6) This lactone is bioavailable and is known to be the major component in sex pheromones of a species of carpenter bee: Wheeler, J. W.; Evans, S. L.; Blum, M. S.; Velthius, H. H. V.; de Camargo, J. M. F.; *Tetrahderon. Lett*. **1976**, 17, 4029-4032.

(7) Weber, F.; Bruckner, R. *Chem. Eur. J.* **2013**, 19, 1288-1302.

(8) (a) Wiley, R. H.; Hart, A. J. *J. Am. Chem. Soc.* **1955**, 77, 2340-2341. (b) Carroll, F. I.; Mitchell, G. N.; Blackwell, J. T.; Soboti, A.; Meck, R. *J. Org. Chem.* **1974**, 39, 3890. (c) McKelvey, R. D.; Kawada, Y.; Sugawara, T.; Iwamura, H. *J. Org. Chem.* **1981**, 46, 4948-4952.

(9) (a) Kamber, N. E.; Jeong, W.; Pratt, R. C.; Lohmeijer, B. G. G.; Waymouth, R. M.; Hedrick, J. L. *Chem. Rev.* **2007**, 107, 5813-5840. (b) Lecomte, P.; Jerome, C. *Adv. Polym. Sci.* **2012**, 245, 173-218.

(10) For 4-methoxy-6-methyl-δ-valerolactone preparation: (a) Huck, W.-R.; Mallat, T.; Baiker, A. *New J. Chem.* **2002**, 26, 6-8. (b) Huck, W.-R.; Mallat, T.; Baiker, A. *Catal. Lett.* **2002**, 80, 87-92. (c) Fehr, M. J.; Consiglio, G.; Scalone, M.; Schmid, R. *J. Org. Chem.* **1999**, 64, 5768-5776. For 6-*tert*-butyl-δ-valerolactone preparation: (d) Hsu, J.-L.; Chem, C.-T.; Fang, J.-M. *Org. Lett.* **1999**, 1, 1989-1991. (e) Hsu, J.-L.; Fang, J.-M. *J. Org. Chem.* **2001**, 66, 8573-8584.